Sapping Features of the Colorado Plateau

A Comparative Planetary Geology Field Guide

Sapping Features of the Colorado Plateau

A Comparative Planetary Geology Field Guide

NASA SP-491

Sapping Features of the Colorado Plateau

A Comparative Planetary Geology Field Guide

Edited by

Alan D. Howard
Department of Environmental Sciences
University of Virginia
Charlottesville, VA 22903

R. Craig Kochel
Department of Geology
Southern Illinois University
Carbondale, IL 62901

Henry E. Holt
U.S. Geological Survey
Flagstaff, AZ 86001

NASA Scientific and Technical Information Division 1988
National Aeronautics and Space Administration
Washington, DC

ON THE COVER Aerial view of the head of Cow Canyon, a tributary to the Escalante River, Utah. This long, narrow box canyon in the Navajo Sandstone has been created primarily by headward erosion due to groundwater sapping. The canyon is approximately 140 meters deep, exposing the underlying flaggy Kayenta Formation, which is a major aquiclude and the locus of many seeps. A small remnant of the shaley Carmel Formation that overlies the Navajo occurs to the right of the canyon head, but elsewhere this formation has been stripped away, permitting recharge of the Navajo aquifer. An arm of Lake Powell appears in the background, and the crest of the Waterpocked Fold anticline (which is the groundwater divide for the regional aquifer) coincides with the strip of dark vegetation beyond the canyon head. The rocks dip about 3 degrees toward the observer. The canyon walls are scalloped by numerous alcoves, some with active seeps, particularly at the headwalls of major tributaries. The head of a tributary canyon is visible at the right. A well-developed slickrock landscape of rounded low domes has formed on the plateau surface on the top of the Navajo Sandstone. See figs. 63 and 64 for location, and chapters 2 and 4 for further discussion of sapping features in this area. Photo by H.E. Holt.

FRONTISPIECE Seepage face and associated alcove at the head of a short canyon in the Navajo Sandstone tributary to North Wash along Utah Highway 95 near the Henry Mountains, Utah. The 1 to 2 m seepage face near the person is wet and covered with algae, mosses, and other phreatophytes. Efflorescences of salts occur 2 to 3 m above the seepage face. An ephemeral wash passes over the center of the canyon headwall at the upper left of the photo. Small quantities of water from the wash flow down the alcove wall, creating the dark streaks. No noticeable plunge pool occurs below the falls. The seepage supports a growth of grasses and shrubs on heavily weathered sandstone debris covering the slope below the seepage face. The alcove has developed by spalling along sheeting joints resulting from unloading stresses caused by backcutting of the seepage face.

Library of Congress Cataloging-in-Publication Data

Sapping features of the Colorado Plateau.

(NASA SP ; 491)
1. Geomorphology—Colorado Plateau. 2. Mars—Geology.
I. Howard, Alan D. II. Kochel, R. Craig. III. Holt,
Henry E. IV. Series.
GB428.C6S27 1987 551.3'55 87-15305

For sale by the Superintendent of Documents, U.S. Government Printing Office
Washington, DC 20402

Contents

Foreword

The exploration of the terrestrial planets by flyby spacecraft, orbiters, and landers has revealed landforms that astounded planetary scientists. The search for an explanation of these landforms has involved many of the most capable scientists of our generation. Many of the surface features are now understood, but others remain enigmatic or controversial in their origin, and the processes responsible for their creation remain unclear.

Mars is the most Earthlike planet with regard to surface environment and landforms. The Mariner and Viking missions revealed immense volcanoes, vast sand seas, polar caps, deep basins, strange "chaotic" terrain, frost-produced features, and numerous channels produced by flowing water. The most spectacular of these fluvial landforms are immense channels, up to hundreds of kilometers wide and thousands of kilometers long, that exhibit features indicative of tremendous floods of water and rock moving through and eroding them. Many hundreds of smaller channels and valleys on the martian surface were probably sculpted by more modest flows fed by precipitation early in martian history when the atmosphere was probably denser and the climate warmer. However, precipitation rates and amounts were considerably lower than those on present-day Earth, indicating that surface water runoff was probably a rather rare event. Many of the smaller valleys exhibit characteristic features, such as abrupt headwater terminations in theater-like box canyons, that suggest the channels were fed and eroded by groundwater emerging as springs in the valley floors.

This volume presents papers that examine the role of groundwater sapping in producing valley networks on Mars and in analogous terrestrial environments. The studies incorporate a variety of methods, including interpretation of Mars images, field investigations of terrestrial valley systems originating from groundwater sapping, experimental development of sapping valleys, and theoretical models of sapping processes. These studies of sapping processes are an excellent example of the scientific benefits resulting from our attempts to explain planetary features revealed during the past 25 years of solar system exploration. The role of groundwater in shaping terrestrial drainage basins has been appreciated and understood within the scientific community as a result of planetary geologic research.

Joseph M. Boyce
Discipline Scientist
Planetary Geosciences Program

Chapter 1

Introduction: Groundwater Sapping on Mars and Earth

Alan D. Howard

The channel and valley networks of Mars are the most exciting geomorphic features discovered by the Mariner and Viking probes (see the general reviews by Baker, 1982, and the Mars Channel Working Group [MCWG], 1983). Most attention has been accorded to the striking 1000+ km long and 20 to 200 km wide outflow channels generally thought to have been formed by single or episodic catastrophic floods or debris flows caused by any of several possible mechanisms, including interception of a large groundwater reservoir by headward-eroding small channels (Soderblom and Wenner, 1978), volcanic melting of ice producing jokulhaupts (Masursky et al., 1977), ground collapse and groundwater release (Carr, 1979), or debris flows generated by sudden liquifaction of unstable rocks with high water contents (Nummedal and Prior, 1981). Although the valley networks, which are located primarily on old cratered terrain near the Martian equator, were recognized quite early in interpretation of Mariner and Viking images (McCauley et al., 1972), they were not studied extensively until recently (the first systematic study was by Pieri, 1976). Other types of channels, such as the stubby networks dissecting the several-kilometer-high walls of some of the martian canyons, and the intermediate-scale longitudinal valley systems, such as Nirgal Vallis, were also described soon after the Mariner 9 mission but were not studied in detail until recently.

The valley networks are very ancient and are contemporaneous with the late stages of accretionary impacts (Baker and Partridge, 1986), which would place their origin during the putative warmer climate at the height of outgassing. The longitudinal valley networks and scarp-wall networks are sculpted in younger but still very ancient units. These higher-relief channels are harder to date than the shallow valley networks, because mass-wasting processes acting on the valley walls give them a deceptively young age based on crater counting techniques.

The superficial resemblance and similarity of scale of the dendritic valley networks to terrestrial stream systems created primarily by runoff erosion prompted immediate suggestions that the martian valleys were sculpted by runoff occurring early in martian history when the atmosphere was denser and temperatures moderate enough to permit liquid water and rain at the surface (Milton, 1973; Sagan et al., 1973). This comparison proved so compelling that the valley networks were initially called "gullies" (Milton, 1973), "arroyos" (Hartmann, 1974), and "runoff channels" (Sharp and Malin, 1975); only more recently have they been given the less suggestive term "valley networks" (Baker, 1982). The suggestion of a runoff origin was initially resisted by many scientists because of skepticism about the presence of a sufficient reservoir of water on Mars as well as doubts about an early temperate climate. However, support for a large supply of water on Mars has come from studies of the expected volatile content of the impact debris and its outgassing, which suggest the presence of initial water equivalent to a layer 10 m to 150 m deep if spread over the surface of Mars (Squyres, 1984). Some of this water is now present in the perennial polar caps, but, in addition, there is a rich suite of nonfluvial geomorphic features indicative of abundant water, including distinctive crater morphology, flow-like mass movements, patterned ground, chaotic and fretted terrain, possible thermokarst, water-related weathering, possible former glaciers, and volcanic-ice interactions (for a general review, see Carr, 1981; Baker, 1982; and Rossbacher, 1986). Thermal budgets also suggest that an extensive water reservoir could be present in permafrost under the present martian climate (Fanale, 1976). Many climatologists feel that enhanced CO_2/H_2O pressures early in martian history during rapid outgassing may have permitted liquid water at the surface (Pollack, 1979; Cess et al., 1980; Toon et al., 1980; Hoffert et al., 1981). However, there are conflicting models (Postawko and Kuhn, 1986), and

Brackenridge et al., (1985) caution against using the presence of valley networks as independent evidence of an early warm climate.

Despite the general acceptance of the presence of abundant water that, early in martian history, may have been stable as water and involved in precipitation events, several lines of evidence suggest an important, and possibly dominant, role of groundwater sapping processes in sculpting the valley networks, the longitudinal valleys such as Nirgal Vallis (chapter 13), and the valley-wall networks such as those dissecting the southern wall of Ius Chasma (see reviews by Pieri, 1980; Baker, 1982; Higgins, 1982; MCWG, 1983; Higgins, 1984; Kochel et al., 1985). Baker (1982; chapter 8) suggests that sapping processes have been responsible for the formation of the deep, U-shaped valleys dissecting Hawaiian volcanoes and similar features on martian volcanic edifices. Sapping processes are postulated based on two lines of reasoning and evidence. Many of the morphometric features of the valley networks, the longitudinal valleys, and the valley-wall networks are similar to those of terrestrial stream networks in which sapping processes are inferred to be dominant. Such features include (1) theater-shaped valley headwalls (particularly in the longitudinal valleys), (2) strong structural control of valley alignment and planform, (3) hanging tributary valleys, (4) long main valleys with short, stubby tributaries, (5) irregular angles of channel junction, and (6) valley widths that remain nearly constant in a downstream direction (Pieri, 1980; Baker, 1982; Laity and Malin, 1985). However, many of these features might be duplicated on young runoff networks in fractured, layered rocks and possibly in valleys eroded by valley glaciers (Lucchitta et al., 1981; Lucchitta, 1982). A low drainage density compared to terrestrial channels and the seemingly abrupt initiation of the channels have also been cited by these authors, although this argument is weakened by the limits of image resolution (and atmospheric hazes) as well as post-origin modification by impact events, mass-wasting, weathering, and eolian modification.

The second line of reasoning for a sapping origin is based on the presumed greater ease of formation of valley networks by sapping than by runoff. The valley networks are formed on heavily cratered terrains, which are likely to be very permeable due to heavy fracturing resulting from impacts and the brecciated and relatively coarse-grained nature of impact debris (little silt or clay-sized debris is formed by impact processes), as noted by Baker and Partridge (1986). Although some weathering would have occurred during early martian history, it was probably rudimentary and limited by the reducing atmosphere. Furthermore, the impact-cratered surface includes numerous craters and other enclosed depressions, encouraging infiltration. Finally, infiltration producing sapping could have occurred by gentle rains or snowfall, whereas runoff requires rains of thunderstorm intensity on relatively permeable materials.

Even though sapping processes can occur as a result of weathering and erosional processes at points of emergence of regional groundwater flow, large volumes of water are required to produce a well-developed sapping network. The most efficient process of sapping erosion occurs in unconsolidated sediments, where the limiting factor is simply the transporting capacity of the spring-fed flows. Experiments by Howard and McLane (in press) (see chapter 5) typically exhibited sediment concentrations in the outflows of about 1%, with a high of 10%. This suggests that a minimum of 10 times more water than volume of eroded sediment must be discharged in order to create a sapping valley network. Even in unconsolidated sediments, a ratio of 100- to 1000-fold is more reasonable. In consolidated rocks, valley erosion is limited by the rate of weathering of rocks at the sapping face by solution of cement (or melting, if the cement is ice), salt-fretting, freeze-thaw, or other process (Laity and Malin, 1985). These processes are generally much slower and may require water to eroded rock ratios of 10^5 or greater. The rocks of the heavily cratered terrain (probably largely impact breccias), the ridged-plains units in which many of the longitudinal valleys are formed (probably lava flows with interbedded tuffs or sediments), and the chasma walls in which the valley-wall networks are eroded (probably lava flows and sediments) are presumably moderately cohesive to well indurated. The implication of these considerations is that valley networks and other putative sapping channels are unlikely to have resulted from one-time dewatering of upland groundwater reservoirs, unless the contributing upland area was much larger than the channel network. Certain of the longitudinal valleys and chasma-wall networks may be of sufficiently small size compared to their potential groundwater source areas to have formed by a one-time dewatering, although it is difficult to envision a scenario for an initial charging of these uplands at a rate much faster than rates of regional groundwater flow unless the water was immobile (frozen). Brackenridge et al., (1985) suggest that heating of groundwater from impact melts produces hydrothermal groundwater that could produce valley networks by sapping. Although they produce estimates of possible water release rates, they do not compare total release volumes to volumes of eroded rock, so that it is difficult to assess the efficacy of the proposed hydrothermal sapping.

Experiments conducted in the University of Virginia sapping tank (see chapter 5) indicated that sapping channels do not generally form in unconsolidated homogeneous sediments with even small percentages of clay or silt. Groundwater flow rates through such sediments are so slow that very high hydraulic gra-

dients (on the order of 0.3 to 0.4) are required to initiate erosion. Under such high gradient conditions, erosion occurs not by grain-by-grain entrainment and channel development, rather by viscous mud flow. This phenonmenon was not further investigated, but it may form a partial analog to debris flows in the chaotic and fretted terrains, such as the types discussed by Squyres (1978, 1979) which have generally been interpreted as periglacial features. Consolidated fine-grained sediments generally do not exhibit such features, eroding by overland flow or by piping erosion.

The role of groundwater sapping in the development of terrestrial drainage networks was long overlooked but is now receiving greater attention. Most of the early literature on sapping processes is reviewed by Dunne (1980) and by Higgins (1982, 1984). With the exception of piping processes in badlands, most of this literature is qualitative and speculative. Piping is the hydraulic erosion of sediments and soils by throughflow along joints and dessication cracks, producing subsurface rills and gullies that in badlands and terraces commonly result in a karst-like landscape. Piping networks are generally of small size and have been qualitatively described in many papers.

Groundwater sapping, as distinct from piping, is a generic term for weathering and erosion of soils and rocks by emerging groundwater, at least partially involving intergranular flow (as opposed to the channelized throughflow involved in piping). Higgins (1984) distinguishes between concentrated erosion at springs ("spring sapping") and "seepage erosion," where groundwater discharge is laterally uniform. These are endpoints of a continuum, and it is debatable whether the distinction is useful. Further discussion of the definition of groundwater sapping is provided by Howard and Kochel (chapter 2). Higgins (1984) provides an extensive discussion of possible examples of groundwater sapping processes and landforms from the pre-1980 literature.

Dunne (1980) suggested that groundwater sapping may be an important process in the development of the headward ends of terrestrial drainage networks in certain physiographic soil settings. However, in these drainage headwaters, runoff erosion and mass-wasting of the soil are also important, so that the strongly incised, gullied, or theater-headed valleys do not occur.

Recently, Pillans (1985) has demonstrated that erosion by emergent groundwater at terrace scarps on New Zealand has created theater-headed sapping valley systems. Schumm and Phillips (1986) note that similar channels at a different location in New Zealand have formed partially by groundwater sapping and partly by runoff erosion, terming these "composite channels." They suggest that certain martian channels may likewise have a composite origin.

Karst landforms in soluble rock are clearly products of groundwater erosion, but with the exception of solutional processes in limestones with high intergranular permeability (Back et al., 1984), solution occurs primarily along joints, bedding planes, and other fractures, producing a landscape of blind valleys, enclosed depressions, subterranean channels, and resurgences that is similar to landforms produced by piping. The literature on karst is extensive; see, for example, Jennings (1985) and papers in LaFleur (1984).

Almost all the literature on landforms produced by groundwater sapping is descriptive. As a result, it has been difficult to quantitatively compare terrestrial networks of sapping origin with potential martian analogs, and comparisons to date have been primarily qualitative (e.g., Higgins, 1982; Laity and Malin, 1985; Schumm and Phillips, 1986). At the resolution of Viking images, the only method of quantitative comparison of martian and terrestrial drainage networks is by use of planimetric morphometric parameters. Pieri (1979, 1980) measured the junction angles within stream networks on Mars and on Earth as a basis for comparison. Kochel et al. (1985) and Baker and Partridge (1986) measured several traditional measures of drainage basin morphometry on martian valley systems for comparison with terrestrial valleys, but both studies had to face the difficult question of defining drainage areas where divides are not evident. It is interesting that all the morphometric comparisons were between the martian channels and typical terrestrial channel networks formed by runoff, with the result that significant differences were found that are primarily related to the distinctive morphometric features described above. To date, such comparisons have not included measurements made on terrestrial stream networks of suspected sapping or composite origin, nor have they included glaciated valley networks, thermokarst valleys, or very immature runoff networks in fractured, layered rocks. The first systematic attempt to distinguish morphometrically between runoff valleys and possible sapping valleys has been the study of Hawaiian valley morphology (Thompson, 1984; chapters 2 and 10).

The processes acting in groundwater sapping have in general not been quantified in terms of mechanisms, rates, or resulting landform morphology. The only exception is the quantitative characterization of groundwater sapping in noncohesive sediments. Howard and McLane (in press) performed experiments on sapping processes in a two-dimensional flow tank and were able to theoretically model the processes and produce a numerical simulation model for the landform evolution (see chapter 5). Experiments on channel network development in sediments in a three-dimensional chamber have been conducted, and progress has been made toward a theoretical simulation model (see chapters 5 and 6).

Because of the complexity of the weathering processes that produce sapping in consolidated rocks (including cement solution, interstitial deposition of minerals, and frost wedging), modeling of these processes can probably only be done in a general way. For example, a reasonable process assumption might be that sapping rates are proportional to a power of seepage rates, with, perhaps, a critical, threshold seepage rate below which no sapping occurs.

Studies of canyon development in the Navajo Sandstone on the Colorado Plateau have provided the strongest documentation for an important role of groundwater sapping processes in a large terrestrial valley system (Laity and Malin, 1985). This book addresses the role of groundwater sapping in forming landforms on the Colorado Plateau. The impressive evidence as well as unresolved questions are summarized in chapters 2-4.

REFERENCES

Back, W., Hanshaw, B.B., and Van Driel, J.N. (1984) Role of groundwater in shaping the eastern coastline of the Yucatan Peninsula, Mexico. In *Groundwater as a Geomorphic Agent*, R. G. Lafleur, ed. Boston, Allen, & Unwin, p. 281-293.

Baker, V.R. (1982) *The Channels of Mars*. Austin, University of Texas Press.

Baker, V.R., and Partridge, J.B. (1986) Small martian valleys: pristine and degraded morphology. *J. Geophys. Res.* **91:** 3561-3572.

Brackenridge, G.R., Newsom, H.E., and Baker, V.R. (1985) Ancient hot springs on Mars: origins and paleoenvironmental significance of small martian valleys. *Geology* **13:** 859-862.

Carr, M.H. (1979) Formation of martian flood features by release of water from confined aquifers. *J. Geophys. Res.* **84:** 2995-3007.

Carr, M.H. (1981) *The Surface of Mars*. New Haven, Yale University Press.

Cess, R.D., Ramanthan, V., and Owen, T. (1980) The martian paleoclimate and enhanced atmospheric carbon dioxide. *Icarus* **41:** 159-165.

Dunne, T. (1980) Formation and controls of channel networks. *Prog. Phys. Geogr.* **4:** 211-259.

Fanale, F.P. (1976) Martian volatiles: their degassing history and geochemical fate. *Icarus* **28:** 179-202.

Jennings, J. (1985) *Karst Geomorphology*. Oxford, Basil Blackwell.

Hartmann, W.K. (1974) Geological observations of martian arroyos. *J. Geophys. Res.* **79:** 3951-3957.

Higgins, C.G. (1982) Drainage networks developed by sapping on Earth and Mars. *Geology* **10:** 147-152.

Higgins, C.G. (1984) Piping and sapping: development of landforms by groundwater outflow. In *Groundwater as a Geomorphic Agent*, R.G. LaFleur, ed. Boston, Allen, & Unwin, p. 18-58.

Hoffert, M.I., Calegari, A.J., Hseih, C.T., and Ziegler, W. (1981) Liquid water on Mars: an energy balance climate model for CO_2/H_2O atmospheres. *Icarus* **47:** 112-129.

Howard, A.D., and McLane, C.F. (in press) Erosion of cohesionless sediment by groundwater sapping. *Water Res. Res.*

Kochel, R.C., Howard, A.D., and McLane, D.F. (1985) Channel networks developed by groundwater sapping in fine-grained sediments: analogs to some martian valleys. In *Models in Geomorphology* , M.J. Woldenberg, ed. Boston, Allen, & Unwin, p. 313-341.

LaFleur, R.G., ed. (1984) *Groundwater as a Geomorphic Agent*. Boston, Allen, & Unwin.

Laity, J.E., and Malin, M.C. (1985) Sapping processes and the development of theater-headed valley networks in the Colorado Plateau. *Geol. Soc. Am. Bull.* **96:** 203-217.

Lucchitta, B.K., Anderson, D.M., and Shoji, H. (1981) Did ice streams carve martian outflow channels? *Nature* **290:** 759-763.

Lucchitta, B.K. (1982) Ice sculpture in the martian outflow channels. *J. Geophys. Res.* **87:** 9951-9973.

Masursky, H., Boyce, J.M., Dial, A.L., Schaber, G.G., and Strobell, M.E. (1977) Classification and time of formation of martian channels based on Viking data. *J. Geophys. Res.* **82:** 4016-4038.

McCauley, J.F., Carr, M.H., Cutts, J.A., Hartmann, W.K., Masursky, H., Milton, D.J., Sharp, R.P., and Wilhelms, D.E. (1972) Preliminary Mariner 9 report on the geology of Mars. *Icarus* **17:** 289-327.

Mars Channel Working Group (1983) Channels and valleys on Mars. *Geol. Soc. Am. Bull.* **94:** 1035-1054.

Milton, D.J. (1973) Water and processes of degradation in the martian landscape. *J. Geophys. Res.* **78:** 4037-4047.

Nummedal, D., and Prior, D.B. (1981) Generation of martian chaos by debris flows. *Icarus* **45:** 77-86.

Pieri, D.C. (1976) Martian channels: distribution of small channels in the martian surface. *Icarus* **27:** 25-50.

Pieri, D.C. (1979) Geomorphology of martian valleys. Ph. D. thesis, Cornell University, Ithaca, N.Y.

Pieri, D.C. (1980) Martian valleys: morphology, distribution, age and origin. *Science* **210:** 895-897.

Pillans, B. (1985) Drainage initiation by subsurface flow in South Taranaki, New Zealand. *Geology* **13:** 262-265.

Pollack, J.B. (1979) Climatic change on the terrestrial planets. *Icarus* **37:** 479-553.

Postawko, S.E., and Kuhn, W.R. (1986) Effect of the greenhouse gasses (CO_2, H_2O, SO_2) on martian paleoclimate. *J. Geophys. Res.* **91:** D431-D438.

Rossbacher, L.A. (1986) Martian geomorphology and its relation to subsurface volatiles: a critical summary. *MECA Newsletter,* no. 7. Houston, Lunar and Planetary Institute.

Sagan, C., Toon, O.B., and Gierasch, P.J. (1973) Climatic change on Mars. *Science,* **181:** 1045-1049.

Schumm, S.A., and Phillips, L. (1986) Composite channels on the Canturbury Plain, New Zealand: a martian analog? *Geology* **14:** 326-329.

Sharp, R.P., and Malin, M.C. (1975) Channels on Mars. *Geol. Soc. Am. Bull.* **86:** 593-609.

Soderblom, L.A., and Wenner, D.B. (1978) Possible fossil H_2O liquid-ice interfaces in the martian crust. *Icarus* **34:** 622-637.

Squyres, S.W. (1978) Martian fretted terrain: flow of erosional debris. *Icarus* **34:** 600-613.

Squyres, S. W. (1979) The distribution of lobate debris aprons and similar flows on Mars: *J. Geophys. Res.* **84:** 8087-8096.

Squyres. S.W. (1984) The history of water on Mars: *Ann. Rev. Earth Planet. Sci.* **12:** 83-106.

Thompson, J.S. (1984) Implications of basin morphometry along the Kohala Mountain in Hawaii. Unpublished paper, University of Virginia.

Toon, O.B., Pollack, J.B., Ward, W., Burns, J.A., and Bilski, K. (1980) The astronomical theory of climate change on Mars. *Icarus,* **44:** 552-607.

Chapter 2

Introduction to Cuesta Landforms and Sapping Processes on the Colorado Plateau

Alan D. Howard and R. C. Kochel

INTRODUCTION

Terrestrial channels are commonly composite channels, formed jointly by runoff and groundwater sapping processes. Schumm and Phillips (1986) describe similarities between composite channels along the New Zealand coast and valley networks on Mars. The objective of this book and much of the recent research related to groundwater sapping processes is to determine what geomorphic criteria can be used to distinguish between channels formed *dominantly* by runoff and those which are sapping dominated. Kochel and Piper (1986) showed, for example, that morphometric parameters describing Hawaiian valleys could distinguish between these two channel types. These remote observations have been supported by field observations in Hawaii by Howard and Kochel in 1985.

The landscape, lithology, and structure of the Colorado Plateau have similarities to areas of Mars, leading geomorphologists to examine the region for possible analogs to such features as volcanoes, wind-deposited and eroded landscapes, and fluvial landforms. In particular, Laity and Malin (1985) have suggested that groundwater sapping processes have been instrumental in sculpting certain valley networks in sandstone. Features of these valleys, such as theater heads, nearly constant valley width downstream, short, stubby tributaries, steep valley headwalls, and strong control of size and orientation by rock structure, are consistent with the observation of seepage-related erosion localized at headwalls. The valleys bear a morphological similarity to some martian valley networks, leading to the suggestion that similar processes led to their development. The Laity-Malin study provided the focal point and null hypothesis model for the field conference described here, which addressed several themes related to the role of groundwater in creating the landscape of the Colorado Plateau:

1. The major conference theme was an evaluation of the relative roles of groundwater sapping and runoff processes in erosion of layered rocks in the Colorado Plateau, and the effects of sapping on valley morphology.

2. Almost all weathering and mass-wasting processes occurring on the Colorado Plateau involve some penetration of water into exposed rocks to produce the physical and chemical changes leading to rock breakup and transport. Thus confusion and semantic controversy can occur until a consensual definition of sapping and seepage erosion emerges.

3. During the field excursion, a wide range of weathering and erosional features were visited that may be martian analogs. Therefore, the field guide discusses the major processes and landforms occurring on the layered rocks of the Colorado Plateau, excluding volcanic, alpine, glacial, eolian, and large-scale structural features. The morphology of sandstone escarpments is emphasized.

4. Interpretation of landforms is complicated to the degree that present features have resulted from processes different from those presently acting. Several authors have suggested that certain landscape elements may be relict from Pleistocene pluvial climates. In a similar vein, we discuss the variation of scarp morphology with areal variations in the present climate.

5. We hope that the discussions held during the field trip and the present document will suggest field or experimental research that can answer questions regarding sapping processes and landforms.

STRATIGRAPHY AND STRUCTURE

The Colorado Plateau is underlaid by layer-cake sequences of Paleozoic and Mesozoic sediments, primarily shales and sandstones, with some formations or interbeds of limestone, gypsum, or more soluble evaporites. The beds are generally nearly flatlying, but are locally faulted or warped into monoclines, domes, and basins. Locally the sediments are intruded by Tertiary laccoliths, plugs, sills, and dikes or capped by lava flows and volcanic cones. Near Moab, large-scale faulted anticlines have been created by flow and intrusion of evaporites and their solution at depth (Doelling, 1985). General geologic references for the area include Rigby (1976, 1977), Hintze (undated), Chronic (1983), and Baars (1983). Geologic maps at a scale of 1:250,000 have been published by the U.S. Geological Survey as follows: Moab Quadrangle, Misc. Invest. Ser., I-360; Grand Junction, I-736; Cortez, I-629; Shiprock, I-345; Gallup, I-981; Salina, I-591; Escalante, I-744; Marble Canyon, I-1003.

Sandstones

The rock types of primary interest during the field conference were sandstones and interbedded shales, particularly the massive sandstones of the Navajo Formation and the Slick Rock member of the Entrada Sandstone. The sandstones generally contain more than 80% by weight of quartz sand, with variable percentages of orthoclase or clay, and generally weak cementation by hematite, calcite, or, less commonly, silica. Even the massive sandstones contain occasional thin beds or partings of shale, chert, and limestone. For more detail on the sedimentology of these units and relationships to groundwater flow, see chapters 3 and 4. Similarly, some layers have considerably greater or much less than average amounts of cementing hematite or calcite. Schumm and Chorley (1966) give unconfined compressive strengths in the range of 2500 to 7200 psi, which are in the low range for sandstones, but strong enough to permit massive vertical cliffs. Porosity commonly ranges from 20 to 35%, and permeability ranges from about 2×10^{-2} to 1 darcy, with the Entrada near the lower end and the Navajo near the upper end of this range (Jobin, 1962; Cooley et al., 1969). Such permeability is at the high end of the range cited by Freeze and Cherry (1979, p. 20) for sandstones and is equivalent to that of unconsolidated silty sand. Curiously, Schumm and Chorley (1966, p. 15) considered the sandstones to be of low permeability while at the same time conducting experiments that demonstrated the ability of water to penetrate 1/2 to 3 inches into Colorado Plateau sandstones within 20 minutes after the beginning of surface wetting (p. 24). Due to high porosity, permeability, and weak cementation, the sandstones weather easily by several mechanisms, including grain-by-grain surface removal, separation along bedding planes, and crumbling. Schumm and Chorley (1966) subjected samples of representative sandstones to two winters and one summer of precipitation and freeze thaw. The samples typically lost 1 to 3% of their initial volume in this exposure, with a high of 23% for Entrada Sandstone samples. This indicates a potential for rapid surficial weathering and erosion under present climates. Schumm and Chorley also note the presence of loosened weathered sediment on bare rock slopes following snow melt and freeze-thaw, with slopes on Entrada Sandstone becoming slippery. Wind and rain rapidly remove such accumulations. Variable amounts of weathering have occurred en mass within the sandstones following lithification and prior to their exposure, both by deeply circulating groundwater and by circulation related to present-day topography (Cooley et al., 1969; Hamilton, 1984). Cooley et al., (1969) suggest that permeability (and, by implication, weatherability) of sandstones increases with the length of time the rocks are exposed near the surface (that is, beneath older erosional surfaces).

Shales

Shales of the Colorado Plateau range from massive marine shales, such as the Mancos Shale, of dominantly silt and illitic clay composition, to sandy lacustrine shale with montmorillonitic clays, such as shales in the Morrison Formation. All of these shales weather readily upon surface exposure, with rock breakup aided by shrink-swell due to changes of moisture content. The montmorillonitic shales break down rapidly as a result of simple wetting, with remarkable volume increases. The illitic shales weather more slowly, yielding yellowish liquors of released salts that must be carried away in solution to continue the weathering process. Despite its weatherability, solid shale is generally encountered within a few inches of the surface on badlands slopes due to the impermeability and self-sealing characteristics of the weathered shale and the restricted supply of precipitation.

MORPHOLOGY AND EROSIONAL PROCESSES ON SANDSTONE CUESTAS

Sandstone units on the Colorado Plateau are generally exposed as bare rock slopes except where mantled with eolian sands or alluvium. However, areas of very low relief, such as the tops, or backslopes, of gently dipping cuestas of sandstones where overlying shales have been stripped away, may be mantled with sandy, cobbly, poorly horizonated soils and scrubby vegetation. Two morphological end members characterize the sandstone exposures; low to moderate relief "slickrock" slopes and cliff or scarp

slopes develop where the sandstones are being undermined. Figure 1 shows terminology used here for the form elements of an escarpment. These two slope types differ significantly in morphology as well as types of weathering and erosional processes and are discussed separately. An intermediate landform type, termed "segmented cliffs" by Oberlander (1977), is also discussed.

Slickrock Slopes

The most striking and unusual landform type occurring on desert sandstone exposures is low, generally rolling relief on bare rock slopes (figs. 2 and 3). Hill forms are generally convex to convexo-concave and rather irregular due to the prevalence of small-scale structural and lithologic controls exerted by the exposed rock on weathering and erosional processes. Slickrock slopes occur most commonly on the tops and crests of sandstone cuestas, being exposed by erosion of weak overlying shales. Erosion rates on these cuesta backslopes are relatively small compared to the rate of sandstone erosion on the scarp faces (Howard, 1970), with correspondingly low relief. However, slickrock topography of moderate and locally high relief occurs on thick sandstone units where long exposure and less effective scarp backwasting contribute to the development of steeper relief. The thick Navajo Sandstone best exhibits this higher relief form of slickrock slopes, such as at Zion National Park (fig. 4). Other descriptive terms applied to such topography include "beehives," "haystacks," "whalebacks," "domes and hollows," "buttresses," and "onionlike" (emphasizing bedding exposure and sheeting fractures).

Where strong structural control by jointing or faulting occur, the fractures tend to be eroded into furrows or valleys, and the sandstone landscape takes on a reticulated or "maze"-like appearance (fig. 3). Doelling (1985) notes that sandy colluvium collecting along depressions developed on joints accelerates weathering of the sandstone by providing a moist environment; thus the influence of fractures on the topography is enhanced by positive feedback on weathering rates. Small-scale horst-and-graben development associated with extensional movement has created the "needles" section of Canyonlands National Park (McGill and Stromquist, 1975).

Slickrock slopes are "weathering-limited" (Carson and Kirkby, 1972, p. 104-106) in that transport processes are potentially more rapid than weathering processes. That is, loose debris is removed from the slopes as fast as it is produced by weathering so that little or no loose residuum covers the bedrock. This contrasts with "transport-limited" slopes with a residual soil in which the rate of erosion is limited by the rate at which slope wash or mass movement can move the soil. Many badland slopes on shales are transport-limited despite their very thin residuum.

On slickrock slopes the bedding is emphasized by the grain-by-grain loosening or disintegration of thin surface crusts or whole layers of the sandstone exposed on these weathering-limited slopes (figs. 5 and 6), particularly on exposures of the massively cross-bedded Navajo Sandstone (fig. 7). Coarser sand layers with fewer grain-to-grain contacts weather and loosen most readily, aiding differential surface expression of minor lithologic variations (Hamilton, 1984). Despite these microscale lithologic controls, the slickrock slopes generally show only minor form control by

Figure 1. The parts of an escarpment. The face is the vertical to near-vertical cliff developed at the top of the escarpment, mostly in the caprock but occasionally extending into the nonresistant layer beneath. The rampart is a slope of lesser inclination extending from the bottom of the face to the base of the escarpment, which is commonly partly mantled with debris from backwasting of the face (from Howard, 1970).

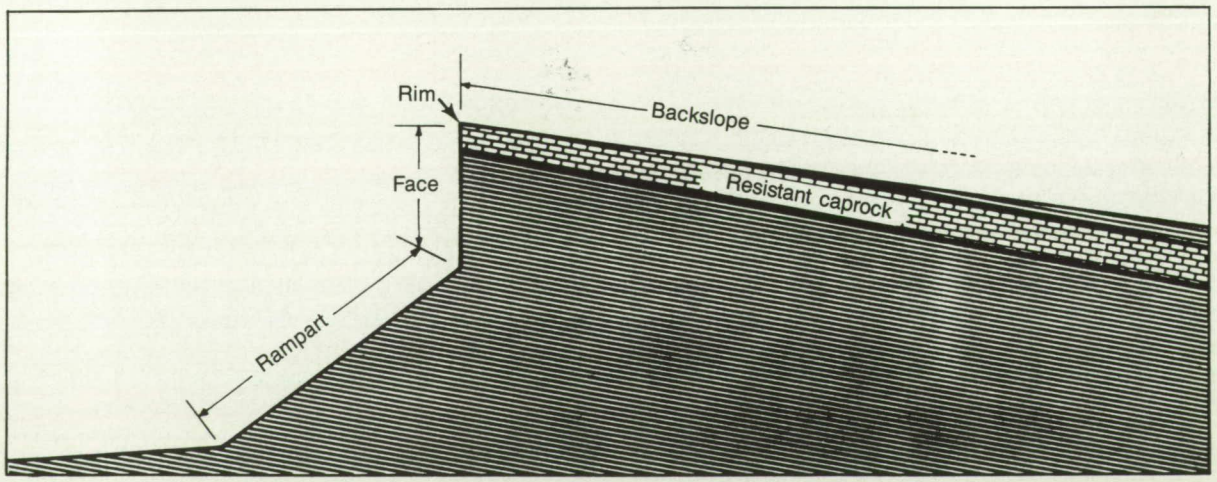

Figure 2. Slickrock slopes in Navajo Sandstone along Utah Highway 12 west of Boulder, Utah.

Figure 3. Slickrock slopes in Cedar Mesa Sandstone in Canyonlands National Park, Utah. Note the strong control by jointing and fractures.

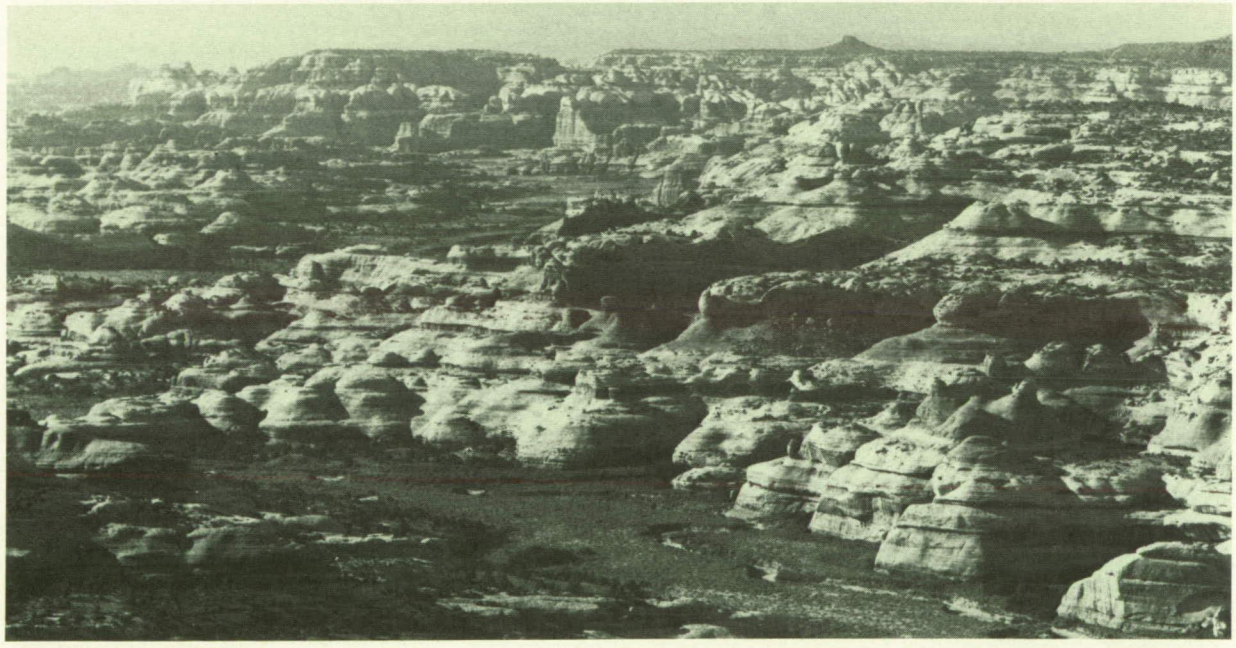

bedding, and the fairly planar to rounded slopes cut across bedding planes (figs. 8 and 9). This propensity for smooth, rounded slopes on a weathering-limited landform is noteworthy and in need of explanation (by contrast, the lateral and downslope grading of transport-limited slopes is well known and readily explained as a result of a direct relationship between slope gradient and the rate of downslope mass movement).

One reason for the development of smooth, generally convex slopes is the development of exfoliation or sheeting fractures (figs. 10 and 11) in massive,

Figure 4. Steep slickrock slopes in Navajo Sandstone along Utah Highway 9 in Zion National Park, Utah.

Figure 5. Slickrock surface in Navajo Sandstone along Utah Highway 12 west of Boulder, Utah. Black iron-rich rock fragments are 5 to 10 cm in length. Note the scaly flaking of the surface. The circular markings suggest the former presence of lichens on the flaky surface.

Figure 6. Disintegration of surface layers of Navajo Sandstone on slickrock surface near Utah Highway 12 west of Boulder, Utah. The large disintegrating rocks are about 50 cm in size.

Figure 7. Expression of bedding in slickrock slopes in Navajo Sandstone near Utah Highway 12 west of Boulder, Utah.

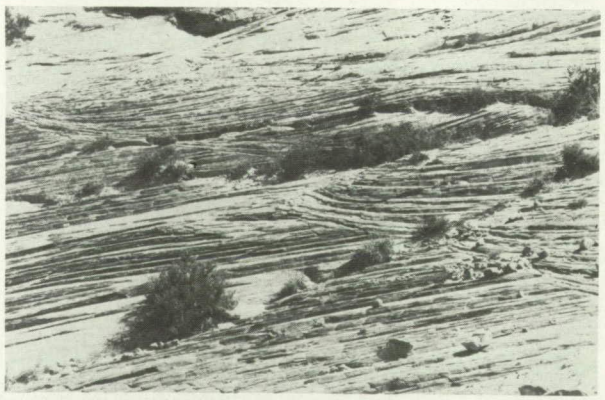

Figure 8. Slickrock slopes in Navajo Sandstone in Zion National Park, Utah, showing smooth grading of slopes crossing bedding.

Figure 9. Slickrock slopes cutting across bedding in Navajo Sandstone near Stop I at the Inscription House Area (Figs. 65 and 66). Some control of slope morphology by sheeting fractures is illustrated by the rounded remnants projecting above the smooth surface at the left and in the middle distance on the right.

Figure 10. Steep canyon slope in Navajo Sandstone near Betakin Ruin, Arizona, showing sheeting along exfoliation fractures.

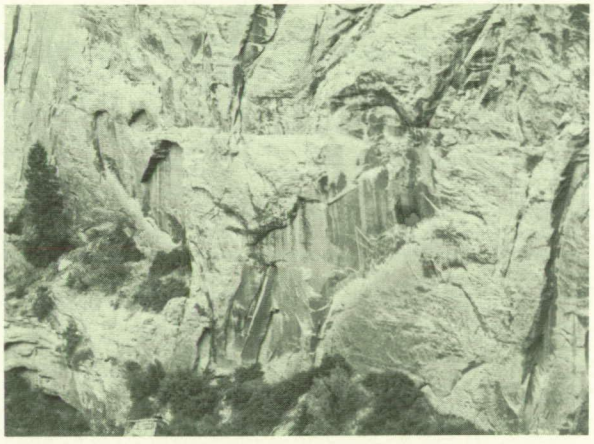

Figure 11. Slickrock slope in Navajo Sandstone near Betakin Ruin, Arizona. Active sheeting failure is apparent on the right near scrubby pinyon-juniper. The remaining slopes with no active sheeting weather primarily by surface attack, with strong expression of lithologic variations.

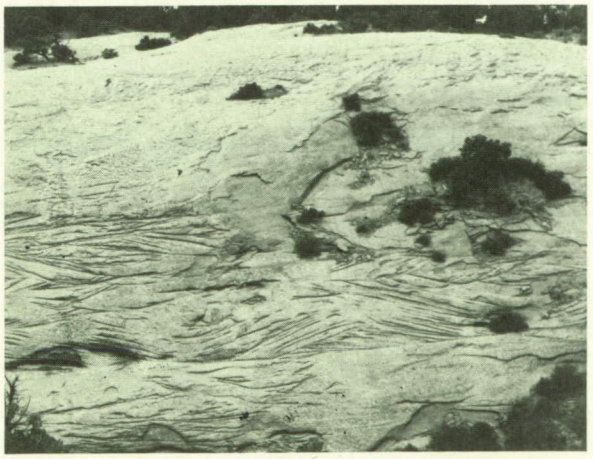

poorly jointed (referring here to preexisting regional or systematic jointing) sandstones such as the Navajo Sandstone (Bradley, 1963). The exfoliation is primarily due to stress-relief fracturing (Bradley, 1963) which produces lenticular sheets of thicknesses ranging from an inch to a few feet, with more widely spaced fractures below these, fading out within 10 to 20 m from the surface. Thus the exfoliation joints form "a crude, somewhat subdued replica of the surface form" (Bradley, 1963, p. 521). The tendency of exfoliation jointing to encourage development of a broadly rounded, domal topography is well known, particularly in granites (fig. 12). However, unlike many of the granitic domes, obvious peeling of exfoliation layers (figs. 13 and 14) is the exception rather than the rule on slickrock topography, where grain-by-grain weathering or peeling of thin (<1 cm) weathered rinds seems to be dominant. Thus, although exfoliation joints are common, their control of surface erosion at present seems generally slight; however, they may exert subtle, long-term effects on weathering rates. Control by exfoliation joints may have been more pervasive during pluvial episodes, when deep freeze-thaw cycling may have caused separation and breakup of sheeting layers. If this is true, the dome-like large-scale hill forms may be inherited from the Pleistocene.

Locally, planar slopes on sandstone may have resulted from exposure of sandstone formerly mantled by talus from overlying cliffs, as discussed below. However, most slickrock slopes lack the association with overlying cliffs and are either too gentle or too steep to have been talus slopes.

Other weathering and erosional processes may aid the development of planar slopes. Strictly surface erosional attack generally does not produce planar surfaces. For example, surface solution of limestones results in irregular surfaces with a tendency toward pointed projections and concave depressions (such surface solution has been termed "uniform decrescence" by Lange, 1959) as well as an intricate expression of bedrock solubility differences (fig. 15 shows uniform decrescence applied to retreat of scarp planforms, showing pointed outliers and smooth, concave

Figure 12. Diagrammatic sketch of exfoliation joints in massive Colorado Plateau sandstones. Arrows show inferred directions of expansion. (A) An exfoliation dome. (B) An exfoliation cave. (C) An overhanging exfoliation plate in a meander scar. (Figure and caption from Bradley, 1963.)

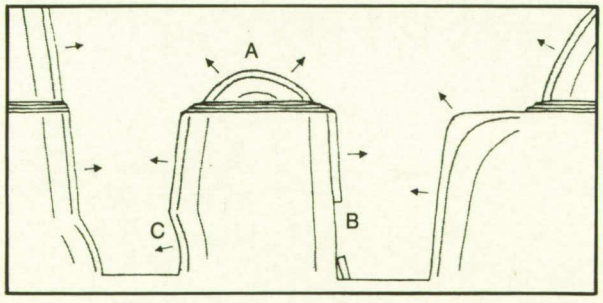

Figure 13. Slickrock slopes near Stop I at the Inscription House Area (figs. 65 and 66) showing control of weathering and erosion by sheeting fractures. The rounded exposures of Navajo Sandstone with strongly dipping bedding planes are sharply cut at their base by a gently dipping sheeting fracture. The beds below the sheeting fracture (where figures are walking) evidently are less subject to weathering than the overlying rock, perhaps due to less influx of water along fractures.

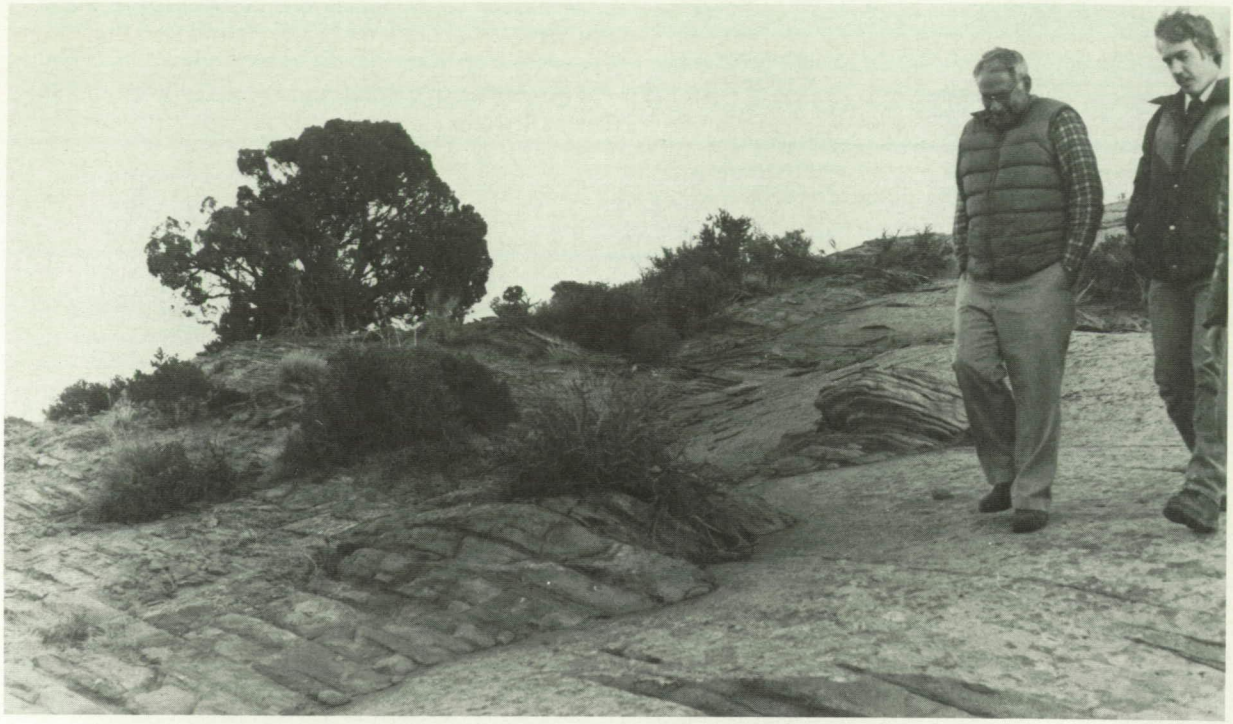

Figure 14. Slickrock slopes near Stop I at the Inscription House Area (figs. 65 and 66) showing control of weathering and erosion by sheeting fractures that cut across the bedding planes (see fig. 13 for further explanation).

Figure 15. Process of uniform erosional attack illustrated on the Redwall, Coconino, and Kaibab escarpments within the Grand Canyon. The rim outline of both the Coconino and Kaibab escarpments (dotted lines) may be approximately duplicated by uniform erosional attack of the Redwall escarpment rim (dashed lines). In a few cases the hollows, or reentrants, are deeper than would be produced by uniform backwasting of the next lower escarpment; sapping backwasting may be involved. (Illustration from Lange, 1959, figure 17.)

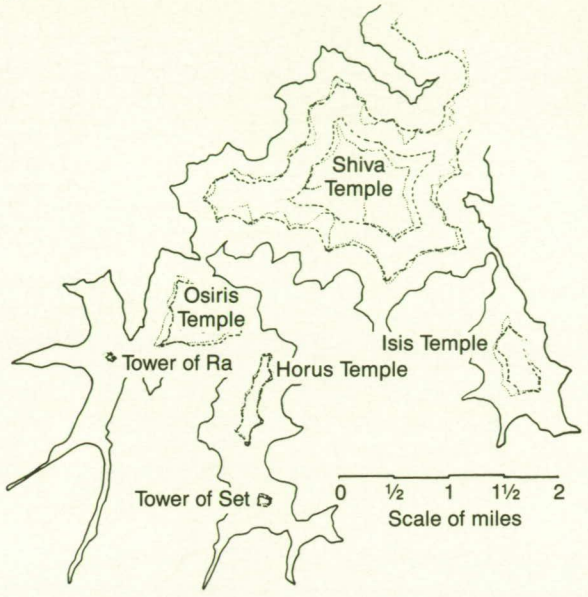

reentrants). However, any weathering process that acts through some depth from the surface will tend to erode away projecting masses due to the greater surface area relative to volume. Such processes may include solution of cement, weathering of feldspars and clays, and disruption of the rock along microfractures and between grains due to differential volume changes produced by temperature changes, freeze-thaw, or shrink-swell of clays.

Since such weathering is necessary before surface grain-by-grain removal can occur, a "grading" of surface slopes should result, with a characteristic scale of action of the same order of magnitude as the depth of weathering (presumably a few centimeters to a few meters). The occurrence of such weathering processes is evidenced by the development of shallow fracture networks on many sandstone exposures. In massive sandstones these surface cracks create a network pattern with a scale of 1 to 5 m that clearly wraps around existing topography (fig. 16), creating an "elephant hide" pattern. Where strong layering is exposed in cross-section, the cracks follow bedding planes and also create fractures cutting across the bedding, forming a "checkerboard" or "waffle" pattern (fig. 17). The effective depth of these fractures is probably about 1/5 to 1/2 of their lateral spacing. Hamilton (1984, p. 32-34) suggests the fractures result from cyclic near-surface volume changes resulting from thermal cycling, wetting and drying, or freeze-thaw.

Figure 16. Polygonal superficial fracturing of Navajo Sandstone along Utah Highway 12 west of Boulder, Utah. Individual "elephant-hide" polygons are about 1 to 2 m in size.

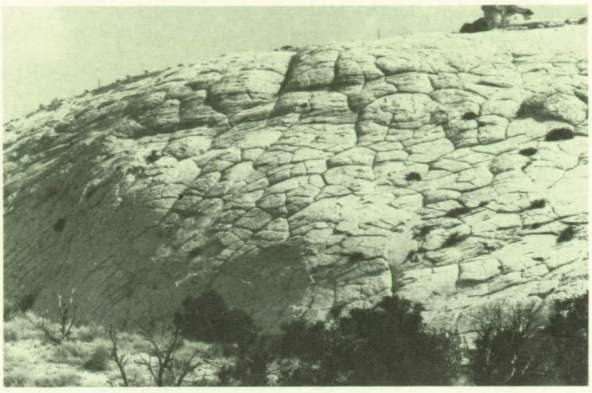

Figure 17. "Checkerboard" superficial fracturing of Navajo Sandstone on Checkerboard Mesa, along Utah Highway 9 at Zion National Park, Utah.

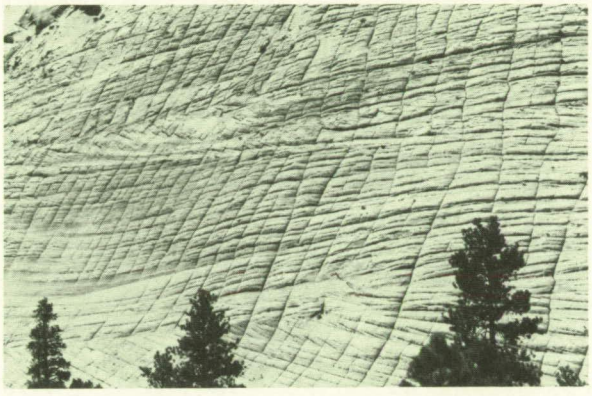

Weather Pits

Solutional removal of calcite cement has locally created karstic landforms on slickrock slopes. The most striking features are enclosed depressions ranging from a few tens of centimeters to tens of meters in diameter and a few centimeters to over 3 m in depth (fig. 18). These "pits," "hollows," "pans," "potholes," "waterpockets," "tanks," or "weather pits" differ from typical karst sinkholes in that most do not drain into obvious solutionally enlarged joints (although some do, as in fig. 19) and are developed on bare rock rather than in surface soil or alluvium. Weather pits also occur on exposed basalt and granite. Solution pits are a similar feature developed on limestones.

Weather pits occur primarily on divides but may occur locally on slopes of 10 to 20 degrees, as discussed below. Sometimes they cause inversion of relief on divides (fig. 20). The important mechanism leading to weather pit development on sandstones is the moderate rate of solution of calcite cement, which

Figure 18. Weather pits on Cedar Mesa Sandstone at Muley Point, Utah (off Utah 261), with goosenecks of the San Juan River in the background and Monument Valley on the horizon.

Figure 19. Weather pits developed along a joint in Cedar Mesa Sandstone at Muley Point.

Figure 20. Weather pits on broad divides in Cedar Mesa Sandstone at Muley Point. Note that the weather pits create a locally inverted relief.

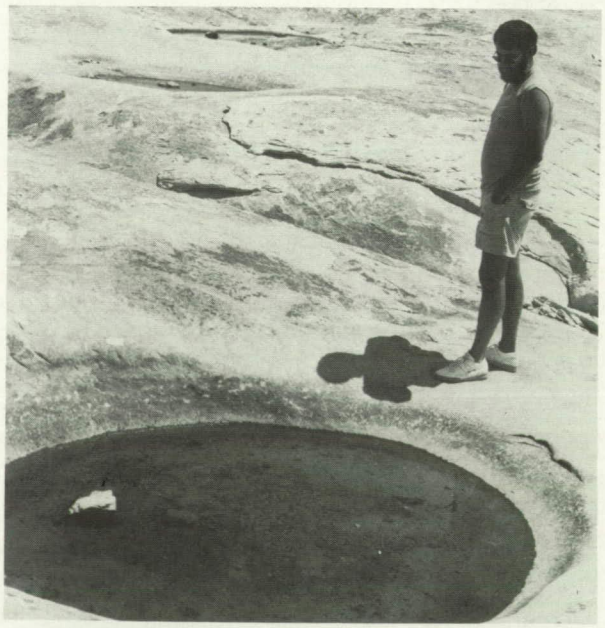

means that standing water has a greater ability to dissolve the calcite than rainfall and runoff over a sloping surface, where the runoff never approaches saturation with calcite. This leads to a positive feedback which tends to deepen and enlarge chance surface depressions. Twidale (1976) attributes the development of weather pits on granite to enhanced weathering by standing water. Many of the depressions act as traps for eolian sand and silt, or for sand transported by runoff. The weather pits generally retain water for hours to weeks after rainstorms. The water may be lost by evaporation, by flow into fractures, or by in-

tergranular percolation into the sandstone. The relative roles of evaporation and downward seepage are uncertain and probably locally variable. The morphological and process similarity to weather pits on granites suggest that infiltration is not a prerequisite to their development on sandstones. A visit to an area of weather pits 2 to 3 days after appreciable rains revealed that some of similar size and surface catchment area were dry, whereas others contained appreciable amounts of water. This suggests that at least some of the weather pits serve as recharge points to the shallow groundwater circulation systems in sandstones that may reemerge as seepage or sapping springs along cuesta scarps. Calcite dissolved from the sandstone may be carried with the percolating water or evaporated on the surface between rains, and removed by the wind, along with the loosened clastic grains. Locally shallow checkerboard or reticulate fractures develop along the edges of the weather pits, presumably due to enhanced weathering from the prolonged presence of water.

George Billingsly (personal communication, 1985) has suggested that the contraction of water frozen in weather pits may pull rock flakes from the walls of the weather pits and help to enlarge and deepen them.

Ephemeral channels draining the sandstone are commonly interrupted by similar weather pits, often resulting in a "beaded" drainage pattern (fig. 21). Even washes draining more than one to tens of square kilometers develop pits (figs. 22 and 23), which, because of their location along channels, are generally called potholes. The beaded pattern is generally limited to slopes less than about 10 to 20 degrees and is replaced by narrow furrows or "gutters" on steeper slopes (figs. 24 and 25). Conventional wisdom ascribes the potholes to corrasional erosion in plunge pools, and this mechanism may be important along some of the larger washes. However, the potholes grade imperceptibly into weather pits near divides, so that solution by standing water between runoff events may also be important along the larger channels. The enhancement of solution rates by fixed turbulent eddies during runoff may also be as or more important than direct abrasion in potholes on calcite-cemented sandstones.

Not all slickrock surfaces exhibit prominent solutional features. The reasons for their variable importance presumably involve differences in climate, lithology (particularly in the amount of calcite cement and rock permeability), slope steepness, ability of wind or running water to remove loosened sand, and degree of mantling of the surface by windblown deposits.

On a larger scale than the solutional features discussed above, Young (1986) draws an analogy between haystack-shaped slickrock slopes in Australia and tropical tower karst, emphasizing the role of solution of the silica cement in these sandstones in producing the rounded slope forms. He also feels that case hardening of rock surfaces plays a role in slope evolution. Young apparently discounts a dominant role for exfoliation fracturing in these sandstones. Also important locally has been the hardening of sandstones adjacent to joints by silica deposition, which results in these hardened zones forming reticulate hillcrests, just the opposite of the typical haystacks of the Colorado Plateau (such as fig. 3), where joints are zones of weakness.

Figure 21. Beaded drainage on rills on Navajo Sandstone north of US 160 west of Kayenta, Utah. The slope gradient is about 15 to 25 degrees.

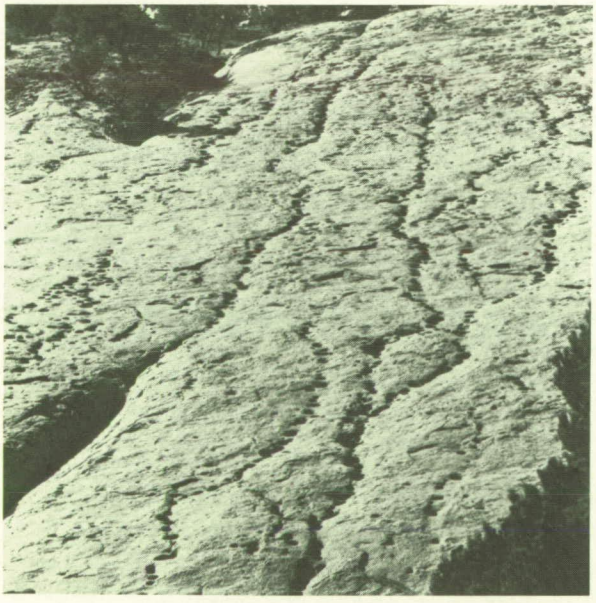

Figure 22. Potholes along a channel in Navajo Sandstone near Newspaper Rock off US 163 and 191 north of Monticello, Utah.

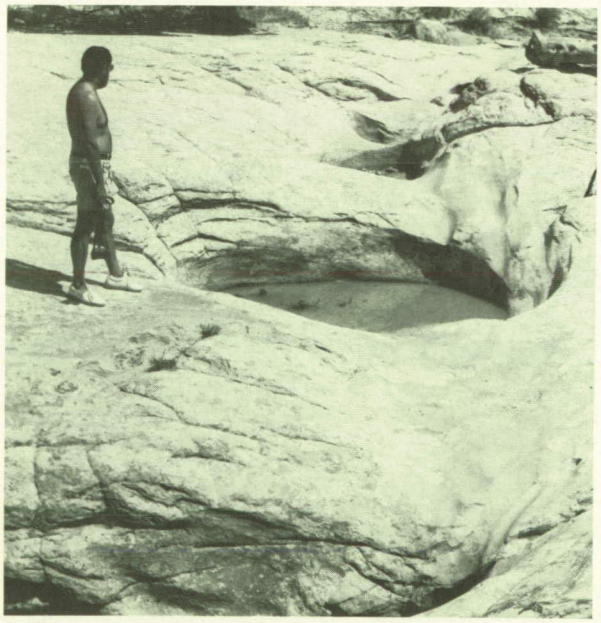

Figure 23. Potholes along wash in Navajo Sandstone along Utah Highway 12 west of Boulder, Utah.

Figure 24. Solutionally deepened superficial joint on Navajo Sandstone near Betakin Ruin, Arizona.

Figure 25. Solutionally deepened rills on Navajo Sandstone north of US 160 west of Kayenta, Arizona.

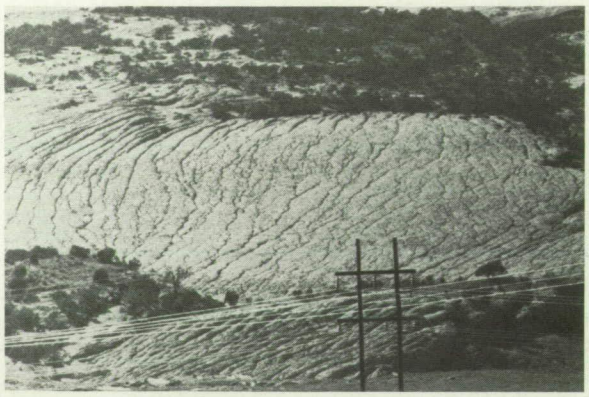

Cuesta Scarps

The exposure of weaker strata (generally shales or highly fractured sandstones) beneath massive sandstones causes undermining of the sandstone, leading to cliff development and rapid scarp backwasting. A far greater volume of rock is initially broken up by scarp retreat than by erosion on slickrock slopes when considering average rates over large areas. Because of the rapid retreat of scarp slopes, the cliffs generally eat back into preexisting slickrock slopes. Figure 26 shows a situation in which updip exposure of shale near the stream level (right side of figure) has caused the development of cliffs and their backwasting into slickrock slopes; such undermining was discussed by Ahnert (1960) and Oberlander (1977).

The relative rates of erosion on different parts of cuestas can be illustrated by considering, as a first approximation, that the form elements maintain a constant gradient and a constant position relative to the stratigraphic layers through time. These assumptions require a constancy of both stream erosion and slope processes through time which probably approximates the long-term average behavior of scarp erosion but not the short-term changes due to climatic fluctuations. The assumption of a constant position of slope elements relative to the stratigraphy (fig. 27B) is clearly a closer approximation to scarp evolution than the assumption that slope elements retain a constant position through time [i.e., a constant rate of vertical erosion on all elements of the scarp (fig. 27A)].

In horizontal stratified rock these assumptions predict a rate of vertical erosion proportional to the slope tangent, whereas the horizontal rate of erosion (lateral backwasting) is identical on all slope elements (fig. 27B). This implies an infinite rate of downwasting for a vertical cliff, which is an artifact of considering cliff retreat as continuous erosion rather than as discrete events such as rockfalls. Therefore, as mentioned above, on a typical escarpment the downwasting of the slickrock slope on top of the caprock is very slow compared to both cliff retreat and to vertical erosion below the rim (fig. 28).

The relative rates of erosion on various slope elements are also affected by the structural dip. If all form elements erode at an equal rate parallel to the structure (that is, in a downdip direction) with constant gradient, then the instantaneous rate of vertical downwasting, V_t, is given by the structural dip, d, the slope angle, s, and the rate of downdip backwasting of the escarpment, D_t. Where the slope is inclined with the dip (fig. 29A).

$V_t = D_t (\sin d - \cos d \tan s)$ for $90° > d > s > 0°$

and (fig. 29B)

$V_t = D_t (\tan s \cos d - \sin d)$ for $90° > s > d > 0°$

Where the slope opposes the structural dip (fig. 29A)

$V_t = D_t (\sin d + \cos d \tan s)$ for $90° > s > 0°$

During continued downcutting by streams draining the escarpment, the relief should adjust until downdip

Figure 26. Landforms of De Chelly Sandstone north of Kayenta, Arizona, along US 163. Slickrock slopes at the left give way to vertical scarps at the right, where undermining is active due to exposure of shaly Organ Rock Tongue at the base of the scarps.

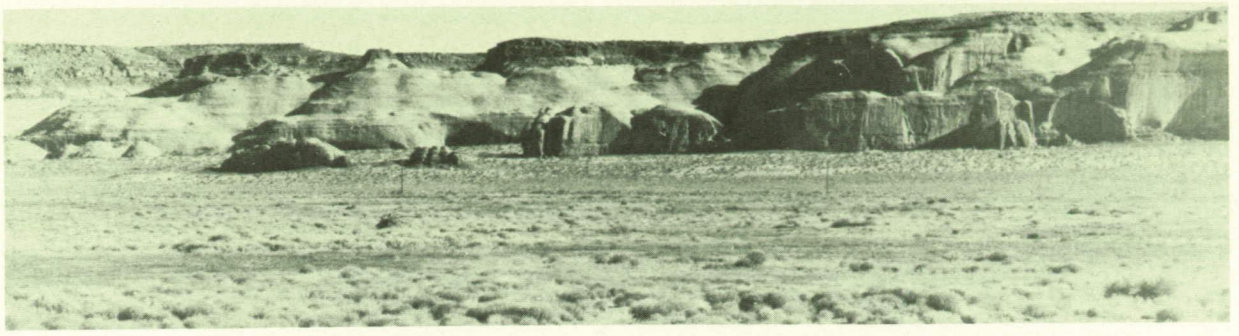

Figure 27. Erosion of a compound hill slope under the assumption of (A) a uniform rate of downwasting on all slope elements and (B) maintenance of correlations between slope elements and stratigraphic units. Both assume that gradients of the respective elements remain constant through time. Under assumption (A), the volume of material removed increases with decrease of gradient, whereas the volume decreases in (B). (From Howard, 1970.)

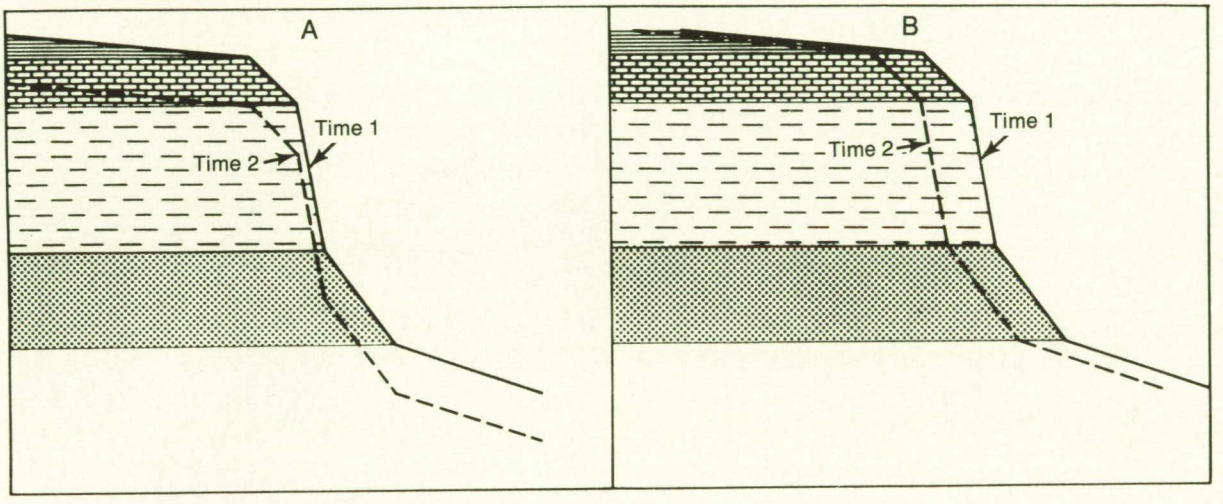

exposure of new caprock and updip removal by backwasting are roughly balanced. Therefore, the rate of vertical reduction of the rim should be independent of the dip (maintaining a constant relief through time), whereas horizontal retreat of the escarpment would be inversely proportional to the tangent of the dip, and the volume of caprock eroded per unit time would be inversely proportional to the sine of the dip. The very rapid rate of horizontal retreat predicted for low dips does not occur because the escarpment becomes segmented by erosion along drainage lines into isolated mesas and buttes whose local relief, distance from the main escarpment, and rate of backwasting increase through time. Nevertheless, these considerations imply that, in general, a greater volume of rock must be eroded per unit time from gently dipping scarps than from steeper ones. The gradients and total relief on a given scarp should increase where the structural dip decreases to maintain relatively constant rates of vertical reduction of the rim. Figure 30 compares relief of escarpments on two sandstones in the Henry Mountains area, Utah, as a function of the reciprocal of the sine of the dip, showing that there is, in fact, a relationship of the type predicted.

Wasting of caprocks occurs primarily by rockfall, undermining, slumping, and fretting. Rockfall includes events ranging from calving of individual blocks to the failure and fall of a wide segment of the face, resulting in a rock avalanche on the scarp rampart. Some sandstone caprocks (especially in the Morrison Formation) are undermined block-by-block by weathering and erosion of the underlying shale without rapid fall of the undermined blocks (figs. 31 and 32). The blocks may be repeatedly lowered with lit-

Figure 28. A typical profile across the escarpment of the Emery Sandstone at North Caineville Mesa. Average gradients on the escarpment front and backslope are indicated by dashed lines. Unit A is sandstone, coal, and shale beds; B is massive sandstone; and C is marine shale. If vertical erosion is proportional to the slope tangent, then the front is downwasting about 15 times faster than the backslope, and the face retreats about 40 feet for every foot of downwasting on the backslope. (From Howard, 1970.)

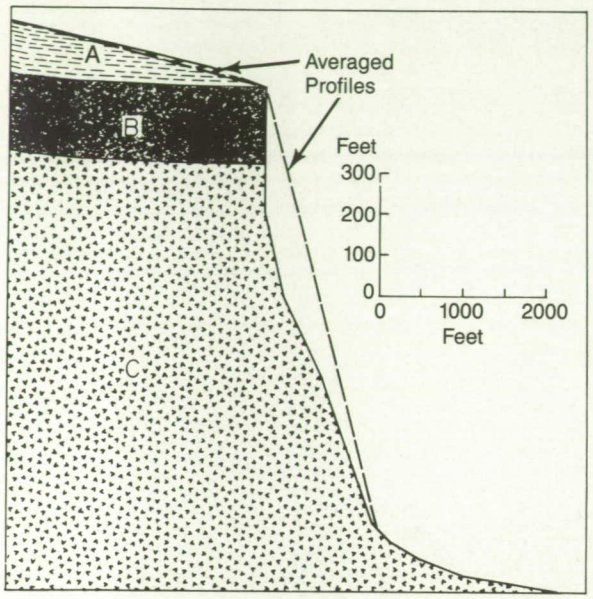

Figure 29. Definition of angles and slope elements on escarpments in dipping strata. (From Howard, 1970.)

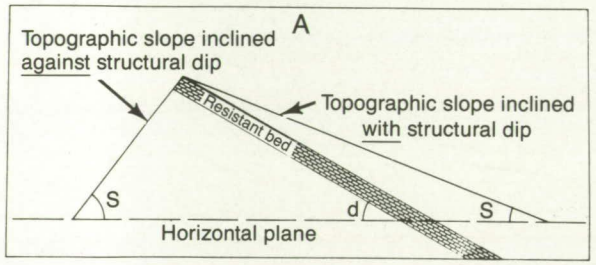

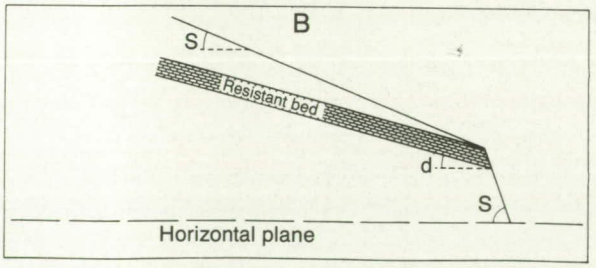

tle downslope sliding or rolling, but typically the blocks slide and occasionally roll a short distance upon being undermined. Block-by-block undermining requires a relatively thin caprock, well-developed jointing, and shale that weathers easily by the addition of water, such as the montmorillonitic Morrison

Figure 30. Relief of escarpments in dipping strata as a function of the angle of dip for two sandstones sandwiched between over- and underlying shales. Relief is measured from the crest of the escarpment to the base of the scarp rampart (see fig. 1). Each data point is a measurement from a separate location along the western edge of the Henry Mountains, Utah. A least-squares regression line has been fitted to observations from each sandstone scarp.

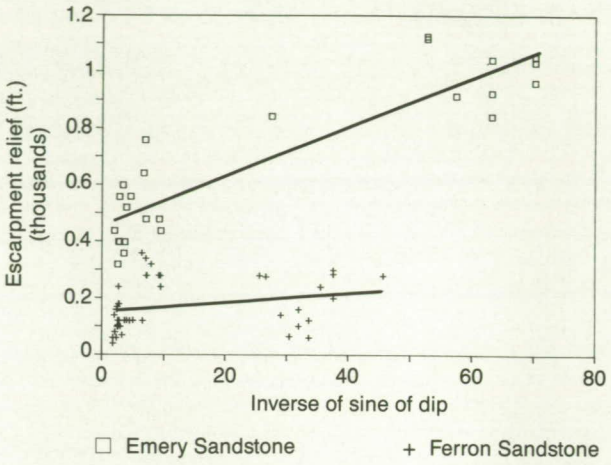

Figure 31. Block-by-block undermining of Cedar Mesa Sandstone at Muley Point by erosion of shale interbed. Goosenecks of the San Juan River are in the background.

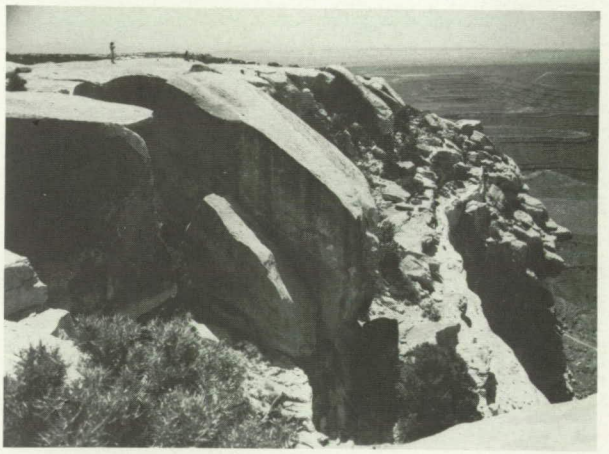

Shale. Slumping is prevalent on relatively few escarpments, where it may dominate as the mechanism of scarp retreat (figs. 33 and 34). The Toreva block slumps are a classic example (Reiche, 1937). Conditions leading to slumping failure have not been firmly established, but a low shear strength of the unweathered sub-caprock unit is probably the major factor. Low shear strength can result from low bulk strength or a high degree of fracturing and/or abundant bedding plane partings. Other factors in some cases may be deep weathering of the sub-caprock unit by groundwater flow and high pore water pressures.

Rockfall is the most common form of scarp retreat (fig. 35). Over time, a rough balance is maintained between the production of debris at the scarp face and its removal from the rampart. Debris produced

Figure 32. Block-by-block undermining of channel sandstones in shales of the Morrison Formation, near Hanksville, Utah.

Figure 33. Slump failures of the Morrison-Summerville escarpment near Hanksville, Utah.

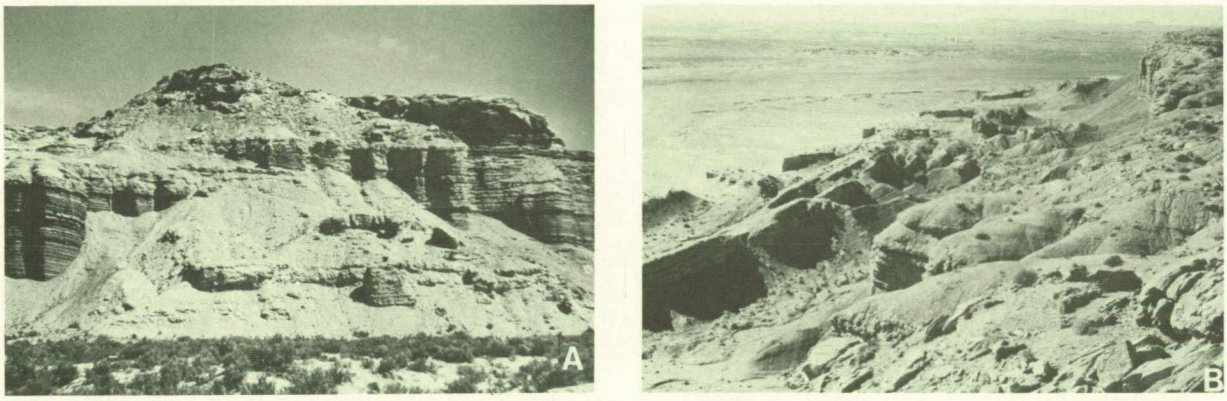

Figure 34. Slumping of a face on the Morrison-Summerville escarpment by slumping (A) before failure, showing failure surface and (B) after failure, showing backward rotation and distortion of bedding. (From Howard, 1970.)

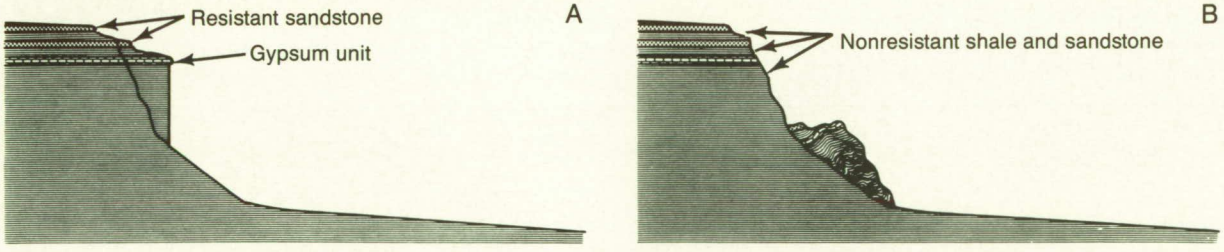

by rockfalls with high potential energy may result in powdering of a large percentage of the original rock (Schumm and Chorley, 1966), but on most scarps the coarse debris produced by the rockfalls must be weathered and eroded before further scarp retreat can occur (fig. 36). Weathering processes acting on the debris are similar to those occurring on slickrock slopes, including splitting or shattering, granular disintegration, and solution of cement (or the rock en mass in the case of limestones). The necessity for weathering of scarp-front debris before further erosion of the sub-caprock unit leads to a natural episodic nature of rockfalls and scarp morphology, as outlined by Koons (1955) (fig. 37). Where caprocks are eroded primarily by large rockfalls, continued erosion of the sub-caprock unit at the margins or base of the rockfall eventually raises the debris blanket into relief, sometimes forming subsidiary small escarpments where the

Figure 35. Portion of escarpment of Emery Sandstone over Mancos Shale on North Caineville Mesa near Hanksville, Utah, along Utah 24. (A) Note extensive deposits of rockfall debris that are dissected by continuing erosion of shale on the rampart. The cliff in the alcove extends far into the underlying Mancos Shale. A seepage line is present at the base of the Emery Sandstone in the alcove. (B) An extensive old debris blanket is strongly dissected at its base. The presence of the debris blanket inhibits further scarp backwasting until the debris is weathered and eroded. The debris blanket is probably a Bull Lake equivalent (Illinoisan?) pluvial deposit. The badlands in the middle distance resulted from the dissection of a Bull Lake pediment extending from the escarpment to Bull Lake gravels (now terraces) along the Fremont River behind the photographer.

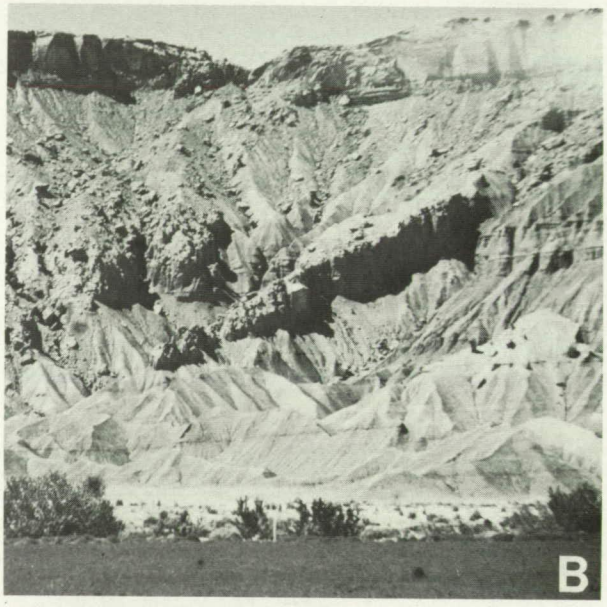

Figure 36. Recent rockfalls in Navajo Sandstone showing abundant rockfall debris. (A) Rockfall northeast of Kanab, Utah. (B) Rockfall in alcove near Stop I at Inscription House Area (figs. 65 and 66).

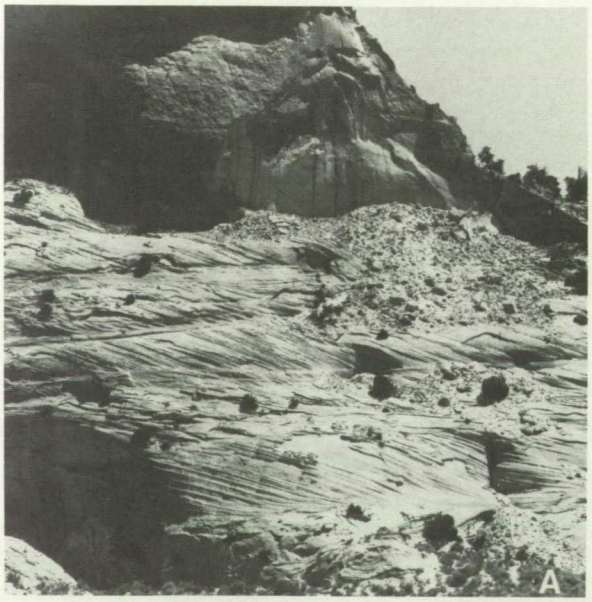

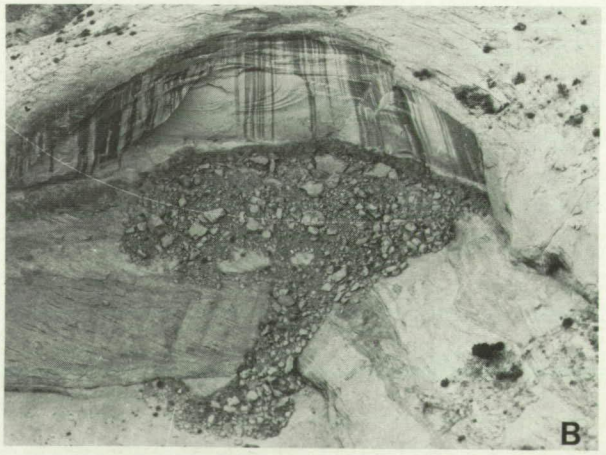

Figure 37. Idealized profiles showing stages in retreat of an escarpment. (Caption and illustration from Koons, 1955.)

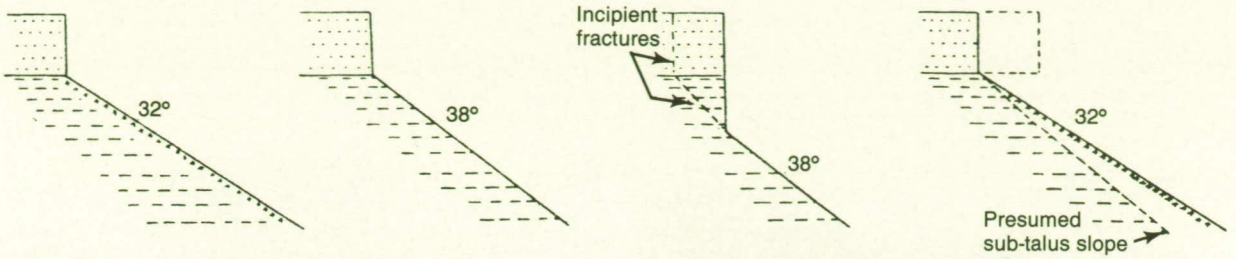

debris blanket is subject to further mass wasting (fig. 35B). Thus old rockfalls stand well above surrounding slopes of both exposed sub-caprock unit and younger rockfalls. The relief and steepness of scarps eroded by rockfalls is controlled not only by necessity to cause failure of the caprock unit, but also by the length of time and relief necessary to weather and erode rockfall debris.

Fretting is used here to refer to surface attack of caprock and sub-caprock units by salt fretting, freeze-thaw, cement dissolution, and similar processes occurring at zones of seepage discharge. Because of the concentrated locus of attack, fretting commonly results in accompanying spalling and alcove development (special types of rockfall). Fretting processes are discussed more fully below.

Most prominent scarps on the Colorado Plateau are formed of massive sandstone underlaid by shale or other easily weathered rock, so that backwasting is caused by loss of bulk strength of the underlying layer accompanied by erosional attack of the scarp rampart. However, some of the incompetent layers producing scarps are strong in bulk but are eroded primarily because of denser fracturing relative to more massive (but not necessarily stronger) overlying sandstones (Oberlander, 1977; Nicholas and Dixon, 1986).

Segmented Scarps

Many areas of moderate relief on sandstones on the Colorado Plateau exhibit a complex topography embodying elements of both slickrock morphology and scarps. Such landscapes developed in the Slick Rock member of the Entrada Sandstone at Arches National Park are the object of a comprehensive study by Oberlander (1977). In this area, slickrock slopes are interrupted by nearly vertical cliffs which Oberlander terms "slab walls" due to their erosion by failure along sheeting (off-loading) fractures parallel to the scarp face. The slab walls terminate at their base at indentations developed in thin weak zones (partings) whose weathering and erosion cause the slab wall backwasting (figs. 38 and 39). Partings that readily weather ("effective partings") are either closely spaced bedding planes with high fractured sandstone

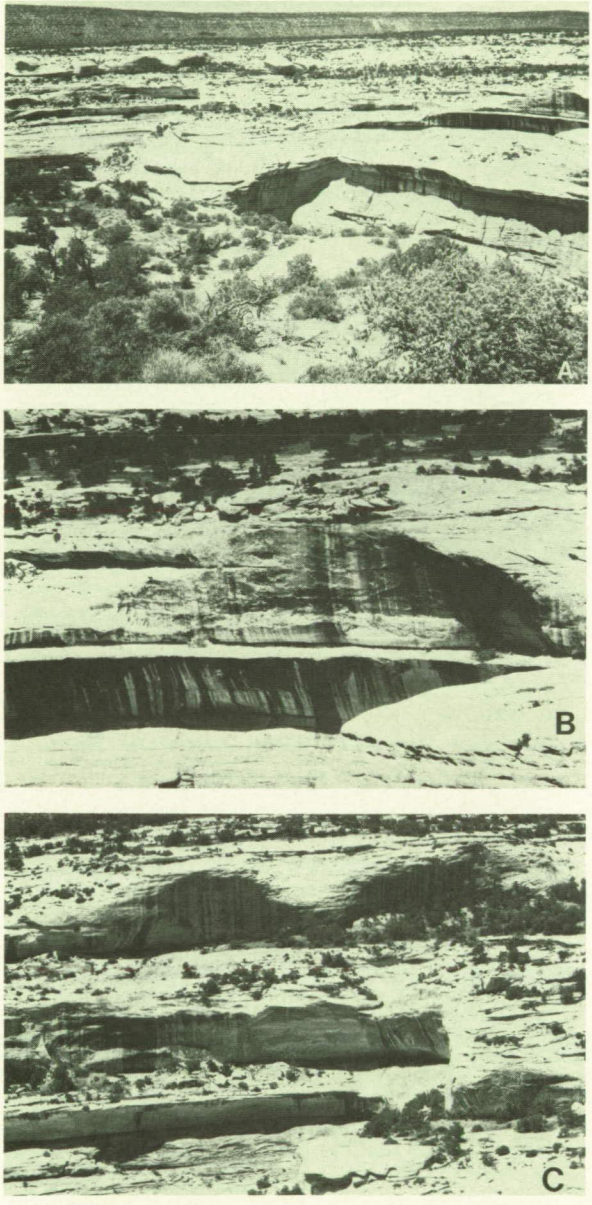

Figure 38. View of segmented scarps in Cedar Mesa Sandstone at Natural Bridges National Monument, Utah. (A) General view. (B) Detail from (A). Note the thinness of effective partings and the absence of fresh rockfall debris. (C) Detail from (A). Note the absence of fresh rockfall debris.

Figure 39. Segmented scarps in the Entrada Sandstone at Arches National Park, Utah. (A) Slickrock slopes and slab walls, showing effective partings at the base of slab walls. Note that the prominent slab wall in the middle of the scarp at the left dies out before the center of the photo due to pinching out of the effective parting. (B) Multiple levels of slickrock and slab walls, showing thin parting layers at the base of the slab walls. Some of the slab walls have been pockmarked by alveolar weathering, indicating lack of recent backwasting.

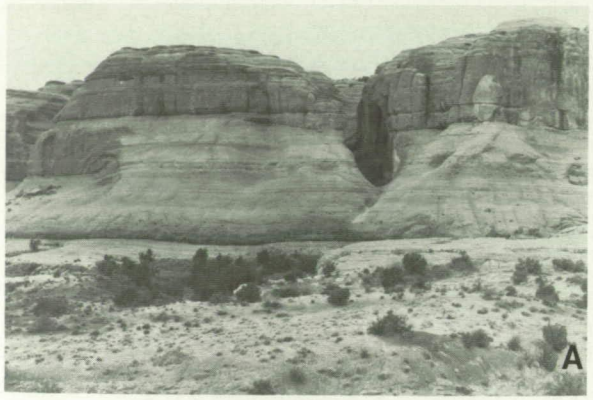

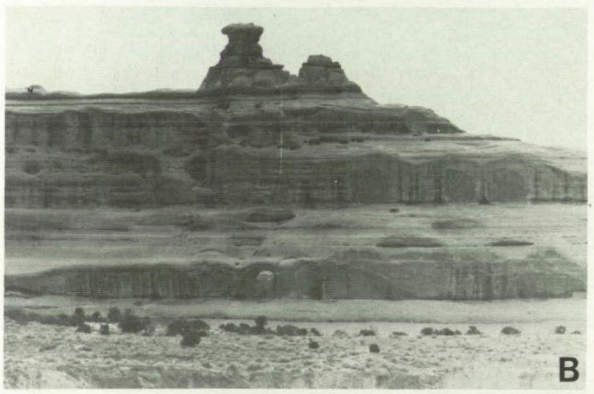

Figure 40. Effective partings in the Entrada Sandstone at Arches National Park, Utah. (A) View of slickrock slopes and short slab wall, located to the extreme left of fig. 39A. Note the embayment at the base of the slab wall at the effective parting. (B) Detail of effective parting in the area in (A). Some evidence of salt efflorescences is present, but there is no evidence of active seepage. Locally, water, held by surface tension, draining down the slab wall, may be delivered to the parting face.

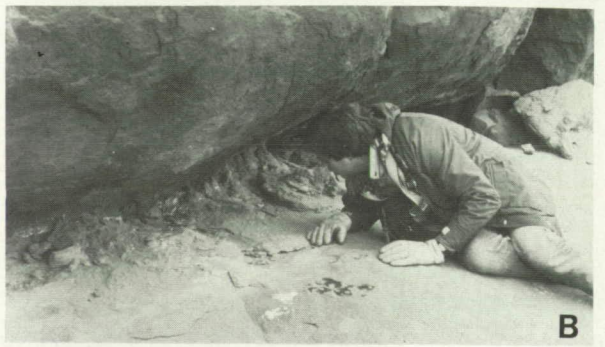

sandwiched in between, or are one or more thin (2 to 5 cm) layers of fissile ferruginous shale (fig. 40). The partings commonly are of limited horizontal extent, so that slab walls die out laterally (fig. 39A). Some slopes may have more than one slab wall where partings occur at two or more levels (figs. 38B, 38C, and 39). Oberlander presents convincing evidence that slope erosion occurs by both erosion of slickrock slopes and slab wall backwasting. This, coupled with intersection of new partings and lateral dying out of other partings during slope retreat, leads to progressive changes in slope profile form (fig. 41). In Oberlander's model, the gradient of slickrock slopes below effective partings depends largely on the relative rates of scarp backwasting by parting erosion and the rate of weathering and erosion on the slickrock slopes, with gentler slickrock slopes associated with rapid parting erosion. Sometimes backwasting at a parting may cease, due to playing out of the parting or to local conditions less conducive to parting erosion. In such cases continued erosion of the slickrock slope below the parting leads to the development of a near-vertical slope below the parting; such slopes are called "secondary walls" by Oberlander. Such inactive slab walls also commonly develop alveolar weathering (fig. 39B), discussed further below. An important conclusion of Oberlander's study is that thin partings in otherwise massive bedrock cause a complicated slope form (in particular the slab wall) so that slope breaks are not necessarily an indication of lithologic differences above and below the scarp, but imply only a thin discontinuity.

Similar slope forms occur in other sandstone units, especially the Navajo Sandstone and the Cedar Mesa Sandstone at Natural Bridges National Monument (fig. 38). In these formations the slab wall is often strongly overhung into a thin two-dimensional arch or alcove presumably backwasted along sheeting fractures. One puzzling aspect of these prominent indentations is a general paucity of mass-wasting debris on the lower floor (figs. 38B and 38C). Schumm and Chorley (1966) cite the ready breakup of the wasted debris as an explanation, but slab wall failures from relatively short cliffs yield abundant debris (fig. 42), and the alcoves are a relatively protected environment. Another possible explanation is present-day inactivity of

Figure 41. Development of scarp forms in massive sandstone through time and space. For simplicity, a constant ground level (dashed line) is assumed during scarp retreat, along with equal thicknesses of removal from major slab walls in each unit of time. At A a through-going cliff is present due to sapping above a thin-bedded substrate. At B the thin-bedded substrate passes below ground level, scarp retreat slows, and effective intraformational partings assume control of scarp form. Effective partings close at C, E, F, G, H, and J, leading to local slab wall stagnation and rounding into slickrock. Partings that open at D, E, F, G, and I initiate growth of new slab walls. Note that the effect of former partings in rocks that have been removed continues to be expressed in the form of slickrock ramps and concave slope breaks. Lowering of ground level during backwearing would cause cliff extension upward from major contact. (Caption and illustration from Oberlander, 1977.)

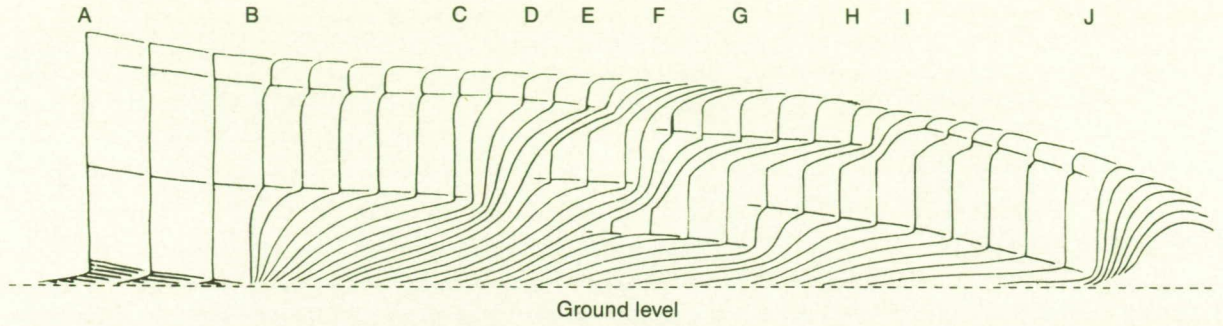

Figure 42. Aerial view of double alcoves in Navajo Sandstone in the Inscription House Area (fig. 65), showing sandstone debris created by recent rockfall.

parting erosion and resulting slab failure due to aridity. The effects of climatic change on scarp morphology are discussed further below.

A different type of slab wall characterized by lack of an obvious parting layer occurs locally on massive sandstones. The lower contact between the slab wall and the lower slickrock slope varies in vertical position (fig. 43). One explanation is that the slab walls are not backwasting at present, whereas the lower and overlying slickrock slopes continue to erode. Thus the vertical wall is similar to the secondary walls of Oberlander. A lack of mass-wasting debris below the slab wall is consistent with this interpretation. The lack of obvious resistant layers or partings makes it unclear why the slab walls developed. However, the present inactivity of the slab walls is consistent with their poor exposures to weathering processes and the lack of undermining.

Figure 43. Slab walls in Navajo Sandstone at Zion National Park, Utah. Note the absence of parting or a sapping zone and the variation in elevation of lower contact between the slickrock slope and the slab wall.

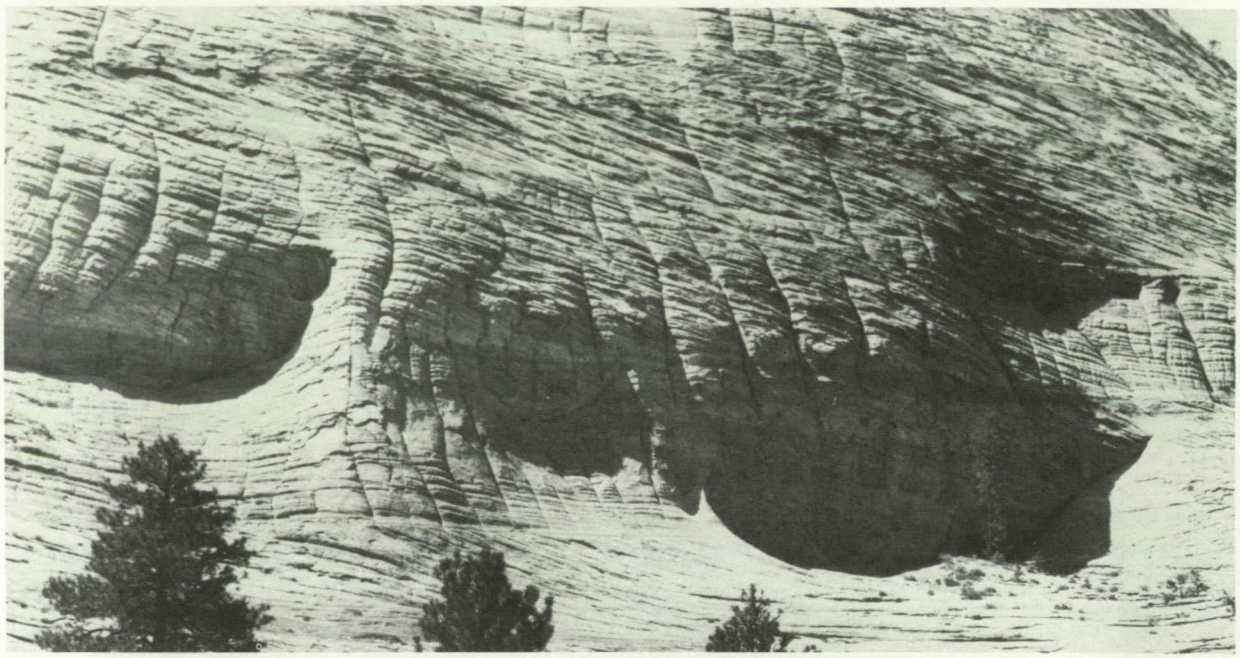

Role of Sapping Processes in Scarp Erosion and Morphology

Various geomorphologists have suggested that rock weathering and erosion at zones of groundwater discharge have contributed to the backwasting of scarps and valleys in sandstones exposed on the Colorado Plateau (Gregory, 1917; Bryan, 1928; Ahnert, 1960; Campbell, 1973; Laity and Malin, 1985). Laity and Malin (1985) define sapping as "the process leading to the undermining and collapse of valley head and side walls by weakening or removal of basal support as a result of enhanced weathering and erosion by concentrated fluid flow at a site of seepage." Higgins (1984) distinguishes between "spring sapping" caused by concentrated water discharge and "seepage erosion" resulting from diffuse discharge at lithologic contacts or other lithologic boundaries. This discussion addresses the general question of the role of groundwater in slope erosion on the Colorado Plateau and the specific question of the role of groundwater in erosion of deeply incised valleys in sandstone that bear a morphological similarity to some martian valleys.

The definitions of sapping and seepage erosion given above are likely to occasion semantic arguments about marginal situations. Scarp erosion processes that are clearly not sapping erosion include plunge-pool undermining and rock weathering by moisture delivered to the scarp face by precipitation, condensation, or absorption of water vapor. However, other circumstances are not as clear-cut. For example, water penetrating into tensional and exfoliation joints close to cliff faces and causing rockfalls as a result of freezing or water pressure would probably not be classified as sapping by most geomorphologists. Similarly, corrasional erosion of shale beneath sandstone by water penetrating along wide fractures (Ahnert, 1960, terms this "subterranean wash") is similar to piping, but probably should not be included as a process of groundwater sapping. On the other hand, rockfall caused by weathering of shales beneath a sandstone scarp in which water is delivered by water flow along joints within the sandstone is more likely to be considered sapping, even in the absence of obvious water discharge along the scarp face. Weathering processes resulting from intergranular flow within sandstone would generally be considered sapping. Seepage and sapping weathering and erosion are defined in the context of this paper as discussed in this paragraph.

Groundwater flow plays an uncertain role in the weathering of the shales and weakly cemented layers whose erosion causes scarp retreat in overlying sandstones. Oberlander (1977) mentions spring sapping as a process of scarp retreat, but felt it is limited to scarps near the top of slopes where flow paths through the sandstone are short. He apparently also felt that flow occurs primarily through fractures. In the 1977 paper it is unclear what processes Oberlander thought were responsible for the erosion of the partings that result in the segmented slopes. However, in a per-

sonal communication, discussed further below, he suggests that weathering can occur by surficial processes unrelated to sapping. Schumm and Chorley (1966), while providing experiments and observations on weathering of caprock units, essentially avoid the issue of processes of scarp retreat. Koons (1955) is similarly vague about the undermining processes. Ahnert (1960) clearly feels that sapping processes are of general importance in scarp retreat in sandstone-shale scarps of the southwest, but he provides little evidence. Laity and Malin (1985) suggest that disruption of surface exposures by salt crystal growth where seepage emerges and sloughing of thin sheets of the bedrock are the major process of sapping erosion in massive sandstones, and that sapping is usually concentrated in thin zones above less permeable boundaries within or below the sandstone. This backwasting and undermining of the overlying sandstone then occasions development of slab failure and, locally, alcove development associated with the development of exfoliation jointing as outlined by Bradley (1963). Laity and Malin discuss primarily spring sapping processes occurring at canyon headwalls, and the degree to which they feel sapping or seepage erosion occurs more generally on sandstone scarps is uncertain. Observations reported below suggest a fairly important role of shallow groundwater circulation in scarp retreat in sandstone-shale sequences of the southwest under present climates.

Positive and Negative Evidence for Surface-Directed Erosion

Oberlander (1977) feels that active backwasting is occurring along the shaly "effective partings" discussed earlier (fig. 40). In a recent personal communication, Oberlander clarifies the processes that he feels cause removal from the partings:

> The active partings I have looked at show *no* evidence of seepage in any recent time. I think that even weak and infrequent seepage would be evident from conspicuous vegetation, moss or fungal growth, or staining of rock by white salts or dark Mn-rich desert varnish similar to that seen in streaks on rock faces. Varnish-forming bacteria do best in spots that are occasionally wetted and then very thoroughly dried so that competing organisms cannot colonize and "acidify" the niche. If wetting is more frequent, fungi and vegetation will show up—as they clearly do at the many active seeps in the area. Where there is seepage today, I feel certain that there are open routes for downward penetration of water, and that joints or exfoliation fissures play a dominant role. I find it hard to accept downward percolation through the pores of a hundred or more feet of sandstone under the present climate of the Plateau. According to studies of downward penetration of water re precip amount (in soil), it just doesn't work—otherwise there would be seeps all over the place!
>
> So how does removal at thin effective partings occur? The finger-thick layer of shale in the shallow recess between the overlying and subjacent massive sandstones seems solid. Yet I presume it is wetted by water working down to it through fissures. Somehow the shale is working out of its recess and onto the cliff face. Here and there on the brow of the subjacent layer are a few mm-size flakes of the shale. I presume that these thin and discontinuous shale interbeds started out as fine sediments washed and blown into flat interdune areas in the ancestral erg, where they were quickly buried by advancing dunes. The lack of depth of these deposits provides a measure of the rapidity of dune advance. Such material would have a high content of salines if there were playas or sabkhas anywhere nearby. The shale could be analyzed for its salinity (I'd bet it's high). If the stuff is rather saline, its exposed edge would absorb water from the ambient air, especially during damp periods. This edge swells, slakes, and crumbles. How it gets scattered outward I can only surmise. Frost creep might be the factor (I can vouch for the winters there being beautiful, but icy—very icy).

On the other hand, many scarps in the southwest are composed of cliffs that extend well below the caprock unit into the underlying shales (fig. 35A). These cliffs are remarkably stable, having persisted and grown vertically (downward) throughout the Holocene (and late Pleistocene?), showing the efficacy of even a small overhang in restricting surface weathering of shales in an arid environment (see further discussion below). The widespread development of tall pedestals of shale supporting sandstone capstones (hoodoos or damoiselles) is further evidence of such protection from weathering processes and the relative inefficiency of wind-blown rain or snow, or moisture condensation in shale (or sandstone) weathering beneath overhangs of more than 2 or 3 feet.

Stream backcutting by corrasion or plunge-pool action is also of questionable importance in scarp retreat, at least for washes with drainage areas less than a few square miles. Washes passing over scarps in sandstone generally occupy only a fraction of the total scarp width. In addition, the scarps are commonly overhung when developed in massive sandstone, and plunge pools are rare and small below the waterfalls (figs. 44 and 45). Even steep streams on thin sandstone beds sandwiched between shale layers exhibit overhangs considerably wider than the stream bed and show little development of plunge pools (figs. 46 and 47). As mentioned previously, small washes developed on slickrock slopes above scarps are commonly interrupted by solution pits, and

Figure 44. Theater-headed valleys in Wingate Sandstone Colorado National Monument, Colorado. Note the narrowness of the stream passing over the headwall compared to the alcove and the absence of plunge pools. Alcoves at valley heads show little sign of active seepage, suggesting either a prevalence of dry sapping or the present inactivity of sapping processes.

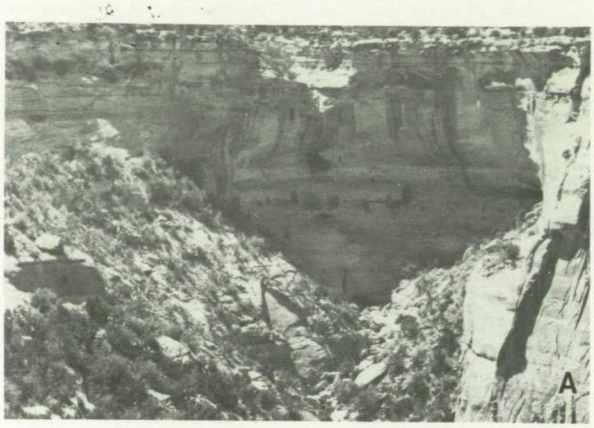

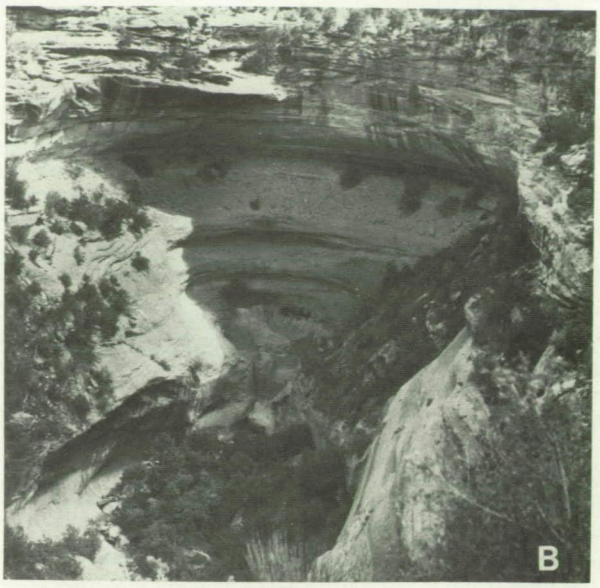

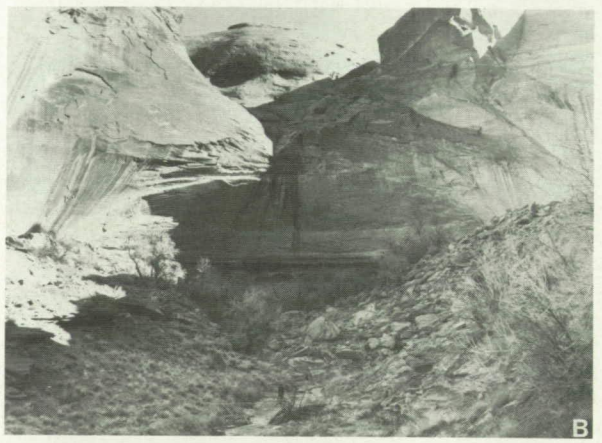

Figure 45. Theater-headed valleys with active seeps. (A) Theater-headed valley in Navajo Sandstone just downstream of the area shown in fig. 22. Water was actively seeping from the parting at the time the picture was taken, a few days after a major rainstorm. The seep was inactive in November after a dry late summer and fall. (B) Theater-headed valley in Navajo Sandstone near Utah 95 along North Wash (southern Henry Mountains area). Note the cottonwood trees and the dark figure in the wash (bottom center) for scale. The active seep is the dark band at the base of the alcove. Note the evidence of offloading fracturing. The stream passing over the top of the alcove is clearly inadequate in size to have created the alcove as a plunge pool. Water draining down the face of the alcove from the lip of the falls has created the dark streaks. However, delivery of water along the alcove walls occurs only locally and is insufficient to account for the backwasting of the alcove.

the washes exhibit flutes and furrows that suggest that solutional removal of calcite cement is more important than mechanical corrasion in bed erosion.

Positive Evidence for Groundwater Sapping

Cavernous Weathering and Alcove Development. Weathering and erosion of sandstone by the effects of crystal growth occur at a variety of scales in sheltered locations. Steep slopes and scarps in sandstone are frequently interrupted by rounded depressions, often overlapping, which intersect sharply with the general slope (figs. 48-50). Such alveolar weathering, or "tafoni," occurs not only in sandstone, but also in granites, tuff, and other massive rocks (Mustoe, 1982, 1983). Both accelerated erosion in the hollows and case hardening of the exposed portions of the slope (Conca and Rossman, 1982) may contribute to the development of tafoni. Salt accumulations are often quite apparent in the cavernous hollows (fig. 51), and the backwasting results in spalling of sheets of weathered rock up to a few centimeters in thickness (fig. 52). Mustoe (1983) notes high soluble cation contents in the spall detritus in tafoni and the presence of the mineral gypsum. Laity (1983) and Laity and Malin (1985) find calcite deposition on spalling walls. The mechanisms by which such mineral deposition may contribute to the spalling include pressure exerted by crystal growth, thermal expansion and contraction of the crystal-filled rock, and expansion and contraction due to hydration of deposited minerals

Figure 46. Steep stream in sandstones at Colorado National Monument, Colorado, showing poor definition of channel, absence of plunge pools, and numerous short overhanging scarps.

Figure 47. Steep gully in interbedded shales and sandstones of the Supai Formation at the north rim of the Grand Canyon, Arizona. Note the absence of plunge pools and the undermining of sandstone ledges along the gully.

Figure 48. Alveolar weathering, or tafoni, developed in Navajo Sandstone at Capital Reef National Monument, along Utah 24. Note the highway reflector for scale. Also note uneroded ribs where surface wash occurs.

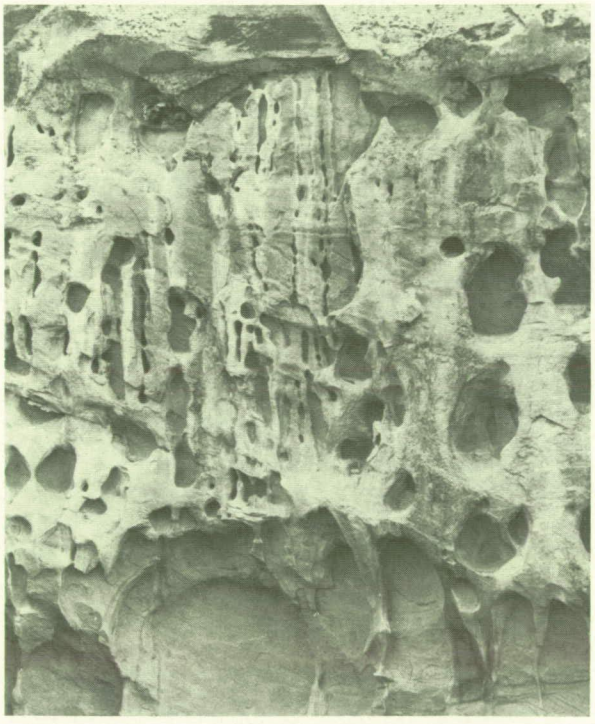

Figure 49. Alveolar weathering at the same general location as that shown in fig. 48.

(Cooke and Smalley, 1968). Freeze-thaw disruption on the moist seepage faces may also contribute, and spalling may be aided by the weight of accumulated winter ice (Laity and Malin, 1985).

A surface protected from surface runoff is a necessary condition for tafoni and alcove development. On steep sandstone scarps, surface runoff commonly flows as sheets down the scarp, held by water tension on slightly overhung slopes. Such runoff paths are commonly accentuated by desert varnish. Where such runoff paths cross zones of tafoni development, backwasting is inhibited, and the tafoni are separated

Figure 50. Tafoni in Entrada Sandstone in an alcove along the road to Needles Overlook off Utah Highway 163 & 191.

Figure 51. Tafoni and salt fretting in an alcove in the Entrada Formation along the road to Needles Overlook. The most concentrated zone of fretting occurs in a 1-m zone at the base of the upper darkcolored unit.

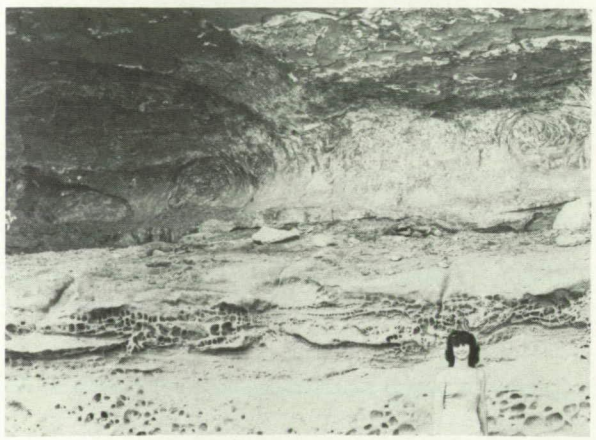

Figure 52. Detail of spalling by salt fretting in the area shown in fig. 51. Note sheets of spalled sandstone on the floor of the alcove.

Figure 53. Alveolar weathering of Cedar Mesa Sandstone along White Canyon near Utah Highway 95 in the Fry Canyon area. Note that alveolar weathering is inhibited where a small wash passes over the scarp face. The zone of alveolar weathering may occur at a zone of emergent groundwater.

by columns that often resemble flowstone columns in caves (figs. 48, 49, and 53). Surface runoff might inhibit salt fretting simply by solution and removal of salts brought to the surface by evaporating groundwater or more actively by case hardening of the exposed surface by deposition of clays or calcite (Conca and Rossman, 1982).

Two intergrading types of sapping landforms develop on massive sandstones. The more exotic form is the development of tafoni on steep scarps and on large talus blocks. Such tafoni may literally riddle certain steep slopes (figs. 48–50), with the tafoni concentrated along certain beds that are either more susceptible to the salt fretting or receive greater groundwater discharge. Talus blocks generally develop tafoni on their lower, overhung portions. The concentration of tafoni development at the base of such blocks may be due to the protection from surface wash as well as upward "wicking" of salts from underlying soils or shales, a process that contributes to weathering of the bases of tombstones (Mustoe, 1983; Hamilton, 1984). Oberlander (1977) points out that tafoni develop most strongly on scarps initially steepened by basal undermining but presently no longer backwasting because alluviation or eolian deposition cover and protect the basal backwasting face. Thus generalized tafoni development on a scarp indicates relative inactivity of backwasting by surface attack or basal undercutting.

On the other hand, large alcoves are common in massive sandstones and are often actively retreating as a result of sapping erosion (figs. 54 and 55). However, direct sapping is usually localized to zones less than 2 m thick along permeability discontinuities where the discharge of groundwater is concentrated (fig. 56), although at major valley heads the seepage zone may be

Figure 54. Explorer Canyon, Utah, and its theater headwall. Explorer Canyon is a tributary of the Escalante River (fig. 63). (A) Aerial view. Explorer Canyon extends upward on the left. Escalante River Canyon, now flooded by Lake Powell, occupies the lower portion of the photo. (B) The headwall of Explorer Canyon, an unbranched tributary of the Escalante River. Groundwater flowing through the Navajo Sandstone emerges at the canyon head in a zone of seepage immediately above the underlying Kayenta Formation. The headwall is 120 m high, and the dark zone of seepage is 20 to 25 m in height. This zone is recessed relative to the upper canyon walls, and evidence of small-scale collapse can be seen. Perched bedding plane seeps are evident on the upper walls. (Figure and caption courtesy of Julie Laity.)

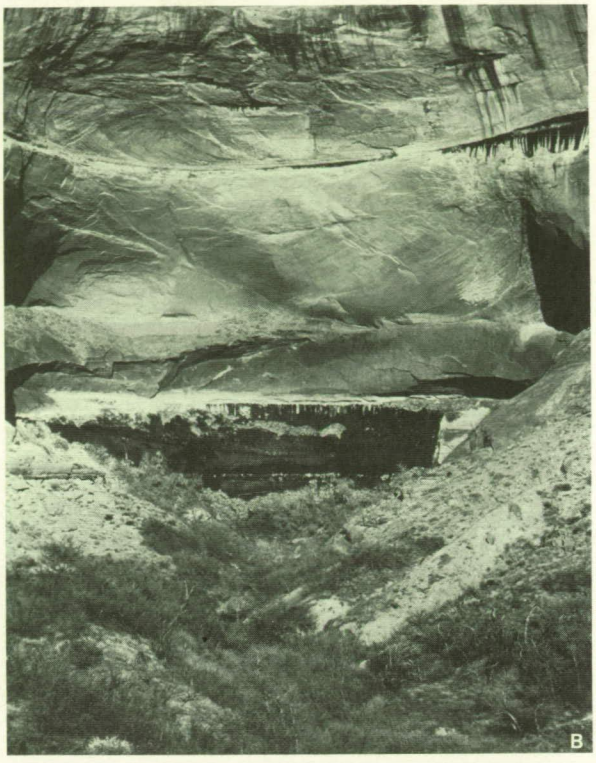

20 to 25 m thick (fig. 57). These sapping zones generally backwaste by processes similar to those of tafoni, and locally tafoni are superimposed on the sapping face. In addition to salt fretting, backwasting by groundwater discharge can also occur by cement dissolution and by weathering of shale beneath or interbedded in the sandstone. The retreat of the active zone of sapping undermines the sandstone above, with the result that occasional rockfalls occur (figs. 36B and 42). In massive sandstone the undermining occasions the development of exfoliation sheeting fractures, resulting in large arches or alcoves, with the deepest parts of the alcoves presumably corresponding to the most rapid sapping attack (figs. 36B, 45, 54B, 55, 56A, and 57B). In well-jointed sandstones, such as the Wingate Sandstone, arches and overhanging cliffs are less common, and the role of scarp retreat by sapping processes is not as obvious but may be just as important (fig. 58).

The major aquiclude for the Navajo Sandstone is the underlying Kayenta Formation, and the major seeps develop at this discontinuity (figs. 54 and 56). However, thin shales and limestone interbeds (interdunal deposits) create minor aquicludes within the Navajo Sandstone (see chapters 3 and 4), leading to frequent development of multiple levels of seeps and associated alcoves at valley headwalls (fig. 59).

A distinction may be made between "wet" sapping with a damp rock face and an effluent discharge and "dry" sapping face, generally encrusted with mineral salts (Laity and Malin, 1985). In general, tafoni are associated with dry sapping because of their localized development, whereas large alcoves are generally associated with a more regional groundwater flow and exhibit faces that are at least seasonally wet. This distinction, like most, admits of many intergrades and transitions from one to the other type as a result of seasonal or long-term climatic fluctuations. For example, dry sapping can lead to alcove development (fig. 60).

Neither active seepage nor deposition of mineral crusts on protected sandstone walls are necessarily correlated with rapid weathering and backcutting of the sandstone walls. For example, the Weeping Wall at Zion National Park is an impressive seep emerging from the Navajo Sandstone, but the associated alcove and canyon are relatively small. Many other examples of fairly high discharge rates but only minor or nonexistent alcoves can be found throughout the Colorado Plateau. Too rapid a seepage may in fact discourage deposition of salts. Although rapid seepage can also cause backwasting by dissolution of calcite or gypsum cement, this would occur only if the groundwater were undersaturated. Similarly, many examples of thick mineral incrustations at seeps lacking evidence of backwasting can be found on sandstones throughout the southwest. Several factors control whether miner-

Figure 55. Alcoves at Betakin Ruin, Arizona. (A) Note the abundant vegetation below alcoves and the thin zones of seepage in the larger alcove. (B) Detail of (A) showing Betakin Ruin.

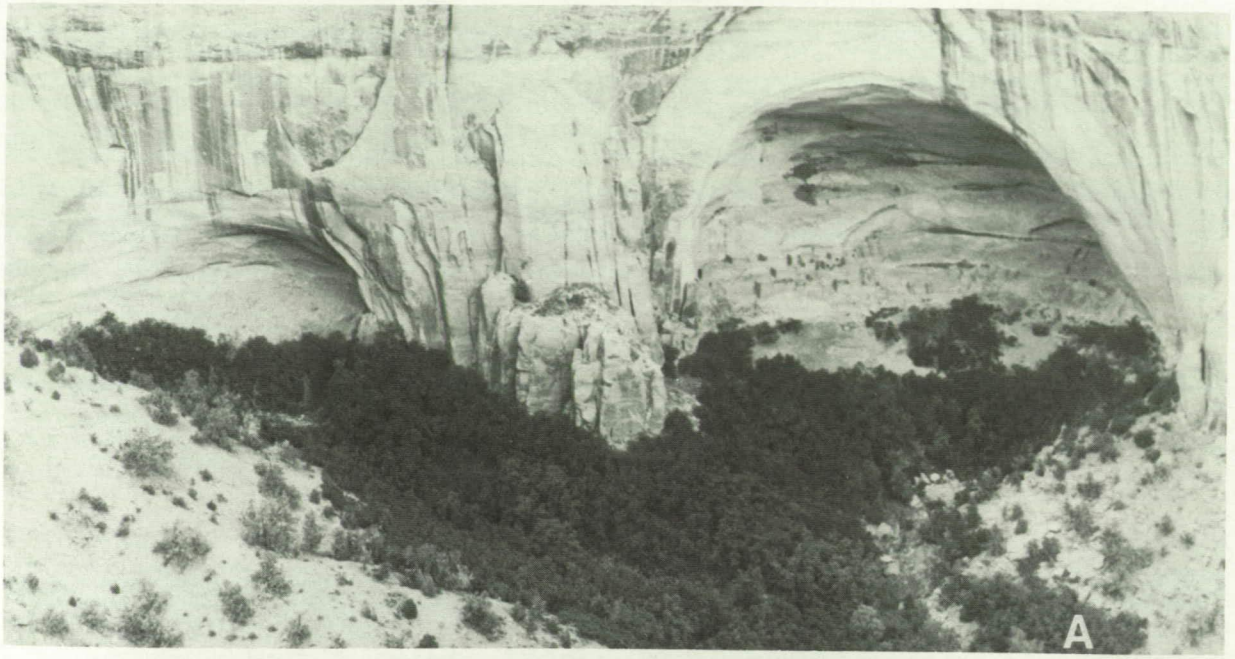

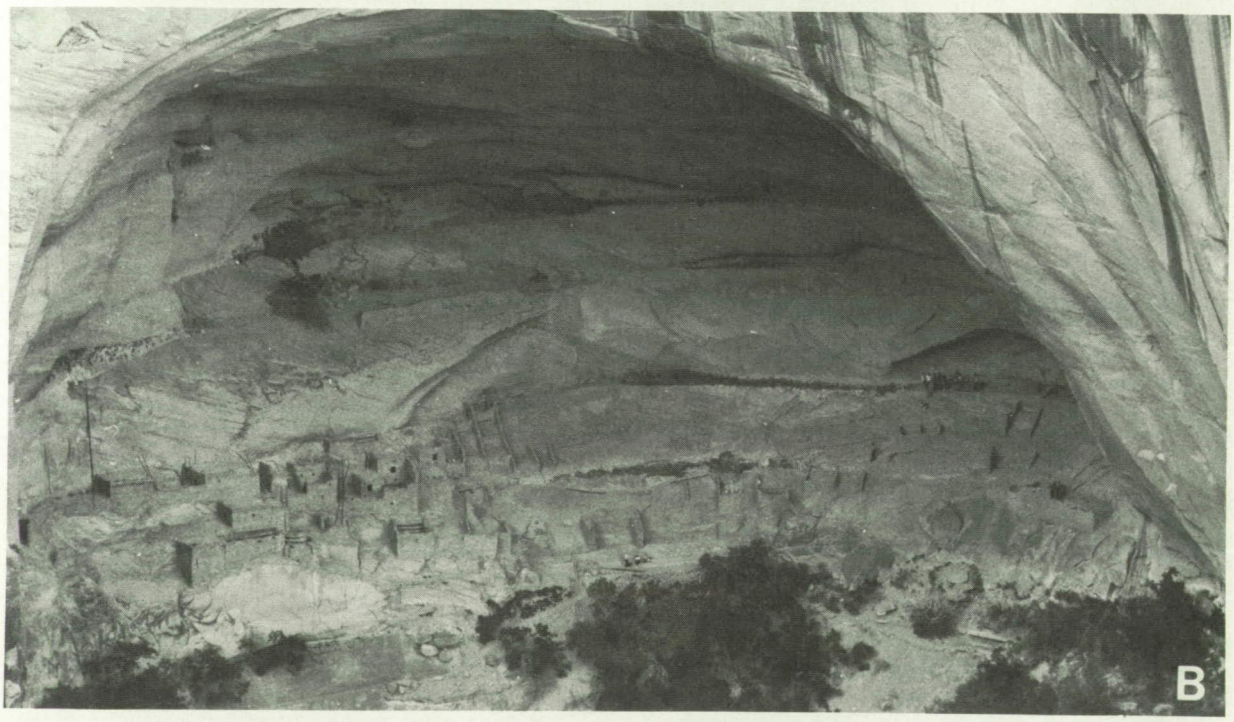

als deposited by evaporating seepage are deposited intergranularly within the rock (encouraging exfoliation and granular disintegration) or at the rock surface (with little resulting sapping), including the type and concentration of salts, the average and variance of water discharge to the surface, the distribution of pore sizes and their interconnectivity, the presence and size of fractures, the temperature regime at the rock face, and the frequency of occurrence of wetting of the rock face by rain or submergence (if along a stream or river). The interaction of these factors is poorly understood. Discrepancies between the size of the alcove or sapping valley and the magnitude of the seep can also result from differences in the length of time that sapping has

Figure 56. Seepage face at the theater head alcove shown in fig. 45. (A) General view of the alcove with 1 to 2 m seepage face. The floor of the alcove is highly weathered sandstone debris supporting a vegetative cover. (B) Detail of seepage face showing vegetative cover of ferns, mosses, algae, and other phreatophytes. Note the salt efflorescences above the moist zone.

been active. Despite these cautions, it is reasonable to expect within a specific physiographic, structural, and stratigraphic setting that the degree of alcove development and the degree of headward erosion of sapping valleys would correlate with the size of the seeps involved (Laity and Malin, 1985).

In summary, most evidence suggests that sapping processes are common in sandstones of the Colorado Plateau and the processes result in the widespread development of tafoni and alcoves. The major caution is the evidence cited by Oberlander suggesting that groundwater sapping is unimportant in erosion of effective partings at thin shale layers in the Entrada and other sandstones. There are several possible explanations for this difference in interpretation of the major process of scarp retreat. The effective shale partings may, in fact, be so readily weathered by atmospheric moisture due to high salt content or other factors that seepage is not required for such partings as it is for cavernous weathering and alcove development elsewhere. The Entrada Sandstone exhibits considerable variation in lithology and cementing both vertically and areally, so that in the Arches National Park the Slick Rock Member may be relatively impermeable. However, well-developed arches and tafoni with evidence of active salt fretting are found a few tens of miles south in this same member (e.g., figs. 51, 52 and 60). Another possibility is that backwasting along effective partings is not very active under present climatic conditions, but was more active during the late Pleistocene. The evidence for relatively inactive scarp retreat (and, by extension, seepage erosion) under present climatic conditions is discussed below.

Large-Scale Morphological Indicators of Sapping Erosion. Groundwater sapping is probably an important process in scarp retreat throughout the Colorado Plateau, as suggested by Ahnert (1960). However, the landform assemblage closest to martian valley systems is the deep, narrow canyon networks of the type discussed by Laity and Malin (1985).

The planimetric form of canyons and escarpments is the most obvious signature of the erosional processes involved in scarp retreat in layered rocks. In the absence of concentrated erosional attack, erosion of caprock units would be by uniform decrescence (fig. 15), resulting in scarp profiles with sharp projections and broadly concave reentrants (Dutton, 1882, p. 258–259; Davis, 1901, p. 178–180; Lange, 1959). Attack of an escarpment by uniform decrescence would gradually make embayments more shallow and the planform of the scarp face closer to linear. Almost all escarpments in gently dipping rocks exhibit deep reentrants and, as erosion progresses, a breaking up into isolated mesas and buttes. This indicates erosion concentrated along generally linear zones of structural

Figure 57. Seepage faces in alcoves in the Navajo Sandstone in the area studied by Laity and Malin (1985). (A) Detail of seepage outflow at the head of Explorer Canyon. The dark zone of seepage is 20 to 25 m in height. Groundwater outflow from the headwall provides about 35% of the baseflow to the stream (see fig. 45). (B) Groundwater emerging from a 20 m high seep at the headwall of a tributary to Iceberg Canyon. Outflow is concentrated at the base of the Navajo Sandstone and is undermining the headwall. Note the two figures for scale. (C) The main valley of Bowns Canyon bifurcates at its tip to form a double theater head. The combined outflow of the headwall springs was measured at 150 to 190 liters/minute (March 1981) and contributed approximately 20% of the stream baseflow. The upper portion of the seepage face (12 to 15 m high) is visible as a dark line at the top of the photo. Much of the seepage is hidden by a dense thicket of brush and trees. The groundwater discharge fills a pond that overflows to form the stream source. (Photos and captions courtesy of Julie Laity.)

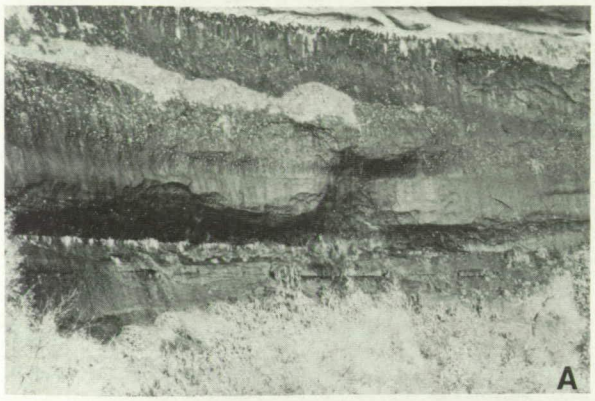

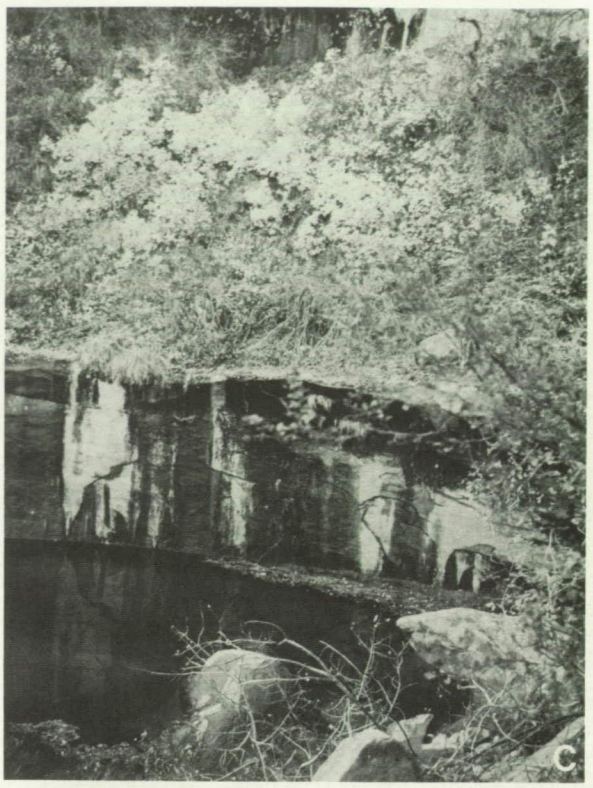

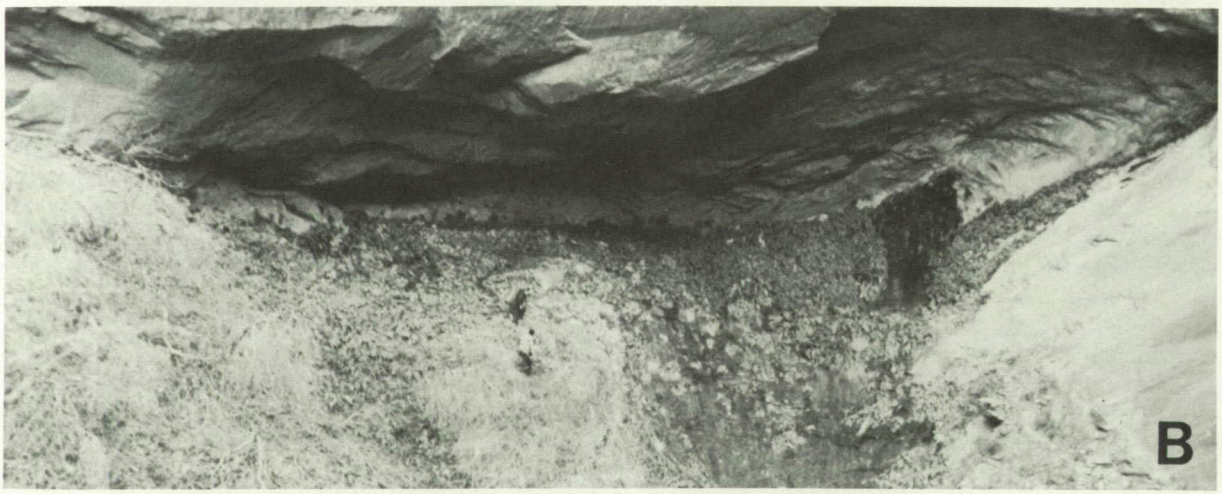

weakness, fluvial erosion, or sapping (often acting in combination). One evidence for the role of either or both fluvial erosion and groundwater sapping is the asymmetry of scarps in gently tilted rocks. The planform of segments where the scarp faces updip is generally similar to that expected by uniform decrescence, since little drainage passes over the scarp, but segments facing downdip ("back scarps" of Ahnert, 1960) are deeply indented as the result of fluvial or sapping erosion (fig. 61) (Ahnert, 1960; Laity and Malin, 1985). Since both fluvial erosion and sapping produce reentrants, the mere presence of deep reentrants is not conclusive evidence for sapping erosion.

Nicholas and Dixon (1986) emphasize the role of variable density of fracturing of incompetent and caprock layers in controlling the rate of scarp retreat and the development of reentrants, projections, and isolated buttes. Their evidence suggests that variable density of fracturing is important on certain scarps, but it probably controls primarily the small-scale planform features. Variable density of fracturing cannot account for the remarkable asymmetry of gently dipping scarps

Figure 58. Scarp in Wingate Sandstone. Scarps at the left and right are typical of this well-jointed sandstone. The smooth cliff and alcove at the center are fairly unusual for scarps in this formation.

Figure 59. Valley headwalls with seeps at multiple levels. (A) Two levels of seeps in an alcove along Geshi Canyon (figs. 64 and 67). The seeps occur on local aquicludes of interdunal shales or limestones within the Navajo Sandstone (see chapters 3 and 4). The bed between the two seeps is approximately 30 m thick. (B) Valley headwall in Toenleshushe Canyon near stop 1 showing a large, nearly dry basal alcove and minor high level seeps and alcoves. The headwall is about 200 m high. See fig. 66 for location and fig. 80 for a general view.

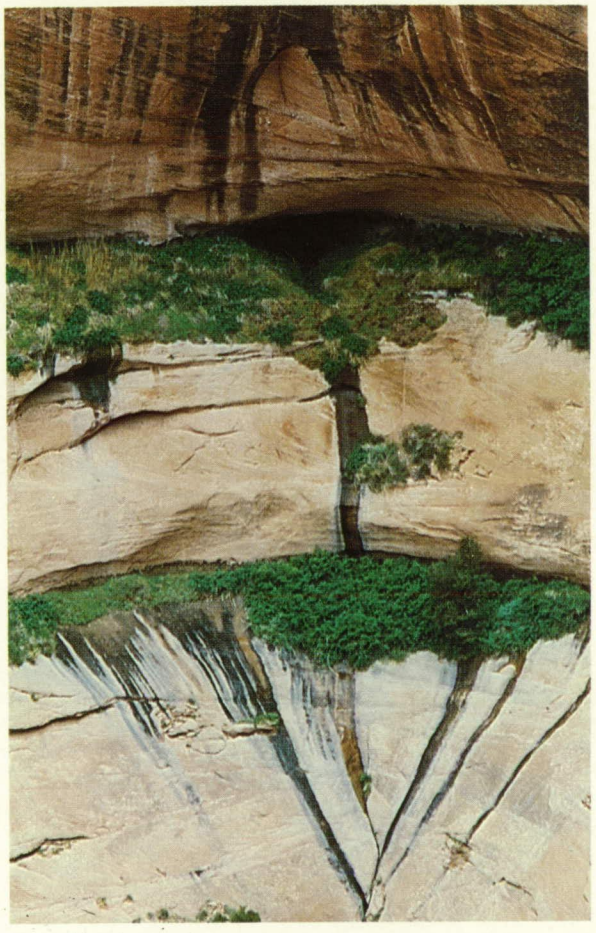

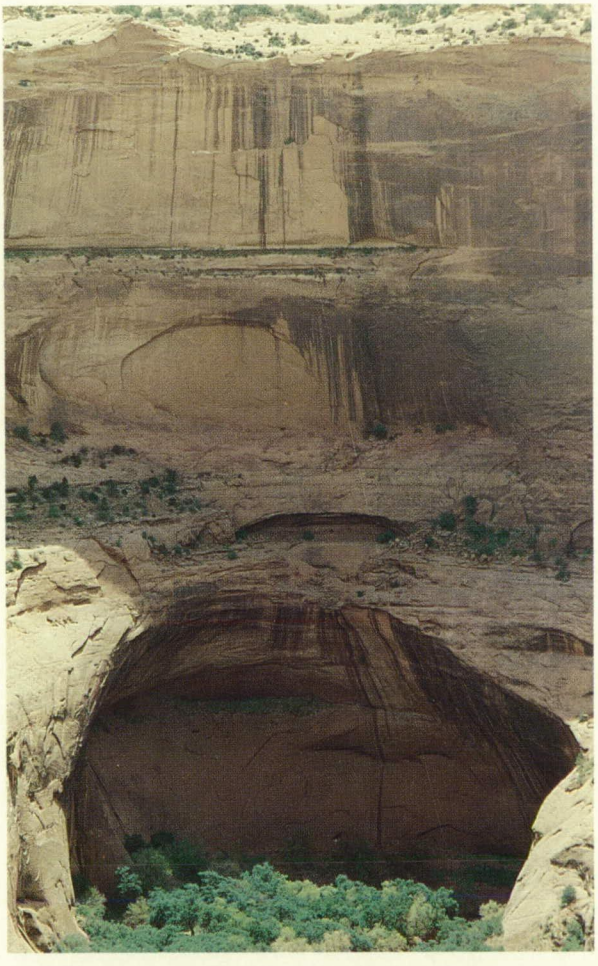

Figure 60. Alcoves in the Entrada Sandstone at the location shown in figs. 51 and 52.

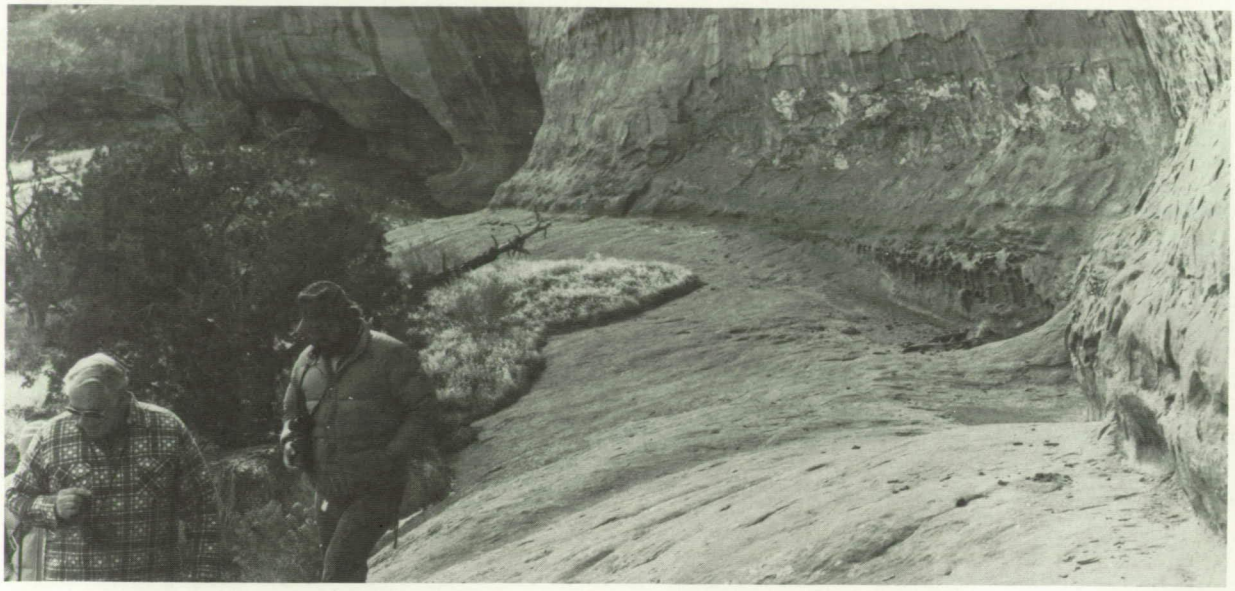

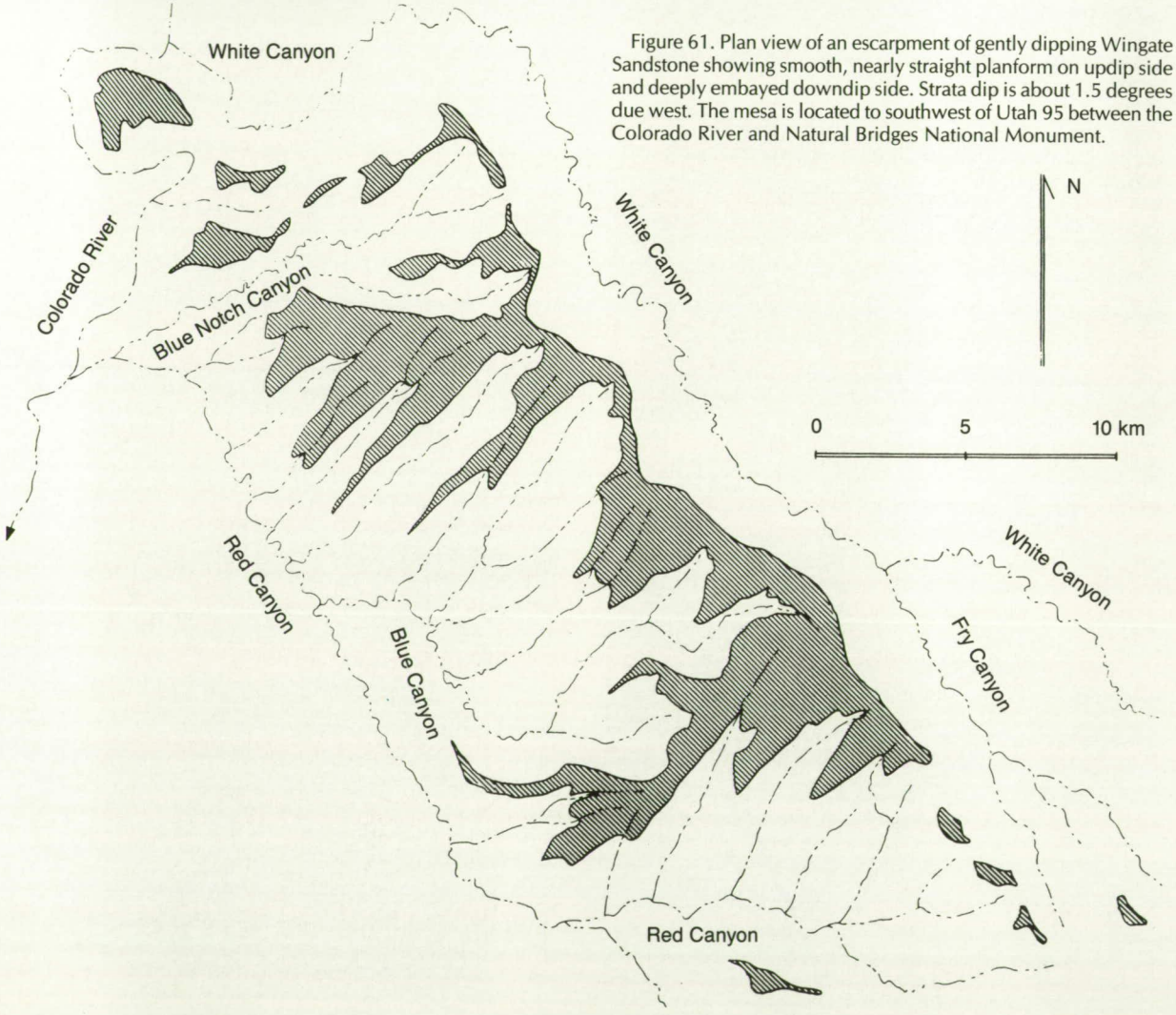

Figure 61. Plan view of an escarpment of gently dipping Wingate Sandstone showing smooth, nearly straight planform on updip side and deeply embayed downdip side. Strata dip is about 1.5 degrees due west. The mesa is located to southwest of Utah 95 between the Colorado River and Natural Bridges National Monument.

(fig. 61) and the general association of embayments with the drainage basins on the overlying stripped surface on the caprock.

Ahnert (1960) and Laity and Malin (1985) suggest that fluvial erosion will produce V-shaped canyon heads that widen consistently downstream, whereas sapping produces U-shaped, or theater-headed canyons of relatively constant width downstream (the terms U- and V-shaped refer here to valley planform, not valley cross-section). Laity and Malin (1985) suggest that the difference in canyon planform for updip- (V-shaped) and down-draining (U-shaped) valleys dissecting the Navajo Sandstone (figs. 54, 62, and 63) is an indication of a prominent role of sapping erosion in the latter and fluvial erosion in the former. However, this comparison is weakened by the difference in dip orientation between the two sets of valleys. The updip-draining valleys do not cut through the resistant sandstone into the underlying shaley Kayenta Formation, so that valley deepening by fluvial plunge-pool action and canyon widening by undermining due to

Figure 62. Aerial view of headwaters of Long (Navajo) Canyon (fig. 63). Note the stripped surface on the top of the Navajo Sandstone and the absence of well-defined drainage on divides. The rocks dip to the left of the photo at about 3 degrees.

Figure 63. Tapered and theater-headed canyons developed in the Navajo Sandstone, attributed to the relative effectiveness of overland-flow or groundwater erosional processes. Dark shaded areas represent the valley floors. West-flowing canyons have theater-shaped terminations and show a greater width/length ratio than do east-flowing valleys. The morphology of theater-headed valleys is analogous to some martian valleys. (Caption and illustration from Laity and Malin, 1985.)

Tributary drainage of the lower Escalante River

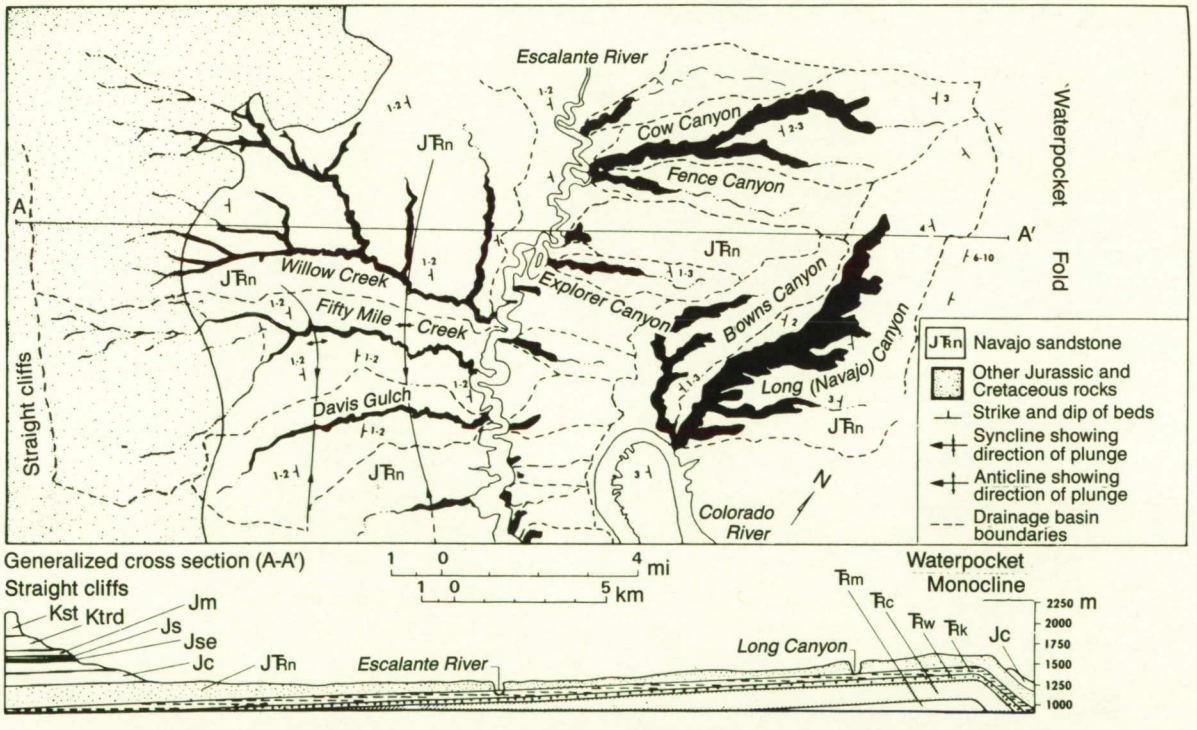

TRm — Moenkopi Formation; TRc — Chinle Formation; TRk — Kayenta Formation; JTRn — Navajo Sandstone; Jc — Carmel Formation; Je — Entrada Sandstone; Jse — Summerville Formation and Entrada Sandstone; Js — Summerville Formation; Jm — Morrison Formation; Ktrd — Tropic Shale and Dakota Sandstone Ksc — Straight Cliffs Formation

non-sapping-related erosion of the shale would not occur, but could be operating in the downdip-draining valleys that do expose the Kayenta Formation. Furthermore, even where updip- and downdip-draining valleys expose the same stratigraphic sequence, headward canyon migration is inhibited in the former by the plunging of the resistant caprock and enhanced in the latter by the updip increase in caprock elevation. A fairer comparison would be between valleys in the same structural setting (same dip and valley orientation), with similar over- and underlying rock units with comparable compressive strength and structural integrity, but having different permeability or different cementing agents (e.g., calcite versus less soluble silica). Finding such a comparative situation may be difficult or impossible.

Fortunately, many of the other diagnostic features cited by Laity and Malin (1985), such as canyons with large theater heads having alcoves and seeps, are much more convincing of a dominant role of sapping in canyon extension and widening. The types of features indicative of a sapping origin proposed by Laity and Malin are discussed below using as an example the box-canyon system tributary to Navajo Creek on

Figure 64. Map of the field trip area. The tour route is shown by a heavy dashed line. The dashed lines show the Inscription House area (fig. 65). Numbers in circles refer to locations discussed in chapter 3.

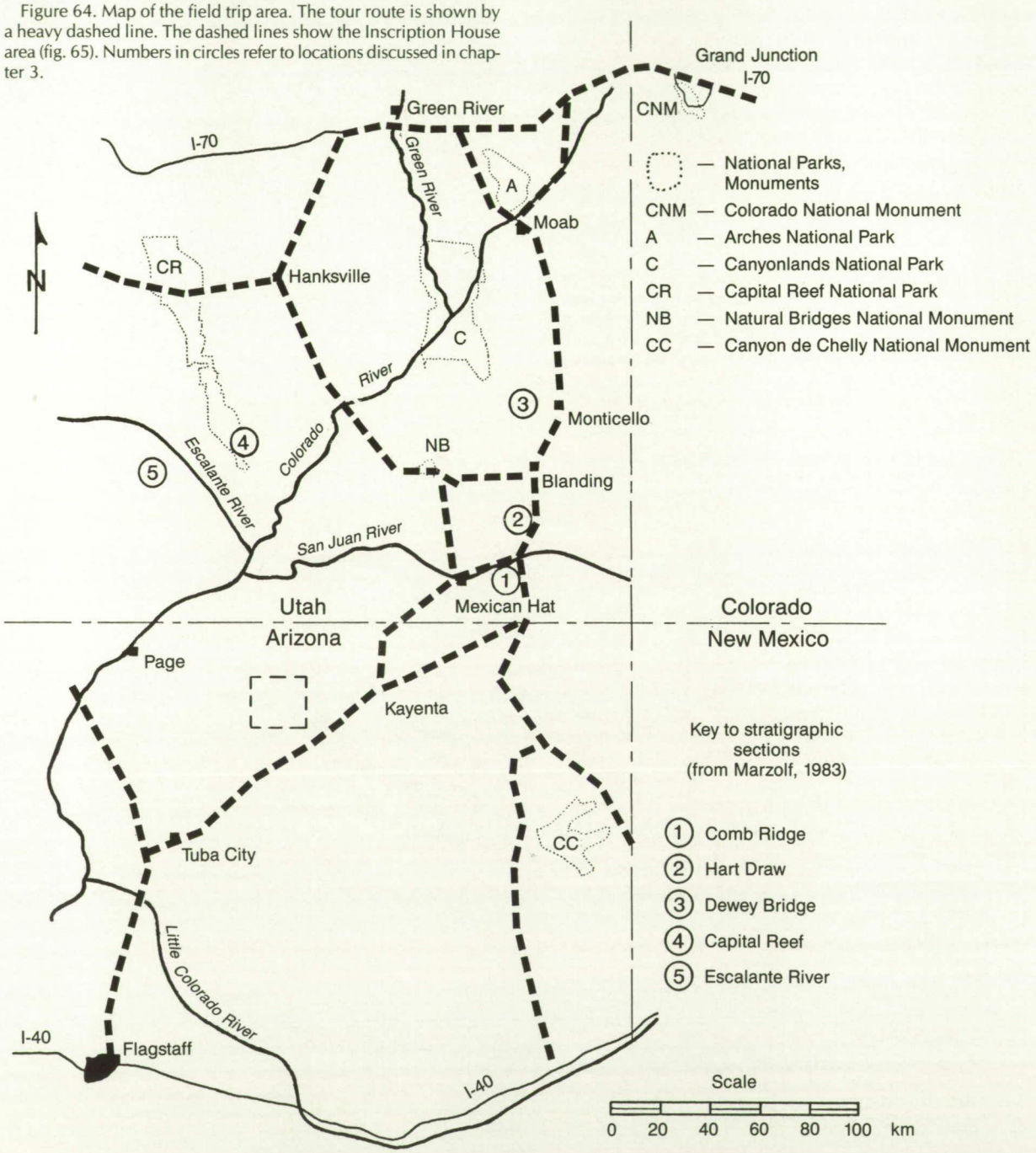

the Navajo Indian Reservation near the Inscription House Ruin (figs. 64–67).

The rocks in the mapped area slope gently to the southwest with dips of 1:80 to 1:40. The center of the mapped area is the crest of a very broad anticlinal flexure superimposed on the regional dip. The canyons are eroded into the Navajo Sandstone. The overlying shales and sandstones of the Carmel formation have been stripped from the Navajo over most of the mapped area except along the southern portions of the divide followed by the Navajo Mountain Road. The underlying flaggy siltstones, mudstones, and sandstones of the Kayenta Formation are exposed in the bottom of all canyons, indicating that the primary locus of backwasting is near this contact. The central sections of Geshi and Far End canyons have a secondary scarp in the center of the valleys developed in Wingate Sandstone exposed along the crest of the anticlinal flexure.

The Inscription House area exhibits the same types of features cited by Laity and Malin (1985) as evidence of sapping processes in a similar area about 50 km north along the Escalante River. These features include theater-shaped heads of first-order tributaries (fig. 59), relatively constant valley width from source to outlet (fig. 65-67), high and steep valley sidewalls,

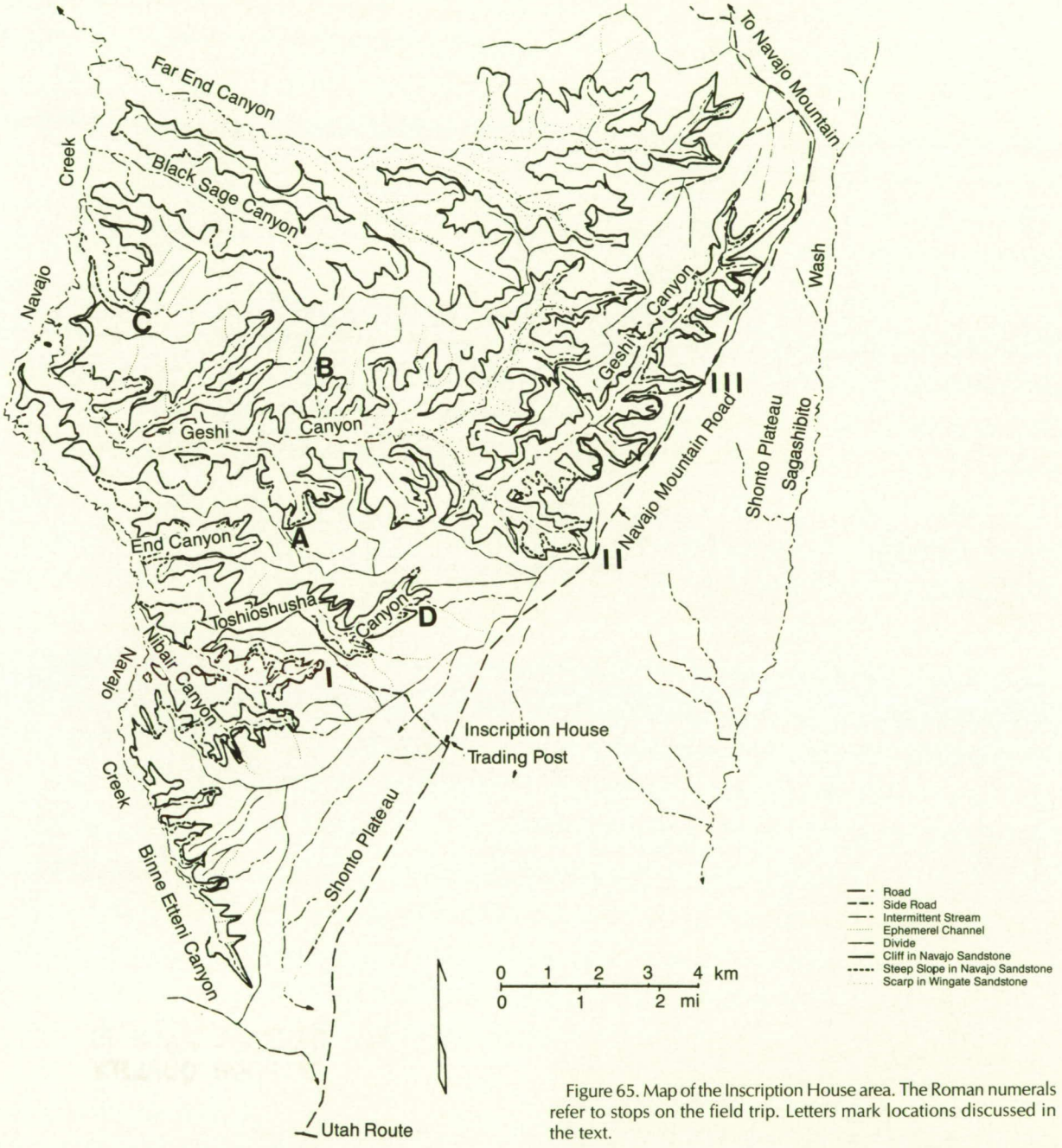

Figure 65. Map of the Inscription House area. The Roman numerals refer to stops on the field trip. Letters mark locations discussed in the text.

Figure 66. Topographic map of the area around Stop I at the Inscription House area.

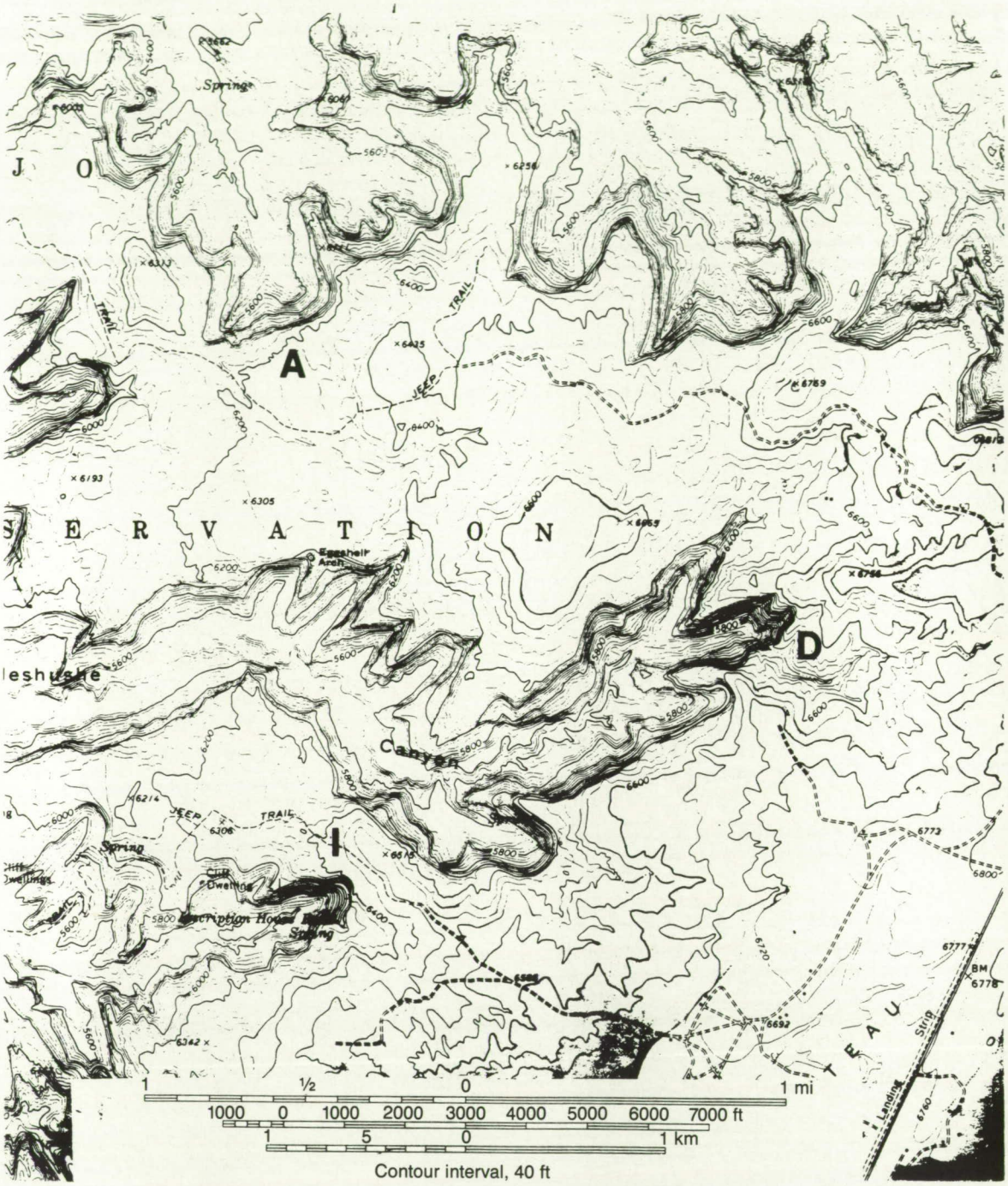

Figure 67. Topographic map of the area around Stops II and III at the Inscription House Area.

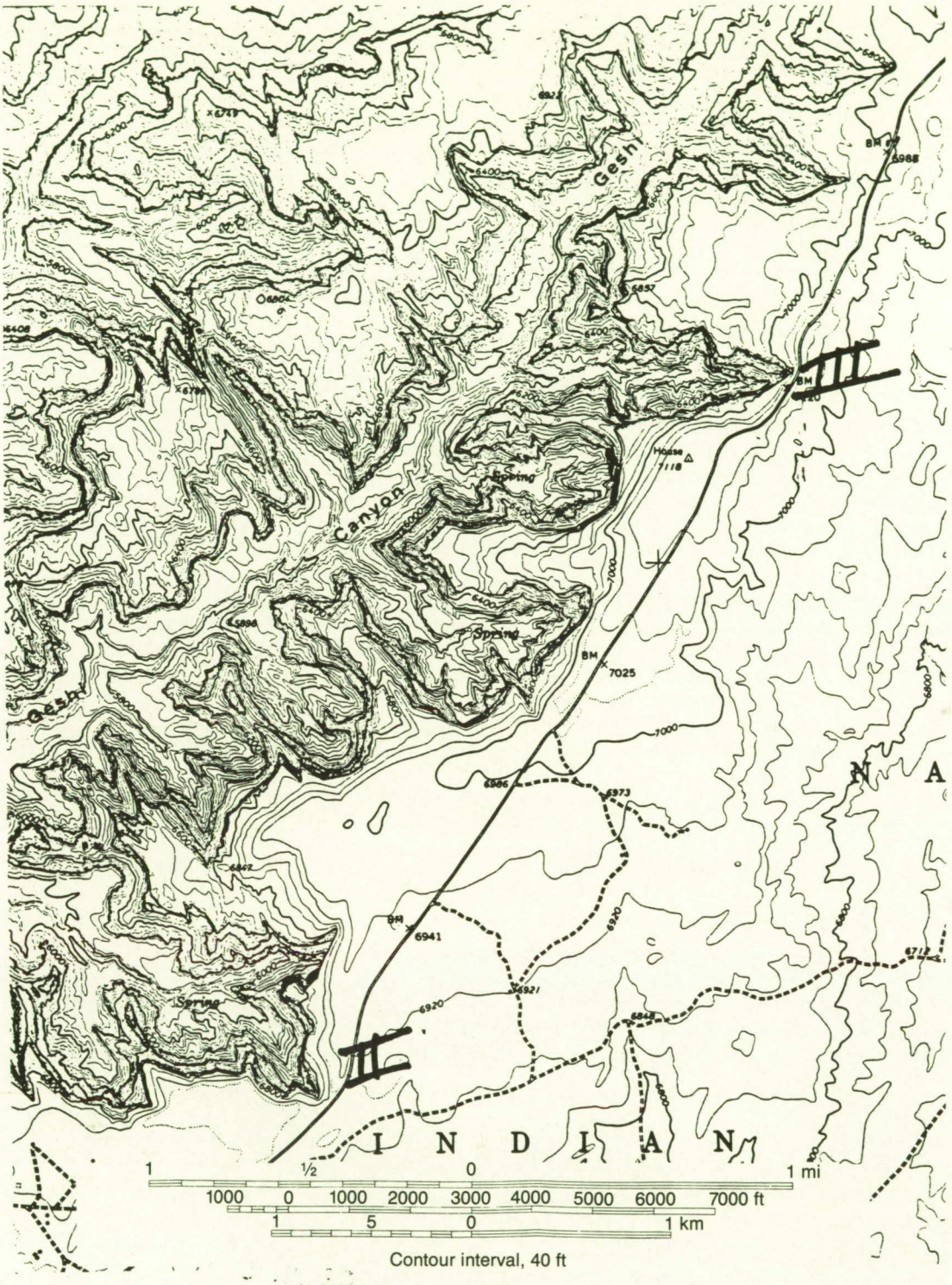

pervasive structural control, and frequent hanging valleys. The most direct evidence of sapping processes are the numerous alcoves, both in valley heads and along sidewalls (figs. 59 and 68). Springs are numerous on the valley walls and bottoms. Although many valley headwalls occur as deeply undercut alcoves, some terminate in V or half-U shapes with obvious extension along major fractures (fig. 69). Although sapping action is fairly evident where alcoves occur at valley heads, sapping may also occur in fracture-controlled headwalls. Evidence for erosion by streams passing over the valley headwalls is slight, and plunge-pools are not obvious. The valley extension along fracture traces suggests control by groundwater flowing along the fractures. The regional joint directions are a strike-oriented NW-SE and a dip-paralleling NNE-SSE set. The latter fracture system exerts the strongest control on the drainage network, with a tendency for valley development to extend updip such as the northeastern ends of Geshi and Tonleshusha Canyons (fig 65). In fact, a preponderance of the major valley heads are oriented updip, which is consistent with sapping by a regional downdip groundwater flow.

One striking feature of the canyon network is a frequent discrepancy between the extent of headward canyon growth and the relative upland area contributing drainage to the canyon head. For example, at A in figs. 65 and 66 a relatively large upland drainage area is associated with a minor canyon. The situations at B, C, and D are even more pronounced, since the upland drainage enters the side rather than the end of the canyon (figs. 65 and 66). Such circumstances suggest that groundwater flow, rather than surface runoff, controls headward extension of the canyons. In fact, such discrepancies are better illustrated in the Inscription House area than in the area studied by Laity and Malin.

Another indication of sapping control is the extension of canyons right up to major divides, such as at stops II and III (fig. 67). In fact, the divide has probably migrated slightly southeastward at II as a result of canyon extension. In contrast to surface runoff, groundwater flow can locally cross divides. Divide migration can also occur in surface runoff drainage basins, but is associated with the presence of slopes that are well graded from stream to divide. In the case of headward migration of canyons, streams above the scarp are perched on the upper slickrock slopes, so that base level control is very indirect.

The pattern of valley development and the relative contribution of sapping processes versus fluvial erosion is influenced by many structural, stratigraphic, and physiographic features. Infiltration may be restricted by overlying aquicludes where not stripped from the sandstone (Laity and Malin, 1985; chapter 4). The permeability of the sandstone is influenced not only by primary minerals, but by diagenetic cements and overgrowths. These secondary minerals vary considerably from layer to layer and location to location (Laity, 1983; chapter 4). Kochel and Riley (chapter 3) and Laity (chapter 4) discuss the important role of thin aquicludes (generally interdune deposits) and bedding strikes and dips in controlling groundwater flow through the sandstone. Primary and offloading (sheeting) fractures are important avenues of groundwater migration (Laity and Malin, 1985; chapters 3 and 4). On the other hand, dense primary

Figure 68. Numerous alcoves in Navajo Sandstone near Stop III in the Inscription House area (figs. 65 and 67).

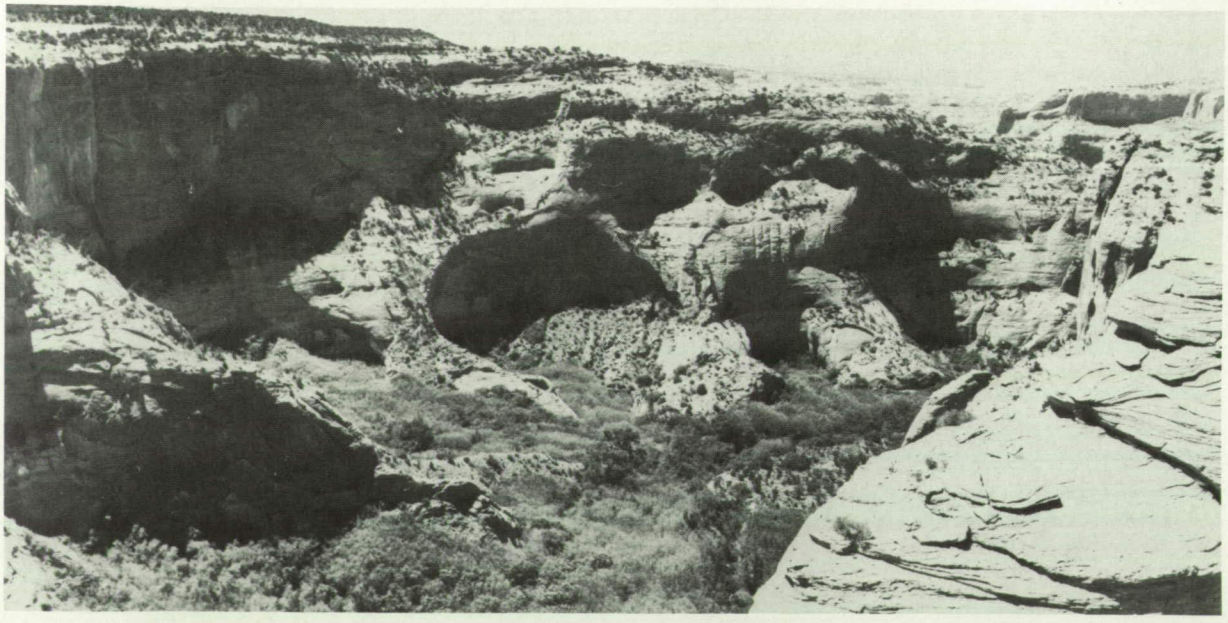

Figure 69. Fracture-controlled valley headwall at Stop III in the Inscription House area (figs. 65 and 67).

fracturing, such as in the Wingate Sandstone, restricts development of alcoves and probably diminishes weathering by cement solution and salt fretting (chapter 4). Sapping processes may still be important, but the spectacular alcoves commonly developed in the Navajo Sandstone are lacking. Relatively flat uplands on sandstones should encourage infiltration, whereas steep slickrock slopes probably lose much precipitation to runoff. Weather pits and thin covers of windblown sand may also encourage infiltration.

EFFECTS OF CLIMATIC CHANGE ON SCARP MORPHOLOGY AND SAPPING PROCESSES

Most recent discussions of scarp morphology and associated weathering and erosional processes have implied that the morphological elements can be explained by presently active processes (e.g., Koons, 1955; Schumm and Chorley, 1966; Oberlander, 1977). However, some escarpments in the Colorado Plateau region appear to be subject to considerably less caprock erosion under the present climate than during the late Pleistocene (Reiche, 1937; Ahnert, 1960; Howard, 1970).

The escarpment of Emery Sandstone near Caineville, Utah, is a case in point. Extensive old rockfall deposits on North and South Caineville Mesas, dissected at their margins as much as 50 m were interpreted by Howard (1970) to be Bull Lake equivalent in age (Illinoisan?) because some of the debris blankets interfinger with pediment deposits of Bull Lake age, whereas the remainder extend no further downslope than the level of the former pediment surface (figs. 35B, 70, and 71). The old debris blankets have been dissected by a similar amount and project concordantly laterally along the escarpment. Much of the scarp rampart is now devoid of extensive debris, so that extensive badlands have developed on the underlying Mancos Shale. In places, the cliff capped by the Emery Sandstone extends downward as much as 70 m into the underlying shale (fig. 35A). Koons (1955) demonstrates that the development of cliff faces in the nonresistant subcaprock unit is a normal occurrence in the cycle of rockfall, debris blanket erosion, and erosion of the subcaprock unit which triggers the next rockfall (fig. 37). However, for reasons outlined above, extensive cliff development in the subcaprock unit may also indicate stagnation of caprock mass wasting, whereas erosion of the subcaprock unit continues on the scarp rampart.

An outstanding example of such morphology is afforded by the escarpment capped by the lower units of the Morrison Formation overlying the thin bedded sand and shale beds of the Summerville Formation near Hanksville, Utah. Much of the escarpment is capped by a thin gypsum layer which is stable enough to support vertical cliffs up to 30 m high in the Summerville Formation (fig. 72C). The gypsum cap has been eroded into small crenelations mimicked in the underlying Summerville Formation (fig. 73), indicating that the caprock protects the vertical face from weathering and erosional processes. The rampart generally consists of debris-free badlands likewise carved in the Summerville Formation, which meet the vertical face at an abrupt angle. The rampart is bordered downslope by dissected pluvial (Bull Lake?) pediments paved with agate derived from the caprock, giving evidence that abundant debris was transported from the escarpment during that time. Where a caprock of gypsum is present, even a thick sequence of overlying sandstone sheds little debris onto the rampart. However, where the gypsum unit is discontinuous or missing (fig. 74), the overlying sandstone wastes by undermining and rockfall. However, during the pluvial climate the gypsum caprock evidently succumbed more readily to rockfall and occasional slumping (fig. 72). The scarps illustrated in photos 3 and 22 of Schumm and Chorley (1966) are probably examples of such presently inactive scarps.

In canyon areas, a cliff in a massive sandstone is often underlaid by a nearly bare rock slope with a gradient of about 30 to 40 degrees. No obvious lithologic break separates these slope elements. In some cases, such as at Canyon de Chelly, examples can be found where such bare rock slopes yield laterally to rock

Figure 70. Map of rockfall debris on the ramparts of the Emery Sandstone escarpment at North and South Caineville Mesas. Older rockfall debris correlates with dissected alluvial surfaces of Bull Lake age; these deposits are identified in the figure as Early Wisconsinan, but present thought suggests that they are Illinoisan. The younger rockfall debris is probably largely Wisconsinan. The older rockfall debris blankets are generally strongly eroded around their margins and stand in considerable relief above both the younger rockfall debris and relatively bare shale slopes on the ramparts. (From Howard, 1970.)

Figure 71. Pleistocene-age (Illinoisan?) rockfall on an escarpment of Emery Sandstone over Mancos shale on South Caineville Mesa near Hanksville, Utah. Note the heavy dissection of the lower end of the rockfall blanket. Note the remnant of a pediment of the same age in front of the escarpment on the left.

Figure 72. Cross-sections through the Morrison-Summerville escarpment showing presumed Pleistocene conditions compared to the present-day profile. During the Pleistocene pluvial backwasting of the caprock units by rockfall and block-by-block undermining was probably rapid, and the debris-covered rampart extended up to the caprock without tall vertical cliffs in the underlying Summerville Formation (cross-section A). Between rockfalls, weathering and erosion eventually removed the sandstone and gypsum debris, and a cliff would begin to form in the Summerville Formation (B). Because of the greater supply of water and lower temperatures, vertical cliffs higher than those in (B) were probably unstable, for another rockfall would return the escarpment to the conditions at (A). However, under the drier and warmer Holocene conditions, the gypsum caprock has become very resistant, and backwasting of the escarpment has essentially halted, with the result that the escarpment rampart is rapidly eroding away, leaving behind high cliffs in the Summerville Formation (C). (From Howard, 1970.)

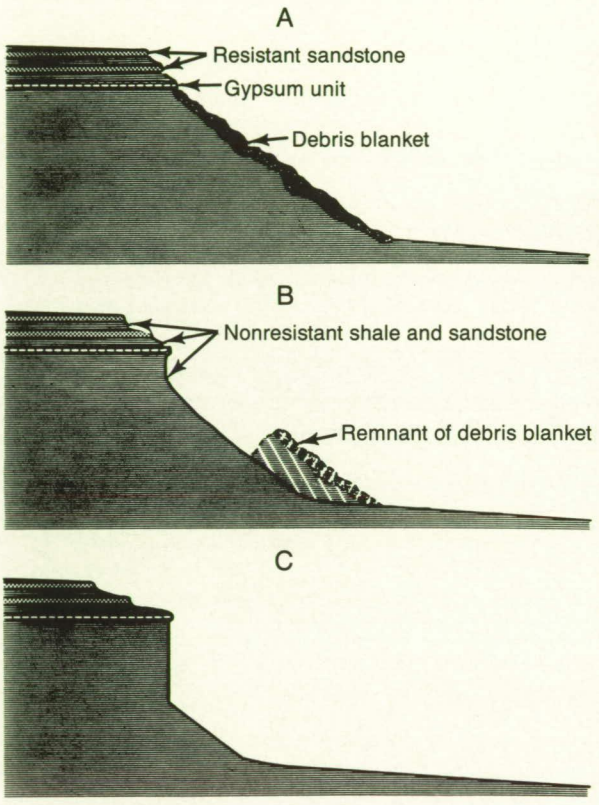

slopes of similar gradient but mantled with rockfall debris (fig. 75). A likely explanation is that the bare rock slopes were formerly mantled with rock debris produced by cliff retreat and that the debris mantle protected the underlying rock from weathering and erosion. The cover of debris on such slopes is now obviously inadequate to protect the rock from weathering and erosion, and the implication is that scarp backwasting is now relatively inactive, which has permitted the weathering and stripping of the former debris mantle. Somewhat similar forms can be found in the areas of segmented scarps in Entrada Sandstone at Arches National Monument (the area studied by Oberlander, 1977) (fig. 76). Oberlander interpreted the low-gradient slickrock slopes to be a normal feature of erosion of segmented scarps (fig.

Figure 73. Typical view of Morrison-Summerville escarpment at Sandslide Point off Utah Highway 95 near Hanksville, Utah, showing the cliff face extending into the weakly resistant Summerville Formation, the badland rampart in the same formation abutting the escarpment face, and the absence of debris on the rampart. Note that the rampart is shallowly underlaid by bedrock and is not a colluvial apron.

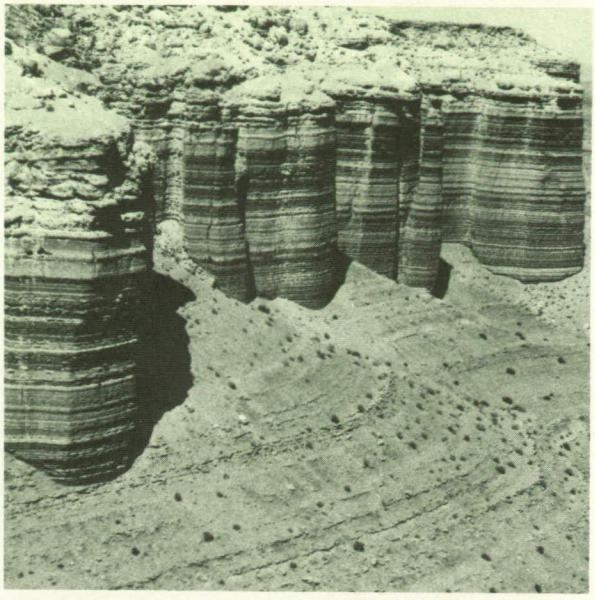

41), but it is possible that some of the slickrock slopes below vertical cliffs may have formerly been mantled by a debris blanket under a different climate (a scattering of debris can be seen in fig. 76).

Ahnert's (1960) historical interpretation of scarp morphology contrasts sharply with the "dynamic equilibrium" interpretations of Schumm and Chorley (1966) and Oberlander (1977). Ahnert suggested that scarp retreat occurs by erosion of shales and other weakly resistant layers by sapping-related processes that have only been active during pluvial episodes characterized by abundant, gentle precipitation. By contrast, he felt that slickrock slopes are eroded largely by sheetwash, which has been active during the sparse but intense rainfall of interpluvials. Ahnert felt that the generally sharp breaks between slickrock slopes and subjacent scarps was evidence of the noncontemporaneous origin of the two features, whereas Oberlander and the present authors feel that such sharp breaks can result from contemporaneous slickrock erosion and scarp retreat. Ahnert's assertion that slickrock slopes are eroded primarily by sheetwash misses the importance of the initial weathering that must occur on these weathering-limited slopes. This weathering, which makes debris capable of slopewash transport, is probably not optimal under the present climatic conditions of brief, intense rainstorms, but is favored by winter precipitation and freeze-thaw.

Despite these objections to Ahnert's interpretations, the examples presented previously suggest that there have been changes throughout the Pleistocene and

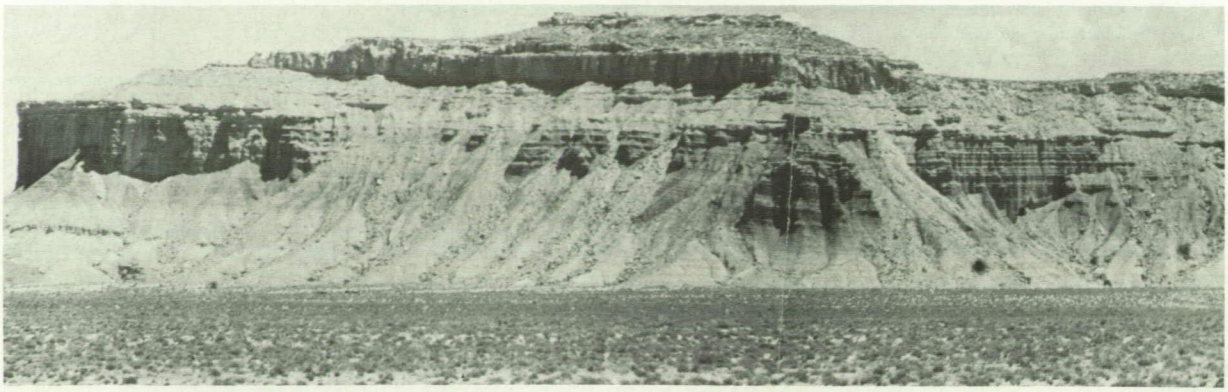

Figure 74. View of the northwest face of Goatwater Point, along Utah Highway 95 near Hanksville, Utah, showing rapid backwashing of the sandstones capping the Morrison-Summerville escarpment in the absence of the gypsum caprock. Vertical cliffs in the Summerville Formation occur only where the gypsum unit is present (especially on the left edge and center in the picture).

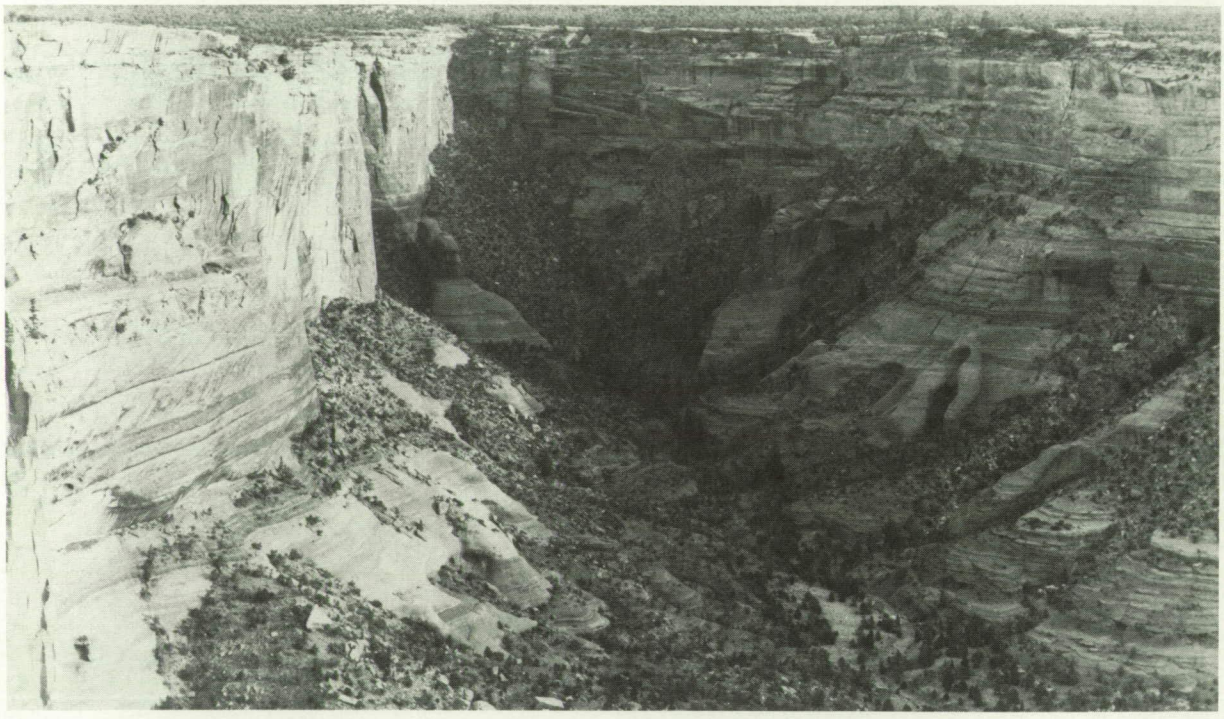

Figure 75. View of a small tributary reentrant to Canyon De Chelly, Arizona, showing prominent vertical cliffs in the upper parts of the De Chelly Sandstone with "slickrock" slopes of 30 to 40 degree inclination below the cliffs and also developed in the de Chelly Sandstone. Note the partial mantling of lower slopes with talus and the suggestion that the other slickrock slopes were formerly mantled.

Holocene in the relative rates of the major processes producing cuesta landforms: scarp undermining by sapping, undermining, or surface-directed weathering; weathering and erosion of rockfall debris; weathering and erosion of slickrock slopes; erosion of interbedded shale layers; and, locally, slumping and landsliding. Changes in the relative importance of these processes have produced landforms that in many cases can only be understood by knowledge of the temporal process changes (i.e., *relict* landforms). These examples of remnant effects of past climates add a complicating element to the interpretation of scarp morphologies. The difficulties in unravelling the geomorphic history of cuesta landforms are compounded by the paucity of stratigraphic evidence, because, unlike fluvial systems, few deposits carry records of past events and climates. The exception is rockfall debris, which contains few

Figure 76. Segmented scarps at Arches National Monument showing partial mantling of slickrock slopes with debris from overlying cliffs. (C) is a detail of fig. 39A. A possible interpretation of such slopes is that they were formerly (during pluvials) mantled with talus that has now been weathered and eroded but not replenished with fresh debris during the present arid climate.

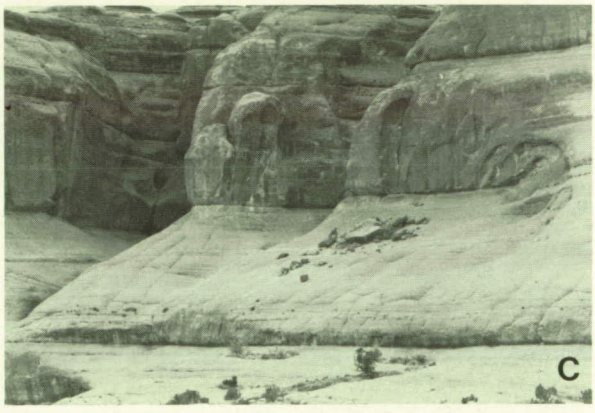

fossils, pollen, organic carbon deposits, or archeological remains, and which is very difficult to examine for stratigraphic relationships.

The occurrence of climatically relict landforms and differences between present and pluvial landform morphology have been discussed in a general way. The question is now directed more specifically to sapping processes and landforms, and to the relative importance of sapping at present compared to the pluvial epochs.

The greater rainfall during the pluvial maxima would suggest greater sapping activity then, but that same moisture supply would also contribute to surface-directed weathering, particularly freeze-thaw weathering. Also, more abundant groundwater does not necessarily produce more sapping in sandstones, because if seepage is sufficient and humidity high enough to permit runoff of the seepage, little salt accumulation will occur. However, other groundwater-related weathering processes would be enhanced by

greater available moisture, such as hydration and leaching of shale interbeds. Thus during the pluvial epochs we might expect more debris production by freeze-thaw, less alveolar weathering, but greater backwasting at the contact between sandstones and underlying shales and along shale interbeds. The present paucity of rockfall debris, rather than indicating nearly complete breakup and rapid weathering of the debris, as suggested by Schumm and Chorley (1966), may simply indicate the relative inactivity of many scarps in present climates. Certainly there are numerous examples of abundant rockfall debris produced by modern rockfalls (figs. 36 and 42).

The Inscription House area offers possible examples of relict landform elements. In some areas the Navajo Sandstone scarps give the appearance of weathering and erosion having cut through preexisting talus and now backcutting along limited portions of the scarp, producing alcoves (fig. 77). If this is the correct interpretation, then the localized sapping, alcoving, and alveolar weathering occurring at present contrasts sharply with pluvial epoch scarps with rapid talus production and more general backwasting. The pluvial-epoch backwasting processes may also have been strongly influenced by groundwater sapping, but primarily by shale weathering and scarp undermining.

Another prominent feature of the theater headwalls at seeps is the paucity of rockfall debris. This contrasts with abundant rockfall debris along the sides of the valley downstream from the seep (figs. 45B, 54B, and 78). Laity (chapter 4) suggests that both initial pulverization of rockfall debris and rapid weathering in the moist environment of the headwall account for the paucity of debris. However, recent rockfalls in alcoves generate abundant debris, and the rockfall debris along valley walls also suggests that the backwasting of scarp walls produces a considerable volume of coarse debris that must be further weathered before it is transported from the rampart and backwasting can continue. Erosion or pulverization from plunge pool activity also seems inadequate to account for the small volume of debris in the alcoves, because little plunge pool development occurs and the alcoves are much wider than the streams passing over the headwall. Thus, as suggested by Laity, particularly rapid weathering at the moist headwall causes rapid disintegration and removal of rockfall debris relative to the rates occurring on the dryer valley sidewall scarps. However, it is unclear why the rapid rockfall debris weathering and erosion are not accompanied by a similar enhancement of headwall sapping and alcove deepening by spalling. Somewhat different processes may be responsible for weathering of rockfall debris than those which produce the primary sapping erosion at the seep face. The weathering of the rockfall debris is likely to involve upward wicking of soluble salts from the seepage flowing at the interface of the rock and the overlying debris. This would produce an active zone of dry salt fretting within the debris (the overhang of the alcove often protects the debris from rainfall and the removal of the soluble salts). However, at the seepage face the constant supply of water would not allow deposition of strongly soluble salts, and the backwasting would have to occur by either deposition of less soluble minerals such as calcite (Laity, 1983) or solution of

Figure 77. Multiple alcoves in a theater-headed reentrant in Navajo Sandstone in the Inscription House area (fig. 65). Note the vegetation in the alcoves, the absence of fresh debris within the alcoves, and the presence of weathered rockfall debris (or possibly eolian deposits) on the finger-like projections between alcoves. These projections are probably bedrock-cored with thin mantles of rockfall or eolian mantles.

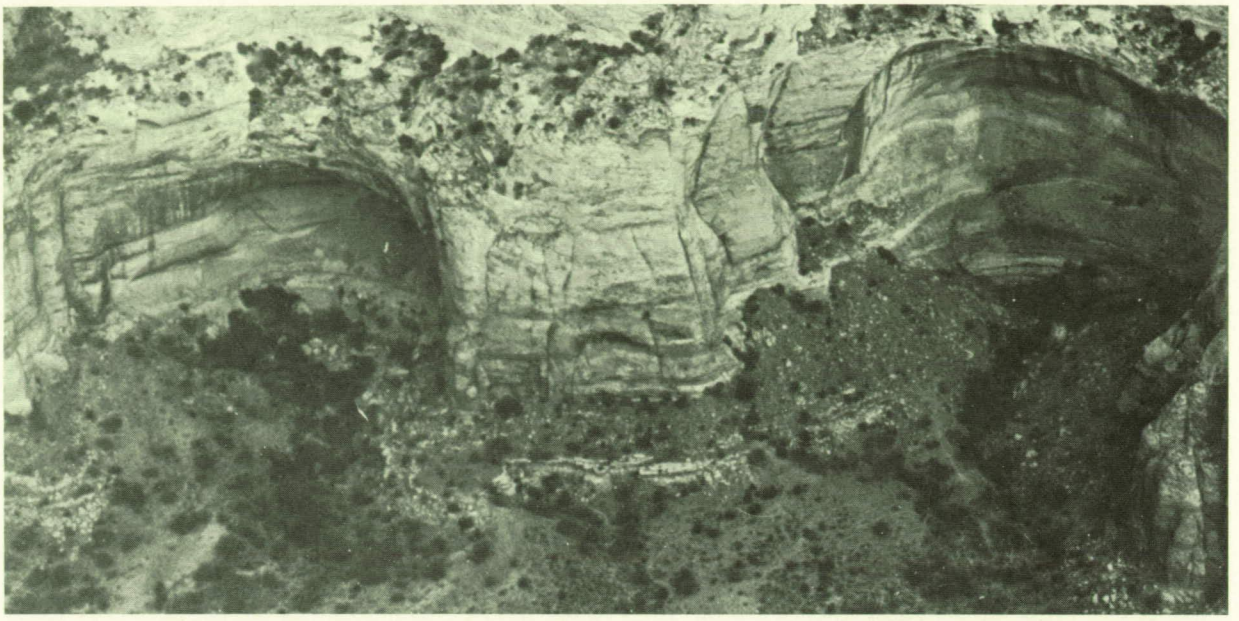

Figure 78. Twin alcoves in Navajo Sandstone in the Inscription House area (fig. 65). Note the absence of fresh rockfall debris within the alcoves, and the presence of weathered rockfall debris on each side of the alcoves.

the intergranular cement. Along the dryer sidewalls the rockfall debris would have less salt fretting and more through-flowing water leaching salts, whereas dry sapping at the base of the rock wall might encourage rockfalls. However, it is possible that the scarcity of recent rockfalls counterbalancing the rapid debris weathering is due to the present inactivity of the sapping erosion (the opposite of the interpretation offered in the previous paragraph). A moister climate might encourage more rapid sapping erosion while causing less enhancement of debris weathering.

The number and extent of active seeps in alcoves in the Navajo Sandstone appear to be less than would be expected for active valley development by sapping processes. Many major alcoves are presently dry or have small seeps that occupy only part of the alcove. Most of the alcoves in which cliff dwellings were built 800-1000 years ago by the Anasazi have few or no seeps. Although a dry environment may have been a factor in alcove selection, seeps must have been active at some time in the past to create the alcove. Similarly, rockfalls have occurred over only a few cliff dwelling ruins since their occupation, and most of those are small. The paucity of fresh rockfalls in general within alcoves on the Colorado Plateau has already been discussed.

Most active seeps in canyons carved into the Navajo Sandstone are located near the tops of cliffs on local interdunal aquicludes (figs. 59 and 80). These seeps are generally derived from very local sources; many of the seeps and associated alcoves occur immediately below surface washes that debouch over the canyon walls (figs. 45 and 59A). Many of these high-level seeps are not associated with strong alcove development (for example, the high-level seeps at the right edge of figure 80). The seeps associated with major alcoves at canyon heads at the contact with the subjacent Kayenta Formation are commonly smaller in volume than the overlying seeps, or are presently dry, suggesting that present volumes of recharge are insufficient to sustain a strong regional groundwater flow, although they are sufficient to maintain perennial streams in many of the canyon bottoms. Many of the present seeps occur either below the alcoves into the stream or its alluvium, or below the layer that defines the furthest zone of backwasting in the alcove. However, Holocene sedimentation has buried the lower portions of many basal alcoves (fig. 80); this burial may also be important in restricting backwasting. Also, many of the seeps at present do not extend across the full width of these basal alcoves. A wetter past climate would have favored the deeper regional groundwater flow and would have contributed to thicker and more extensive seeps.

These subjective observations on reduced levels of seep activity as compared to a past pluvial climate at the time of major alcove development and valley extension pertain primarily to canyons in the Navajo Sandstone in the northern Arizona portions of the Navajo Indian Reservation, such as around the Inscription House area (fig. 64). Basal seeps at canyon headwalls in tributaries to the Escalante River described by Laity and Malin (1985) appear to be more active than described above. However, Laity and Malin note that many sidewall alcoves are presently dry, and Laity notes in chapter 4 that sapping processes may have been more active in the past. The deeper canyons (and thicker Navajo Sandstone)

in the Inscription House area as compared to the Escalante River area (200 m compared to 130 m) may contribute to the difference, since vertical flow will be intercepted by more interdunal aquicludes. The box canyons carved into the Navajo Sandstone are so difficult to traverse that objective regional characterization of seep activity is impractical except locally, such as the fortuitous access afforded by Lake Powell to the canyons studied by Laity and Malin (1985).

Figure 79. Scarp in Navajo Sandstone northeast of Kanab, Utah. Note the abundant mass-wasting debris and the absence of alcoves and segmented scarps.

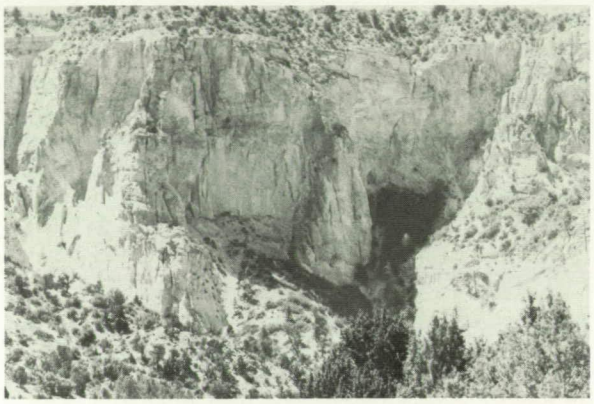

Figure 80. The head of Toenleshushe Canyon, showing deeply dissected alluvial fill. Wide-angle photo taken from near stop 1 (fig. 66). The depth of dissection is about 10 to 15 m. Also note prominent basal alcoves with seeps supporting dense vegetation and high-level seeps. Figure 59B is a detailed view of the valley head at left center.

The difficulties involved in interpreting the geologic history of slope processes will probably mean slow progress toward direct resolution of the question of relict landforms. Another approach might be to study the comparative morphology of scarps in different present-day climates. Such comparisons have their own problems in equivalence of lithology, structure, and relief. As an example of the potential usefulness and difficulties associated with this approach, Navajo Sandstone scarps northwest of Kanab, Utah, exhibit much less alveolar weathering and alcove development and more evidence of coarse physical weathering and talus production than in the Inscription House area, which lies at a similar elevation and in which the scarps have similar relief (fig. 79). It is uncertain whether these differences are due to climatic, structural, or lithologic factors.

Other methods might be used to assess the history of sapping processes on the Colorado Plateau and the degree to which sapping landforms might be relict. Detailed study of alluvial chronology in association with rockfalls (rockfalls burying alluvium and vice versa) could be used to estimate the relative frequencies of rockfalls (fig. 80). Similarly, the occurrence of rockfalls onto archaeological sites in alcoves can give an indication of the degree of recent rockfall activity in alcoves.

UNRESOLVED QUESTIONS AND RESEARCH OPPORTUNITIES

From the preceding discussion it should be evident that our understanding of the processes involved in sapping erosion is fragmentary, and that it is difficult to make conclusive statements about the past and present roles of sapping processes in scarp evolution on the Colorado Plateau, although there are strong indications that sapping processes are important and perhaps dominant in scarp retreat. Any studies of the processes or history of scarp processes would be welcome, particularly those involving the role of sapping and seepage.

The problems of interpretation become even more acute when we attempt to extrapolate to Mars from possible terrestrial analogs, because many of the morphological details indicative of sapping, such as alveolar weathering and alcove development, are not visible at the resolution of martian imagery. Furthermore, the great age of the fluvial features, together with landform modification by eolian and impact processes, means that many large-scale but subtle features, such as shallow drainageways on uplands, may have been obliterated. Even some of the large-scale features cited by Laity and Malin (1985) as being indicative of sapping processes must be regarded as tentative, such as the updip and downdip valley comparison discussed previously.

Quantitative morphometric characterization of scarp and canyon morphology may help to distinguish sapping-related features from those produced by runoff processes (Kochel et al., 1985). As an example, relatively constant down valley canyon width should be easily distinguishable from gradually increasing width downstream by plotting valley width versus order or drainage area. Another characteristic of scarp backwasting by sapping mentioned by Laity and Malin is that the rate of backwasting should in general be positively correlated with the drainage area contributing to the scarp face; this would not be true for scarp backwasting solely by surface attack. Conversely, backwasting by sapping implies that the removal of the last remnants of a caprock should be more difficult than earlier stages. Many gently dripping escarpments on the Colorado Plateau have a wide zone of thin salients, small buttes, and needles (fig. 61), with a classic example being Monument Valley. A high proportion of such forms may characterize sapping retreat of scarp fronts. Parts of the fretted terrain on Mars have a similar appearance. However, the research of Nicholas and Dixon (1986) demonstrates that variable density of rock fracturing affecting rock strength may also be an important factor leading to the development of isolated buttes; some of the fretted terrain on Mars has clearly developed by erosion localized along fracture zones (although sapping dominated by groundwater flow through the fractures could be the controlling process).

Recent studies by Kochel and Piper (1986) have shown that morphometric parameters can be used to distinguish between runoff-dominated and sapping-dominated valleys on Hawaii. Figure 81 shows an example of principal component analysis applied to valleys on the islands of Hawaii and Molokai. These plots show a clear separation in most cases between runoff and sapping valleys. Table 1 summarizes the mophologic and morphometric attributes of sapping and runoff valleys formed in Hawaiian basalts.

Table 1. Morphologic Comparison of Hawaiian Valleys

Parameter	Runoff dominated	Sapping dominated
Basin shape	Very elongate	Light bulb shaped
Head termination	Tapered, gradual	Theater, abrupt
Channel trend	Uniform	Variable
Pattern	Parallel	Dendritic
Junction angle	Low (40°–50°)	Higher (55°–65°)
Downstream tributaries	Frequent	Rare
Relief	Low	High
Drainage density	High	Low
Drainage symmetry	Symmetrical	Asymmetrical
Basin area/canyon area	Very high	Low

Experimental development of sapping stream networks also permits qualitative or quantitative comparisons with possible martian analogs, and such an approach is being pursued. Such experiments offer the advantage of controlled conditions and known structure and material composition, but they are somewhat limited by small physical size and problems of scaling to the target (martian) features.

One approach to moving from strictly qualitative comparisons is to model scarp retreat numerically, making assumptions regarding the processes involved, structural influences, and lithologies. A fairly heuristic approach to such modeling is discussed in chapter 5.

ROAD LOG

The sapping road log follows the field trip as it occurred. Suggestions for additional stops and side excursions are included. George Billingsly provided valuable information on stratigraphic nonmenclature.

Day 1

Mile 0 Junction of US 89 and US 180 at the east end of Flagstaff, Arizona. Proceed North on US 89. The route is shown in fig. 64 by heavy lines. The initial portion of the tour route passes over Quaternary

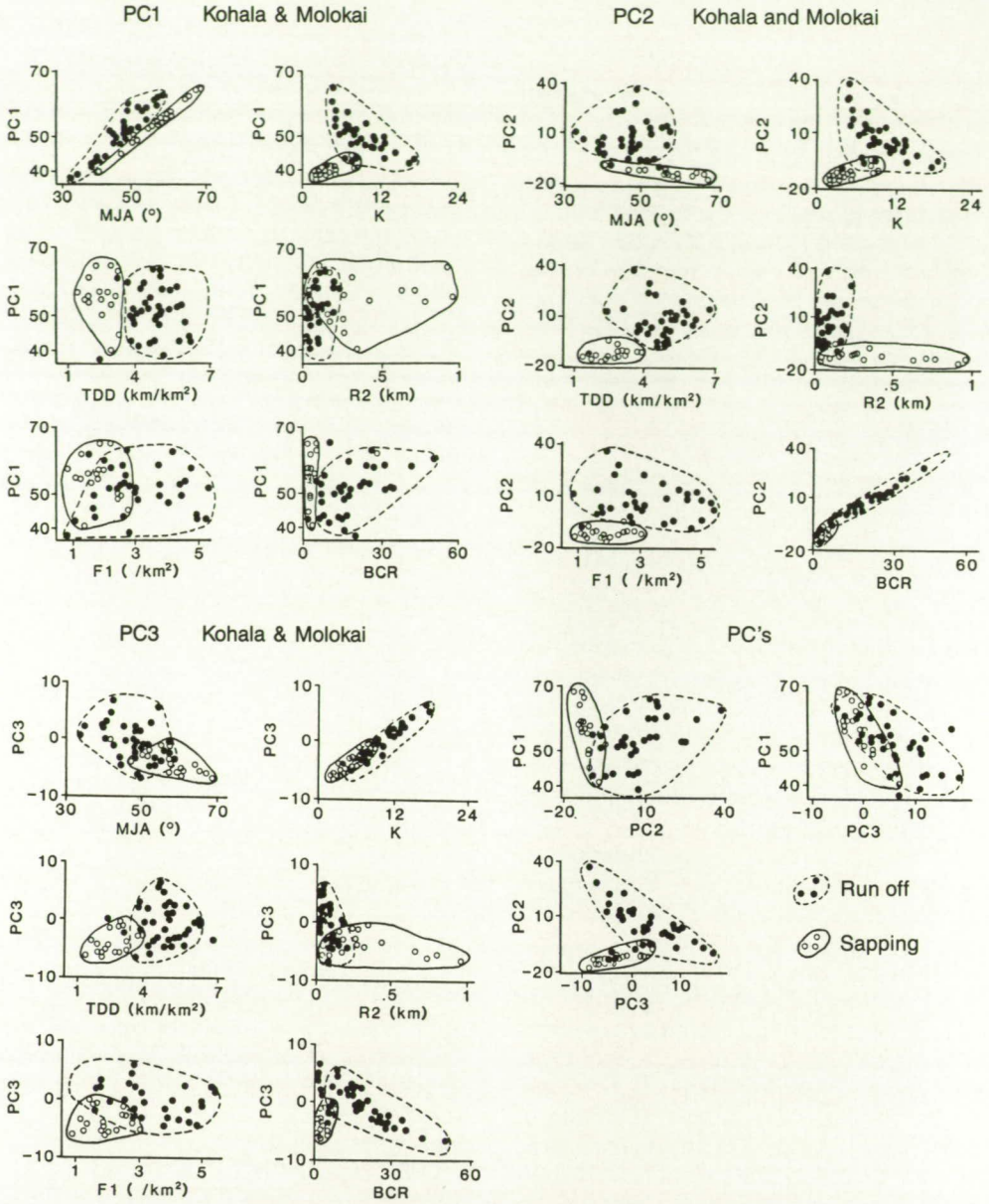

Figure 81. Principal component analysis of drainage basin morphometry on parts of the islands of Hawaii (Kohala area) and Molokai. Basins containing large deep canyons with abrupt headwalls are classified as "sapping," whereas shallower basins with a more linear profile are classified as "run-off." The variables measured on these basins are the mean junction angle (MJA), the basin shape as a lemniscate (K), the total drainage density (TDD), the cross-sectional basin relief measured at mid-basin (R2), the first-order channel frequency (F1), and the ratio of the total basin area to the area of the canyon (BCR). The measured values of these variables for individual basins are plotted against the principal component score for each basin for the first three principal components. Principal component scores for the first three components are also plotted against each other. The database for the principal components incorporated additional variables of basin morphometry not included in the plots. Although in this analysis the initial classification of the basins into sapping versus runoff was subjective, a distinction between the two basin types is consistently manifested in the principal component scores. Objective statistical classification techniques are now being investigated.

volcanic features associated with the San Francisco Peaks.

Mile 11.6 Sunset Crater loop road. Stay on US 89. (The Sunset Crater area is a nice sidetrip to see young basaltic flows and cinder cones.)

Mile 25.9 Other end of Sunset Crater loop road. Stay on US 89.

Mile 35 The road drops off Quaternary basalt flows onto the Moenkopi Formation and Kaibab Limestones.

Mile 46.8 Junction of US 89 and AZ 64. Stay on US 89.

Mile 51.4 Badlands in Chinle Formation.

Mile 61.4 [0] Junction of US 89 and US 160. Turn right onto US 160 and reset the mileage counter. The road now climbs upward in section through Moenave and Kayenta Formations onto plateau on Navajo Sandstone mantled with eolian deposits. Over the next 50 miles the road passes near Tertiary and Quaternary geomorphic surfaces (pediments) mapped by Cooley et al. (1969).

Mile 35 The road lies on Navajo Sandstone with an eolian mantle. Black Mesa, capped with Cretaceous shales and sandstones, lies to the southeast of US 160 for the next 30 miles.

Mile 49.7 [0] Junction of US 89 and AZ 98. Turn left onto AZ 98 and reset the mileage counter.

Mile 12.1 Junction with NAV 16, the road to Navajo Mountain. Turn right onto this dirt road. You are entering the area shown in fig. 65.

Mile 17.5 Inscription House Trading Post. Four-mile round trip on dirt road to overlooks of Toenleshusha Canyon and Inscription House Canyon areas with excellent examples of alcove development. Inquire locally for road shown on map. Discussion themes: slickrock versus undercut morphologies; discrepancies between surface drainage and pattern of valley extension; processes of sapping and alcove development; role of fractures, crossbeds, and impermeable interbeds in controlling sapping processes; role of sheeting fractures in controlling slickrock topography and alcove development; entrenched valley fills. (figs. 9, 13, 14, 36B, 59, 67, and 80)

Mile 22.5 [0] Return to NAV 16 and turn left (north), resetting mileage counter.

Mile 2.9 Brief STOP to look out over deep canyon in Navajo Sandstone. Small alcoves, but valley head not alcoved due to prominent fracture(s). Discussion question: are sapping processes important in strongly joint-controlled headwalls? (fig. 67).

Mile 5.3 STOP at deep canyon in Navajo Sandstone. Hike down to valley overlook. Discussion of evidence for seepage in alcoves, nature of sapping processes, development of alcoves, differences in morphology in strongly jointed versus massive sandstones, and role of sapping in strongly jointed sandstones. Discussion of large-scale features indicative of sapping. Backtrack to US 160. (figs. 67-69)

Mile 28.1 [0] Junction of AZ 98 and US 160. Left onto 160 and reset mileage counter.

Mile 12.6 [0] Junction of US 160 and AZ 564. Reset mileage counter.

Optional sidetrip. Turn left onto AZ 564. The road climbs a steep dip slope on top of Navajo Sandstone.

Mile 5.6 Top of monocline. STOP at solution pits developed on nearly flat-lying plateau of Navajo Sandstone. Discussion theme: processes developing solution pits—factors controlling size—secondary jointing similar to mudcracks—possible role of eolian fills in larger weather pits—effect of surface gradient—"beaded" drainage and solutional grooves—relative amounts of rainwater loss through evaporation versus infiltration—role of solution pits to introduce through-flowing water into sandstone, contributing to sapping on sideslopes—why are solution pits developed strongly on some Navajo Sandstone exposures, whereas other nearly flat surfaces have none?

Mile 9.1 Optional continuation to Navajo National Monument with 1-hour roundtrip walk to Betakin alcove overlook. Return to US 160. (figs. 10, 11, 24, and 55)

Mile 11.2 (18.2) [0] Junction of AZ 564 and US 160. Turn left onto US 160 and reset mileage counter.

Mile 0-5 Continuing on US 160, notice large landslides in Cretaceous shales and sandstones to the right of the road for the next 5 miles.

Mile ≈4.8 Brief STOP to view beaded drainage and solutionally deepened rills on dip slope of Navajo Sandstone to the left. Discussion theme: relative roles of corrasional and solutional fluvial erosion in rills on slickrock slopes. (figs. 21 and 25)

Mile ≈9.0 Note intrenched valley fills of Laguna Creek on the left. The valley is not intrenched further upstream.

Mile 23.3 [0] Junction of US 160 and US 163 at Kayenta. Overnight stop. Reset mileage counter. Turn left on US 163.

Day 2

Mile 2.4 STOP at entrenched fills of Laguna Creek. Note extensive piping and futile attempts at control using old automobiles, etc. Some structural grabens formed as a result of undermining by piping. Discussion theme: contrast the corrasional development of

piping with groundwater sapping processes in sandstone. Also note that piping seems limited to clay-rich alluvium, although sapping probably is important in valley-head extension in dissected sandy alluvium.

Mile 10.6 Escarpment of Navajo over Wingate over Chinle. Escarpment primarily backwastes by rockfall rather than alcoving due to pronounced vertical jointing in Wingate. Discussion theme: is some form of sapping important in such rockfall-wasted scarps?

Mile 17.7-18.6 STOP to discuss role of undermining in creating vertical slopes and alcoves in De Chelly Sandstone. Where the shaly Organ Rock tongue is not exposed at the scarp base, the De Chelly has typical slickrock morphology, but this is being eaten back into by cliffs where underlying Organ Rock is exposed. Discussion of Ahnert's climatic change hypothesis. (fig. 26)

Mile 27 Heart of Monument Valley. Possible picture stops. The "monuments" are composed of thin caprock of Shinarump Conglomerate (Chinle Formation) over a thin layer of shaly Moenkopi Formation over prominent vertical cliffs in the De Chelly Sandstone (Cutler Formation) and underlaid by ramparts of Organ Rock member (Cutler Formation). Ahnert suggests that the monuments are not actively backwasting due to a scarcity of debris from the De Chelly Sandstone. Most rocks on the Organ Rock ramparts are the very resistant Shinarump and are commonly on pedestals (damoiselles). Ahnert suggests more active backwasting by spring sapping during the pluvials. Notice that small "mittens" and the end of linear mesas produce less debris on the ramparts than along straight or indented portions of the scarps, due to a smaller area of cliff per area of rampart.

Mile 30-40 The road gradually passes down through Organ Rock Member, Cedar Mesa Sandstone Member, and Halgaito Tongue (shaly) of Cutler Formation and onto the Honaker Trail Formation (formerly the Rico Formation).

Mile 44.0 Bridge over the canyon of the San Juan River at Mexican Hat.

Mile 48.0 [0] Junction of US 163 and UT 261. Left turn onto UT 261 and reset mileage counter. View of dissected monoclinal flexure to the right exposing lower Cutler and underlying Hermosa Formation.

Mile 0.9 Junction with road to overlook of San Juan River goosenecks. (Optional sidetrip to gooseneck overlook.) Continue on UT 261.

Mile 7.4 Begin steep climb in valley headwall developed in Cutler Formation (Permian). Lower slopes in Halgaito Tounge, Organ Rock Shale, and caprock of Cedar Mesa Sandstone. The valley is only vaguely theater-headed, probably due to the thin-bedded nature of sandstone layers with shale interbeds and partings, which limits downward percolation.

Mile 8.9 STOP along the road in cliffs of Cedar Mesa Sandstone. Well-developed cavernous weathering and sapping in sandstones at contacts with underlying shaly units. Note salt concentration in crusts in tafoni and evidence of active spalling. Sapping is probably important in backwasting of thin-bedded sandstones despite lack of alcoves and strongly theater-headed valleys. Note the paucity of evidence of active fluvial erosion by plunge pools. The profile of the Cedar Mesa scarp is moderately convex, probably due to more rapid wasting at the top due to sapping processes in upper layers (groundwater is restricted from percolating lower due to shale interbeds).

Mile 9.1 Brief stop at overlook. View of monocline and Mexican Hat.

Mile 9.5 [0] Muley Point overlook turnoff. Reset mileage counter.

Mile 3.8 Time-permitting round trip to Muley Point. This side excursion can also be taken on the return portion of the trip. STOP at the overlook of Monument Valley and goosenecks of the San Juan River. Pronounced development of solutional pits, some very deep, on sandstones capping escarpment. Good slickrock morphology. Also backwasting of escarpment by calving of very large joint-bounded blocks. (figs. 18-20 and 31)

Mile 5.1 End of the road at Muley Point. STOP for magnificent views. Return to UT 261.

Mile 10.2 [0] Turn left onto UT 261. Reset mileage counter.

Mile 22.7 [0] Junction of UT 261 and UT 95. The high ridge to the north is underlaid from bottom to top by upper Cutler (de Chelly), Moenkopi, and Chinle Formations (with cliffs in Mossback Member). The "Bears Ears" at the crest of the escarpment are in Wingate Sandstone. Turn left onto UT 95 and proceed to Natural Bridges National Monument (NBNM). Reset mileage counter.

Mile 1.8 Turn right off UT 95 onto UT 275 toward NBNM.

Mile 18.3 Continue to NBNM and take the loop drive, returning to UT 95 and turning east. Discussion theme: well-developed slickrock and alcoving in canyon walls in Cedar Mesa Sandstone, sometimes resulting in natural bridges. Good illustration of most of the morphological features discussed by Oberlander. (fig. 38)

Mile 20.1 [0] Junction of UT 95 and UT 261. Continue on UT 95 and reset mileage counter. At approximately mile 9 cross the Comb Ridge Monocline and rise rapidly into Jurassic-Cretaceous strata.

Mile 29 [0] Junction of UT 95 and US 163. Turn north and reset mileage counter. The road from here to beyond Monticello generally lies on Cretaceous Dakota and Burro Canyon Formations (mostly sandstone), locally mantled by pediment and fan deposits from the Abajo mountains to the northwest. Local eolian mantling. Morrison Formation exposed in deeper valleys.

Mile 4 Blanding

Mile 21 Monticello. Overnight stop.

Day 3

Mile 21 Continue north on US 163.

Mile 34 Road drops sharply off Cretaceous sandstones, through the Morrison Formation onto alluvial plain developed on the Entrada Formation. Steep buttes in the Slick Rock Member of the Entrada Formation are visible on both sides of the road. These are often sculpted into deep alcoves and thin projecting fins.

Mile 39 [0] Junction of US 163&191 with UT 211. Reset mileage counter and turn left onto UT 211.

Mile 10.9 STOP at alcove along ephemeral stream in massive Navajo Sandstone. Active seep below stream in alcove. Ephemeral stream with weather pits or waterpockets in stream bed. The stream bed in the area of waterpockets is steep and devoid of alluvium, although the bed is gravelly alluvium upstream. Discuss the relative roles of macroturbulence (kolks) and solution in creating the waterpockets. Return to US 163&191. (figs. 22 and 45A)

Mile 21.8 [0] Junction of UT 211 and US 163 and 191. Turn left onto US 163&191. Reset mileage counter.

Mile 6.7 [0] Junction of UT 211 with the road to Needles Overlook. Reset counter and turn left onto Needles Overlook Road.

Mile 7.5 Pull off onto short dirt road leading to strongly alcoved exposure of Entrada Sandstone after passing several examples of alcoves in the same formation en route. Well-developed tafoni and honeycomb weathering. Good examples of salt crusting and spalling. Good examples of surface wash and possible resulting case-hardening preventing tafoni development in otherwise ideal circumstances. Discussion topic: role of surface wash in developing alveolar weathering. (Optional 8.4-mile roundtrip to Needles Overlook). Return to US 191&163. (figs. 50-52 and 60)

Mile 15.0 (23.4) [0] Junction with US 191&163. Turn left and reset mileage counter.

Mile 2 Casa Colorado Rock in Entrada Sandstone about 2 miles east of the highway (no stop). Pronounced alcove and fin development, with deep natural cisterns on top of rock. Cisterns may be precursors to the development of arches.

Mile 2-17 Good views of alcoving and natural arches in Entrada Sandstone.

Mile 7.5 Junction with UT 46. Continue on US 191&163.

Mile 17.8-33.4 Fault grabens and salt anticlines. Discussion of their origin and possible analogs to martian grabens.

Mile 33.4 Moab.

Mile 35.4 Junction with UT 128. Continue on US 163&191.

Mile 39.1 [0] Entrance to Arches National Park. Reset mileage counter. Turn right into park and visit Courthouse and Windows sections. Contrast of slickrock slopes on Navajo Sandstone with blades, alcoves, and arches of Entrada Formation. Tafoni and spalling in incipient arches. Discussion of Oberlander paper—role of joints, shaly beds in landscape morphology. Comparison of slopes on Entrada and Navajo Formations. (figs. 39, 40, and 76)

Mile 23.4 Return to US 163&191. Turn left onto US 163&191. Continue 2 miles to junction with UT 128. (Optional sidetrips to Dead Horse Point, Grandview Point, or potash workings.)

Mile [0] Turn left onto UT 128 and reset mileage counter.

Mile 0-35 The road follows the canyon of the Colorado River, which here flows across a broad anticline. The road crosses Navajo, Wingate, Chinle, Moenkopi, and Cutler Formations and then back upward through the section, eventually into the Cretaceous sandstones and shales.

Mile 50 Junction with I-70. Turn east onto I-70. Bluffs in Cretaceous sandstones and shales of Mesaverde Group to the north of the road.

Mile ≈102 [0] Grand Junction and Airport. Overnight stop. Reset mileage counter.

Day 4

Approximately 20-mile side trip through Colorado National Monument with good examples of theater-headed valleys in Wingate, Kayenta, and Entrada Formations. (figs. 44 and 46)

Return to I-70 and turn west, continuing past the junction with UT 128 (mile 58), past Green River (mile 111), Utah, to junction with UT 24.

Mile 143 Turn south onto UT 24. Pass through badlands in Morrison Formation. Note the spectacular monoclinal east limb of the San Rafael Swell to the west, exposing hogbacks in Navajo and Wingate Formations. Cross the San Rafael River. The road climbs onto broad desert with extensive eolian mantle on En-

trada Formation (miles 160-180). Most of the sand is probably derived from this formation.

Mile ≈163 Pass the turnoff to Goblin Valley. Goblin Valley is an excellent example of hoodoos in the Entrada Formation.

Mile 188 [0] As Hanksville is approached, note isolated buttes in the Entrada Formation and, to the west of the road, cliffs of the Summerville Formation capped by the lower part of the Morrison Formation. The laccolithic Henry Mountains are visible to the south. Reset mileage counter at Hanksville. At Hanksville continue west on UT 24.

Mile 12 After climbing escarpments in the Summerville Formation capped by Morrison (note occasional slumps), rounded badlands in variegated montmorillonitic shales of the Morrison Formation and prominent escarpment of Ferron sandstone over Tununk shale (Cretaceous), turn left onto prominent terrace of the Fremont River. Good view of the Fremont River, three levels of pre-Wisconsonan gravel fill terraces of the Fremont, and the 800 to 1000 foot high escarpment of the Emergy Sandstone over Blue Gate shale (Cretaceous). Note the steep, linear-sloped badlands with knife-edged divides in the illitic Blue Gate shale. The badlands have formed from dissection of a pediment graded to the lowest prominent terrace, of Bull Lake age (Illinoisan?). Some remnants of this pediment are visible. The Emery sandstone escarpment primarily backwastes by rockfall and avalanching, but the backwasting is less active now than during the Bull Lake pluvial. To the west, the lava-covered plateaus of Thousand Lake and Boulder Mountain are visible. The latter was glaciated during the Bull Lake pluvial. (figs. 35 and 71)

Mile 19 Continue west on UT 24. Just before the road bends at a hogback of the Ferron Sandstone, pull off the road on the right and climb to the top of the prominent terrace of Bull Lake age. Good examples of the formation of badlands by dissection of the Bull Lake pediment and of dissected rockfalls of the same age on the ramparts of the Emergy Sandstone escarpment.

Optional roundtrip to Capital Reef National Park, following upstream along the Fremont River as it passes downward through the geologic column section through prominent eastward-dipping monoclines (the Waterpocket Fold). Excellent examples of tafoni in exposures of Navajo Sandstone near road level. Also good examples of domal topography in Navajo Sandstone with strong joint control (the "Capitals"). (figs. 48 and 49)

Mile 38 [0] Return to Hanksville, reset mileage counter, and turn south onto UT 95.

Mile 11 Travel for several miles on exposures of the Entrada Formation mantled with eolian sands. Stop at the view of escarpments of the Summerville formation capped with Morrison gypsum and sandstone to the west of the road. This escarpment has been largely inactive in backwasting since the last major pluvial. (figs. 33, 73, and 74)

Mile 26 [0] Continue on UT 95, passing dissected pediments from the Henry Mountains and hoodoos in the Entrada Formation. Turn left onto UT 276 and reset mileage counter. Overnight stop at Ticaboo (mile 27) or Bullfrog Basin (mile 40).

Day 5

Mile [0] Return to UT 95 and reset mileage counter. Turn south on UT 95. The road follows downstream in the canyon of North Wash, descending the geologic column through the Carmel, Navajo, Kayenta, Wingate, Chinle, and Moenkopi Formations, eventually reaching the Colorado River at Hite.

Mile 3.2 Stop along UT 95 and hike to the northeast to the head of a prominent theater-headed alcove with active seep (approximately 1.5 mile roundtrip). Note the impressive alcove, lack of plunge pool of small stream passing over scarp, and paucity of rockfall debris at the base of seep and alcove (as contrasted with abundant rockfall debris along valley sidewalls). Minor theater headwalls with largely dry alcoves are passed along the hike. (figs. 45B and 56).

Mile 13.9 and 15.1 Continue southeast on UT 95. Turn off for scenic views of Lake Powell.

Mile 20.3 Cross the Dirty Devil River (also known as the Fremont River). The bridge is on the Cedar Mesa Sandstone.

Mile 22.3 Cross the Colorado River.

Mile 23.5 Hite Marina turnoff. Continue on UT 95. Over the next 70 miles the road follows a stripped surface on the Cedar Mesa Sandstone. Bluffs to either side of the road expose, in ascending order, the upper Cutler Formation (Organ Rock Member), the Moenkopi Formation, the Chinle Formation, and, on the highest mesas, the Wingate Sandstone.

Mile 37.4 Overlook into canyon carved in Cedar Mesa Sandstone to the left, with good exposures of tafoni. (fig. 53)

Mile 46.4 Settlement of Fry Canyon.

Mile 58.5 Junction with UT 263, the Halls Crossing Road. Continue on UT 95.

Mile 66 Junction with UT 275, the Natural Bridges National Monument road. Continue on UT 95.

Mile 67.8 [0] Junction with UT 261. Turn south onto UT 261, retracing an earlier part of the trip as far as the junction with US 163. Reset mileage counter.

Mile 33 [0] Junction with US 163. Turn left onto US 163 and reset mileage counter.

Mile 15.8 Pass through Comb Ridge Monocline which successively exposes at the Cutler, Moenkopi, Chinle, Wingate, Kayena, and Navajo Formations.

Mile 18.1 Junction with US 191. Turn south onto US 191. After crossing the San Juan River, the road lies on sand-mantled Navajo Sandstone, with the bluffs to the east exposing the Carmel, Entrada, Summerville, Bluff, and Morrison Formations.

Mile 47 Turn right (west) at the junction with US 160, passing through Mexican Water. The road still lies on Navajo Sandstone.

Mile 49.6 Turn left (south) onto US 191.

Mile 75.0 Alcoves in Navajo Sandstone are visible to the left. The road now drops in the stratigraphic section, exposing the Kayena Formation, the cliff-forming Wingate Sandstone, and finally the Chinle Formation.

Mile 85.1 Junction with NAV 12 at Round Rock. Continue on US 191. The road from here to Chinle lies on the Chinle Formation, locally eroded into rounded badlands. Scarps in the Wingate Sandstone lie to the west of the highway, and Black Mesa, developed on Cretaceous sandstones and shale, forms the western horizon.

102.9 Junction with NAV 59 at Many Farms. Continue on US 191.

Mile 118 [0] Town of Chinle. Overnight stay. Reset mileage counter.

Day 6

Take 54-mile roundtrip from Chinle on NAV 7 through Canyon de Chelly, New Mexico, as far as Spider Rock overlook and return, stopping at all turnoffs and lookouts. Good views of alcoves, some created by sapping processes, and some by undercutting. Many have associated cliff dwellings. Some of the lower canyon slopes in the De Chelly Sandstone have approximately 30 to 40 degree slopes. Some are debris mantled, whereas others are nearly bare. The latter may be slopes formerly protected from erosion by a debris cover which is now eroded due to lack of cliff retreat. (fig. 75)

Mile [0] Returning to Chinle, reset mileage counter and continue south on US 191. The road continues on the Chinle Formation.

Mile 33.2 Triple junction of US 191 with AZ 264 and NAV 16. Turn southwest on NAV 16, which joins with NAV 15 in 13 miles. The road initially follows the canyon of Ganado Wash, exposing the Wingate, Moenave, Carmel, Entrada and Cow Springs Sandstone Formations on the northwest side, but then the road rises onto the Pliocene lake bed and tuff deposits of the Bidahochi Formation.

Mile 70.6 Junction of NAV 15 with AZ 77 at Bidahochi. Turn south on AZ 77. The road lies primarily on the Chinle Formation to the junction with I-40.

Mile 69-84 Tertiary volcanic flows and cones at the eastern edge of the Hopi Buttes are scattered over the landscape.

Mile 107.2 Junction with I-40. Turn west onto I-40.

Mile 207.4 Flagstaff at US 89 junction. End of trip.

REFERENCES

Ahnert, F. (1960) The influence of Pleistocene climates upon the morphology of cuesta scarps on the Colorado Plateau. *Ass. Am. Geogr. Ann.* **50:** 139-156.

Baars, D.L. (1983) *The Colorado Plateau, A Geologic History*. Albuquerque, University of New Mexico Press.

Bradley, W.A. (1963) Large-scale exfoliation in massive sandstones of the Colorado Plateau. *Geol. Soc. Am. Bull.* **75:** 519-528.

Bryan, K. (1928) Niches and other cavities in sandstones at Chaco Canyon, N. Mexico. *Zeit. Geomorph.* **3:** 125-140.

Campbell, I.A. (1973) Controls of canyon and meander forms by jointing. *Area* **5:** 291-296.

Chronic, H. (1983) *Roadside Geology of Arizona*. Missoula, Mountain Press.

Conca, J.L. and Rossman, G.R. (1982) Case hardening of sandstone. *Geology* **10:** 520-533.

Cooley, M.E., Harshbarger, J.W., Akers, J.P., and Hardt, W.F. (1969) Regional hydrogeology of the Navajo and Hopi Indian Reservations, Arizona, New Mexico, and Utah. U.S. Geological Survey Professional Paper 521-A.

Cooke, R.U., and Smalley, I.J. (1968) Salt weathering in deserts. *Nature* **220:** 1226-1227.

Davis, W.M. (1901) An excursion to the Grand Canyon of the Colorado. *Harvard Mus. Comp. Zool. Geol. Ser.* **5:** 105-201.

Doelling, H.H. (1985) *Geology of Arches National Park*. Utah Geological and Mineral Survey, Map 74.

Dutton, C.E. (1882) Tertiary history of the Grand Canyon district. U.S. Geological Survey Monograph 2.

Freeze, R.A., and Cherry, J.A. (1979) *Groundwater*. Englewood Cliffs, Prentice-Hall.

Gregory, H.E. (1917) Geology of the Navajo country. U.S. Geological Survey Professional Paper 93.

Hamilton, W.L. (1984) *The Sculpturing of Zion*. Zion Natural History Assoc., Zion National Park.

Higgins, C.G. (1984) Piping and sapping: development of landforms by groundwater flow. In LaFleur, R.G., ed., *Groundwater as a Geomorphic Agent*. Boston, Allen & Unwin, p. 18-58.

Hintze, L.F. (undated) Geologic history of Utah. *Brigham Young Univ. Geology Studies* vol. 20, part 3.

Howard, A.D. (1970) A study of process and history in desert landforms near the Henry Mountains, Utah. PhD dissertation, Johns Hopkins University, Baltimore.

Kochel, R.C., Howard, A.D. and McLane, C. (1985) Channel networks developed by groundwater sapping in fine-grained sediments: analogs to some martian valleys. In Woldenberg, M.J., ed., *Models in Geomorphology*. Boston, Allen & Unwin, p. 313-341.

Kochel, R.C. and Piper, J.F. (1986) Morphology of large valleys on Hawaii: implications for groundwater sapping and comparisons to martian valleys. *17th Lunar Planet. Sci. Conf.* p. 424-425.

Jobin, D.A. (1962) Relation of the transmissive character of the sedimentary rocks of the Colorado Plateau to the distribution of uranium deposits. U.S. Geological Survey Bulletin, 1124.

Koons, D. (1955) Cliff retreat in the southwestern United States. *Am. J. Sci.* **253:** 44-52.

Laity, J.E. (1983) Diagenetic controls on groundwater sapping and valley formation, Colorado Plateau, as revealed by optical and electron microscopy. *Phys. Geogr.* **4:** 103-125.

Laity, J.E., and Malin, M.C. (1985) Sapping processes and the development of theater-headed valley networks in the Colorado Plateau. *Geol. Soc. Amer. Bull.* **96:** 203-217.

Lange, A.L. (1959) Introductory notes on the changing geometry of cave structures. *Cave Studies* no. 11.

McGill, G.E., and Stromquist, A.W. (1975) Origin of graben in the Needles District, Canyonlands National Park, Utah. Four Corners Geological Society Guidebook, 8th Field Conference, p. 235-243.

Mustoe, G.E. (1982) The origin of honeycomb weathering. *Geol. Soc. Am. Bull.* **93:** 108-115.

Mustoe, G.E. (1983) Cavernous weathering in the Capitol Reef Desert, Utah. *Earth Surf. Proc. Landforms* **8:** 517-526.

Nicholas, R.M., and Dixon, J.C. (1986) Sandstone scarp form and retreat in the Land of Standing Rocks, Canyonlands National Park, Utah. *Zeit. Geomorph.* **30:** 167-187.

Oberlander, T.M. (1977) Origin of segmented cliffs in massive sandstones of southeastern Utah. In Doehring, D.O., ed., *Geomorphology in Arid Regions*. Boston, Allen & Unwin, p. 79-114.

Reiche, P. (1937) The Toreva Block, a distinctive landslide type. *J. Geol.* **45:** 538-548.

Rigby, J.K. (1976) *Field Guide, Northern Colorado Plateau*. Dubuque, Kendall/Hunt.

Rigby, J.K. (1977) *Field Guide, Southern Colorado Plateau*. Dubuque, Kendall/Hunt.

Schumm, S.A., and Chorley, R. (1966) Talus weathering and scarp recession in the Colorado Plateaus. *Zeit. Geomorph.* **10:** 11-36.

Schumm, S.A., and Phillips, L. (1986) Composite channels of the Canterbury Plain, New Zealand: a martian analog? *Geology* **14:** 326-329.

Twidale, C.R. (1976) *Analysis of Landforms*. New York, John Wiley.

Young, R.W. (1986) Tower karst in sandstone: Bungle Bungle massif, northwestern Australia. *Zeit. Geomorph.* **30:** 189-202.

Chapter 3

Sedimentologic and Stratigraphic Variations in Sandstones of the Colorado Plateau and their Implications for Groundwater Sapping

R. Craig Kochel and Gregory W. Riley

Previous workers have shown that groundwater sapping processes have been important in concert with runoff processes in the formation of channel networks on the Colorado Plateau (Baker, 1982; Laity and Malin, 1985). The deeply incised box canyons with uniform valley width and amphitheater heads, characteristic of sapping valley morphology, are common in the highly transmissive sandstones of the Navajo and Entrada Formations. Significant groundwater discharge occurs along vertical exposures of these sandstones despite the semi-arid climate because of the high porosity and permeability of these rocks formed dominantly by aeolian processes.

Laity and Malin (1985) showed that structural dip and joint orientations exert major regional controls on the development of sapping canyons on the Colorado Plateau. They attributed the asymmetry of sapping canyons on opposite sides of the Escalante River to the capture of groundwater by valleys on the updip sides of the river. Valleys on the down-dip sides appear to be dominated by runoff (Laity and Malin, 1985). Structural factors appear to be most important in controlling sapping features on a regional scale.

Recent investigations of aeolianites have demonstrated that considerable complexity exists in the lateral and vertical variation of textures and facies (Kocurek, 1981). Vertical and lateral inhomogeneities in permeability are frequent and widely distributed throughout the major aquifers of the Colorado Plateau such as the Navajo and Entrada Sandstones (Brookfield 1977; Kocurek, 1981). Few workers have discussed the significance of sedimentologic and stratigraphic variations upon direction and discharge of groundwater. Sedimentologic parameters may be important subregional and local controls on groundwater flow. They appear to play a major role in the evolution and location of channels dominated by sapping processes.

SEDIMENTOLOGY AND STRATIGRAPHY

Regional Stratigraphy

The Navajo Formation and its western equivalent, the Aztec Sandstone, is essentially a westward-thickening wedge of sandstone that reaches a maximum thickness of over 650 meters in southwestern Utah and southern Nevada (Marzolf, 1983). In northern Arizona and southern Utah, the Navajo Sandstone is unconformably overlaid by the Entrada Sandstone and younger Jurassic rocks of the Carmel Formation.

The Navajo Sandstone is the uppermost unit of the Glen Canyon Group, which also includes the Kayenta and Wingate Formations (fig. 82). The Navajo is a light gray to red sandstone over most of the field trip region, composed dominantly of well-sorted fine-to-medium quartz sand (Peterson and Pipiringos, 1979).

General Characteristics of Aeolianites

The most diagnostic feature of aeolianites, aside from their good sorting, is the abundance of large-scale, high-angle cross-beds of various types. Cross-bed sets are variable in size, but are commonly in the range of 5 to 20 meters in thickness. Less conspicuous horizontally bedded interbeds of poorly sorted sandstones, mudstones, and cherty limestones and dolomites also occur between cross-bed sets. These deposits are related to deposition in interdune environments and are first-order bounding surfaces (see figs. 84 and 85). These minor facies exert considerable control on the regional and local variations in permeability, which greatly affect the flow of groundwater. These features, and the regional trends of other sedimentary structures play a significant role in subregional control of directional permeability. These sedimentary controls are the focus of our discussion

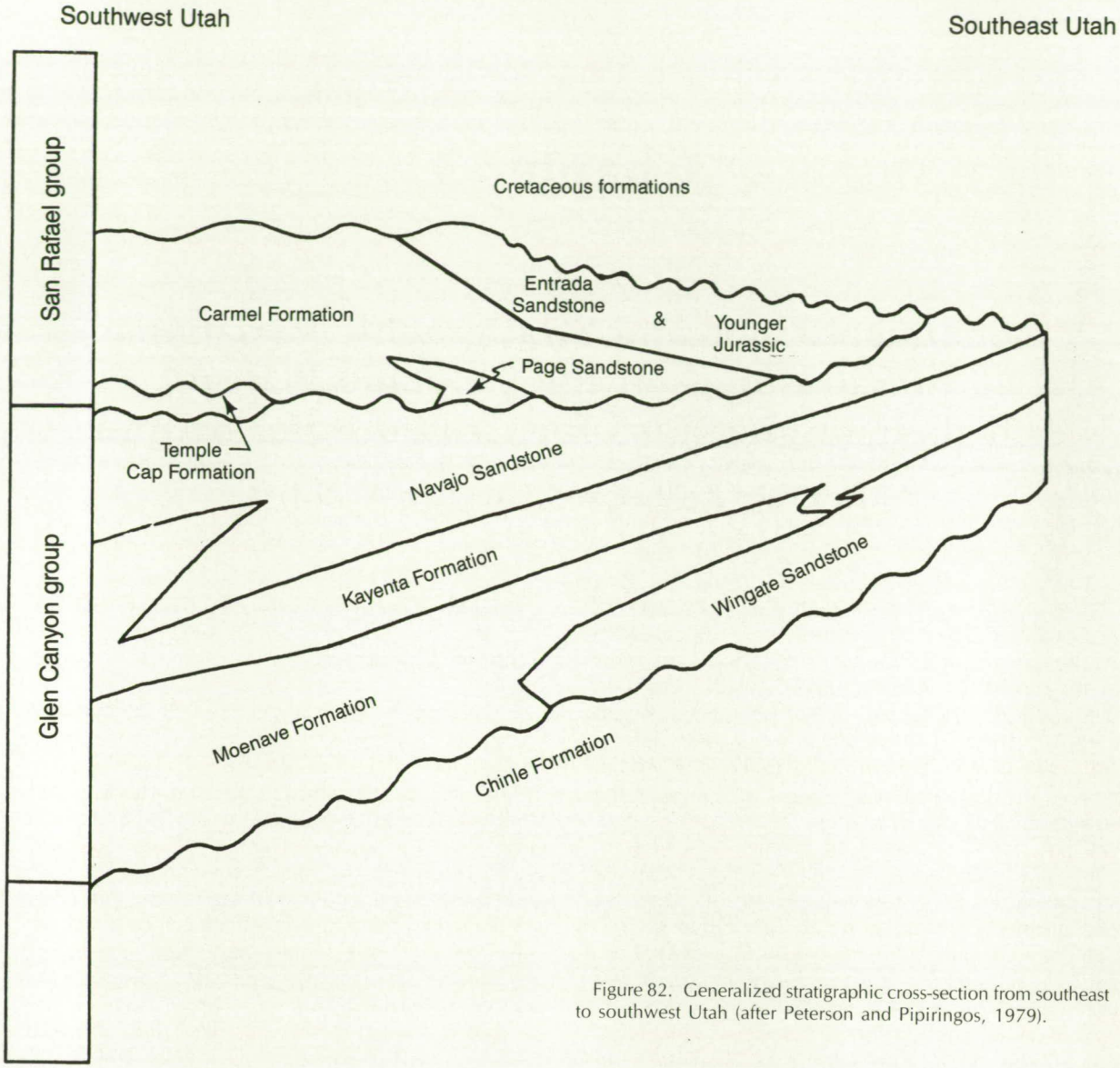

Figure 82. Generalized stratigraphic cross-section from southeast to southwest Utah (after Peterson and Pipiringos, 1979).

because of their importance to groundwater sapping. Figure 64 shows the extent of the field conference trip and the area of Colorado Plateau that will be treated.

Facies Variations in the Navajo Sandstone

The following discussion details the variations within the Navajo Formation. Facies relations are similar to those found in the Entrada Sandstone (Kocurek, 1981).

Cross-Bedded Facies. The Navajo Sandstone is dominantly a feldspathic quartz arenite composed of well-rounded, well-sorted sand. Marzolf (1983) noted that the exposures in southern Utah and northern Arizona are dominated by large-scale trough, tabular-planar, and wedge-planar cross-stratification.

Marzolf (1983) measured cross-bed orientations in vertical increments of 15 to 30 meters at numerous localities between Utah and southeastern California and found that orientations were regionally consistent. Figure 83 shows a summary of the cross-bed data from southern Utah. Throughout the area, Marzolf (1983) found cross-bed azimuths dipping consistently toward the southeast (fig. 83), with a range from 75° to 171°. He calculated vector-resultant cross-bed dip azimuths from a large sample of over 1850 measurements to demonstrate the consistency of regional paleocurrent patterns. Marzolf (1983) interpreted this data to indicate aeolian deposition from northwesterly paleowinds across the field trip region. Similar observations of regionally consistent dips of cross-strata in modern and other ancient sand seas have also been observed.

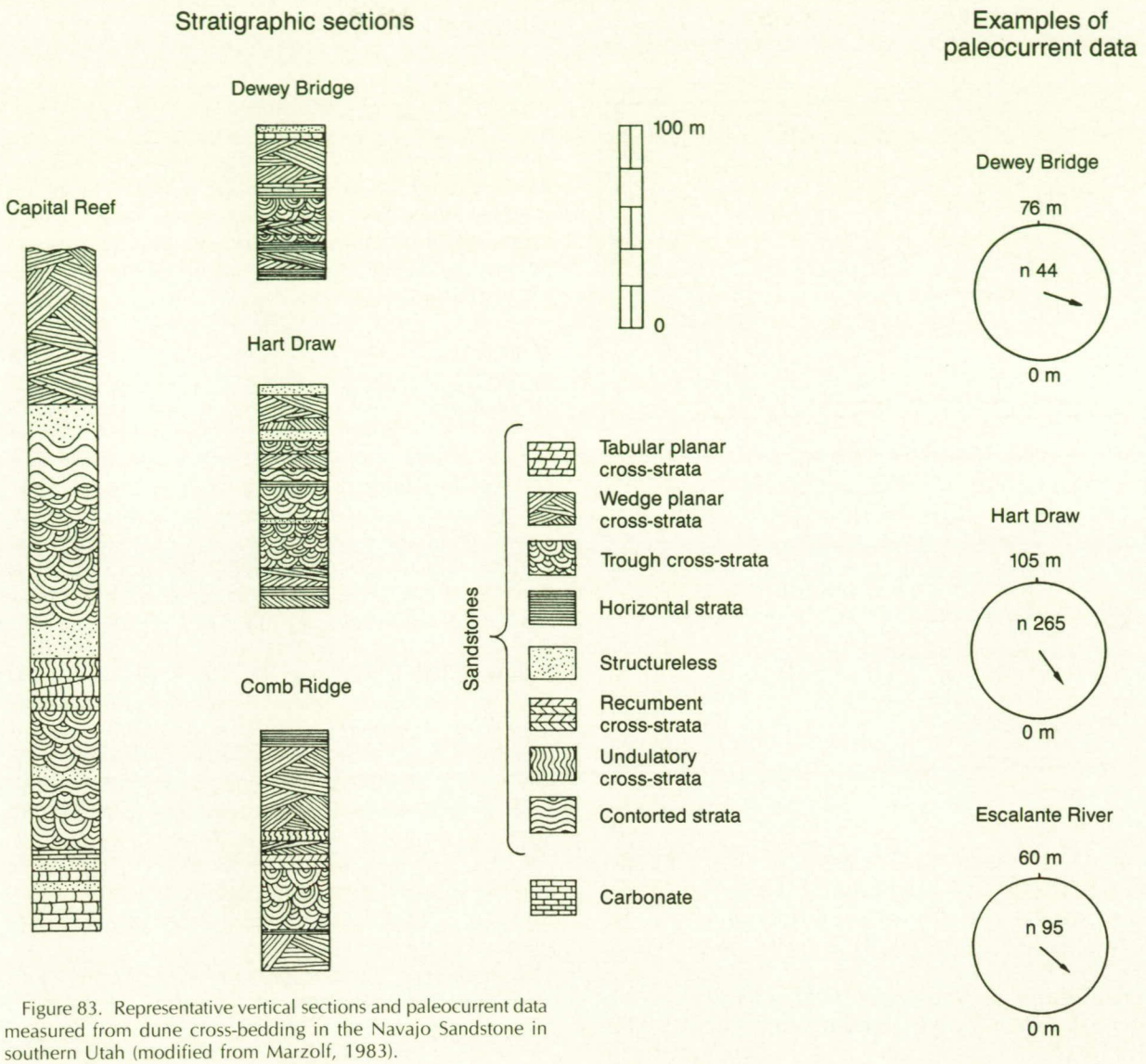

Figure 83. Representative vertical sections and paleocurrent data measured from dune cross-bedding in the Navajo Sandstone in southern Utah (modified from Marzolf, 1983).

Non-Cross-Bedded Lithologies. The thick, cross-bedded sandstones are the most volumetrically dominant and conspicuous lithofacies in the Navajo Sandstone; however, a significant portion of the formation is characterized by other lithotypes. Nonstratified facies include (1) limestone lenses, (2) mudcracked, horizontally stratified sandstones, (3) contorted beds, and (4) structureless sandstones (fig. 84). These deposits are typically formed in interdune swales, but some can result from groundwater modification prior to lithification. These units generally account for less than 35% of the total Navajo strata; however, they exert a significant control on groundwater movement. Therefore, they deserve special attention with regard to sapping.

Limestone lenses between 1 to 2 meters thick are common throughout vertical sections described in southern Utah by Marzolf (1983). Limestone lenses are typically underlaid by silts or mudstones and contain freshwater fossils (Harshbarger et al., 1957). Marzolf (1983) interpreted these lenses as the result of shallow lakes and ponds that temporarily occupied small interdune depressions.

Horizontally stratified, dark red, silty sandstones are also common between major cross-bedded units in the Navajo Sandstone. These strata often contain wavy lamination, adhesion ripples, and mudcracks (Kocurek and Fielder, 1982; Marzolf, 1983). Marzolf interpreted these silty sandstones as erosional surfaces resulting from deposition in or modified by an aqueous environment. He noted the absence of ripples and suggested that the horizontally stratified sands resulted from slow lateral percolation of groundwater through the sand soon after deposition (Marzolf, 1983).

Contorted and structureless sandstones range between a few meters to over 35 meters thick and are scattered throughout the Navajo Sandstone (Marzolf,

Figure 84. Schematic distribution of aeolian facies and corresponding groundwater flow paths (modified from Lindquist, 1983).

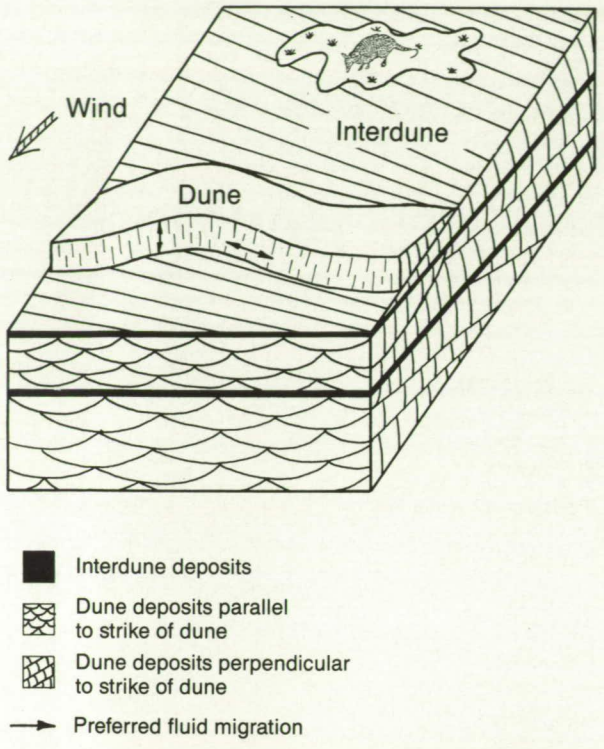

1983). These stratification types have been attributed to liquifaction and fluidization from overpressured groundwater after deposition of the sand (Marzolf, 1983; Doe and Dott, 1980; Horowitz, 1982).

Distribution of Non-Cross-Bedded Facies. The sections shown in fig. 83 represent the vertical distribution of major sedimentary features within the Navajo Sandstone in southeastern Utah described by Marzolf (1983). Kocurek (1981) described similar facies distributions within the Entrada Formation. These non-cross-bedded interdune facies occur in all the sections, accounting for an average of about 30% of the total thickness of measured section in the Navajo Sandstone. The horizontally stratified silty sandstone is most abundant near the base of the Navajo Formation. These beds form minor aquicludes and inhibit the downward movement of groundwater near the base of the Navajo Sandstone. The abundance of these interdune units near the base of the Navajo Sandstone accounts for the high frequency of seeps near its base. The occurrence of multiple horizons of interdune deposits explains the presence of major seepage zones at other levels throughout the Navajo Formation. Figures 59, 68, and 80 show examples of several distinct stratigraphic levels where active seepage and alcove formation are occurring.

Directional Permeability

Variations in grain size and sorting between beds accounts for significant anisotropy related to facies variations in aeolian deposits (Lindquist, 1983). This distribution of facies controls the migration of groundwater through units like the Navajo and is important in determining the location of seepage facies. This is especially important to subregional groundwater flow patterns because of the regional consistency of cross-stratification orientation.

Bounding Surfaces. Aeolian deposits contain a hierarchy of bounding surfaces (Brookfield, 1977), some of which play a role in the migration of groundwater. We will limit this discussion to first- and second-order bounding surfaces because third-order surfaces are small-scale, nonhorizontal features. First-order bounding surfaces are overlaid by horizontally laminated strata and represent deposition within interdune areas. Second-order bounding surfaces separate sets of cross-strata and represent the migration of a single dune (fig. 85).

Permeability Variations. First-order bounding surfaces act as subregional controls on groundwater migration. These surfaces are overlaid by horizontally laminated sands and silts. These deposits inhibit the downward migration of groundwater. Within the package of sediments between two first-order surfaces, permeability and transmissivity are generally very high (fig. 86). Lateral permeability is generally greater than vertical permeability within these packages due to heterogeneities caused by cross-stratification (Lindquist, 1983, 1986).

Second-order surfaces and cross-bed dip direction determine local variations in directions and rates of

Figure 85. Hierarchy of bounding surface in aeolianites (based on Brookfield, 1977).

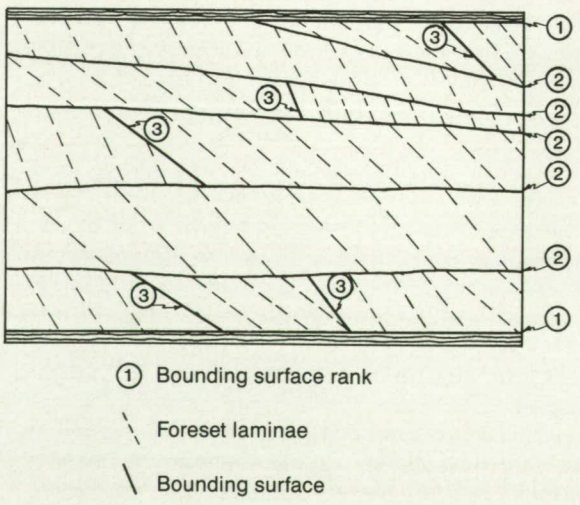

Figure 86. Examples of the variations in permeability in aeolian sandstones showing the effects of facies stratification types (from Lindquist, 1983, 1986).

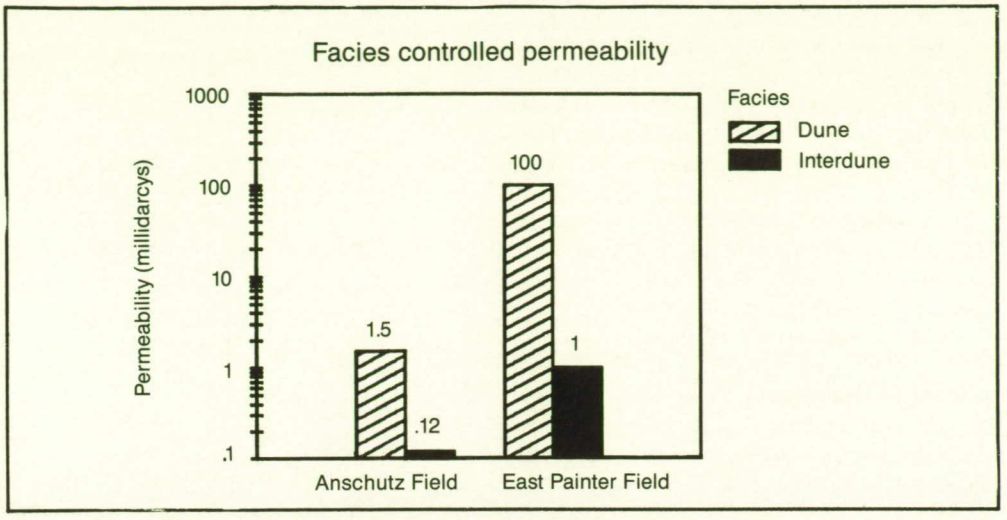

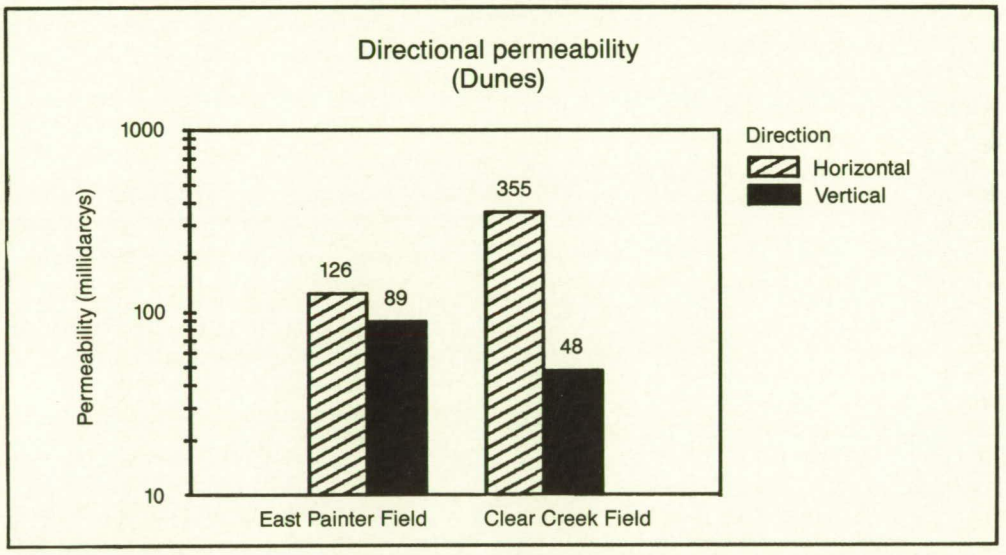

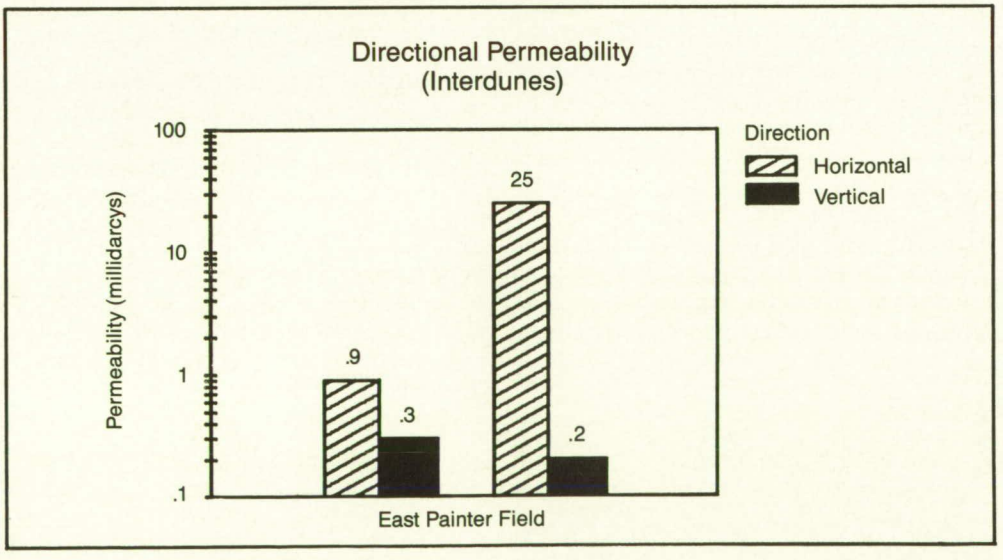

fluid migration. Second-order surfaces typically act as aquicludes, resulting in vertical, subequally spaced levels of alcoving. Preferential migration of fluids occurs along bedding planes; therefore, the preferred direction of migration in dune facies will parallel the strike of cross-beds and will parallel dune foreset dip (Lindquist, 1986). Migration of fluids parallel to strike is limited by dune size, while migration along the foresets is limited by the thickness of the foresets (fig. 84).

Figure 86 shows examples of the variability of directional permeability in aeolianites studied for petroleum purposes. Permeability in dune facies can be as much as three orders of magnitude higher than interdune facies. Horizontal permeability is generally higher than vertical permeability in both dune and interdune deposits. Lindquist (1986) showed that within dune deposits horizontal permeability is significantly greater parallel to the strike of cross-beds than perpendicular to cross-beds.

CONCLUSIONS

Aeolian sandstones are characterized by a complex set of lateral and vertical variations in facies which may have significant influence upon movement of groundwater and the evolution of valleys formed by groundwater sapping.

1. Facies present within aeolianites control groundwater movement in both vertical and horizontal directions.
2. Interdune deposits act as aquicludes, preventing the downward migration of fluids.
3. Cross-bed dip direction plays an important role in the lateral permeability variations important in groundwater movement. Regional cross-bed dips are remarkably consistent; hence, they may have significant effects on regional groundwater flow.
4. Occurrence and positioning of sapping canyons appears to be controlled on a regional scale by structural dip and fracture patterns. Sedimentologic variations are important in controlling the vertical occurrence of sapping features and local arrangement of sapping canyons.
5. Bedding planes are major pathways of groundwater movement in aeolianites. Therefore, cliff faces that intersect few bounding surfaces should exhibit infrequent, widely spaced (vertically) alcoves. Cliff faces that intersect several bounding surfaces should be characterized by multistacked alcove morphology.

REFERENCES

Baker, V.R. (1982) *The Channels of Mars.* Austin, University of Texas Press.

Brookfield, M.E. (1977) The origin of bounding surfaces in ancient aeolian sandstones. *Sedimentology* **24:** 303-332.

Doe, T.W., and Dott, R.H. (1980) Genetic significance of deformed cross bedding—with examples from the Navajo and Weber Sandstones of Utah. *Sediment. Petrol.* **50:** 793-812.

Harshbarger, J., Repenning, C.A., and Irwin, J.H. (1957) Stratigraphy of the uppermost Triassic and Jurassic rocks of the Navajo country. U.S. Geological Survey Professional Paper 291.

Horowitz, D.H. (1982) Geometry and origin of large-scale deformation structures in some ancient wind-blown sand deposits. *Sedimentology* **29:** 155-180.

Kocurek, G. (1981) Significance of interdune deposits and bounding surfaces in aeolian dune sands. *Sedimentology* **28:** 753-780.

Kocurek, G., and Fielder, G. (1982) Adhesion structure. *Sediment. Petrol.* **52:** 1229-1242.

Laity, J.E., and Malin, M.C. (1985) Sapping processes and the development of theater-headed valley networks on the Colorado Plateau. *Geol. Soc. Am. Bull.* **96:** 203-217.

Lindquist, S.J. (1983) Nugget Formation Reservoir characteristics affecting production in the overthrust belt of southwestern Wyoming. *Petrol. Technol.* July, p. 1355-1365.

Lindquist, S.J. (1986) Practical characterization of heterogeneous aeolian reservoirs, Nugget Sandstone, Utah-Wyoming thrust belt. In Kocurek, G., ed., *Upper Paleozoic and Mesozoic Aeolianites of the Western United States.* Tulsa, Society Economic Paleontologists and Mineralogists.

Marzolf, J.E. (1983) Changing wind and hydrologic regimes during deposition of the Navajo and Aztec sandstones, Jurassic (?), southwestern United States. In Brookfield, M.E. and Ahlbrandt, T.S., eds., *Eolian Sediments and Processes.* Amsterdam, Elsevier, p. 635-660.

Peterson, F. and Pipiringos, G.N. (1979) Stratigraphic relations of the Navajo Sandstone to Middle Jurassic formations, southern Utah and northern Arizona. U.S. Geological Survey Professional Paper 1035-F.

Chapter 4

The Role of Groundwater Sapping in Valley Evolution on the Colorado Plateau

Julie Laity

The development of sapping networks is limited by lithologic, structural, and climatic constraints, and, as such, sapping is not widespread on the Colorado Plateau. Characteristic requirements for groundwater sapping include (1) a permeable aquifer, (2) a rechargeable groundwater system, (3) a free face at which subsurface water can emerge, (4) some form of structural or lithologic inhomogeneity, such as jointing in sandstone or dikes in volcanic material, that locally increases the hydraulic conductivity and along which valleys grow, and (5) a means of transporting material released from the scarp face.

The most telling characteristics of sapping are morphologic ones. Valleys terminate in steep-walled headcuts that have been variously described as cuspate or theater-shaped in form. In addition, the valleys show near-vertical sidewalls and relatively straight drainage segments with apparent structural control. Observed on aerial images or maps, the network properties of the valleys are distinct owing to competition for available groundwater rather than surface water. The areal extent of groundwater drainage basins does not always correspond with surface catchment boundaries.

Valleys with aforementioned characteristics have been noted in a number of different localities on the Colorado Plateau. However, many sapping forms may be representative of relict processes or of processes that act discontinuously or exceedingly slowly in today's environment. Map and photo analysis as well as field reconnaissance indicate that the best-developed and most areally extensive theater-headed networks occur in the Navajo Sandstone in the Glen Canyon region of south-central Utah. In addition to a well-developed morphology, theater-headed valleys in the Navajo Sandstone display active groundwater seepage, sustaining base flow in streams. The aquifer properties of the Navajo Sandstone and its stratigraphic relation to an underlying aquiclude provide the potential for groundwater sapping. However, the interplay of other structural and stratigraphic factors are important in determining the relative role of groundwater in the evolution of the valley networks.

Whereas the Navajo Sandstone has an extensive and well-developed network of theater-headed valleys, other sandstones of the region (for example, the Wingate Sandstone and Entrada Formation) lack such development. These differences will be addressed by analyzing the properties of some of the principal aquifers of the Colorado Plateau and examining their relationship to overlying and underlying lithologies.

PRINCIPAL AQUIFERS OF SOUTHERN UTAH

The Colorado Plateau is characterized by aquifers composed of sandstones interbedded with, and confined by, relatively thick and impermeable siltstones, mudstones, and a few thin limestones. The chief aquifers are the Coconino and Navajo Sandstones, but all units yield some water to springs or wells. The sandstones have moderate to great mean thickness and permeability, and consequently have relatively high uniform gradients of regional transmissive capacity. In the Glen Canyon area, the Carmel, Kayenta, and Chinle Formations act as aquicludes and are interbedded with the moderately permeable and transmissive Entrada and Wingate Sandstones and the highly transmissive Navajo Sandstone.

The basins and uplands control the principal movement of groundwater in the sedimentary rocks. The main areas of recharge to the groundwater reservoirs are on the highlands that form the structural divides between the hydrologic basins. Vertical movement of fluid into aquifers is restricted primarily to strongly folded and fractured regions found chiefly along the major monoclines, to narrow zones surrounding igneous intrusions, and to areas in which the imperme-

able upper confining layers have been stripped back by erosion. Groundwater recharge to the Navajo Sandstone in the area of Glen Canyon is probably greatest in a zone around the base of the Henry Mountains, along the intensely fractured Waterpocket Fold, and in large areas of exposed bedrock along the lower Escalante River basin and south of the Colorado River, particularly where the surface is mantled by eolian material that inhibits surface runoff. Lateral movement of groundwater is generally downdip from the highlands toward the Colorado or San Juan Rivers and their major tributaries (Cooley et al., 1969). The aquifer properties of the principal formations and factors affecting the erosional development of valley networks are discussed below.

Aquifer Properties of the Principal Formations

Chinle Formation. The uppermost part of the Chinle Formation, the Owl Rock Member, is composed of interbedded siltstones, limestones, mudstones, and poorly sorted very fine grained sandstones. It forms an aquiclude to the overlying Wingate Sandstone in most areas.

Wingate Sandstone. The Wingate Sandstone is a moderately well sorted, very fine grained sandstone that is a good aquifer. It has a very uniform permeability owing to a consistent grain size and similarity in character and amount of interstitial matrix material over the extent of the formation (Jobin, 1962). Horizontal bedding planes are few, and the formation is easily recognized by its dense vertical jointing. The formation exhibits features associated with groundwater seepage, including tafoni and alcove development, but these features are less common than in the Navajo Sandstone and are associated principally with weathering of the sidewalls.

Several factors contribute to the absence of theater-headed valley forms in the Wingate Sandstone. These include an intrinsic transmissivity (3.6) that is lower than that of the Navajo Sandstone (6.1) (Jobin, 1956); very intense jointing, so that no one fracture acts to focus groundwater flow along the valley trend; areally limited surface exposure of the formation that restricts groundwater recharge to small exposures around volcanic intrusions or highly fractured zones; and vigorous incision by runoff from the overlying Kayenta Formation.

Kayenta Formation. The Kayenta Formation is composed of interbedded sandstone, siltstone, and mudstone. In regions where the Glen Canyon Group is highly fractured, such as around the Navajo Mountain dome, water may percolate from the Navajo Sandstone through the Kayenta Formation into the Wingate Sandstone, forming what Cooley et al., (1969) termed the N multiple-aquifer system. Sandstone beds of the Kayenta Formation are moderately permeable, and small amounts of seepage occur in some areas as a result of leakage from the overlying Navajo Sandstone. Cavernous weathering is observed in some of the sandstone beds. However, the overall permeability and regional transmissivity of the formation are greatly reduced by the many interbedded seams of silt and clay, so that, in many areas, the Kayenta Formation acts as an aquiclude for the Navajo Sandstone (Jobin, 1962; Laity and Malin, 1985). The Navajo Sandstone/Kayenta Formation boundary has long been recognized as an important zone at which springs occur (McKnight, 1940; Cooley et al., 1969).

In samples of the Kayenta Formation obtained immediately below the contact with the Navajo Sandstone at Explorer Canyon and at North Wash, the most significant factor in porosity reduction was the abundance of clay filling the pores. Other factors included the development of quartz overgrowths, which result in tight grain packing, and extensive carbonate deposition (Laity, 1983). However, it should be noted that the Kayenta Formation shows considerable lateral variation.

Navajo Sandstone. Studies of regional transmissivity of sedimentary rocks on the Colorado Plateau by Jobin (1962) and Harshbarger (1961) show the Navajo Sandstone to be the most transmissive of all sedimentary rocks as a function of its permeability and geometrical configuration and continuity. The recharge potential of the aquifer is high because of its widespread surface exposure at low dip angles, relatively uniform permeability of the rock, and pervasive fracturing. The saturated thickness of the sandstone varies according to local structure, but in regions to the west of Glen Canyon it attains a thickness of 60 to 150 meters (Gates, 1965; Goode, 1965; Cooley, et al., 1969).

Aquifers are recharged principally during winter and spring, in response to precipitation of generally low intensity and large areal extent. Sporadic summer downpours are usually short and intense and result in surface runoff, but little replenishment of groundwater. The maximum groundwater discharge at seeps occurs during the spring, and seepage discharge and well water levels decline during the summer.

Movement of water through the Navajo Sandstone is generally slow owing to the fine grained nature of the material. Sandstone yields water in part from intergranular openings only partly filled with cement, and in part from fractures. Cores of the Navajo Sandstone obtained from the Navajo Reservation immediately south of Glen Canyon by Cooley et al. (1969) had an overall porosity ranging from 25 to 35 percent. Permeability variations in the Navajo Sandstone result from changes in grain size within the rock unit, from diagenetic processes that change the original porosity of sandstone by modifying pore spaces, from fracturing of the rock, and from the presence of less

permeable layers that cause perched water bodies. The permeability of cores drilled parallel to the bedding is higher in most sites than that of cores drilled perpendicular to the bedding (Marzolf, 1976).

Jointing in the rock can significantly increase permeability perpendicular to bedding. Harshbarger (1961) demonstrated that the yield to wells in highly fractured areas is commonly several times greater than normal. The effect of jointing on permeability may decrease with depth as joint spaces become more closed and more water moves through intergranular spaces (Gates, 1965).

Small discontinuous bodies of perched water occur extensively throughout the Navajo Sandstone and at three or four levels in cliff faces in the Glen Canyon area. Perched water tables develop above thin, relatively impermeable units of limestone, siltstone, or shale horizontally interbedded in the formation. Recharge is from local precipitation, and during periods of below-normal rainfall the perched water bodies do not receive enough recharge to maintain seepage. Alcove development associated with perched water levels is important in terms of modifying canyon walls. However, it is insignificant in the evolution of canyon networks that are dependent for their growth on sustained seepage at valley headwalls fed by regional aquifers.

Carmel Formation. The Carmel Formation, of sandy siltstone and limestone, forms an aquiclude of moderate effectiveness to the overlying Entrada Sandstone. It is also significant in the morphologic development of canyons in the Navajo Sandstone, as its presence as a caprock limits local groundwater recharge and increases the amount of surface runoff. Well-developed sapping networks in the Navajo Sandstone develop only in regions where the Carmel Formation has been extensively stripped back from basins.

Entrada Sandstone. The Entrada Sandstone has about half the transmissive value for groundwater as the Navajo Sandstone, and the springs emerging from it are of very small volume. The permeability of the Entrada Sandstone in a given area reflects the relative proportions of sandy and earthy material. In south-central Utah the Entrada Sandstone has a relatively low permeability, and the lower siltstones form an aquiclude of moderate effectiveness (Jobin, 1962). Jointing is uncommon in both the Entrada Sandstone and the Carmel Formation.

Many of the beds of the Entrada Sandstone weather to form nonresistant slopes and plains. Broad uplands of subdued relief are covered with earthy and sandy soil and some sand dunes. Mechanical weathering of the Entrada Sandstone has been shown to be extremely fast (Schumm and Chorley, 1966). The lack of theater-headed valley development may be attributed to the low permeability of the material, lack of jointing, and rapid breakdown of the rock.

Summary

Aquifer properties of a material as well as structural and stratigraphic relationships, weathering rates, transport mechanisms, climatic conditions, and other factors are all significant in determining the role of sapping on the Colorado Plateau. Whereas cliff recession by basal sapping and cavernous weathering processes are not uncommon, extensive valley networks are limited to the Navajo Sandstone and are absent from other aquifers in the region.

THE ROLE OF JOINTING IN DRAINAGE DEVELOPMENT IN THE NAVAJO SANDSTONE

The spatial relations of the regional joint pattern in southern Utah exert considerable control on the drainage pattern in the Navajo Sandstone. Exfoliation jointing, developed parallel to canyon walls, affects local morphology. A modified trellis drainage pattern, with pronounced elongation in a northeast-southwest direction, is clearly evident on topographic maps and aerial photographs and has been attributed by Gregory (1950) and Campbell (1973) to some degree of joint control. Faulting in the region is limited.

Regional Jointing

Systematic joints trending toward the northwest dominate many areas of Utah, Colorado, and Wyoming (Heylum, 1966). In southern Utah the orientation of regional joints may remain relatively constant over areas as large as a few thousand square kilometers. The joints comprising each set are parallel to subparallel in plan, and the angle of any two sets ranges from less than 15° to 90° but remains essentially constant within a given area. In the vicinity of Glen Canyon, the principal fractures trend N 65° - 75° E. Lesser fractures trend about N 25°W across the principal set (Kelly and Clinton, 1960). In section, the dip of the joints remains within 25° either side of normal to the bedding (Hodgson, 1961). The surfical expression of a joint is usually a fissure resulting from the mechanical separation of the joint faces, commonly enhanced by weathering.

The pervasive fracturing greatly increases the overall permeability of the plateau surface and increases the contribution of precipitation to the groundwater system. The fractures also act at depth to increase the transmissivity of the bedrock, and laterally flowing groundwater exploits the major joints. The water subsequently emerges at seepage points along cliff faces, and the canyons migrate headward along joint trends as sapping undermines the steep cliff faces and causes the collapse of massive sandstone slabs.

Exfoliation Jointing

Exfoliation joints on the Colorado Plateau are best developed in the more massive units such as the Wingate and Navajo Sandstones and are less developed in well-bedded units. In the Navajo Sandstone exfoliation joints appear to result from pressure release owing to canyon cutting, and therefore joints develop essentially parallel to the sidewalls. The sets of parallel joints are usually restricted to a depth of less than 100 meters, and the distance between joints increases with depth (Bradley, 1963; Lasson, 1963). The collapse of massive slabs developed by exfoliation jointing and undermined by seepage results in a canyon morphology characterized by high and steep valley sidewalls. Mechanically weak sandstone shatters readily upon impact, and the material is further comminuted by active weathering processes. The blocks are extremely friable, particularly when saturated. Boulders round in situ and are commonly surrounded by aprons of loose sand. Evidence for rapid breakdown in place is provided by exposures in stream terraces and in talus cones. In section, these are primarily sand bodies, with remarkably few boulders or cobbles.

THEATER-HEADED VALLEY NETWORKS IN THE NAVAJO SANDSTONE

Groundwater outflow and sapping are proposed as significant processes in the formation of theater-headed valleys in the Navajo Sandstone. These valleys develop where large exposures of gently dipping and highly fractured sandstone allow high rainfall infiltration rates. Groundwater encounters a permeability boundary (the Kayenta Formation) and moves laterally down the hydraulic gradient through intergranular pores and fractures. Where groundwater is intercepted by valley heads, the flow converges and emerges in concentrated zones of seepage, where small-scale erosional processes slowly reduce the support of steep cliffs and contribute to their collapse (fig. 87). Valleys grow headward by successive slab failure, aided by processes that break down the debris produced by slope collapse and transport away the disintegrated materials.

In the initial stages of valley development, growth of the main canyon proceeds more rapidly than that of tributary canyons owing to its larger subsurface drainage area. In time, a network of canyons may

Figure 87. Seepage from the headwall region of Bowns Canyon. Combined flow from the double theater head of Bowns Canyon was measured at 150 to 190 liters/minute. The seepage faces discharge water into ponds that overflow to form the stream source. The headwall is 125 meters in height.

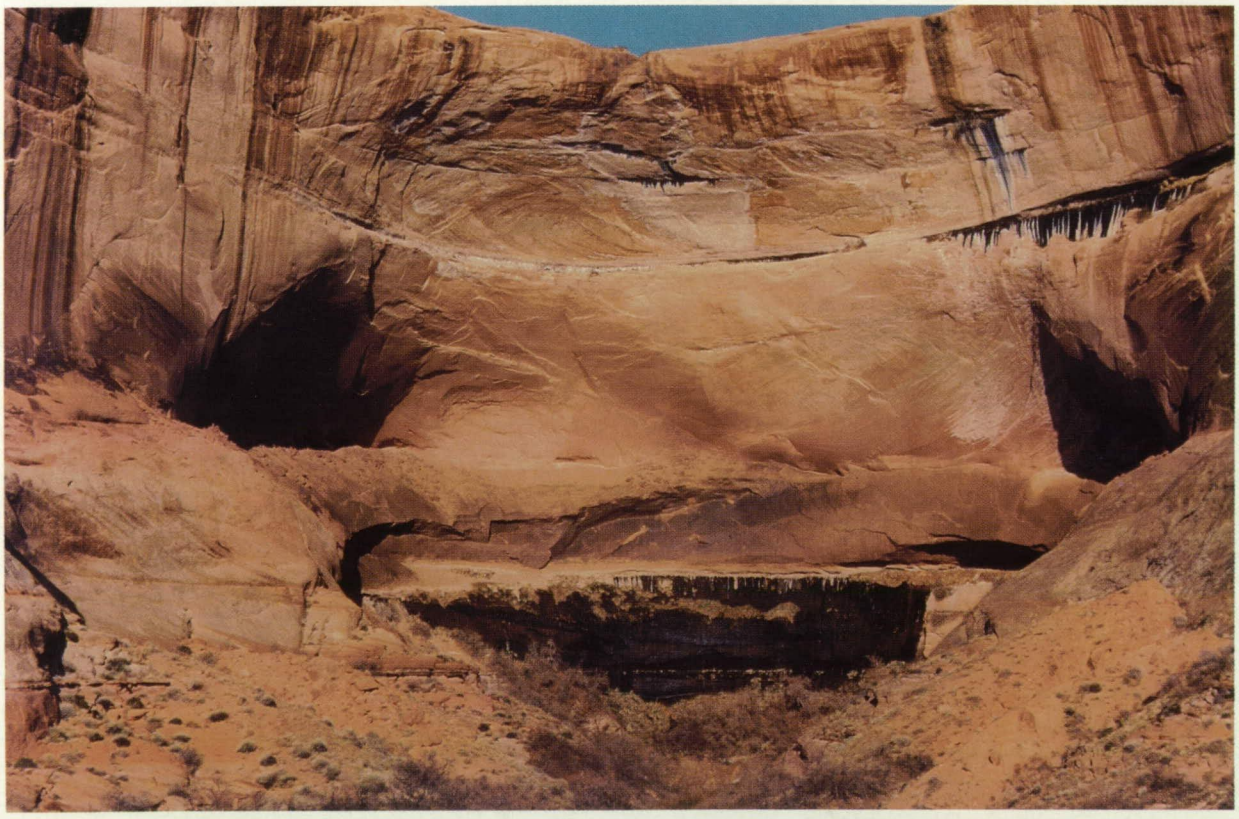

result from headward retreat. Given a constant climate, headward growth rates probably decline as the system enlarges and the drainage area of the spring heads lessens. In an advanced stage of valley development, lateral retreat by sidewall seepage approaches that of headward retreat, and valleys widen. They may continue to grow until adjacent tributaries merge, leaving only isolated buttes and remnants of the original surface.

Sapping is an erosional process that produces unique landforms. Sapped drainage systems differ from fluvially eroded networks in morphology, pattern, spatial evolution of the network, rate of erosion, and degree of structural control. Some characteristics of sapping network structure and morphology in the Navajo Sandstone include:

1. Elongated networks and basins.

Valleys elongate first and widen subsequently in response to the availability of groundwater that diminishes as the source area is approached by the canyon head. Figure 88 illustrates elongation of a network into a basin. As the valley approaches the headward limits of the groundwater basin, the rate of valley extension slows, and lateral widening of the canyon becomes increasingly significant. The canyons occupy a large proportion of the drainage basin and may continue to grow until adjacent systems merge.

The drainage basins of theater-headed valleys are markedly elongate, having a length to width ratio that averages 3.8:1 (fig. 89). The length of the drainage area was measured from the outlet to the drainage basin perimeter, and the maximum width of the basin was determined.

Figure 88. Cow Canyon illustrates elongation of a canyon network during an extensional phase of development. Sapping basins are generally elongate, and Cow Canyon has a length to width ratio of 3.4:1. The canyon is 10 km in length. Stevens Canyon: following headward extension of the main canyon, valley widening has become the dominant process. Stevens Canyon is 18 km in length.

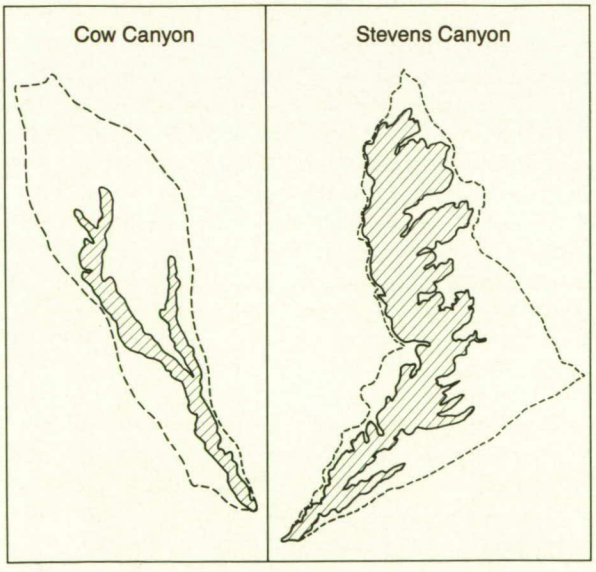

Figure 89. Elongation ratios for 30 theater-headed basins developed in the Navajo Sandstone. The average length to width ratio is 3.8:1.

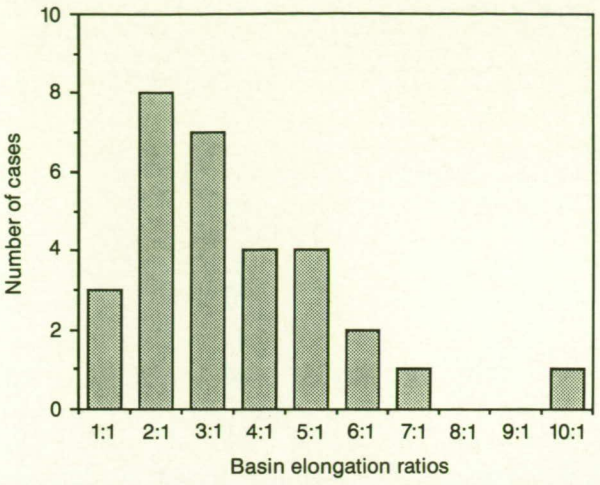

2. Simple network structure with little branching.

Of the 30 networks examined, more than 90% were Strahler order 1 or 2. No basins with Strahler orders greater than 3 were observed. Most (>50%) of the networks were single unbranched valleys (fig. 90). These observations are comparable to those of Kochel et al. (1985) for channel networks generated in fine-grained sediments of an experimental sapping box.

Unbranched tributaries are most common in basins with high length to width ratios, in valleys that grow parallel to the dip of beds, and in systems at an early stage of extension. The elongate nature of the drainage basins causes most of the groundwater to be intercepted by extending main valleys, with little available for bifurcation in down-valley areas of the basin. Branching is favored by conditions that enhance groundwater contribution along the length of the main valley. This occurs where valleys develop in synclines or extend transverse to the dip of the beds.

3. Strong structural control of canyon orientation.

Valleys grow as groundwater, emerging along the valley sidewalls, exploits zones of greater hydraulic conductivity, usually joint planes. Thus, canyon networks are often highly asymmetric, show unusual constancy of tributary-junction angles into the mainstream, and exhibit pervasive parallelism of tributary orientation over large geographic areas.

Because groundwater is also sensitive to changes in gradient resulting from regional folding, theater-headed valleys are observed to grow in an up-dip direction. However, as bed dip or topographic slopes steepen, surface runoff increases, and canyon morph-

Figure 90. Eastern tributaries to the Escalante River grow up the gently dipping (2° - 4°) slopes of the Waterpocket Fold. These unbranched canyons are at an early stage of extension.

ology tends toward forms with tapered heads. Theater-headed canyons are found principally on surfaces with low dip angles (1° - 4°) that favor a large proportion of infiltrated precipitation.

4. Relatively straight longitudinal profiles.

The longitudinal profiles of theater-headed valleys result primarily from the removal of mass along a permeability boundary. Steep headwalls (120 to 150 meters in height) appear as distinctive steps in the profile, and divide the drainage into upper and lower zones (fig. 91). On the plateau above the headwall the channels are usually floored with bare rock and sand, and may be interrupted by large weathering pits. Although the runoff from the larger of the plateau channels is considerable, surface drainage area and length of drainage area above an amphitheater are not related to the depth, width, or length of the canyon into which it drains.

Because the profile below the headwall was initiated along a permeability boundary, many of the canyons, including such large drainages as Fence, Cow, and Long Canyons, form "hanging valleys" above the base level of the Colorado, San Juan, and Escalante Rivers. Surface runoff acts to modify the shape of the profile.

CONCLUSIONS

Groundwater processes on the Colorado Plateau are manifested by scarp recession, cavernous weathering on exposed rock faces, and by the development of large-scale theater-headed valleys. In some lithologies, theater-headed valley forms may be relict of previous climatic conditions. However, the numerous deeply entrenched canyons developed in the Navajo Sandstone show abundant seeps and collapse features that indicate that groundwater erosion remains an ongoing process under present semi-arid conditions.

The process of sapping is much less common than fluvial erosion owing to the many limiting constraints on concentrated groundwater erosion. Among these are the qualities of the aquifer (areal extent, geometrical configuration and continuity, uniformity of permeability, structural and stratigraphic relationships, zones of recharge); jointing which affects local wall morphology as well as providing a conduit for groundwater flow; material properties, that is, rock must be of sufficient competency to support canyon growth at a given scale, but must break down rapidly to a size that is readily transported out of the basin; limited surface runoff, that in larger quantities would degrade the cuspate morphology of the headcuts; and a free face at which groundwater emerges and undermines basal support for overlying material. As a result of this complex interplay of conditions, groundwater sapping is not effective as an agent of valley growth in all permeable lithologies of the Colorado Plateau, even within a region where climatic conditions and regional structure are broadly similar.

Where spring sapping is an effective process, the valleys that develop are unique in terms of their morphology and network pattern. Some of the distinctive attributes of the systems include elongate networks and basins, simple networks with little branching, strong structural control of canyon orien-

Figure 91. The longitudinal profiles of Cow and Explorer Canyons, theater-headed tributaries to the Escalante River. Groundwater flows through the Navajo Sandstone and emerges at a permeability boundary formed by the underlying Kayenta Formation. The canyons grow headward by sapping along this lithologic contact.

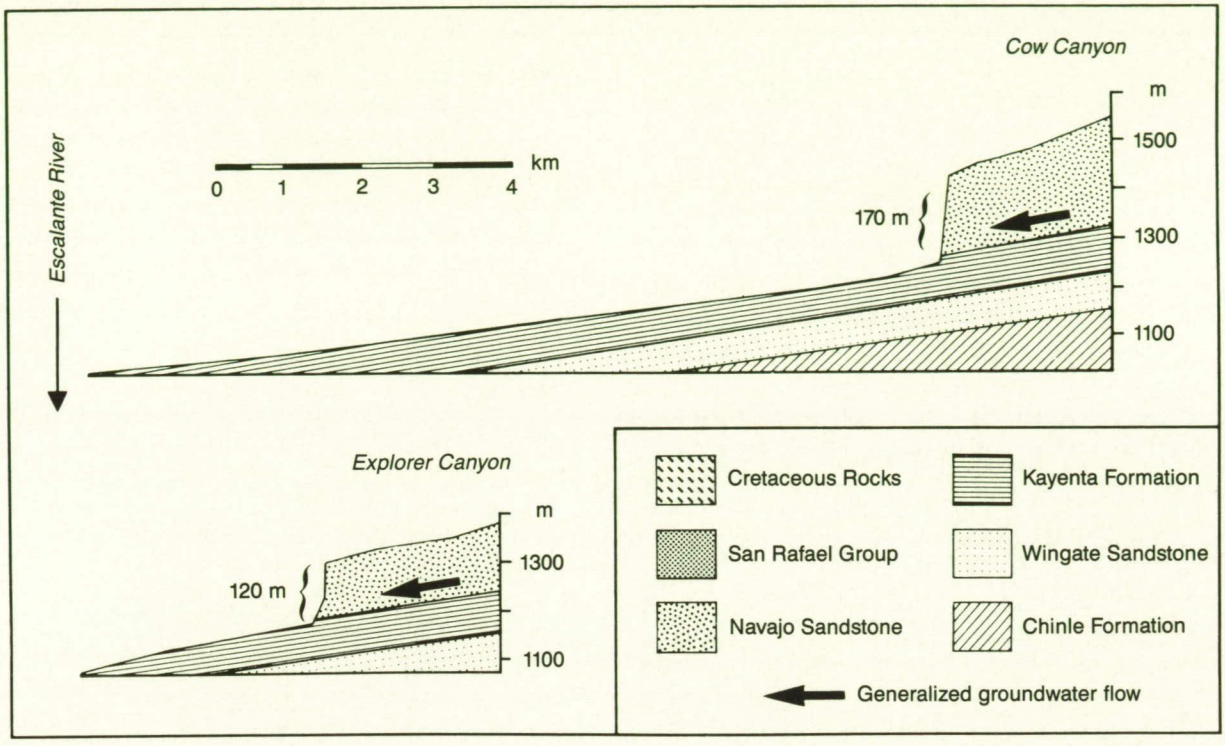

tation and wall morphology, and a relatively straight longitudinal profile that is sensitive to permeability boundaries rather than to local base level.

REFERENCES

Bradley, W.C. (1963) Large-scale exfoliation in massive sandstones of the Colorado Plateau. *Geol. Soc. Am. Bull.* **74:** 519-527.

Campbell, I.A. (1973) Controls of canyon and meander form by jointing. *Area* **5:** 291-296.

Cooley, M.E., Harshbarger, J.W., Akers, J.P., and Hardt, W. F. (1969) Regional hydrogeology of the Navajo and Hopi Indian Reservations, Arizona, New Mexico, and Utah. U.S. Geological Survey Professional Paper 521-A.

Gates, J.S. (1965) Groundwater in the Navajo Sandstone at the east entrance of Zion National Park. In *Geology and Resources for South-Central Utah.* Utah Geological Society Guidebook 19, p. 151-161.

Goode, H.D. (1965) Sources of water to supply coal-fired electric power plants in Kane County, Utah. In *Geology and. Resources for South-Central Utah.* Utah Geological Society Guidebook 19, p. 143-150.

Gregory, H.E. (1950) Geology and geography of the Zion Park region, Utah and Arizona. U.S. Geological Survey Professional Paper 220.

Harshbarger, J.W. (1961) Techniques of groundwater development in the Navajo Country: Arizona, New Mexico, and Utah, U.S.A. In *Groundwater in Arid Zones.* Symposium of Athens, 1961: International Association Scientific Hydrology Publication 57, p. 657-679.

Heylum, E.B. (1966) Systematic rock joints in parts of Utah, Colorado, and Wyoming, and an hypothesis on their origin. Ph.D. thesis. University of Utah.

Hodgson, R.A. (1961) Regional study of jointing in the Comb Ridge and Navajo Mountain area, Arizona and Utah. *Am. Assoc. Petrol. Geol. Bull.* **45:** 1-38.

Jobin, D.A. (1956) Regional transmissivity of the exposed sediments of the Colorado Plateau as related to distribution of uranium deposits. U.S. Geological Survey Professional Paper 300, p. 207-211.

Jobin, D.A. (1962) Relation of the transmissive character of the sedimentary rocks of the Colorado Plateau to the distribution of uranium

deposits. U.S. Geological Survey Professional Paper 300, p. 207-211.

Kelley, V.C., and Clinton, N.J. (1960) Fracture systems and tectonic elements of the Colorado Plateau. University of New Mexico Publications in Geology, no. 6.

Kochel, R.C., Howard, A.D., and McLane, C. (1985) Channel networks developed by groundwater sapping in fine grained sediments: analogs to some martian valleys. In Woldenberg, M., ed., *Models in Geomorphology*. The Binghamton Symposia in Geomorphology International Series, no. 14, p. 313-341, Allen and Unwin, London.

Laity, J.E. (1983) Diagenetic controls on groundwater sapping and valley formation, Colorado Plateau, revealed by optical and electron microscopy. *Phys. Geogr.* **4:** 103-125.

Laity, J.E., and Malin, M.C. (1985) Sapping processes and the development of theater-headed valley networks on the Colorado Plateau. *Geol. Soc. Am. Bull.* **96:** 203-217.

Lasson, G.D. (1963) Engineering geology of the Glen Canyon dam site, Colorado River, Arizona. In *Abstracts for 1962*. Geological Society of America Special Paper 73, p. 89.

Marzolf, J.E. (1976) Sand-grain frosting and quartz overgrowth examined by scanning electron microscopy: the Navajo Sandstone (Jurassic(?)), Utah. *J. Sediment. Petrol.* **46:** 906-912.

McKnight, E.T. (1940) Geology of the area between Green and Colorado Rivers, Grand and San Juan Counties, Utah. U.S. Geological Survey Bulletin 908.

Schumm, S.A., and Chorley, R.J. (1966) Talus weathering and scarp recession on the Colorado Plateau. *Zeit. Geomorphol.* **10:** 11-36.

Chapter 5

Groundwater Sapping Experiments and Modeling

Alan D. Howard

Studies of groundwater sapping processes and landforms at the University of Virginia involve a combination of experiments, theoretical modeling, analog studies, and comparison with martian valley networks. This discussion will concentrate on experimental development of three-dimensional valley networks by sapping processes and numerical simulation modeling of network development.

EXPERIMENTS

Our early experiments of sapping erosion of cohesionless sediments were conducted in a narrow, essentially two-dimensional chamber (Howard and McLane, *in press*). The primary purpose of these experiments was to gain insight into the processes involved and the factors controlling sapping rates and sapping zone morphology. These experiments revealed that three distinct zones occur at a sapping face (fig. 92). At the headward end, the backcutting of the sapping face causes intermittent undermining of the dry or damp sand face at intervals of several minutes. In this "zone of undermining" the dry sand is at the angle of repose, while below this is damp sand in the capillary fringe, and gradients can become vertical or overhanging due to the capillary cohesion. Most of the hydraulic erosion is concentrated in the uppermost zone of seepage outflow, where there are steep surface gradients and rapid, upward seepage. This "sapping zone" is about 2.5 to 25 cm in length, depending on flow conditions and the type of sand, with gradients of 13 to 17 degrees. The surface of this zone is wet, although flow depths are barely sufficient to cover the grains. The surface of this zone is generally smooth. Individual surface grains move downstream, but the predominant mode of movement is intermittent bulk flow failures occurring at intervals of tens of seconds to a few minutes, depending on grain size and flow conditions. The thickness of the flow failures is a few millimeters. Downstream from the sapping zone is the "zone of fluvial transport," in which the water flow is generally more than several grain diameters thick and grains move individually. Channel gradients range from 5 to 7 degrees at the outflow to 10 to 13 degrees at the junction with the sapping zone. In contrast with the sapping zone, low bedforms, generally oblique bars, are common in the fluvial zone. Whereas the height of the zone of undermining decreases during each experiment and the length of the sapping zone remains relatively constant, the fluvial zone expands as the sapping face retreats (fig. 93). Most of the experiments were conducted by maintaining a fixed groundwater head at the upstream end of the chamber (fig. 93).

Processes acting in the two-dimensional experiments were analyzed by computer simulation modeling of the evolution of the experiments based on a theoretical model of sediment entrainment by the combined forces of gravity, surface flow, and outward seepage (Howard and McLane, *in press*). These simulations indicate that the factor controlling the rate of backwasting of the sapping face is the rate at which sediment can be transported through the zone of fluvial transport, which in turn depends on the sediment characteristics, the morphology of the sapping face, and the imposed hydraulic gradient through the sand. Because the flow pattern in turn depends on the morphology of the sapping face, the temporal evolution of the sapping face results from a complicated interaction of groundwater flow, surface flow, sediment transport, and the morphology of the sapping face. The sapping zone, characterized by intermittent shallow bulk failures, is characterized by gradients near the threshold of failure as determined by the balance of seepage and gravity moments and the angle of internal friction of the sediment (direct surface tractive stresses are relatively unimportant in this zone).

The three-dimensional experiments have been conducted in an aluminum tank 5 feet square and 2 feet

Figure 92. Experimental two-dimensional groundwater sapping chamber.

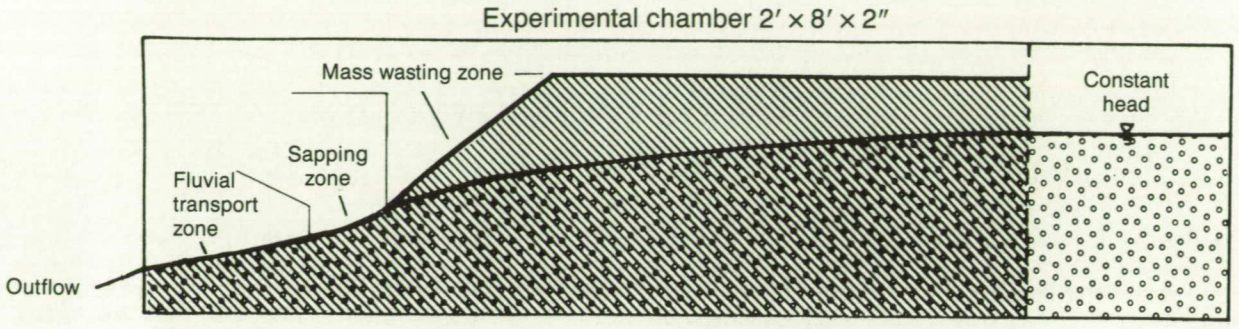

Figure 93. Evolution of sapping erosion in an experimental chamber for five experiments. Elapsed time is given in seconds.

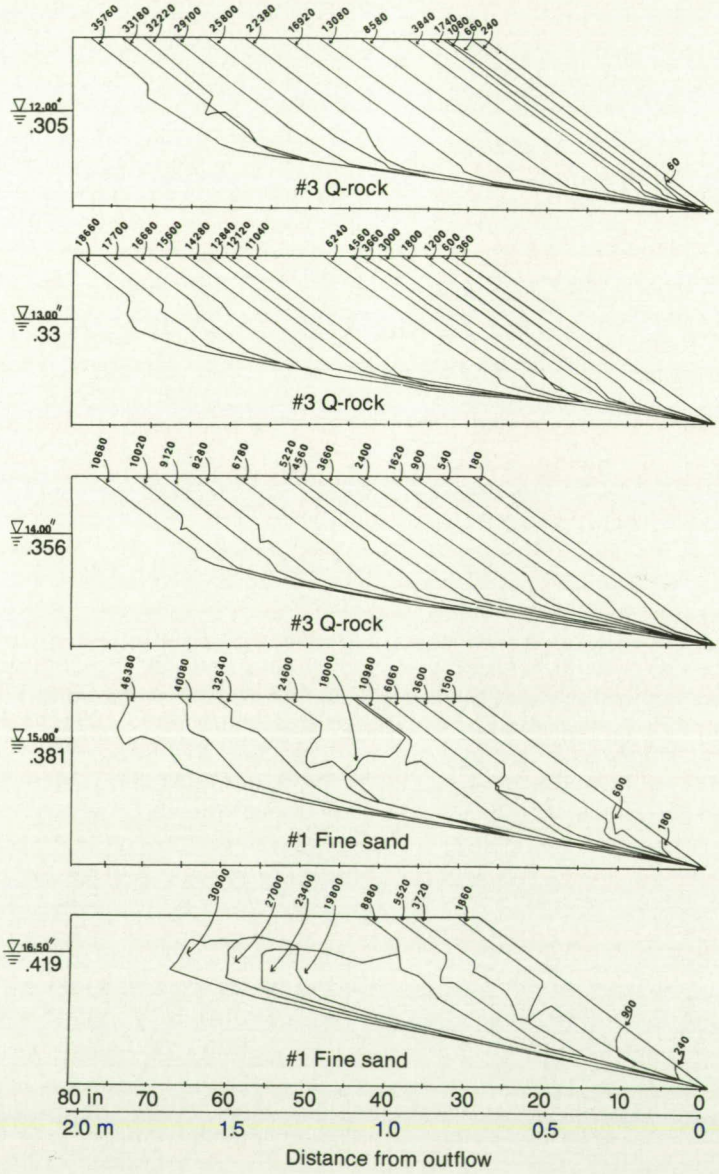

Figure 94. Three-dimensional groundwater sapping chamber.

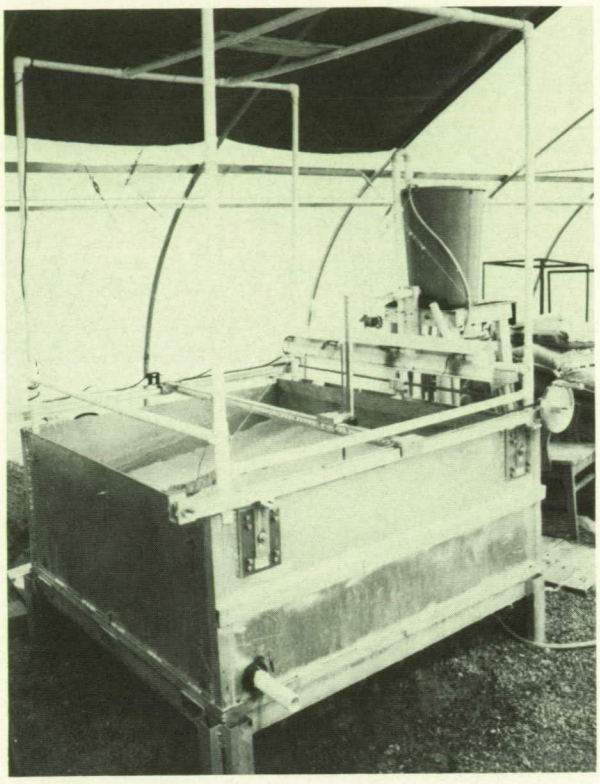

Figure 95. Cross-sections through three-dimensional groundwater sapping chamber with (A) and without (B) a downstream scarp in the sediment. Note the water reservoir to the left and the drain for water and sediment at the right end of the tank. In (A) seepage emerges at the scarp face, whereas in (B) seepage occurs along most of the upland surface, causing development of a dense rill network.

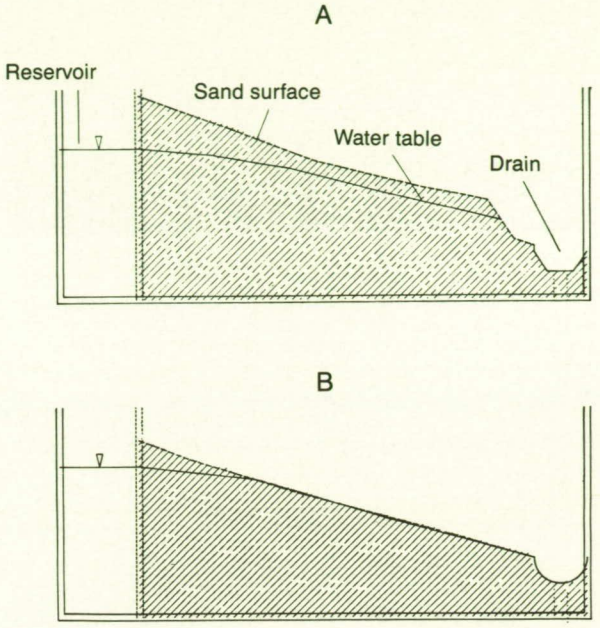

high (fig. 94). Flow originates from an upstream reservoir whose head can be controlled. A screen separates the sand from the reservoir. After flowing through the sand, the flow, and any sediment in transport, exit into a level trough and then out of the tank. A grid of piezometers on the bottom of the tank allows a rough mapping of the water table configuration during the experiments.

Most of the experiments have been conducted with essentially homogeneous, isotropic sand mixtures. In most experiments the sand surface was constructed with a slight slope (the upland surface) from the reservoir to the vicinity of the collecting trough. Also, for most experiments a small to large scarp was placed in the sand near the trough (fig. 95). Experiments have been conducted with both cohensionless and slightly cohesive sands. The experiments with cohesionless sands are discussed first.

The experiments are conducted by raising the head in the reservoir until erosion commences. Several distinct channels are initially formed (fig. 96A). However, competition between adjacent channels is very strong, so that after a few inches of headcutting along the main channels, only one to three channels remain active (fig. 96B). The channels that by chance have stronger flow due to slightly higher permeability of the sand feeding the channel erode more rapidly. As suggested by Dunne (1980), these channels, by virtue of the lower and more forward position of their headward terminus, cause convergence of flow lines and resultant "capture" of groundwater from adjacent, less advanced channels. As the channels extend headward and flow convergence increases discharge, erosion rates increase. During most experiments this was offset by decreasing the head in the reservoir to maintain a roughly constant erosion rate. Competition becomes less strong after the one to three main ("trunk") channels are established. The drainage density of one two three major channels in the box is controlled primarily by the geometry of the groundwater flow through the sand mass, particularly the depth of flow relative to the length of flow, as well as the depth of the channel (that is, the magnitude of its "cone of depression"); these factors, plus the magnitude of the critical flow needed to initiate erosion, determine the lateral influence of a given channel on groundwater flow.

In experiments in which flow rates were only slightly above the threshold for sediment entrainment, short tributaries often developed from the trunk channels (fig. 97). Sometimes both channels remained active after the bifurcation, but often one channel became inactive after a time due to competitive disadvantage. As a result, tributary channels are generally short and stubby, and are actively growing for only a short period. Three factors act concurrently to create tributaries. First, as the trunk channels erode headward, the flow convergence becomes stronger, and

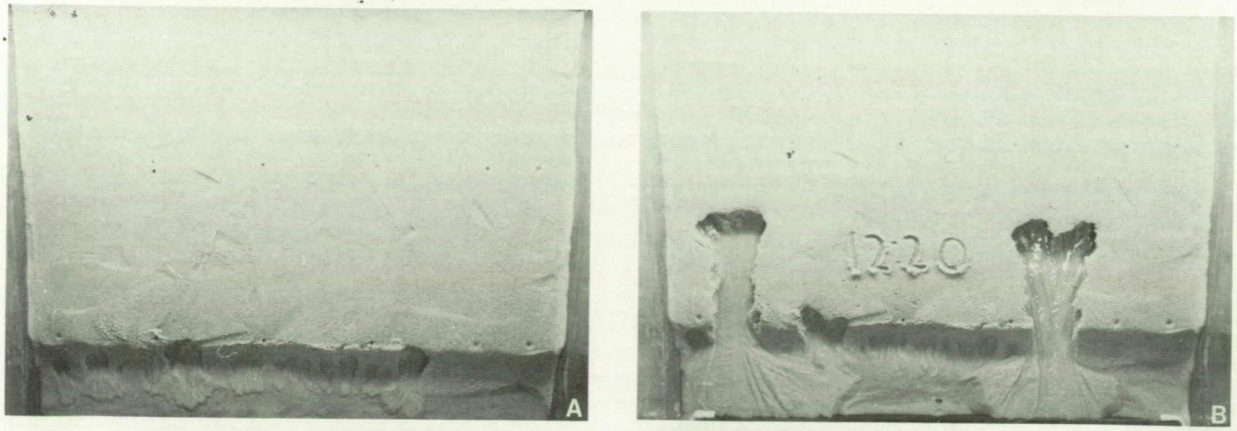

Figure 96. The temporal evolution of drainage networks developed in coarse cohesionless sand in the three-dimensional sapping chamber. The groundwater enters the sand from the reservoir beyond the top of the picture through the permeable back wall. The water and sediment drains into the gutter at the bottom of the picture. Note the numerous initial channels in (A), the development of tributaries in (B), and the mass-wasting that occurs on the valley walls upon drying after the conclusion of the experiment (C).

Figure 97. Temporal evolution of drainage networks in coarse cohesionless sand with discharge slightly above the erosion threshold.

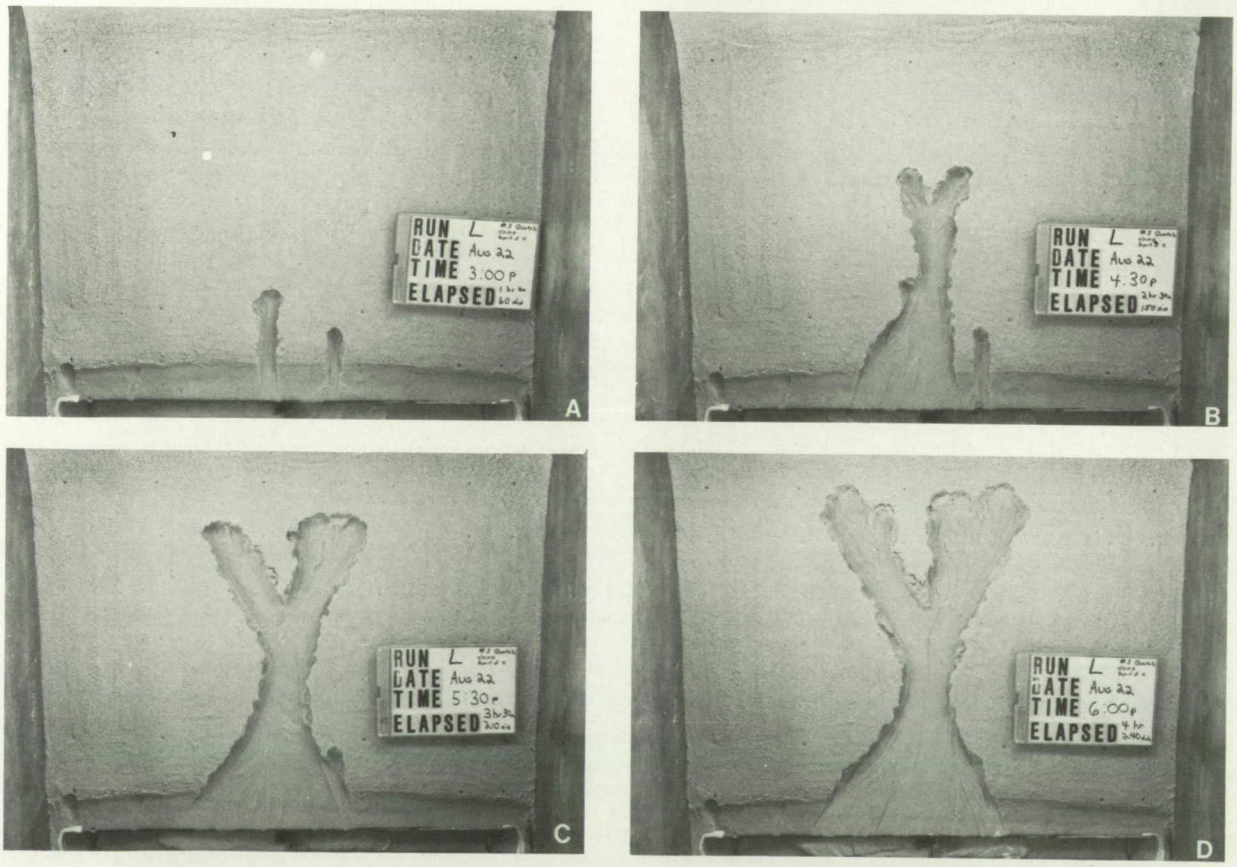

there is a tendency toward widening of the valley head. This factor alone would probably not produce bifurcation. Small differences in permeability at the valley headwall can create two zones of headwall extension surrounding a zone of lower permeability. Groundwater competition can then continue this process, with the two channels growing along diverging paths. Another factor that is important in the sand box is the occurrence of headwall slumps. As with the two-dimensional box, the valley headwalls are eroded episodically by mass wasting. When undermining creates a local slump, the infilling of material raises the channel bed and pushes the zone of groundwater emergence downstream, temporarily reducing the rate of erosion. Adjacent portions of the headwall that have not recently experienced slumps may gain a competitive advantage, causing a bifurcation.

Even with low flow rates and slow rates of erosion, the channels become rather wide relative to their depth in cohesionless sand. The reason for this is the lateral meandering and small-scale avulsion around bars that occurs in the shallow, wide alluvial channels below the headscarp. The lateral valley walls are constantly being undermined, widening the valleys.

At high flow rates and with correspondingly more rapid erosion, the competition between adjacent channels becomes less pronounced. More trunk valleys are active and valley heads are wider (fig. 98). Lateral erosion often destroys the intervalley divides a short distance below the headwall. Tributaries are rare.

Several methods were tried to introduce small amounts of cohesion into the sand to study the effects of cohesion on channel form. Introduction of small quantities of clay into the sand proved unsatisfactory, because appreciable cohesion was obtained only with quantities of clay sufficient to severely restrict groundwater flow rates and inhibit sapping. Plaster was also unsuitable, largely because the solubility of gypsum tended to create surface crusts by evaporation of water at the sand surface. Portland cement in concentrations of 1:125 to 1:175 provides moderate cohesion to the well-sorted coarse sand matrix without a strong effect on permeability; it was used for a series of experiments.

Experiments with cemented sand in which the groundwater flow regime was similar to the experiments with cohesionless sand produced a drainage pattern similar to those with low flow rates in cohesionless sand in that one to five trunk channels developed. However, the valley form differed in that it was narrower and deeper (fig. 99). Erosion rates were much lower for the same discharge, so that lower channel gradients were required. However, the channels near their head end were steeper than an alluvial channel would be for the same regime of water and sediment; the channel floor lacked an alluvial cover. That is, the headward portions were "bedrock" channels in the sense described by Howard (1980). These bedrock channel sections commonly were irregular in gradient with occasional potholes. The potholes probably formed primarily in zones of below-average cohesion. Under such circumstances the overall rate of erosion was determined by the rate of detachment at the headwall and along the upper bedrock channel rather than by the sediment transport capacity as in the case of cohesionless sand. Much less lateral erosion of valley walls occurred along the lower portions of the trunk channel than was the case for cohesionless sand. This was due to both the cohesion of the sand and the lower channel gradient in the lower parts of the trunk valleys.

Figure 98. Temporal evolution of drainage networks in coarse cohesionless sand with discharge well above the erosion threshold.

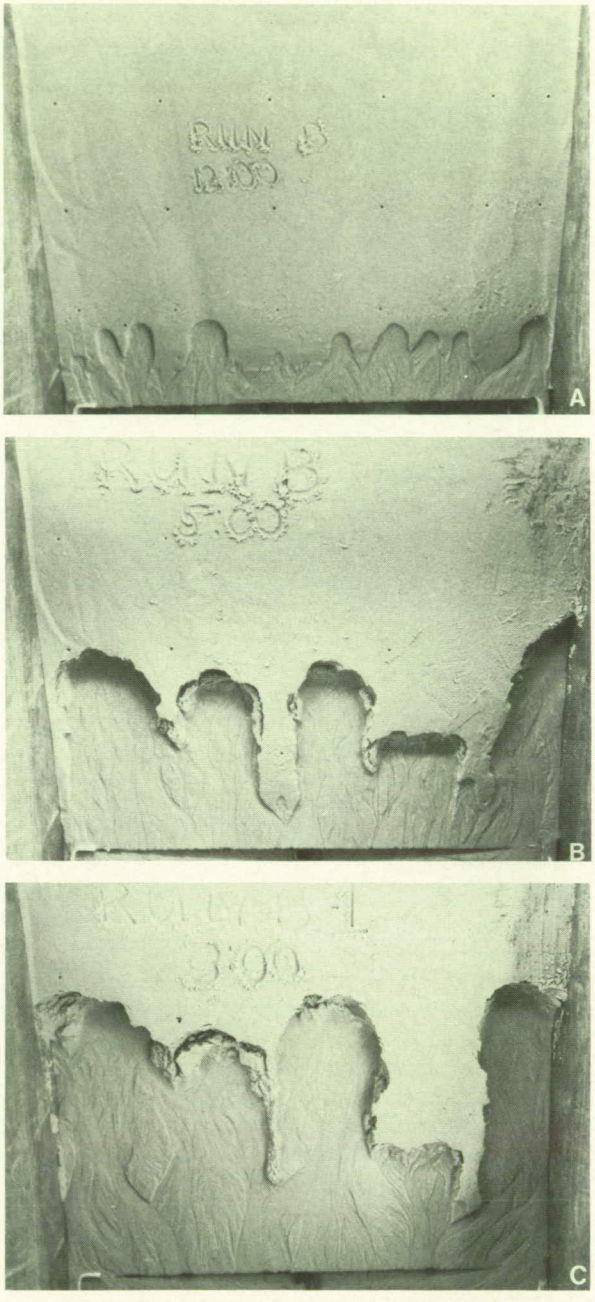

Figure 99. Temporal evolution of drainage networks in slightly cohesive coarse sand. Note the narrow, steep-walled valleys with slab failures where the walls are undermined by seepage.

Figure 100. Temporal evolution of drainage networks in slightly cohesive coarse sand. Note the shallow rills developed on the upland surface from emergent seepage and the terminal and levee deposits formed where the reabsorption of water into the sand decreases transport capacity. Narrow, steep-sided valleys have eroded headward from basal scarp.

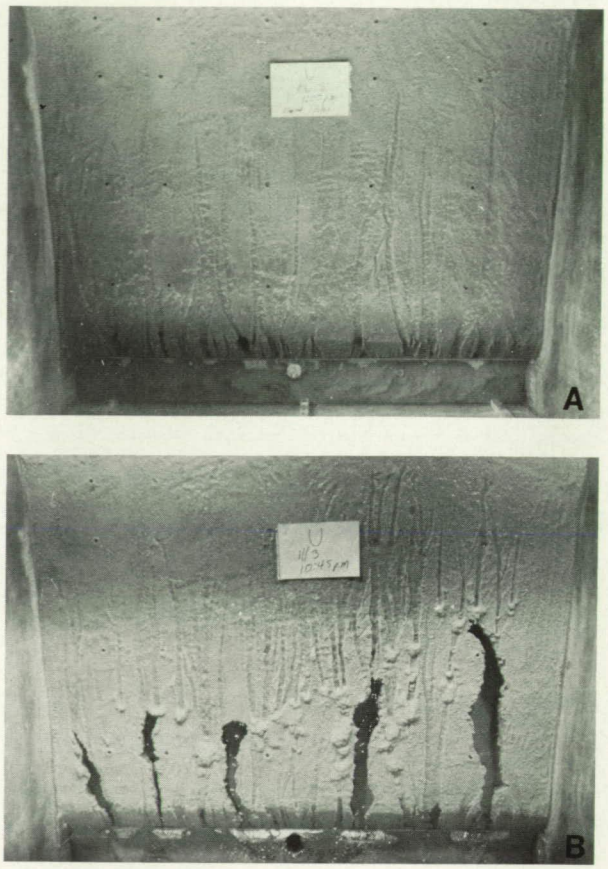

Due to the somewhat reduced permeability with the admixed Portland cement and the cohesion, hydraulic gradients about 20 to 50% higher than those for cohesionless sand were required to initiate erosion. As a result, in these experiments an unintended circumstance occurred in which groundwater flowed from the reservoir through the sand, emerged as surface flow on the middle portions of the upland surface, and then once again sank into the sand near the scarp close to the exit trough. The flow then reemerged near the base of the scarp (fig. 100). This flow pattern produced an erosional morphology that was strikingly different from previous experiments. As a result of the 8 to 10 degree slope on the upland surface, a rill system formed on the upland surface. These rills were initially nearly parallel, but as erosion progressed, they became integrated into a crude dendritic pattern. The initial rills died out as they approached the lower scarp due to loss of water through the channel bottom. As a result, the sediment transported through the rills was redeposited as marginal and terminal levees along the lower portions of the rills (fig. 100). Headward erosion along trunk channels occurred relatively independently of the rill development on the upland surface.

The development of the upland channels was further investigated with a series of experiments in which the sand surface morphology and the hydraulic gradients were varied. If the hydraulic gradient is increased, or if the slope of the upland surface is increased (generally requiring a decrease in the height of the basal scarp), the drainage over the upland surface does not sink into the sand prior to passing over the basal scarp. As a result, rapid rill incision occurs on the steep scarp surface at the downstream end of the upland, and the rill network grows by a combination of downward cutting of the upland portions of the rills and headward retreat of the gullies cutting the lower scarp (fig. 101). Toward the end of the period of erosion, the gradients of the lower portions of the rills on the upland surface steepen somewhat, and the gully heads become more gentle, so that the rill profiles are more uniformly graded. However, due to inhomogeneities in the cement binding, local gradient scarps and scour holes occur along most rills.

If the scarp is eliminated, so that the upland surface slopes smoothly down to the trough (fig. 102),

rill development occurs fairly uniformly over the upland surface within the zone of emergent seepage. Rill incision is most rapid near the lower end of the upland surface where discharges are greatest, so that the rills develop a generally concave profile. Lateral channel migration and divide erosion cause local captures that result in a crudely dendritic network developing through time (fig. 102).

The differences in rill and gully development as the slope of the upland surface and the height of the basal scarp are varied are similar to the variations in drainage pattern developed on runoff rill networks on slopes of different steepness described by L. Phillips (chapter 14). In cases where the upland surface is nearly flat and a relatively large lower scarp occurs, runoff (produced either by emergent groundwater or by excess precipitation) erodes primarily as channels cutting headward as a "wave of dissection." Where the scarp is relatively lower or absent and the upland surface is steep, rills develop and subsequently deepen over most of the upland surface. Little of the erosion occurs through headward migration of a wave of dissection.

Figure 101. Temporal evolution of drainage networks in slightly cohesive coarse sand. In contrast to fig. 100, the upland seepage is strong enough to pass over the basal scarp. The network develops jointly by rill erosion on the upland and by headward erosion of gullies from the scarp (partly from water contributed from the rills, and partly from seepage emerging at the scarp face).

Figure 102. Temporal evolution of drainage networks in slightly cohesive coarse sand. No basal scarp is present, and seepage emerges on the lower portions of the upland surface, producing a rill network that deepens progressively. Many of the scour holes developed at a network of locations where the surface was marked for positional reference. Note the dendritic drainage pattern that develops in the deeply incised network. The water head in the upstream reservoir was raised during the course of the experiment; in (A) seepage first emerges about halfway along the slope. In (B) the seepage emerges along the lower two-thirds of the slope (due to an increase in the head), and in (C), about four-fifths of the slope experiences seepage.

A feature of these experiments with cohesive and cohesionless sands that is particularly noteworthy is the difference in drainage density between situations in which channel development is solely by headward scarp retreat (where only one to three trunk channels eventually survive) and the dense network that forms where groundwater emerges near the top of a sloping plain (where 20 to 30 rills may occur across the plain). This may have application to drainage networks on Mars. The coarse-textured, deeply incised drainage networks dissecting the walls of Valles Marineris (fig. 103) have been argued to be of sapping origin (Kochel et al., 1985), and they may be closely analogous to the experimental networks developed by headward scarp retreat (figs. 96, 97, and 99). Particularly suggestive is the valley form that results in the experiments with cohesionless sand after the sand has dried and the valley walls slump to form angle-of-repose slopes (fig. 96C). The more elongated, but also deeply incised Nirgal Valles (fig. 104) may be of similar origin. Brakenridge et al. (1985) have recently suggested that many of the small valley networks on Mars may have formed by hydrothermal spring sapping. These small, subparallel networks have drainage densities many times those of the Valles Marineris or Nirgal Valles types, and they have formed on broad, but reasonably steep regional slopes. The morphometric similarity to the rill networks developed on upland slopes in the experimental chamber suggests a similar origin by groundwater emergence. One important similarity is that the networks head along a fairly well-defined line below the crest of the slope that in the experimental chamber is the head of the zone of seepage. The experiments described above indicate that higher drainage densities would be expected under such circumstances. Baker (chapter 7) and Baker and Partridge (1986) also note that the small valley networks are characterized by two types of channels, numerous subparallel networks developed on the regional slopes, and a few deeply incised channels developed along the lower courses of the networks. They suggest that the incised channels are late-stage modifications of the shallow channel network; crater counts lend some support to this interpretation, although counting techniques are problematical on these narrow, linear features. However, the experiments described above raise another possibility: the dense, subparallel network may be analogous to the rill networks developed on the upland slope, and the incised channels may have developed concurrently by headward scarp retreat (sapping in the incised channels also may have continued as the water table dropped below the level of the upland). Other experiments directed toward explanation of Hawaiian valley morphology are discussed by Kochel et al. (chapter 6).

SIMULATION MODELING

Although the sand tank experiments described above provide insight into sapping processes and sapping valley morphology and suggestive analogs to martian valley networks, the experiments necessarily form a limited and potentially misleading analog. Foremost is the problem of scale; the processes and materials producing the small-scale experimental are necessarily different from those acting in the martian networks several orders of magnitude larger. There is little justification for assuming that morphologies of groundwater sapping networks in the laboratory and on Mars would be geometrically similar. The processes acting to produce scarp retreat in the experimental networks are primarily those of hydraulic entrainment together with mass-wasting triggered by sediment removal at the base of the scarp. Rocks exposed in martian valley networks are almost certainly more indurated than those in the experiments, and the processes of groundwater erosion at the headwalls should primarily involve physical and chemical weathering, as occurs in the Colorado Plateau and in Hawaiian valleys discussed elsewhere in this volume.

One way of gaining insight into the interactions of processes, materials, structure, topography, and flow patterns that can form groundwater sapping valley networks is through theoretical modeling. Such an approach is being undertaken through computer simulation of the interaction of erosional processes and groundwater flow. Theoretical approaches offer the advantage of being able to numerically scale process and material properties. In addition, temporal and spatial boundary conditions can be extensively varied to examine their effects. On the other hand, simulation modeling can be limited due to finite computer resources, lack of appropriate theory, numerical instabilities or errors, and difficulty of testing theoretical assumptions against empirical data.

Our initial simulations of valley development by groundwater sapping have utilized simplistic assumptions about sapping processes, materials, and flow conditions.

The Flow Model

Initial numerical experiments have been conducted using a regional finite-difference numerical flow model for an unconfined aquifer of finite thickness, and permeability that is vertically uniform but areally variable. The gradients of the piezometric surface are assumed to be small enough to permit the DuPuit assumption. Erosion rates are assumed to be slow enough that a steady-state flow model is appropriate. Under these assumptions the governing flow equation is

Figure 103. A portion of the scarp wall of Valles Marinaris showing stubby, theater-headed valley networks.

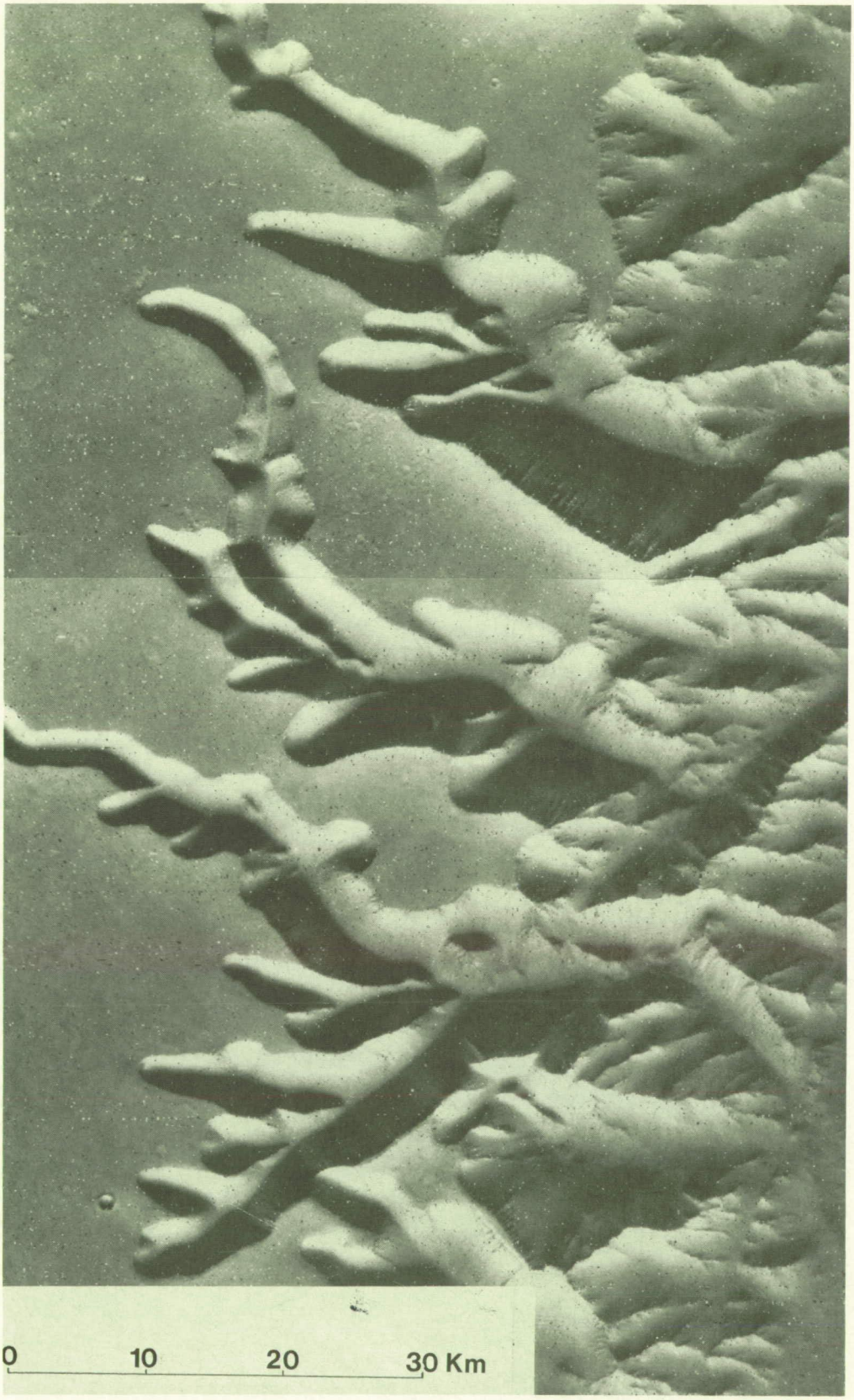

Figure 104. A portion of the headward end of Nirgal Valles showing stubby tributaries with theater heads.

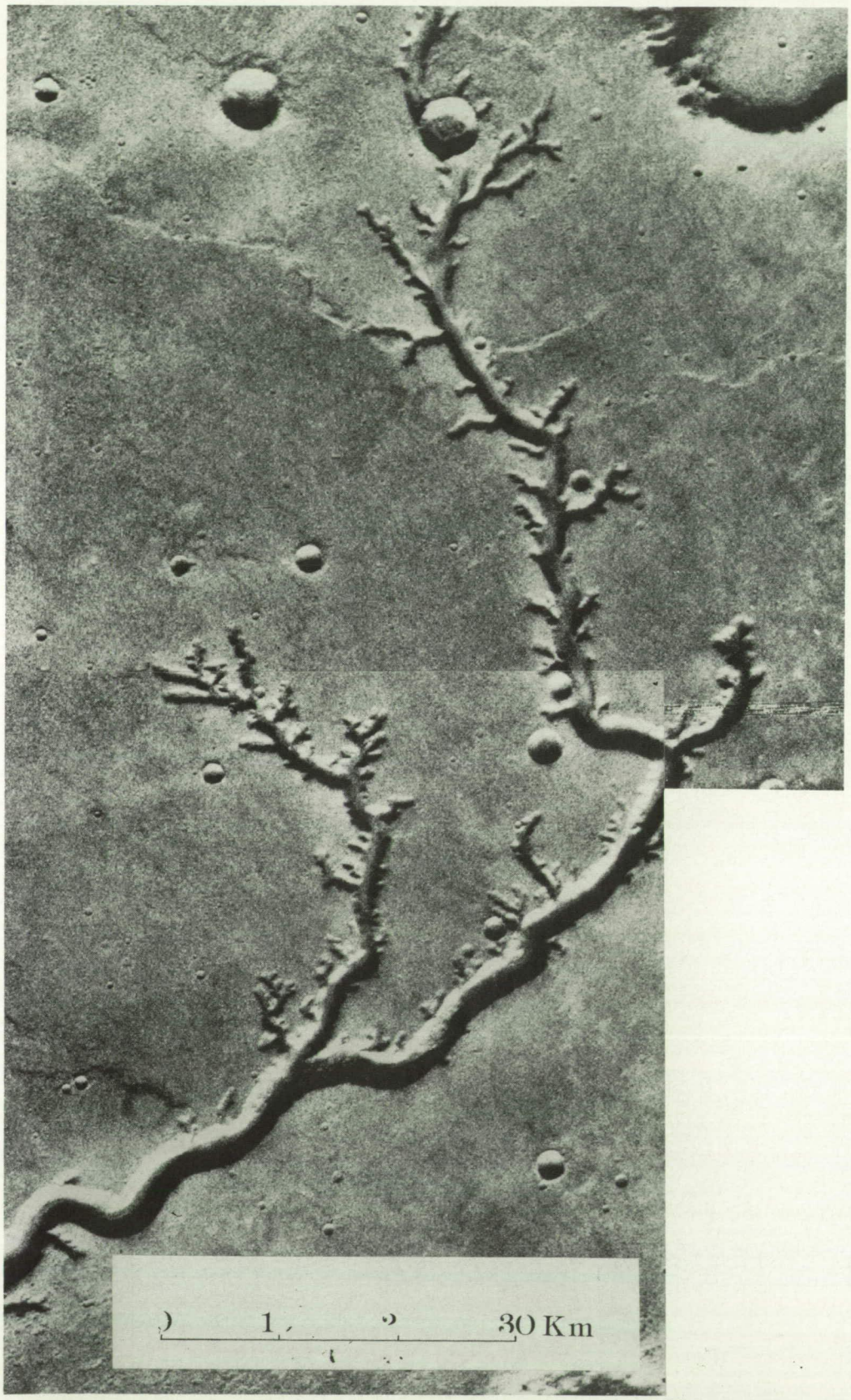

$$\frac{\partial}{\partial x}\left(K\,h\,\frac{\partial h}{\partial x}\right) + \frac{\partial}{\partial y}\left(K\,h\,\frac{\partial h}{\partial y}\right) = R \qquad (1)$$

where h is the hydraulic head, x and y are the horizontal axes, K is the hydraulic conductivity, and R is the recharge (positive) or withdrawal (negative) rate (volume of water per unit time per unit surface area). The groundwater flow pattern is solved using Gauss-Seidel iteration with successive over relaxation (Wang and Anderson, 1982, chapter 3).

For the simulations discussed here, a 50 × 50 point square grid defines the active flow area. The boundary conditions were no-flow boundaries (groundwater divides) on the left, right, and top, and a fixed head boundary on the bottom (the outflow). Uniform areal recharge was assumed. A nominal hydraulic conductivity, K_n, was assumed, and the actual conductivity of each cell, K_a, was defined as

$$K_a = K_n\, e^{CN} \qquad (2)$$

where N is a random normal deviate (zero mean and unity standard deviation) and C is a scaling factor. Once assigned, the conductivities remained constant. The randomization of conductivity was included to simulate natural areal variability.

The Erosion Model

For simplicity, the simulated area was assumed to have uniform erodibility, and valley walls and heads were assumed to erode horizontally (zero downstream gradient). Erosion was assumed to occur only along the valley walls and heads, where groundwater emerges to the surface. In other words, the simulation corresponds to very low gradient valleys eroding headward into a level upland. The rate of valley wall erosion was assumed to be proportional to the excess of lateral inflow of groundwater per unit width of valley wall, q, above a critical flow rate, q_c:

$$E = E_c\,(q - q_c) \qquad (3)$$

where E_c is a scaling factor.

Initially the eroding scarp face was assumed to be along the lower, fixed head boundary of the flow domain. As valleys eroded headward, the head and side walls were likewise treated as fixed head locations. In order to increase resolution of the valley morphology above the 50 × 50 matrix, each *active* node representing the furthest extension of erosion has an array of 8 *virtual* nodes that represent the fractional extension of erosion beyond the actual node in eight directions (N, NE, E, SE, S, SW, W, and NW). If erosion in any direction progresses to the distance that the fractional extension exceeds the internode spacing, then the next node in that direction becomes an active node. Furthermore, to increase the flow net resolution, a procedure was developed to force the water table to pass through the fixed head of each virtual node. This was accomplished by defining an *apparent* head for each direction that represents the groundwater table projected through each virtual node to the actual node.

Test Simulations

The evolution of the valley network and the corresponding flow network was simulated by an iterative procedure. First, the flow net was calculated for the existing pattern of fixed heads representing the valley headwalls (initially the lower flow domain boundary). Each calculation of the flow net required 75 to 200 successive approximations. Then, based on equation 3, lateral erosion was simulated by moving the virtual nodes. Any resulting new active nodes were added to the list, and apparent heads for the active nodes were calculated. Total erosion was scaled for the entire collection of virtual nodes such that the maximum rate of lateral erosion was equal to a preassigned fraction of the internode spacing. Such flow and erosion calculations are alternated through a specified number of iterations or until no further erosion was possible ($q < q_c$ everywhere).

The end results of two simulations are shown in figs. 105 and 106. Figure 105 shows a simulation for an assumed value of q_c of zero. Under these circumstances all active nodes undergo some erosion. However, even for this case there is a competitive effect such that erosion becomes concentrated along a few wide valleys. The flow net at the close of the simulation is shown in fig. 105B. The end result is similar to the pattern that occurs for high discharge rates (high q relative to q_c) for cohesionless sand (fig. 98). An additional simulation was run for a value of q_c that was about 0.8 times the maximum value of q at the start of the simulation. Under these circumstances only a small fraction of the active nodes has sufficient discharge to undergo erosion. Competition is very strong, with only a few, narrow valleys forming (fig. 106). Note that there is a weak tendency to form tributary valleys. The competition is due to groundwater capture, as discussed above. Many short valley heads and sidewalls experience a decrease in discharge through time as more advanced portions of the drainage network receive their former drainage. The resultant network has narrower valleys than any of the networks in cohesionless sand (for example, figs. 96 and 97). This is due to two factors. First, it is difficult to run the experiments at flow conditions very close to the critical value because of the length of time required to conduct the experiment and the necessity for very diligent control by the experimenter. Second, lateral planation by the fluvial channels tends to widen the valleys, as discussed previously. Planation effects are not included in the simulation model. The valley networks produced by scarp retreat using cohesive sand are more similar to the simulation with high q_c (fig. 99).

Figure 105. Plan view of a simulated valley network developed by groundwater sapping with a critical discharge, q_c of zero. (A) The lines show the position of the edge of the valley at intervals of 25 iterations, with erosion progressing from the bottom edge of the matrix. (B) Vectors showing the flow field at the end of the simulation (the vectors are assumed to be of zero length within the valleys).

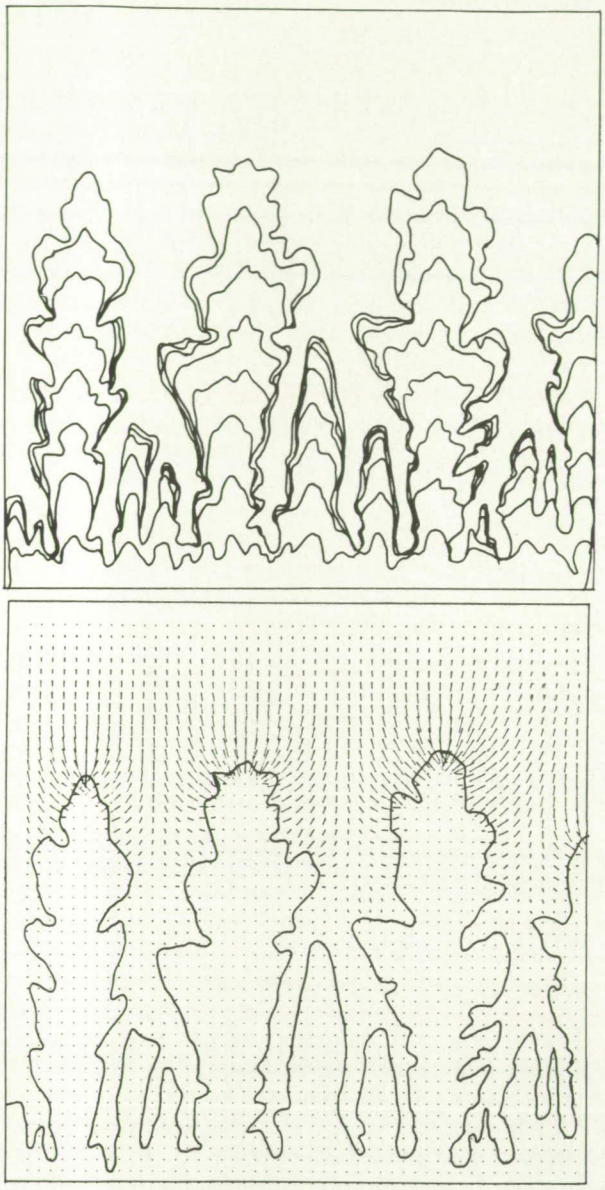

Figure 106. Plan view of a simulated valley network developed by groundwater sapping with a high value of the critical discharge, q_c. See fig. 105 and text for explanation.

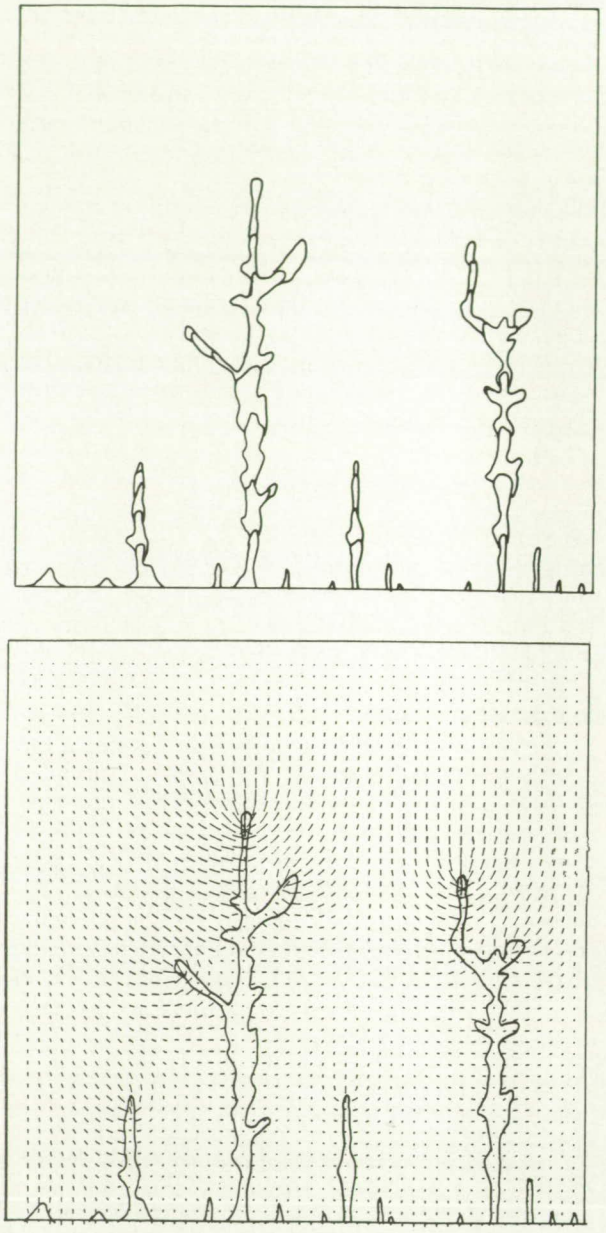

FUTURE RESEARCH

Laboratory experimentation of sapping processes has essentially been completed. These experiments, together with those completed by Craig Kochel at Southern Illinois University, provide an extensive data base for extrapolation to terrestrial or martian analogs as well as a basis for testing simulation models. The primary emphasis in future research will be a combination of computer simulation and field analog studies.

The first stage of development of simulation models will be to program general purpose models and to test the validity of model assumptions. The first stage will be an assessment of whether regional groundwater flow models (quasi three-dimensional) are adequate for modeling sapping processes under simple boundary conditions (e.g., single-layer confined or unconfined aquifers). If they are not, then either more general three-dimensional modeling will be required, or adjustments will have to be introduced to correct for model inadequacies. The primary problem to be addressed is that the regional flow models do not

model discharge to seepage faces. In fact, near such locations the hydraulic gradients are sufficiently high that the model assumption of a near-horizontal piezometric surface is violated. In the present simulations the assumption is made that most of the groundwater discharge to the valleys occurs as seepage close to the valley walls, so that the calculated q values crossing the fixed-head boundaries at the valley walls primarily represent seepage flow (or at least are proportional to seepage flows).

Assuming that an accurate and numerically efficient numerical flow model can be created (as seems very likely), the next step is to validate the process assumptions and numerical techniques used in the erosion modeling. The primary means of such validation will be to model valley development under conditions corresponding to the flow tank experiments.

The validated model can be used to investigate the effects of changing material parameters, differing assumptions pertaining to the rate laws governing erosion, and different boundary conditions (topography, sources and sinks of water, thickness and layering of sedimentary layers, and structural features such as faults, craters, etc.). We will be particularly interested in the effects of varying model parameters on the morphology of simulated valleys. Such comparisons can be the basis for inferring the hydrologic and geologic setting of martian valleys of sapping origin.

REFERENCES

Baker, V.R., and Partridge, J.B. (1986) Small martian valleys: pristine and degraded morphology. *J. Geophys. Res.* **91:** 3561-3572.

Brakenridge, G.R., Newsom, H.E., and Baker, V.R. (1985) Ancient hot springs on Mars: origins and paleoenvironmental significance of small martian valleys. *Geology* **13:** 859-862.

Dunne, T. (1980) Formation and controls of channel networks. *Progr. Phys. Geogr.* **4:** 211-259.

Howard, A.D., and McLane, C.F. (in press) Erosion of cohesionless sediment by groundwater sapping. *Water Res. Res.*

Howard, A.D. (1980) Thresholds in river regime. In Coates, D.R., and Vitek, J.D., eds., *Thresholds in Geomorphology*. Boston, Allen, and Unwin, p. 227-258.

Kochel, R.C., Howard, A.D., and McLane, C.F. (1985) Channel networks developed by groundwater sapping in fine-grained sediments: analogs to some martian valleys. In Woldenberg, M. J., ed., *Models in Geomorphology*. Boston, Allen, and Unwin, p. 313-341.

Wang, H.F., and Anderson, M.P. (1982) *Introduction to Groundwater Modeling*. San Francisco, W.H. Freeman.

Chapter 6

Groundwater Sapping Experiments in Weakly Consolidated Layered Sediments: A Qualitative Summary

R. Craig Kochel, David W. Simmons, and Jonathan F. Piper

Recent laboratory experiments have produced channels by groundwater sapping processes in weakly consolidated sediments (Kochel et al., 1983, 1985). Currently, this type of research is being conducted jointly by Southern Illinois University (SIU) (Kochel and others) and University of Virginia (UVa) (Howard and others).

The SIU recirculating flume has been modified for groundwater sapping studies by the installation of a perforated, screened headwall that allows a constant head reservoir to recharge a groundwater table established in a wedge of sediment (fig. 107). By varying the characteristics and geometry of the sediments, this system is capable of modeling processes acting in a variety of natural settings. Experiments to date at SIU have examined the effects of the following parameters on sapping channel morphology: surface slope, stratigraphic variations in permeability cohesion and dip, and structure—joints and dikes.

Gently dipping layers of varying permeability, combined with joint patterns, are used to simulate conditions analogous to those found on the Colorado Plateau. Channels formed in these experiments were characterized by long valleys, short tributaries, and amphitheater heads, similar to the valleys described by Laity and Malin (1985). Our discussions focus only on the experiments mimicking conditions expected on the Colorado Plateau.

Figure 107. Schematic of the modified flume at Southern Illinois University. The upper third of the recirculating, tilting flume is shown in the sketch. Reservoir level is maintained at constant head by the use of the overflow pipe. The dimensions of the sediment wedge vary with slope angle and internal stratigraphy.

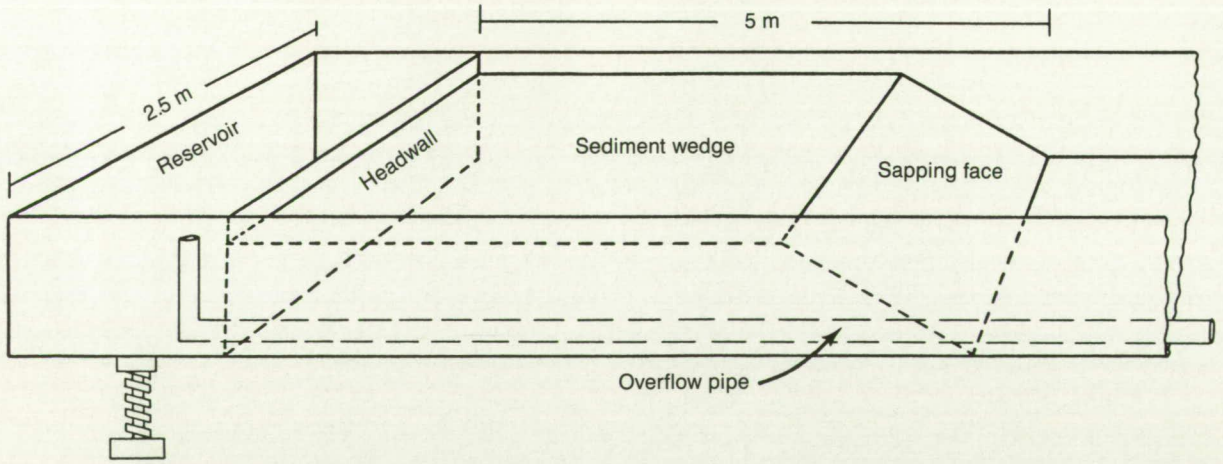

FLUME EXPERIMENTS

Experimental Design

Figure 108 illustrates the variety of designs used to simulate the gently dipping strata and joints characteristic of the Colorado Plateau. Run 3 can be viewed as a control because it used uncemented, homogeneous sediment. Runs 8–11 were designed to observe the effect of joints in a variety of stratigraphic settings. Joints were constructed by excavating the fine sand in linear troughs and backfilling with coarser, more permeable sand. Runs 27 and 28 investigated the effects of varying cohesion. Cohesion was varied by mixing different amounts of cement (between 0.5 and 5% cement) or loess in the fine sand and by using sediments of varying grain size.

Figure 108. Summary schematic of the experimental runs discussed in the text. Vertical scale of the cross-sections is exaggerated twice. The joint network shown in the plan view was used for runs 8–11.

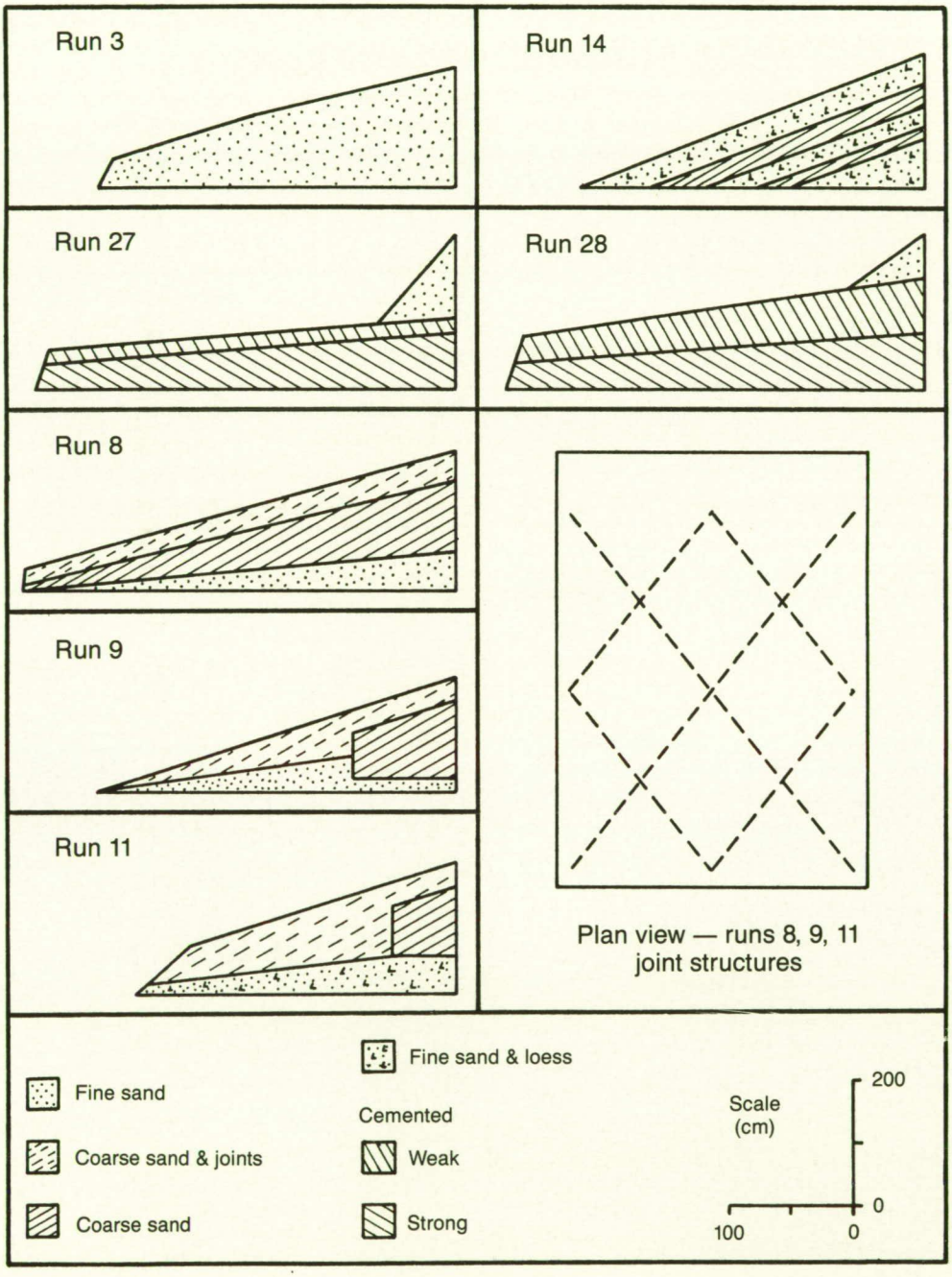

Variations in Slope and Stratigraphy

The slope of the sediment surface and the slope of the internal stratigraphy were varied between runs to determine the effect of slope on sapping processes. In particular, we were interested in how slope affects the rate of sapping, measured by the rate of channel development, and how the slope affects the morphology of sapping channels. Most of the slope variations were not designed with distinct Colorado Plateau analogies in mind. Aside from minor structural warpings, the rocks of the Colorado Plateau typically range in dip between 1° and 3°. However, several observations may be of general interest in the evolution of sapping channels.

Our experimental sapping processes were partly transport limited because of scaling problems inherent in the relative size of the sand compared to the dimensions of the channels produced. We also cannot effectively scale the weathering processes that have been shown to be important in the disintegration of debris falling from weakly cemented sandstone outcrops like those in the Navajo Sandstone (Schumm and Chorley, 1966).

Homogeneous Sediment. Initial experiments using homogenous sediment (fig. 108, run 3) indicated that there exists a threshold slope of about 9° below which no sapping channels formed (fig. 109). Below this critical slope, a seepage face formed, but channel incision failed to occur because sediments were not entrained. This slope value is probably diagnostic of the fine sand used in these experiments.

Experiments with initial slopes above 11° experienced significant slumping at the expense of channel formation. Kochel et al. (1985) observed that sapping channels sometimes formed in this slump debris. The slumping decreased slope gradient to the range where sapping channels could form.

Layered Stratigraphy. The effects of slope in experiments with layered stratigraphy appear to be more complex. Variations in the dip of strata seem to be more important in channel development than surface slope. Runs 14 and 27 (fig. 108) contained layered strata with markedly different surface and dip slopes. The 9° surface slope of run 14 should have resulted in rapid channel formation. However, only small channels formed directly above the toe of the coarse layer. Slumping occurred downslope from this point (fig. 110). The stratigraphy in run 14 was parallel to the surface slope, and no layering was exposed on the seepage face. Most of the groundwater discharge through the coarse layer either flowed along the flume floor to induce slumping or emerged directly above the toe of the coarse layer, taking the shortest route through the fine layer. The surface slope of run 27 was only 3°, well below the threshold of transport seen in homogeneous fine sand, but experienced significant channel development. Channels developed because

Figure 109. Oblique photograph of run 3 after 46 hours. This run, using homogeneous, uncemented fine sand, serves as a control to which subsequent photographs of other runs can be compared. Note the abandoned channel on the right whose groundwater was pirated between hour 6 and 10 during the run by the two neighboring channels.

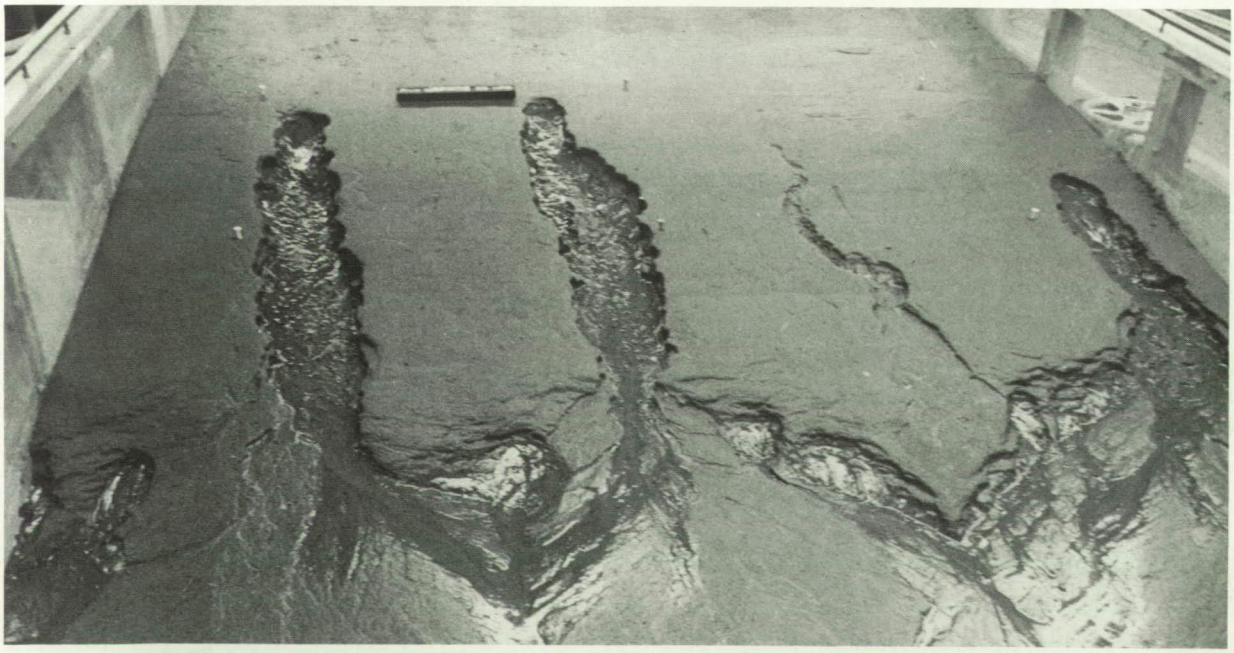

ORIGINAL PAGE IS OF POOR QUALITY

Figure 110. Oblique photograph of run 14 after 58 hours. Note the shallow channels that formed only in the lower portion of the seepage face. Channels were unable to extend up the seepage face as they did in run 3 (fig. 109) in homogeneous sediments. Groundwater was prevented from reaching the seepage face by the less permeable loess-sand unit on top (see fig. 108).

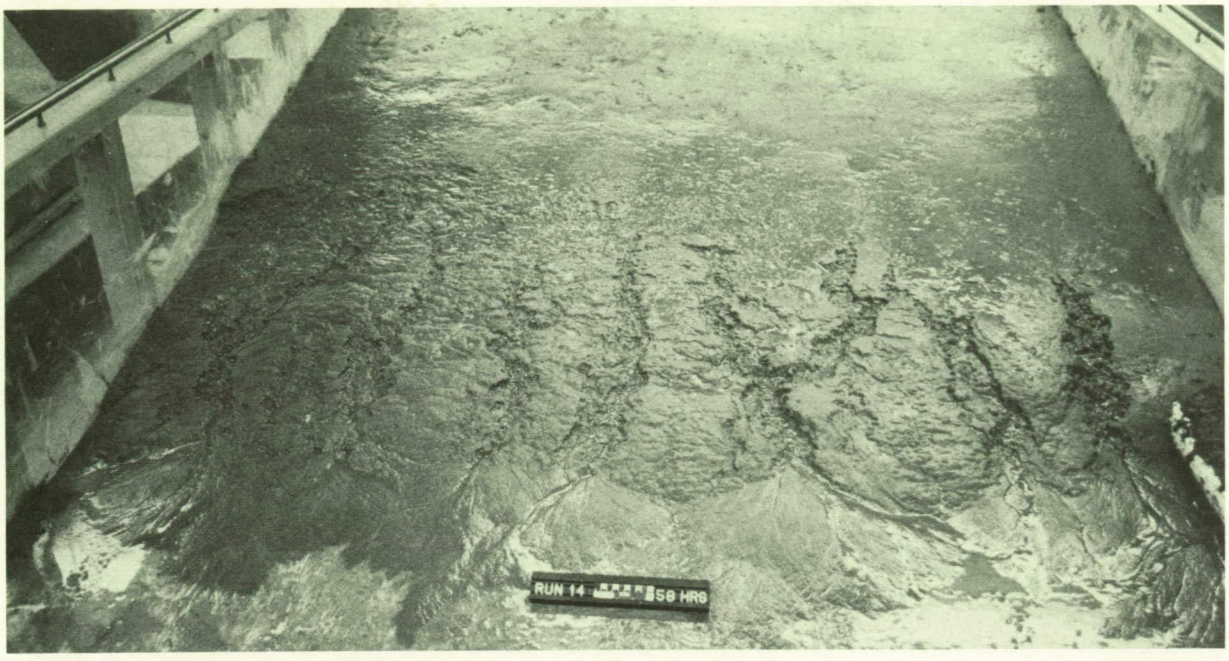

the coarse, permeable layer was exposed on the face of a low scarp at the toeslope. Sapping rapidly produced small slumps which extended headward into channels (fig. 111). The coarse sand used in the more permeable bed armored the channels, which inhibited incision as the run continued. Therefore, these channels were not incised as deeply as those in homogeneous sediments (fig. 109).

The depth of the sapping canyons also appeared to have been directly related to the thickness of the sediment in the upper strata. In situations where there is a more permeable upper layer (weakly cemented) over a less permeable base (strong cement or loess mixture), the basal layer acts as a base level control on incision. Thick, cemented upper layers prevented good channel development in the experiments because channels were clogged by massive slumps from valley walls. Coarse debris from the large slump blocks could not be eroded and formed boulders of cemented sand that armored the channel. Less cemented upper strata were readily eroded by fluvial processes downstream from the sapping face.

The width of the sapping channels varied considerably with the thickness of the strata and with cohesion (compare run 3, fig. 109 and run 27, fig. 111). Channels were wider in less cohesive sediments (run 3) where lateral migration of streams downstream from the sapping face was extensive. Cohesion limited the rate of lateral cutting by retarding the rate of channel wall slumping, resulting in narrower valleys.

Structural Variations

Asymmetry of Tributaries. Laity and Malin (1985) drew attention to the role of structure in controlling the pattern of channel networks developed by sapping in the Navajo Sandstone of the Colorado Plateau. They noted that on a regional scale tributaries to the Escalante River were asymmetrically distributed on opposite sides of the channel. Tributaries were much more frequent on up-dip slopes, which indicated the importance of groundwater flow down the regional stratigraphic dip. Note that the right (up-dip) walls of the channel indicated by the arrow in fig. 112 are scalloped by sapping alcoves and incipient tributaries, while down-dip slopes (left) are smooth. The up-dip walls were receiving significant groundwater flow. This asymmetry is also visible in the large sapping valleys developed in layered volcanic rocks of the Kohala volcano on Hawaii (fig. 113; see Waimanu Canyon in particular) and on slope valleys along sapping in basalt (fig. 114).

Joints. Structural features such as joints and faults create zones of increased permeability in consolidated rocks which are preferred paths for groundwater flow.

Figure 111. Oblique photograph of run 27 after 88 hours. Compare the channel development to run 14 (fig. 110). Channels in run 27 extended much further up-slope because the permeable bed was exposed on the lower seepage face, which permitted headward extension by sapping.

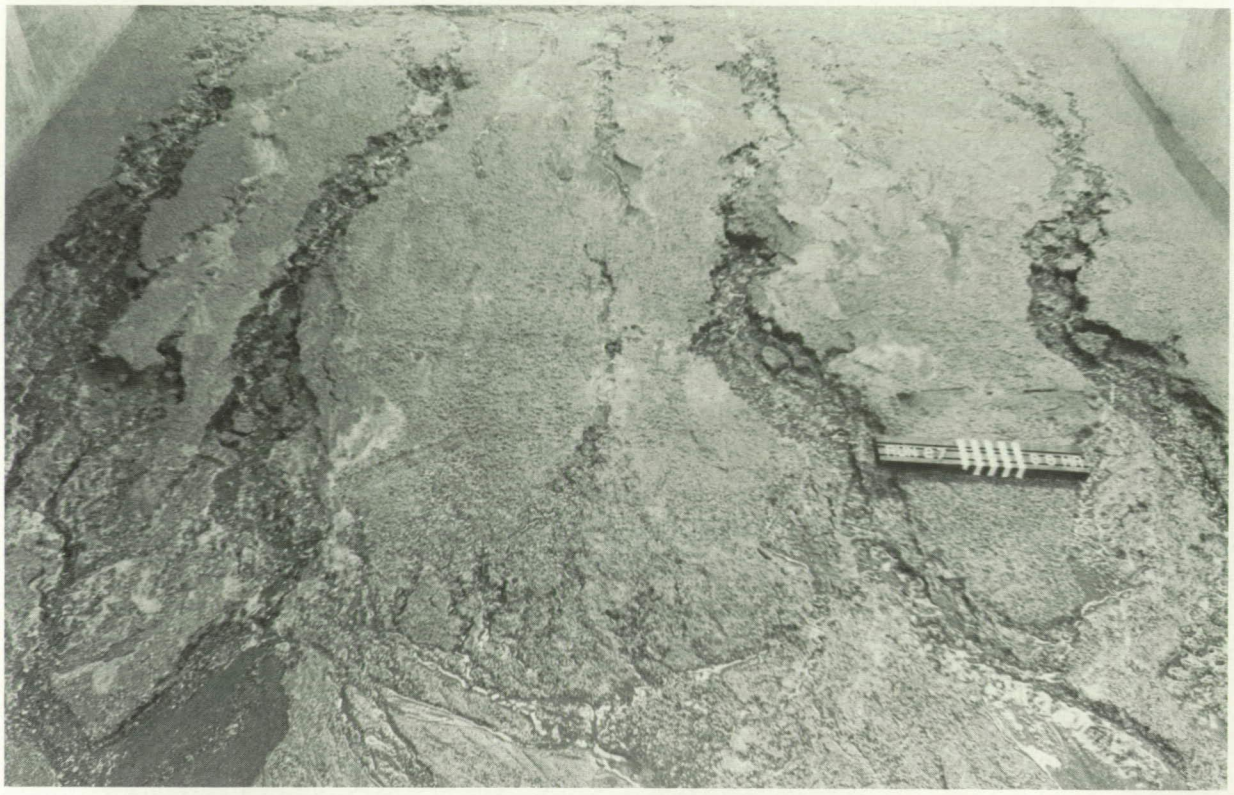

Figure 112. Oblique photograph of the central portion of run 18 after 22 hours. Note the asymmetry of the morphologic expression of channel walls. The up-slope walls (arrow) are scalloped by alcoves where sapping is occurring while down-dip walls are smooth.

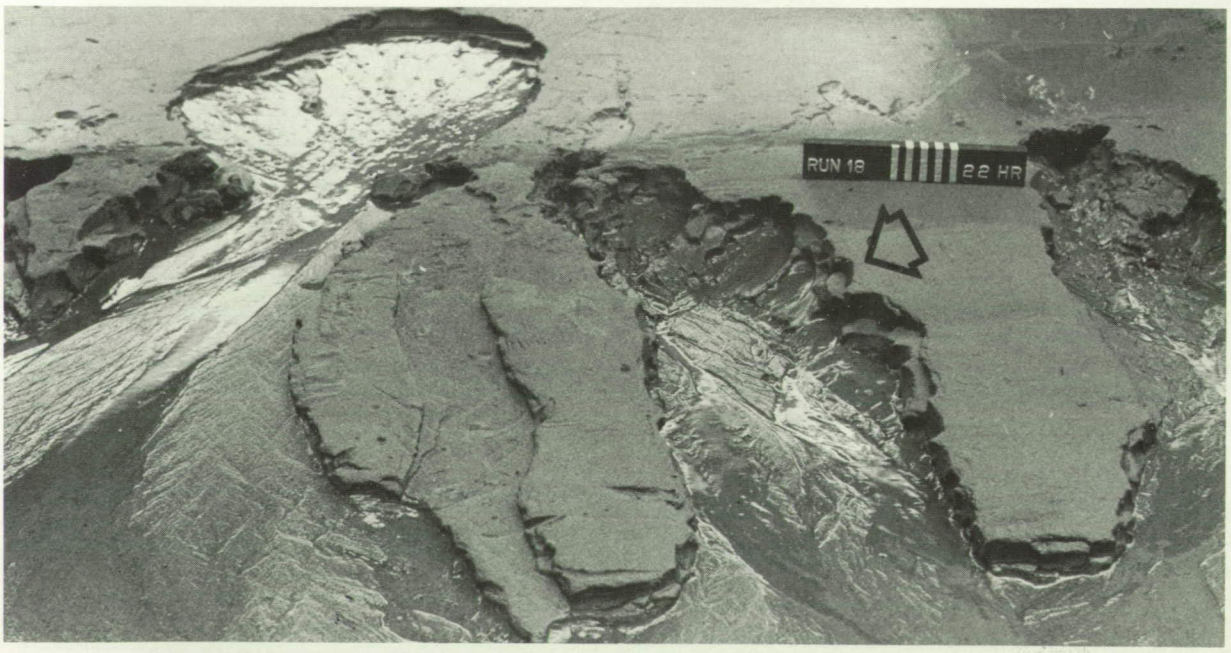

Figure 113. Map of the valleys and drainage of the northeastern slope of Kohala volcano on the island of Hawaii. Sapping valleys have the deep, wide valleys indicated by the shaded pattern. Note the asymmetry of tributaries to many of these canyons, in particular in Waimanu Valley. Valleys are absent on down-dip sides of the channel. Note also the absence of downstream tributaries for many of the valleys, such as Honokane Valley.

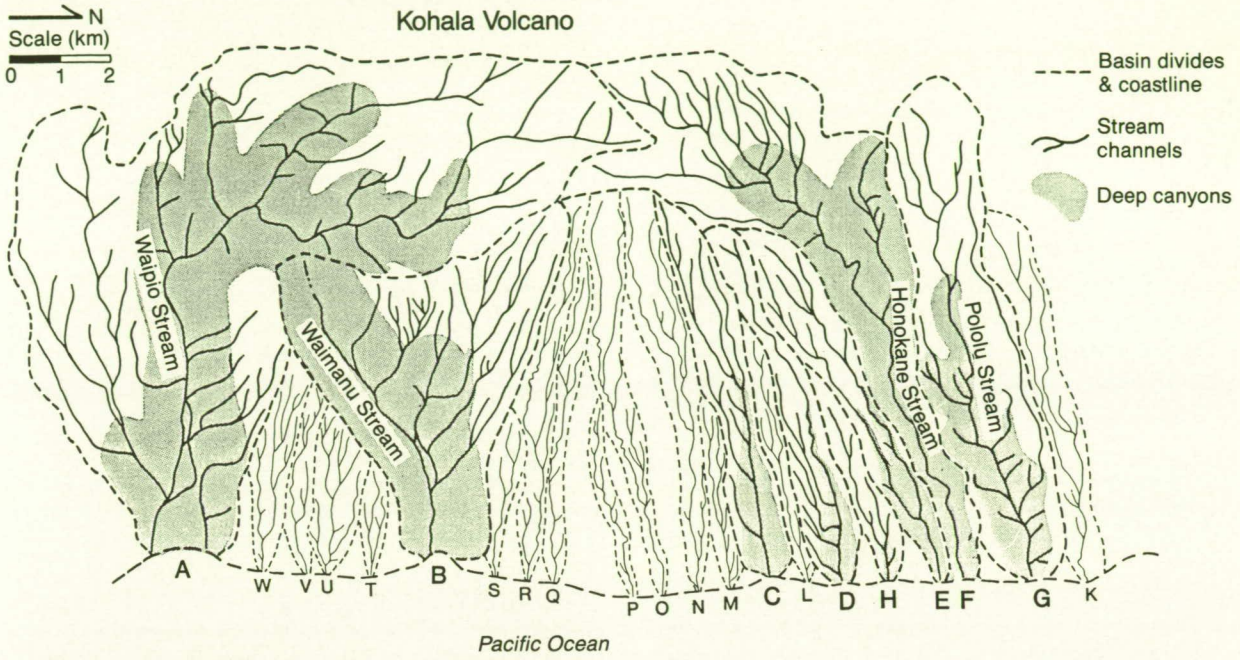

Figure 114. Viking Orbiter frames 923A13–14 of some of the slope valleys along Valles Marineris, Mars. Note the symmetry of tributaries to the main sapping valleys. On a much larger scale, there is a marked asymmetry of valleys along opposite margins of Valles Marineris that also appears to reflect the effect of groundwater migration through gently dipping strata.

Laity and Malin (1985) showed that orientations of channels in the Escalante River region closely corresponded to regional joint trends on the Colorado Plateau. Some of the sapping canyons on the Plateau terminate in tapered heads where joints intersect. Similar tapered heads are also seen on Mars (see fig. 119b). Joint spacing also appears to play a major role in controlling the width of alcoves. The width of these alcoves is limited by the spacing of the joints.

Experimental runs 8–11 (fig. 108) were designed to observe the effect of joints on the development of sapping channels. In general, main channel trends followed joint patterns and tributaries developed parallel to joints. Channels in run 11 followed the joints exclusively (fig. 115). During the first few hours seepage occurred in the slope over a large range of elevation but exclusively along the joints. Two main channels formed and enlarged headward along the joint pattern (fig. 115a). The left channel was favored during the latter hours of the run because it reached an intersection of joints first and pirated water from the neighboring channel (fig. 115b).

In runs 8–10, the channels did not follow the joints exclusively, but were strongly influenced by their presence. Run 8 began with a period of parallel scarp retreat by slumping at the toe of the slope. An indentation appeared along the scarp at the right by hour 30 (fig. 116a) which extended into a joint intersection. By hour 9 (fig. 116b) this grew into a large channel showing a bifurcated head. The bifurcation was due to groundwater inflow from two diverging joints above the intersection. The early development of run 9 followed the joint pattern (fig. 117a) until major joint intersec-

Figure 115. Oblique photographs of channels in run 11 showing the effects of joints on channel development. (A) After 2 hours, groundwater is preferentially flowing along joints. (B) By 4 hours, the channels continued to enlarge and incise along joint trends. Note that the left channel has developed further at the expense of the right channel, probably due to piracy after the major joint intersection between the channels was first encountered by the left channel.

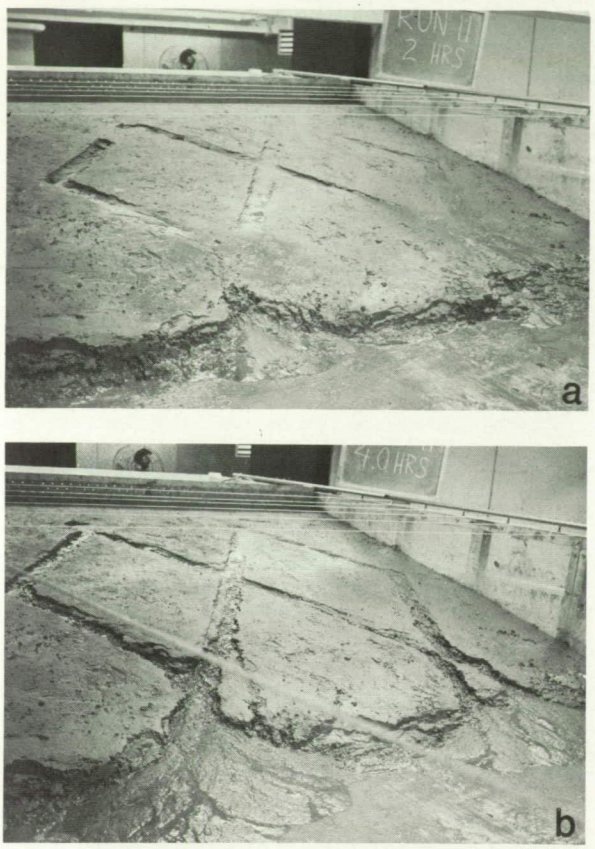

Figure 116. Oblique photographs of run 8. (B) After 9 hours, a distinct embayment appears along the right half of the backwasting escarpment due to slumping. Eventually, slumping in this area extended to the joint intersection visible upslope. (A) By hour 40, a large channel formed by sapping processes fed by the augmented groundwater flow at the intersection of the two joints.

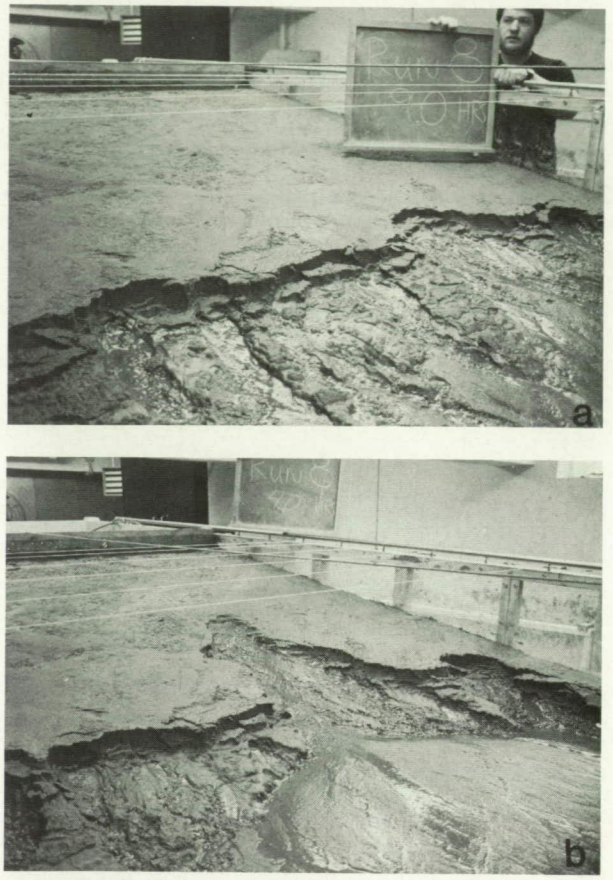

tions were encountered. Then, the left channel widened rapidly following a major joint trend (fig. 117b) creating the diagonal channel. The right channel bifurcated at a joint intersection and followed two diverging joints as it continued to cut headwardly. This is well illustrated in the graphs of data from run 9 (fig. 118). The rate of headcutting in channel 2 (left channel) was rapid during the first 19 hours as the diagonal channel was forming. The rate of growth of channel 2 then slowed as channels 4 and 5 enlarged (right bifurcation). Apparently, channels 4 and 5 pirated more water from the neighboring channels after reaching the joint intersection on the right.

In summary, our experiments with linear zones of increased permeability suggest that if significant joints are present, sapping valleys will preferentially extend along these avenues of increased groundwater discharge. The degree of influence joints will have on channel location probably depends on the relative differences between the permeabilities of the joints and the host rock. As this difference becomes greater, the influence of jointing should become more pronounced. Our current experiments are testing this idea by developing sapping channels in jointed systems in cemented sand.

Martian sapping valleys display numerous examples of structural control in their valley patterns. Figure 119 shows that headward extension of slope valleys along Valles Marineris was controlled by the influence of grabens. Similar features have been observed by Kochel and Burgess (1983) along the margins of major Martian outflow channels. Kochel and Capar (1983) showed close correspondence of structural features with sapping channels throughout the Valles Marineris region.

Runoff and Sapping

Most investigators of channel-forming processes agree that sapping and runoff processes are jointly responsible for valley development in field situations. Schumm and Phillips (1986) suggested that both processes were important in the development of large valleys along the coast of New Zealand. Kochel and

C-2

Figure 117. Oblique photographs of run 9. (A) Initial channel development along major joint trends during hour 3. (B) After 11.5 hours, the left channel widened rapidly along a diagonal joint. The left channel enlarged first because its headward extend reached the intersection of two joints before any of its neighbors.

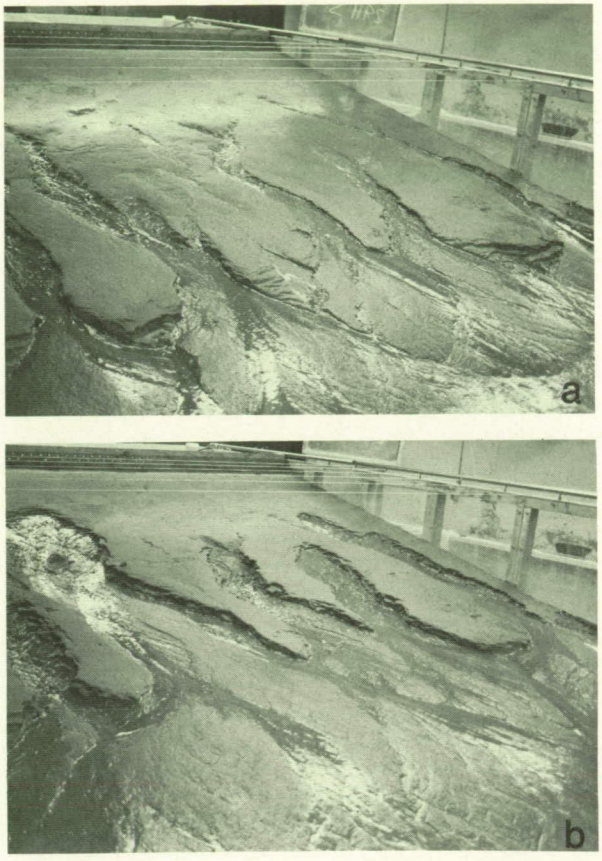

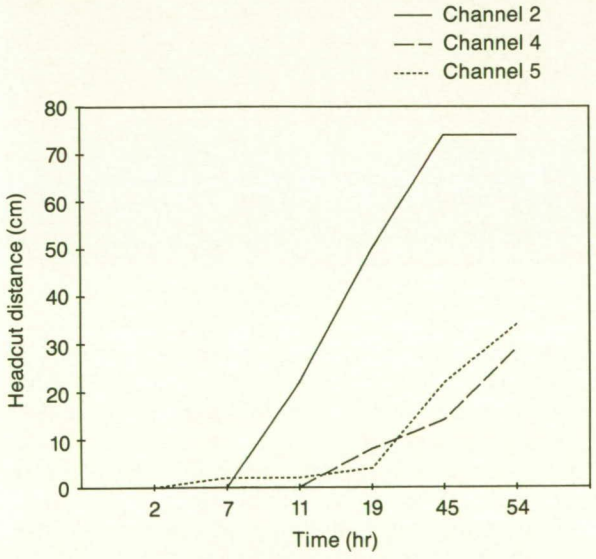

Figure 118. Plot of channel headcutting with time for run 9. Note the rapid extension of channel 2 (left channel in fig. 117). Channels 4 and 5 did not extend significantly until later in the run, when they succeeded in pirating some of the water from channel 2. At the time, the rate of headcutting in channel 2 decreased.

Figure 119. Examples of structural control of sapping valleys on Mars along Valles Marineris. (A) Viking frames 921A11–19 showing canyons extending up linear grabens. (B) Viking frames 923A07–14 showing right angle bends in the channels where grabens were encountered.

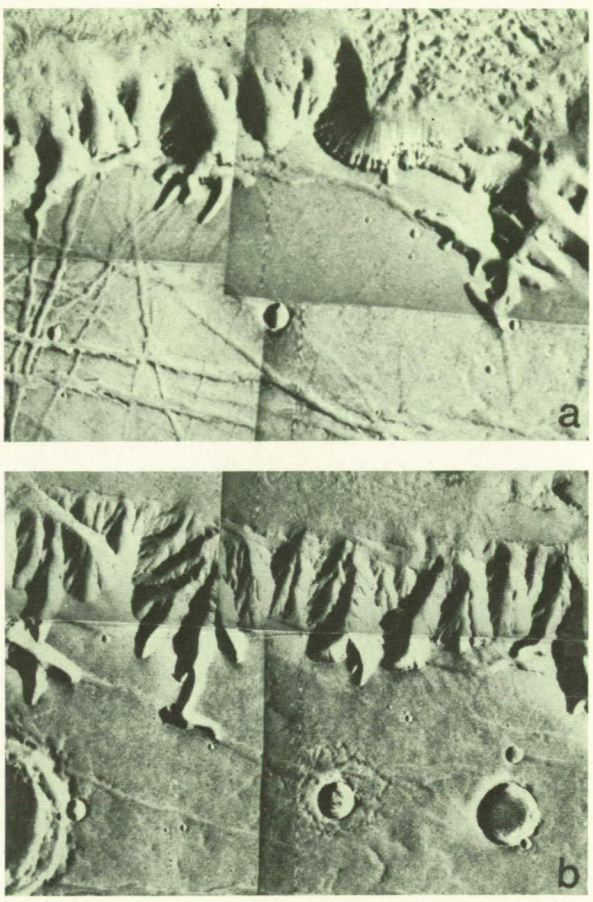

Piper (1985) showed that a combination of runoff and sapping processes was responsible for the formation of large valleys on Hawaii. However, detailed morphometric analyses could successfully differentiate valleys dominated by sapping from those dominated by runoff processes.

We are currently experimenting with the development of channels by the combination of groundwater sapping and rainfall runoff processes. Channels formed in run 28 were established first by sapping during hours 0–12 (fig. 120). After hour 12, sapping continued, but the flow was supplemented with periodic intervals of rainfall. The resulting channels (fig. 120) exhibited a tapering head area more indicative of runoff valleys and was also characterized by more bifurcation than the normal sapping valleys produced in runs where only sapping had occurred. However, close inspection of fig. 120 reveals a distinctive scalloped morphology of alcoves developed along the channel walls. Although the overall morphology appeared more like runoff valleys, the influence of sapping could definitely be observed along the valley

walls. The head of one of the valleys (fig. 120, right channel) was also bowl shaped due to the significant basal sapping that was occurring there.

Channel Morphology and Piracy

The morphology of experimental channels developed by groundwater sapping is remarkably similar to that of terrestrial and martian valleys presumed to have formed by sapping processes. The most distinctive features include the amphitheater head region; long main valley with infrequent, stubby tributaries; the presence of alcoves along valley walls, particularly along up-dip sides of the valleys; asymmetry of tributaries; and absence of tributaries in the downstream reaches of the channels. These features have all been recognized in the valleys thought to have been strongly influenced by groundwater sapping in the Colorado Plateau.

We noticed the importance of groundwater piracy in the evolution of channel networks during most of the sapping experiments. Subsurface piracy was commonplace in all types of stratigraphic settings and regardless of the presence of joints. Three to six channels typically formed at regularly spaced positions across the seepage face during the initial few hours of sapping runs. During the course of a run, one or two of these channels extended headward more rapidly until it captured groundwater from surrounding areas that would have flowed into neighboring channels. Once dominance of a given channel began, the process became self-enhancing and the disparity between development of neighboring channels became even more apparent. Eventually the pirated channels became inactive and channel evolution was terminated. Figure 121 shows examples of channel piracy during run 7.

Groundwater piracy was best developed during several runs (runs 7 and 18) where conditions were established to mimic the intersection of channels with subsurface high-level aquifers in experiments designed to simulate channel development on Hawaii (Kochel and Piper, 1985). Head regions of the first channels that reached the high-level aquifers widened dramatically and grew at the expense of neighboring channels that were pirated. This process is probably responsible for the light-bulb-shaped valleys typical of sapping valleys on the Hawaiian Islands (fig. 113).

Figure 120. Oblique photograph at the conclusion of run 28. Note the amphitheater head of the right channel and the scalloped appearance of channel walls formed into alcoves by sapping. The overall form of the channels is more runoff-like because the channels have been produced by rainfall and sapping combined.

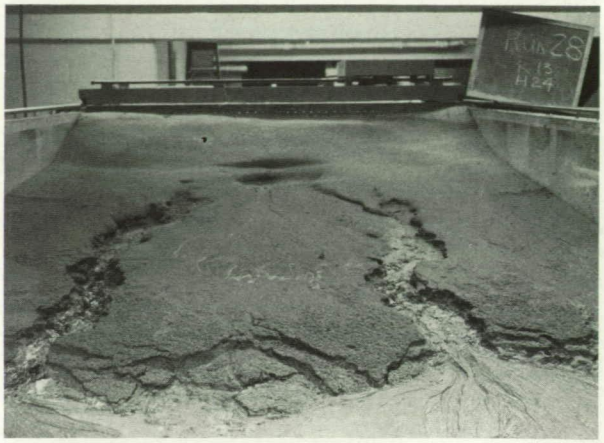

Figure 121. Oblique photograph of run 7 after 42 hours. Note the wide sapping heads of the two large channels that tapped into high-level aquifers. The growth of these large channels pirated flow to the neighboring channels, which were abandoned early in the run. The bifurcated abandoned channel now looks like a tributary to the left channel, but it was eroded by lateral extension of the left channel, which removed the downstream portion of the bifurcated channel. Note that the abandoned channels are at much higher elevation than the active sapping channels.

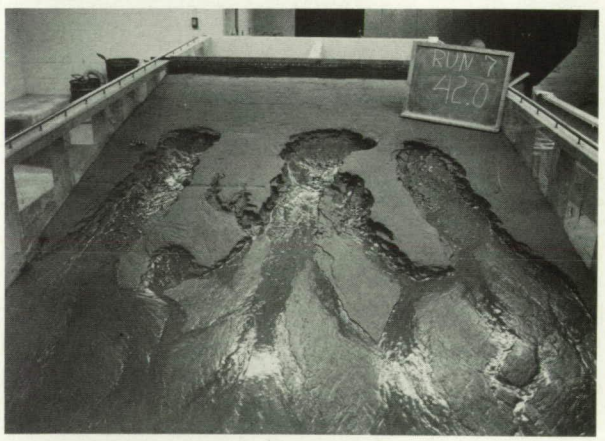

SUMMARY

Experimental modeling provides a convenient way of making direct observations of process and morphology of valleys formed by groundwater sapping. It is very difficult to resolve or observe formative processes in field situations. Controlled laboratory settings are required to directly observe processes over a short time frame. We cannot mimic all of the attributes of a field setting, such as the important role of weathering and removal of the sapped debris, actual rock strength, and sediment size to channel size scaling. However, we can make valuable observations of channel morphology, channel evolution, and sapping processes using experimental models.

Our experiments have successfully demonstrated the following features which have been suggested to be important in the evolution of channels on the Colorado Plateau: joint control of groundwater flow and subsequent orientation of channels, the importance of groundwater piracy, the importance of stratigraphy in controlling the location of seepage faces on layered rocks, and how impermeable strata can inter-

act with the geometry of permeable strata as important controls on the dimensions of channels developed by groundwater sapping.

These kinds of modeling experiments are particularly good for testing concepts, developing a suite of distinctive morphologies and morphometries indicative of sapping, helping to relate process to morphology, and providing data necessary to assess the relative importance of runoff, sapping, and mass-wasting processes on channel development. The observations from the flume systems can be used to help interpret features observed in terrestrial and martian settings where sapping processes are thought to have played an important role in the development of valley networks.

REFERENCES

Kochel, R.C., and Burgess, C.M. (1983) Structural control of geomorphic features in the Kasei Vallis region of Mars. *NASA TM-85137,* p. 288–290.

Kochel, R.C., and Capar, A.P. (1983) Structural control of sapping valley networks along Valles Marineris, Mars. *NASA TM-85127,* p. 295–297.

Kochel, R.C., and Piper, J.F. (1985) Morphology of large valleys in Hawaii: evidence for groundwater sapping and comparisons to martian valleys. *17th Lunar and Planetary Science Conference,* p. 424–425.

Kochel, R.C., Baker, V.R., Simmons, D.W., and Lis, C.J. (1983) Surface channel networks developed by groundwater sapping in a laboratory model: analog to sapping channels on Mars. *NASA TM-85127,* p. 227–229.

Kochel, R.C., Howard, A.D., and McLane, C. (1985) Channel networks developed by groundwater sapping in fine-grained sediments: analogs to some martian valleys. In Woldenberg, M., ed., *Models in Geomorphology*. Boston, Allen, & Unwin, p. 313–341.

Laity, J.E., and Malin, M.C. (1985) Sapping processes and the development of theater-headed valley networks on the Colorado Plateau. *Geol. Soc. Am. Bull.* **96:** 203–217.

Schumm, S.A., and Chorley, R. (1966) Talus weathering and scarp recession in the Colorado Plateau. *Zeit. Geomorph.* **10:** 11–36.

Schumm, S.A., and Phillips, L. (1986) Composite channels of the Canterbury Plain, New Zealand: a martian analog? *Geology* **14:** 326–329.

Chapter 7

Evolution of Small Valley Networks in the Heavily Cratered Terrains of Mars

Victor R. Baker

The equatorial heavily cratered uplands of Mars are dissected by two classes of small valleys that are intimately associated in compound networks (Baker and Partridge, 1984a). Pristine valleys, exhibiting steep valley walls, preferentially occupy downstream portions of compound basins. Degraded valleys, exhibiting eroded walls, are laterally more extensive and have higher drainage densities than pristine valleys (Baker and Partridge, 1984b). Morphometric and crater-counting studies indicate that relatively dense drainage networks were emplaced on Mars during the heavy bombardment about 4.0 billion years ago. Over a period of approximately 10^8 years, these networks were degraded and subsequently invaded by headwardly extending pristine valleys.

The great lateral extent of degraded networks, as indicated by their high network dissection ratios, certainly indicates a different process for their evolution than for the pristine valleys. Cross grading (Horton, 1945) as opposed to simple headward extension (Abrahams, 1977) might explain the differences between degraded and pristine network morphology. However, degraded networks are so difficult to map that this distinction may have to await the acquisition of higher quality imagery of Mars.

Pristine network segments possess numerous attributes associated with an origin by sapping (Pieri, 1980; Baker, 1982). The pristine valleys probably evolved by headward growth and structurally-controlled bifurcation, as modeled for terrestrial networks by Dunne (1980). Paleoenvironmental implications of this process center on the need for an active hydrologic cycle to recharge the high water tables necessary to sustain spring discharge at the valley heads.

Figure 122 shows a hypothetical sequence of valley network evolution on Mars that is consistent with the data generated in this study. In scene A, a relatively dense network of valleys has developed during the heavy bombardment, approximately 4.0 billion years ago. The valleys formed on slopes dictated by large (> 20 km-diameter) craters that already had been emplaced by this time. Valley formation may have contributed to the obliteration of smaller craters that formed coeval with the large ones.

Scene B shows the formation of intercrater plains (IC), which broke the densely cratered terrain into zones of rugged, cratered plateau (HC) and intervening plains (IC). Plains formation probably buried portions of the older valleys. However, the intercrater plains became sites for the initiation of new headwardly extending pristine valleys. As these grew into the now-relict predecessor network (scene C), relatively small craters were superimposed on the landscape. Unlike the large craters, which are now highly degraded in appearance, the small craters are relatively fresh. Nearly all are less than 10 km in diameter, and this population dominates the final configuration of the compound network (scene D). The high density of these craters indicates that they were part of the heavy bombardment, but probably were emplaced during the rapid decline of cratering rates about 3.8 to 3.9 billion years ago.

The data indicate that in a relatively short period after the emplacement of large craters, perhaps 10^8 years, the extensive networks were formed, degraded by erosional processes, and invaded by headwardly extending pristine valleys. It is tempting to hypothesize that the degradation of the valleys may have been the same degradation interpreted to have affected the large craters (Hartmann, 1973; Chapman and Jones, 1977). This period of high erosion rates seems to have been coincident with the rapid decline in cratering rates about 3.8 to 3.9 billion years ago.

The relict compound valleys on Mars are morphometrically distinct from most terrestrial drainage

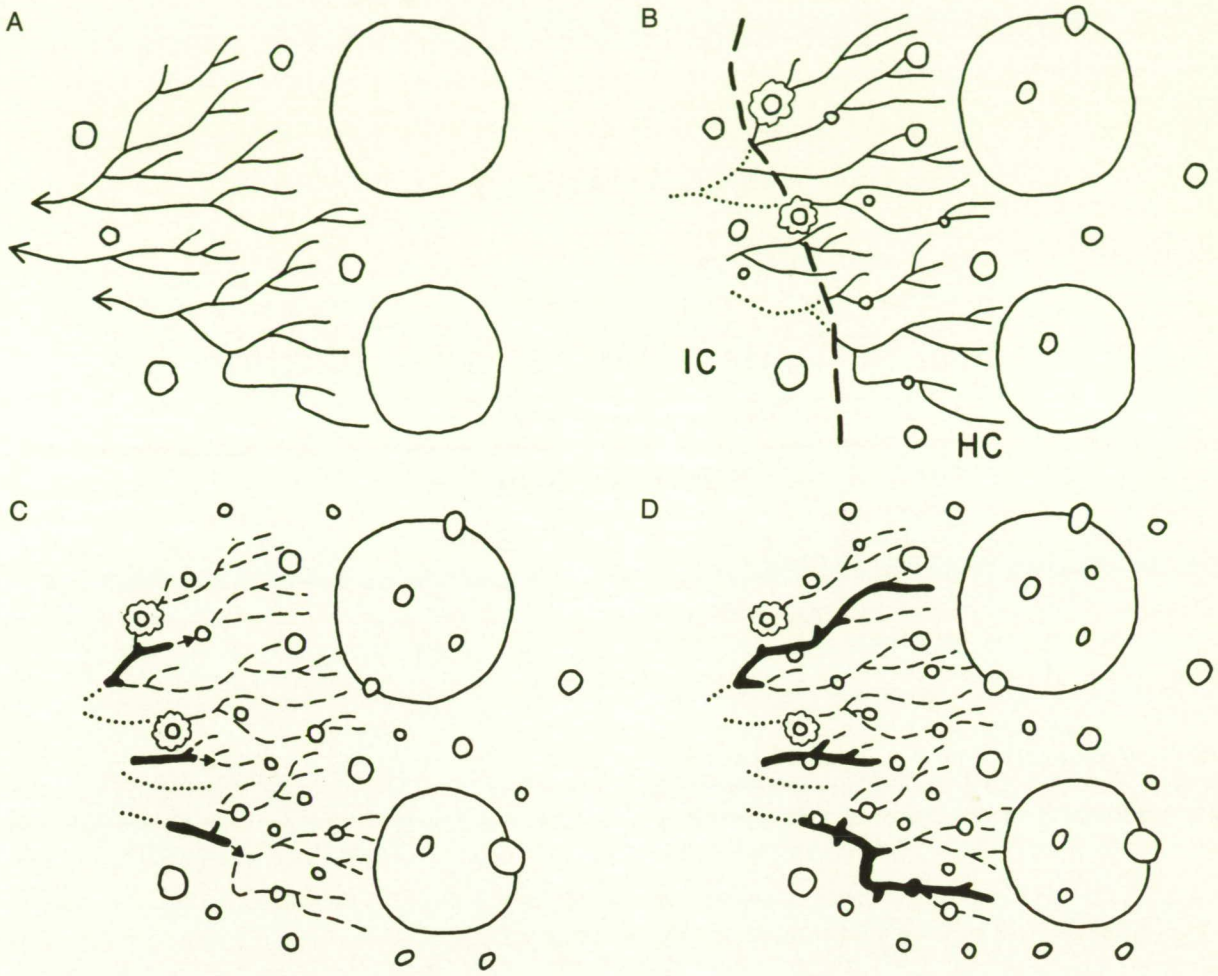

Figure 122. Hypothetical sequence of valley development in the equatorial highlands of Mars. (A) Relatively dense network of valleys forms coeval with heavy bombardment approximately 4.0 billion years ago. (B) Intercrater plains (IC) begin formation, burying downstream extensions of some valleys (dotted lines). Intercrater plains become distinct from the rugged, densely cratered plateau (HC). (C) Pristine valleys (heavy lines) form in intercrater plains and migrate headward (arrows) into areas of now-inactive degraded valleys (dashed lines). (D) Pristine valleys cease headward migration about the same time as the termination of the heavy bombardment, approximately 3.8 to 3.9 billion years ago. Landscape experiences extremely slow degradation up to the present.

systems. The differences might be caused by a martian valley formation episode characterized by hyperaridity, by inadequate time for network growth, by very permeable rock types, or by a combination of factors. Clearly the valleys have had a complex history that is intimately associated with the cratering of the heavy bombardment. Because cratering and other erosive processes have removed so much of the evidence, it may not be possible to discern an unequivocal origin.

REFERENCES

Abrahams, A.D. (1977) *Am. J. Sci.* **277:** 626-645.

Baker, V.R. (1982) *The Channels of Mars.* Austin, University of Texas Press.

Baker, V.R., and Partridge, J.B. (1984a) *Lunar and Planetary Science XV.* Houston, Lunar and Planetary Institute, p. 25-26.

Baker, V.R., and Partridge, J.B. (1984b) *Lunar and Planetary Science XV.* Houston, Lunar and Planetary Institute, p. 23-24.

Chapman, C.R., and Jones, K.L. (1977) *Annu. Rev. Earth Planet. Sci.* **5:** 515-540.

Dunne, T. (1980) *Prog. Phys. Geogr.* **4:** 211-239.

Hartmann, W.K. (1973) *J. Geophys. Res.* **79:** 3951-3957.

Horton, R.E. (1945) *Geol. Soc. Am. Bull.* **56:** 275-370.

Pieri, D. (1980) *Science* **210:** 895-897.

Chapter 8

Evolution of Valleys Dissecting Volcanoes on Mars and Earth

Victor R. Baker

Drainage evolution on volcanoes proceeds according to the functional relationship

$$D = f(c, r, p, t)$$

where D is drainage density, c is climate, r is relief, p is rock type, and t is time. Because most volcanic rocks are highly permeable, drainage will not develop until a less permeable ash mantle is emplaced or until weathering reduces infiltration. Examples of both phenomena occur in Hawaii. Kilauea Volcano, youngest of the Hawaiian shields, displays little dissection except where the 1790 Keanakakoi ash was emplaced (Malin et al., 1983). The older Mauna Loa and Mauna Kea shields display V-shaped ravines where steep slopes on their eastern flanks were mantled by Pahala ash. Dissection is more pronounced on Mauna Kea, which is older than Mauna Loa. Kohala Volcano, dated at 700,000 years B.P., is the oldest shield on the island of Hawaii. Deep weathering of its basalt has reduced infiltration sufficient to promote high-density drainage on its northeastern slopes (fig. 123).

On volcanic cones, dissection by closely spaced V-shaped ravines produces a characteristic "parasol ribbing" in which valley sides intersect to form sharp-edged ridges (Ollier, 1970). The radial drainage results in a convergence of valley heads toward the volcano summit. Stream abstraction and capture are very common and may be enhanced by orographic effects on precipitation. The result is greater incision on the upper slopes that may leave the relict surface of the original volcano preserved as triangular facets ("planezes") on the low slopes (Ollier, 1970). Continued erosion then reduces the cone to a residual volcano, exposing resistant dikes and vents. Relief inversion may occur where valleys are filled by lava flows that are more resistant than adjacent valley walls.

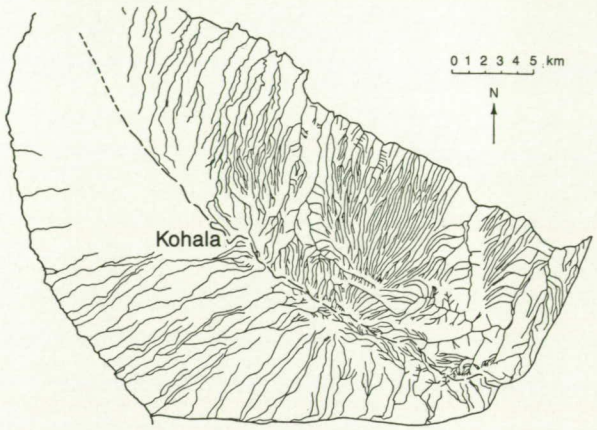

Figure 123. Drainage map of Kohala Volcano at the northern end of the island of Hawaii. This map emphasizes V-shaped ravine development.

On shield volcanoes parallel ravine systems incise to expose deeper layers where groundwater activity becomes more important. The deepest incision produces trough-shaped theater-headed valleys (fig. 124). Once the latter form, they dominate the dissection of the shield. The largest theater-headed valleys probably grow fastest since they tap the largest supplies of groundwater. The groundwater locally produces spring sapping, but a more general process may be enhanced chemical disintegration of basalt at the water table, which intersects the slope toes at the valley wall/floor junction. This leads to exceptionally steep valley walls (Wentworth, 1928). On Kohala and the older Hawaiian volcanoes of Maui the characteristic deep valley form is U-shaped in cross section, and valley sides are subject to active soil avalanches, slumps, and other mass movement (Wentworth, 1943). Continued headward retreat of such valleys

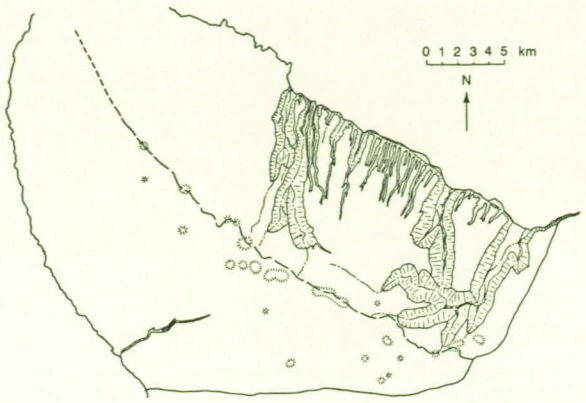

Figure 124. Drainage map of Kohala Volcano at same scale as fig. 123 emphasizing U-shaped, theater-headed valleys.

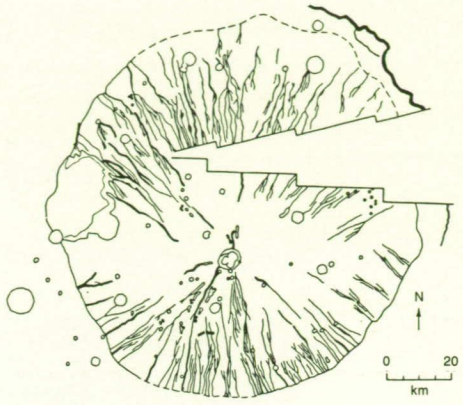

Figure 125. Sketch map of drainage features on Hecates Tholus. Heavy lines indicate relatively deep, U-shaped valleys in contrast to high-density ravines.

isolates uplands drained by V-shaped ravines (fig. 124) producing hanging valleys. Divides may eventually be reduced to knife-like ridges, as in the pali of northeastern Oahu (Macdonald and Abbott, 1970).

Especially large theater-headed valleys occur on Maui, where two such valleys, Kaupo and Keanae, have grown headward into the caldera of Haleakala Volcano. The relationship is remarkably similar to that shown on Tyrrhena Patera of Mars (Baker, 1982). Such large valleys may become conduits for lava flows and lahars, thereby adding to the complexity of their origin.

The climatic factor exerts a strong influence on Hawaiian volcano dissection. The northeastern, windward slopes of Kohala are much more dissected than the southwestern, leeward slopes (figs. 123 and 124). Similar relationships occur on Mauna Kea, where the northeastern Hamakua Coast shows moderate drainage development of long, parallel V-shaped valleys experiencing cross grading by capture. Leeward slopes of Mauna Kea are essentially undissected.

Hawaiian volcano dissection has been suggested as an analog for sapping valleys in the martian heavily cratered terrains (Baker, 1980a, 1982) and as a model for volcano dissection on Mars (Baker, 1980b). Several older shield volcanoes, including Hecates Tholus (fig. 125), appear to display fluvial dissection. New crater dating studies of these volcanoes suggest that the dissection is coincident with the terminal heavy bombardment on Mars. Thus, the valleys probably formed at the same time as those in the heavily cratered terrains. Both areas of valley formation show two types of valleys: (a) slightly older, more dense networks on higher, probably relict land surfaces, and (b) younger, less dense networks of deeply incised valleys that seem to have grown headward at the expense of type (a) valleys. It is hypothesized that these relationships indicate an evolutionary sequence similar to that observed in the Hawaiian volcanoes. High-density surface water ravines formed initially because of low-permeablity rock types, appropriate climate, adequate relief, or some combination of these factors. With time, some valleys deepened sufficiently to tap groundwater flow in deeper, more permeable rock types. These valleys then enlarged by headward growth at the expense of the older network. The latter was isolated as relict, degraded components of the landscape. The entire system ceased functioning and was "frozen" in its approximate present configuration at the termination of the heavy bombardment on Mars.

REFERENCES

Baker, V.R. (1980a) NASA TM-81776, p. 286-288.

Baker, V. R. (1980b) NASA TM-82385, p. 234-235.

Baker, V. R. (1982) *The Channels of Mars*. Austin, University of Texas Press.

Macdonald, G.A., and Abbott, A.T. (1970) *Volcanoes in the Sea*. Honolulu, University of Hawaii Press.

Malin, M.C., Dzurisin, D., and Sharp, R.P. (1983) *Geol. Soc. Am. Bull.* **94:** 1148-1158.

Ollier, C.D. (1970) *Volcanoes*. Cambridge, Mass., MIT Press.

Wentworth, C.K. (1928) *J. Geol.* **36:** 385-410.

Wentworth, C.K. (1943) *Geol. Soc. Am. Bull.* **54:** 53-64.

Chapter 9

Flow Modeling of Cataclysmic Flood Discharges

Victor R. Baker

The indirect calculation of flow hydraulics from paleochannel dimensions is generally accomplished using semi-empirical formulae such as the Manning equation:

$$Q = VA = n^{-1} AR^{2/3} S^{1/2}$$

where Q is discharge (m^3/s), V is mean flow velocity in m/s, A is channel cross-sectional area (m^2), n is the Manning roughness coefficient, R is the hydraulic radius (m), and S is the energy slope. This equation also serves as the basis of the slope-area procedure, which accounts for nonuniform flow (Chow 1959; Dalrymple and Benson, 1967). In applications to paleochannels it may be necessary to substitute flow depth (D) for hydraulic radius (R) and to substitute channel bottom slope or water surface slope for energy slope (S). An additional source of error derives from the specification of Manning's n.

Slope-area procedures have been applied to paleoflood discharge calculations in the Channeled Scabland (Baker, 1973). Maximum Missoula flood outflow in the Rathdrum Prairie area was found to be approximately 21 x 10^6 m^3/s. This is the largest known terrestrial fresh water discharge.

Paleoflood discharge calculations for martian outflow channels have followed terrestrial experience. The Manning equation, modified for martian gravity and flow depths

$$Q = VA = 0.5\ n^{-1} AR^{2/3} S^{1/2}$$

can be used to calculate discharges based on outflow channel dimensions (Nummedal et al., 1976; Carr, 1979; Baker, 1982). However, because of the complexity of the gravitational influence, Komar (1979) proposed an alternative calculation procedure based on frictional drag of the flow boundaries:

$$Q = VA = C_f^{-1/2} A (gDS)^{1/2}$$

where C_f is a dimensionless drag coefficient and g is the acceleration of gravity. Although this procedure has interplanetary versatility, it remains highly sensitive to a very uncertain parameter (C_f), and it assumes uniform flow (which would rarely occur in a cataclysmic flood situation).

Because of the above uncertainties, we have investigated a relatively new approach to paleoflood reconstruction employing step-backwater analysis (Feldman, 1981). The method employs computer programs (Hydrologic Engineering Center, 1979) to generate energy-balanced water surface profiles for various discharges in reaches where channel geometry is well specified. The modeled profiles are then matched to geologic evidence of high-water levels to establish the optimum discharge. Advantages of this procedure include the following: it provides a more accurate accounting of flow-energy losses associated with steady, nonuniform (gradually varied) flow in irregular channels; it allows multiple cross sections to accurately define channel constrictions and expansions; and it is relatively insensitive to uncertainties in specifying various friction loss coefficients, such as Manning's n (O'Connor and Webb, in preparation; Webb, 1985). All these factors make flow modeling the procedure of choice in various paleoflood reconstruction studies (O'Connor et al., in press).

A reach of North Kasei Vallis (fig. 126) was selected to apply flow modeling to Mars. It was assumed that canyon depths (calculated by shadow measurements on Viking images) corresponded to maximum probable depths of paleoflood water. Channel slope was established from the regional slope indicated by radar data (Lucchitta and Ferguson, 1983). A gradient (S) of 2.5 km/Km was used. Roughness (n) was assumed to be 0.010, or about one-half a reasonable terrestrial value. For the six cross sections (fig. 126) a discharge of 20 x 10^6 m^3/s results in a modeled water surface profile that nearly matches the canyon depths. For this modeled discharge the flow was found to be sub-

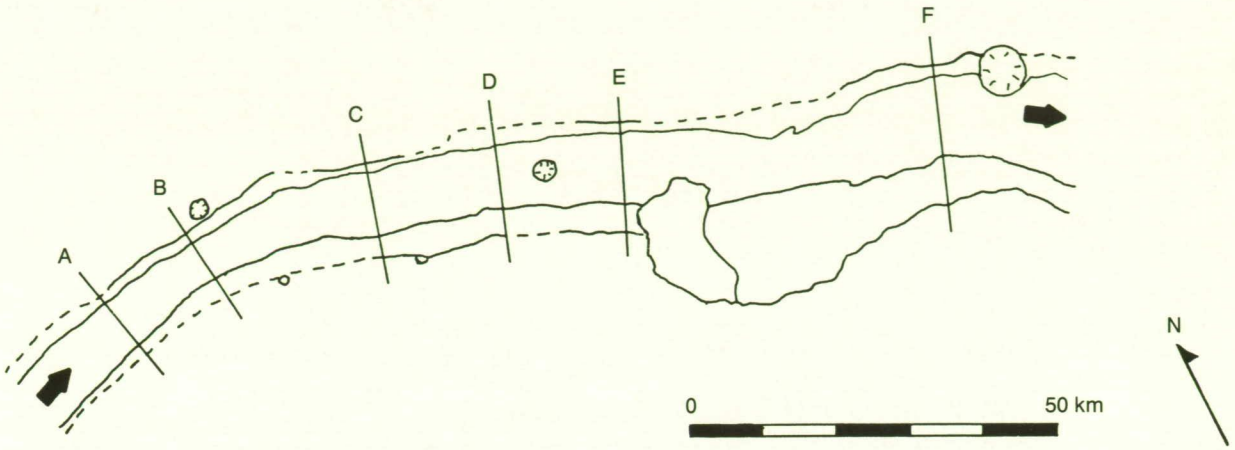

Figure 126. Sketch map of a portion of North Kasei Vallis prepared from Viking Photomosaic 211-5882, rev. 665A. Note locations of cross sections used in flow modeling of this outflow channel reach.

critical in all cross sections. In general, channel slopes, discharges, and Froude numbers are remarkably similar to values obtained for the Channeled Scabland employing both slope-area (Baker, 1973) and flow modeling (O'Connor and Baker, in press) procedures.

Present topographic data for Mars are sufficiently crude that the simpler paleohydraulic equations are adequate. However, proposed radar altimetry measurements by the Mars Observer Mission will greatly enhance our ability to specify outflow channel geometry. The computerized flow modeling procedures reported here will allow accurate paleodischarge calculations to be made from this new data base.

REFERENCES

Baker, V.R. (1973) *Geol. Soc. Am. Special Paper* **144:** 1-79.

Baker, V.R. (1982) *The Channels of Mars.* Austin, University of Texas Press.

Carr, M.H. (1979) *J. Geophys. Res.* **84:** 2995-3007.

Chow, V.T. (1959) *Open Channel Hydraulics.* New York, McGraw-Hill.

Dalrymple, T., and Benson, M.A. (1967) U.S. Geological Survey Tech. of Water Resources Inv., Book 3, Chapter A-2, p. 1-12.

Feldman, A.D. (1981) In *Advances in Hydrosciences.* New York, Academic Press, p. 297-423.

Hydrologic Engineering Center (1979) *HEC-2 Water Surface Profiles, User's Manual.* U.S. Army Corps of Engineers.

Komar, P.D. (1979) *Icarus* **37:** 156-181.

Lucchitta, B.K., and Ferguson, H.M. *J. Geophys. Res.* **88:** A553-A568.

Nummedal, D., Gonsiewski, J.J., and Boothroyd, J.C. (1976) *Geologica Romana* **15:** 407-418.

O'Connor, J.E., and Baker, V.R. (in press) *Quatern. Res.*

O'Connor, J.E., and Webb, R.H. (in preparation). In *Flood Geomorphology.*

O'Connor, J. E., R.H. Webb, and Baker, V.R. (in press) *Geol. Soc. Am. Bull.*

Webb, R.H. (1985) Late Holocene Flooding on the Escalante River, South-Central Utah. Ph.D. thesis, University of Arizona.

Chapter 10

Role of Groundwater Sapping in the Development of Large Valley Networks on Hawaii

R. Craig Kochel

Stream channels draining the windward slopes of the islands of Hawaii, Maui, and Molokai display greatly variable degrees of dissection relative to their leeward counterparts. Leeward slopes are slightly dissected with numerous high-density channel networks developed in parallel arrangement. These channels are in the minority on windward slopes. Windward channels are dominated by deeply dissected valleys having broad U-shaped cross-sections and amphitheater headward terminations (fig. 127). It is unlikely that the asymmetry of rainfall-runoff between opposite sides of these volcanoes can account for these differences, especially since dissected valleys occur on windward slopes as well. Groundwater sapping processes are suspected to play a major role in explaining the morphology observed in these Hawaiian valleys. Evidence supporting the importance of sapping comes from a combination of studies of imagery and topographic maps, field observations, and laboratory experiments.

The contribution of groundwater to the formation of large Hawaiian valleys was discussed by early workers (Stearns, 1966; Macdonald et al., 1983). In particular, they noted the apparent coincidence of central dike swarms with headward terminations of large valleys like those on the northeast slope of Kohala Volcano. It was suggested that once surface runoff incision proceeded to the depth where it intersected perched dike water, the influx of groundwater to these valleys caused dramatic increases in the rate of valley enlargement.

Drainage basins were outlined on 7.5-foot topographic maps (aided by observations of aerial photographs) from which morphometric measurements could be made. Measurements included basin area, various indices of relief, canyon area/basin area, drainage density, junction angle, basin shape, and channel orientation. Table 1 summarizes the results of these studies. Principal components analysis (PCA) of the morphometric data showed that valleys could be distinctly separated on the basis of morphometry.

Field reconnaissance of several valleys verified the significance of groundwater discharge into the large valleys. In most instances, valleys appear to be retreating headwardly by plunge pool erosion at valley-head waterfalls combined with basal sapping and associated mass-wasting of headwalls. Plunge pool erosion appears to be minor in most cases based on the following observations: large plunge pools are uncommon; waterfalls are not always present at valley heads; and significant talus and colluvium can be seen in some valley heads. Although no direct discharge measurements were made, large discharge springs were found at the base of valley heads, even in valleys without waterfalls or where falls were diverted by upstream irrigation tunnels. Piracy of groundwater flow appears to have played a major role in the development of these sapping valleys much as it does in the evolution of surface runoff networks.

Finally, experimental studies of groundwater sapping processes in unconsolidated sediments (Kochel et al., 1985) provide useful analogs to the Hawaiian situation. The effect of a sudden increase in groundwater contribution to a channel system was mimicked with the use of stratigraphic variations in sediments of varying hydraulic condivity. Surface channels were established on a smooth slope by groundwater sapping through the sediments from a headward reservoir. A more permeable and porous medium was put in the headward area of the slope which was progressively tapped as sapping channels cut headwardly. The rate of channel widening and extension increased significantly after the headward aquifer was tapped. These experiments and others in progress lend support to the model of increased dissection in the Hawaiian valleys caused by channels incised to the level of perched dike waters near the volcano summits. Widening of the headward portions of the large

Figure 127. Drainage networks on the northeast slope of Kohala Volcano, Hawaii. A-G are valleys influenced by sapping. A, B, F, and G are actively enlarging by sapping today. C, D, E, and parts of B may not be enlarging rapidly because of upslope groundwater piracy by valleys A and F. H-W show little evidence of sapping because of piracy of upslope groundwater by the large valleys.

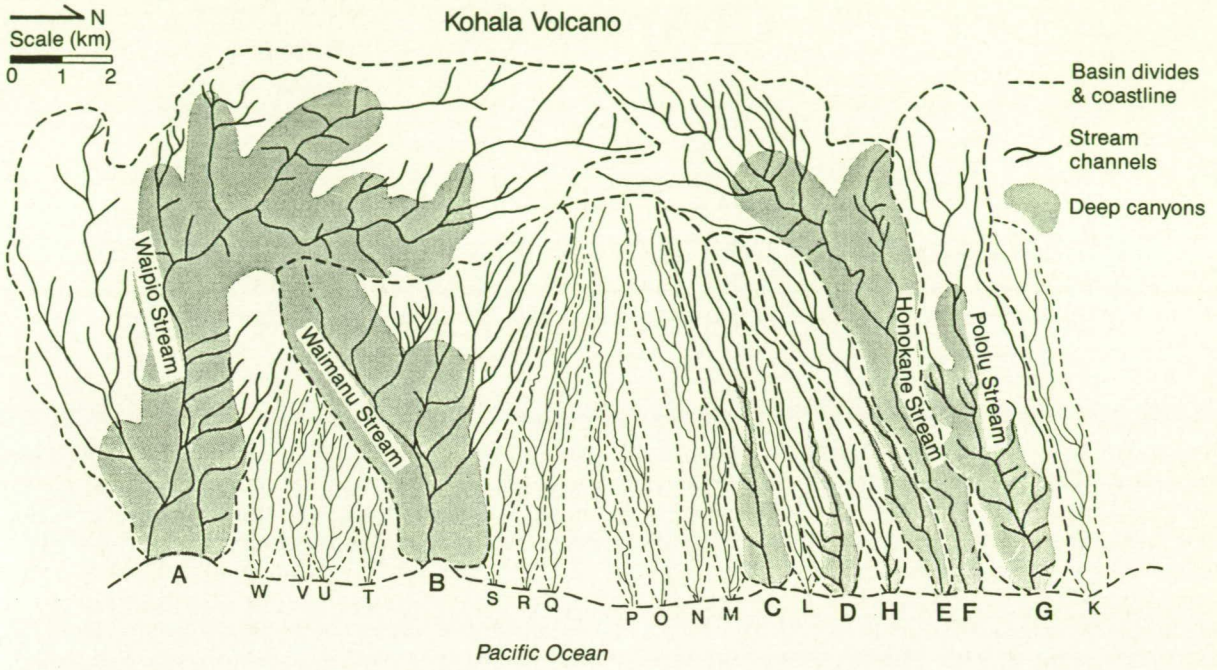

valleys on Kohala (fig. 127) by subsurface piracy is similar to the valley head widening that occurred in experimental runs at the level of the major aquifer.

Table 1. Comparison of Runoff-Dominated and Sapping-Dominated Valleys on Kohala Volcano

Characteristic	Runoff-dominated	Sapping-dominated
Basin shape	Extremely elongate	Lightbulb shaped
Head terminations	Tapered, gradual	Amphitheater, abrupt
Trend of channel segments	Uniform	Variable
Downstream tributaries	Frequent	Rare
Local relief	Low	High
Drainage density	High	Low—canyons High—plateaus
Drainage symmetry	Symmetrical	Asymmetrical Low down-dip
Canyon area/basin area	Low	High

REFERENCES

Kochel, R.C., Howard, A.D., and McLane, C. (1985) Channel networks developed by groundwater sapping in fine-grained sediments: analogs to some martian valleys. In Woldenberg, M.J., ed., *Models in Geomorphology*. New York, Allen and Unwin, p. 313-341.

Macdonald, G.A., Abbott, A.T., and Peterson, F.L. (1983) *Volcanoes in the Sea, the Geology of Hawaii*, 2nd ed. Honolulu, University of Hawaii Press.

Stearns, H.T. (1966) *Geology of the state of Hawaii*. Palo Alto, Calif. Pacific Books.

Chapter 11

Harmonic Shape Analyses of Streamlined Landforms on Earth and Mars

Paul D. Komar, Karen E. Clemens, and Nicklas G. Pisias

Harmonic shape analyses have been undertaken on streamlined islands within rivers, on glacial drumlins, and on the streamlined landforms found within the outflow channels on Mars. The objective was to determine whether subtleties in shapes of the martian erosional residuals offer evidence as to their origin and thus to the erosion of the outflow channels.

Past studies have described these various landforms as elliptical to airfoil shaped (Chorley, 1959; Reed et al., 1962; Trenhaile, 1971; Komar, 1984), so that harmonic analyses were first performed on these ideal end-member forms, the geometric lemniscate representing the airfoil. The harmonic shape analysis technique was first employed by Schwarcz and Shane (1969) and Ehrlich and Weinberg (1970) and has been applied to investigate the shapes of lunar craters by Eppler et al. (1983). Our analyses follow much the same procedures. The shape analyses of the ellipses and lemniscates demonstrated that all harmonics vary systematically with the length-to-width (L/W) elongation. For a given L/W ratio, the even harmonics of an ellipse and lemniscate are almost the same and so offer little potential for distinguishing landforms of different origins. In contrast, the odd harmonics largely reflect shape asymmetry and are zero for the perfectly symmetrical ellipse while having finite though small values for the lemniscates.

Harmonic analyses of the drumlins yield odd harmonics that are intermediate between the values for ellipses and lemniscates, but the lack of trends for the odd harmonics and best agreement of the even harmonics with the ellipses indicate that drumlins are more elliptical than airfoil shaped. The streamlined river islands show reasonable conformity with the harmonic trends of the lemniscate, both odd and even. The martian landforms yield still higher odd harmonics than the lemniscates, especially the triangular third harmonic. This is apparently due to their erosion in most cases having been controlled by flow separation around impact craters, producing more length-wise asymmetry than for the ideal lemniscate as well as a more triangular tail.

Discriminant function analysis is a statistical technique that permits simultaneous consideration of all of the harmonics in the landform comparison. A discriminant function first was determined using the ellipses and lemniscates as end members, and then the harmonic representations of the landforms were entered into this function, yielding scores according to their similarities to these geometric end members. The scores for the drumlins ranged from ellipses to lemniscates, while the scores for the river islands distributed evenly around the mean score for the lemniscates, none falling into the ellipse range. Many of the martian islands had scores that placed them in the lemniscate range, but more than half had scores indicating a significant departure. This departure is away from ellipses and drumlins, being in the direction of "super-lemniscates." The results indicate that the martian islands are not at all drumlin like in shape, whereas they do overlap in shapes with the terrestrial river islands. The extreme scores of many martian islands indicate, however, that they do have subtle shape differences from the river islands.

Diversion of flowing water by impact craters can be expected to have produced the observed contrasts in harmonic shape analyses between river and martian islands, but this interplay between flow hydraulics, structural control, and the resulting shapes as reflected in harmonic analyses requires further investigation. Flume experiments are now under way with this objective. Although the harmonic shape analyses do not provide a definitive conclusion as to the origin of the streamlined landforms on Mars, the results are consistent with their erosion by channelized water floods.

REFERENCES

Chorley, R.J. (1959) The shape of drumlins. *J. Geol.* **3:** 339-344.

Ehrlich, R., and Weinberg, B. (1970) An exact method for characterization of grain shape. *J. Sediment. Petrol.* **40:** 205-212.

Eppler, D.T., Ehrlich, R., Nummedal, D., and Schultz, P.H. (1983) Sources of shape variation in lunar impact craters: Fourier shape analysis: *Geol. Soc. Am. Bull.* **94:** 274-291.

Komar, P.D. (1984) The lemniscate loop—comparisons with the shapes of streamlined landforms. *J. Geol.* **92:** 133-145.

Reed, B., Galvin, C.J., and Miller, J.P. (1962) Some aspects of drumlin geometry. *Am. J. Sci.* **260:** 200-210.

Schwarcz, H.P., and Shane, K.C. (1969) Measurements of particle shape by Fourier analysis. *Sedimentology* **13:** 179-212.

Trenhaile, A.S. (1971) Drumlins: their distribution, orientation and morphology. *Can. Geogr.* **15:** 113-126.

Chapter 12

Sapping Processes and Valley Formation in the Navajo Sandstone of the Colorado Plateau

Julie Laity

The primary erosional mechanism in the development of entrenched theater-headed canyons in the Navajo Sandstone of the Glen Canyon region appears to involve groundwater sapping. Sapping results from the undermining and collapse of valley head and side walls by weakening or removal of basal support as a result of enhanced weathering and erosion by concentrated groundwater outflow at a site of seepage. The Navajo Sandstone is a highly transmissive aquifer underlaid by essentially impermeable rocks of the Kayenta Formation. Seepage occurs at a zone a meter or two above the contact because of diagenetic changes in the Navajo Sandstone that have reduced permeability near the base. As emerging groundwater approaches the vertical evaporative surface, calcite is deposited in pore spaces, wedging apart grains, and weakening the wall rock. Concurrently, macroscopic tunnels 200 to 600 μ in diameter are formed within this deposit that maintain flow to the surface. Efflorescent gypsum is deposited on the outer wall. As the weathering surface grows in thickness, the weakened material is sloughed off, aided in winter by the formation of icicles that cause a plucking action. The geomorphic consequence of sloughing and grain release is the enlargement of alcoves in cliff faces. These undermine basal support and cause eventual slab failure, facilitated by pressure release joints that develop parallel to canyon walls. Other processes break down the debris produced by slope collapse and carry away the disintegrated materials. Over the long term, large-scale valley networks form by headward sapping.

The canyons that develop differ in morphology, drainage pattern, network spatial evolution, rate of erosion, and degree of structural control from their fluvial counterparts. Valleys maintain relatively constant widths from source to outlet with high and steep sidewalls. The longitudinal profile is essentially straight in the lower segment (with some modification by fluvial erosion) because sapping occurs along a permeability boundary formed by the Kayenta Formation. Structural control results because groundwater flow is sensitive to changes in hydraulic gradient resulting from regional folding, as well as to deep fractures in the sandstone that act as conduits for laterally moving groundwater. This is demonstrated by network patterns that are highly asymmetric, show unusual constancy of tributary junction angles into the mainstream, parallelism of tributary orientation consistent with regional jointing over large geographic areas, and growth axes aligned up-dip. Theater-headed canyons are restricted in occurrence to surfaces with low dip angles (1° to 4°) and gentle topography that favors infiltrated precipitation over surface runoff.

Growth rates and development of canyons vary with the contributing subsurface drainage area and changes in climate which affect the amount of seepage and the effectiveness of surface runoff. Given a constant climatic regime, growth rates by sapping probably decline as the network enlarges and the drainage area of the spring heads lessens. In an advanced stage of development, the amount of lateral retreat approaches that of headwall retreat and valleys widen. Adjacent tributaries may merge, leaving isolated buttes and remnants of Navajo Sandstone, and a new drainage system of surface runoff develops on the exposed Kayenta Formation.

Chapter 13

Geomorphology of Nirgal Vallis

Timothy J. Parker

Nirgal Vallis is located in the southwest Margaritifer Sinus subquadrangle at −27° to −30° latitude, 37° to 45° longitude. It lies on the west side of the broad, northward-dipping Chryse Trough. Its mouth is cut into the west wall of Uzboi Vallis (Sharp and Malin, 1975; Pieri, 1980; Baker, 1982).

Nirgal developed within the Smooth Plains and Channel Modified materials of Parker and Pieri (1984) west of Uzboi Vallis. The Smooth Plains is a lightly cratered unit relative to surrounding units it appears to overlie. It also exhibits less concentrated structural lineaments and wrinkle ridges than surrounding units. These structural lineaments and wrinkle ridges display many orientations similar to those of segments of Nirgal Vallis (fig. 128).

The total length of Nirgal Vallis (distance from the mouth to its headward terminus measured along the valley floor) is about 685 kilometers. The width of the valley (across the entire system measured at the upper plains surface) averages 5 kilometers for the eastern (lower) half, with a maximum width of 20 kilometers at a point 65 kilometers from the mouth. The average width of the valley across the valley floor is 3 kilometers for the lower third and about 1.5 kilometers for the remaining two-thirds.

A longitudinal profile for the valley and 26 of its tributaries was obtained by taking 73 shadow measurements of the main valley and a total of 106 of the tributaries (fig. 129). These were obtained from moderate-resolution (about 70 m/pixel) Viking Orbiter 1 images (orbit 466A). The surface of the Smooth Plains material and Channel Modified material of Parker and Pieri (1984) was used as a datum. The maximum depth for the entire valley is 2 kilometers at a point 65 kilometers from the valley mouth. From here to a point 10 kilometers from the mouth the depth decreases to 500 meters. The minimum depth of the valley is 200 meters at its headward termination.

The slope of the valley floor (relative to the datum) from 480 kilometers from the mouth of the valley to

Figure 128. Comparison of structural lineaments; wrinkle ridges, and Nirgal Vallis.

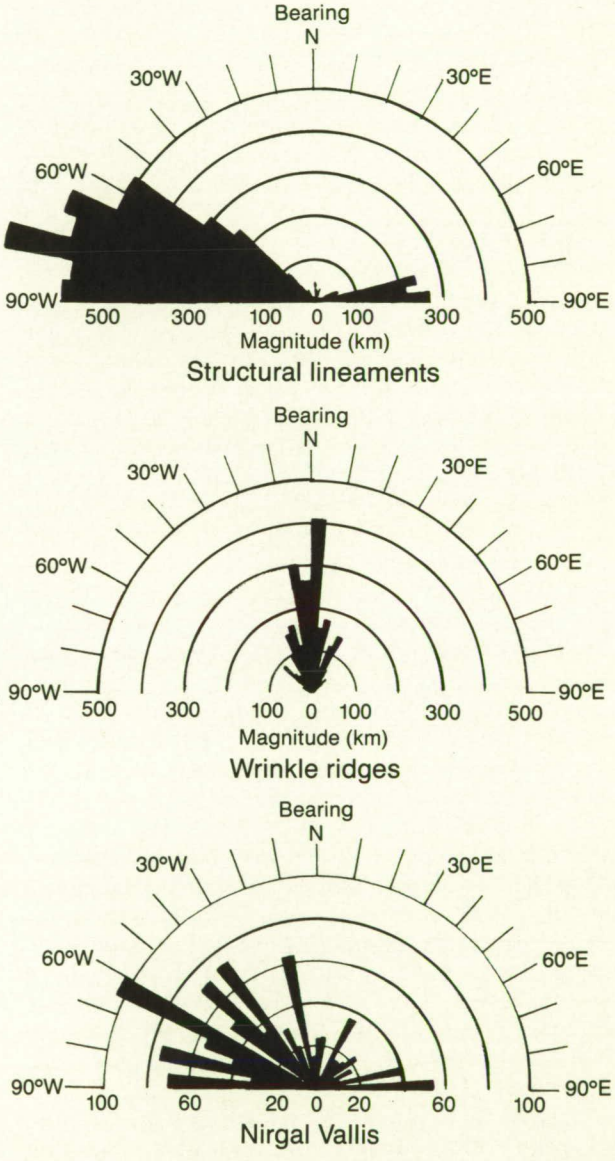

Figure 129. Longitudinal profile of Nirgal Vallis and tributaries.

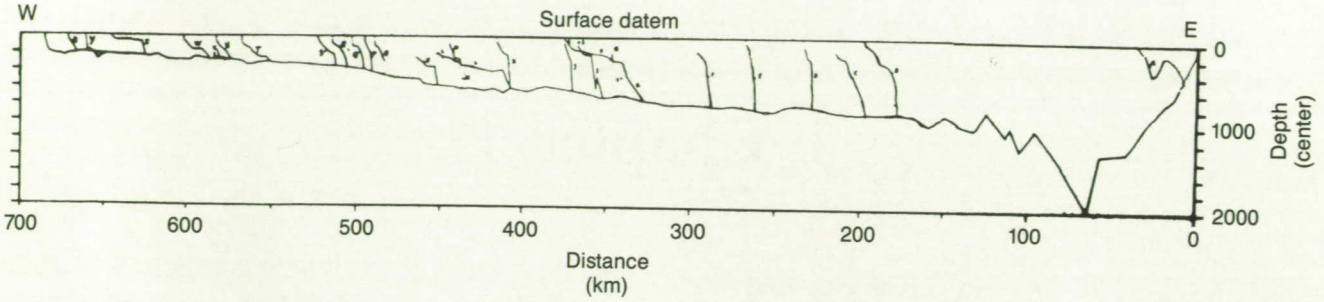

its headward termination is 1.04 meters per kilometer. From 480 kilometers to 460 kilometers from the valley mouth it increases to 5 meters per kilometer. This increase in slope does not correspond to any visible change in the surface, so it likely reflects an actual change in the slope of the valley floor. From 150 kilometers to 460 kilometers from the valley mouth the slope is 1.19 meters per kilometer. From 65 kilometers to 150 kilometers from the valley mouth, the data points show considerable scatter. The slope value here may be as low as 5 meters per kilometer or as high as 13 meters per kilometer. This scatter may be due to uncertainties in the depth measurements introduced by the increasing width of the valley floor resulting in an increasing separation of the data points from the thalweg (not positively identified). Or it might be due to an increase in the roughness of the valley floor in the lower reaches caused by wall collapse. Another possibility is that it might be due to a greater topographic variability in the Smooth Plains surface. From 10 kilometers from the valley mouth to 40 kilometers from the valley mouth, where the depth progressively decreases, the slope is −24.67 meters per kilometer. This negative slope is more probably due to a downward slope in the Smooth Plains and Channel Modified materials' surface toward Uzboi Vallis than to debris choking the valley floor. The data points within this range show very little scatter. The influence on the valley profile by Uzboi Vallis' wall from 0 to 10 kilometers from Nirgal's mouth is undetermined, as no reliable shadows were found.

Tributaries to Nirgal are more plentiful and are longer in the valley's western than in its eastern half. The number of tributaries identified (down to the limits of recognizability) in the eastern half of the valley is about 45. Of these, 24 lie on the south side of the main valley. In the western half of the valley, however, the number of recognizable tributaries was about 110, 60 of which lie on the south side of the main valley. The number of tributaries longer than about 5 kilometers is 9 for the eastern half and 19 for the western half. The average separation between tributaries longer than 5 kilometers along the main valley is 43 kilometers for the eastern half and 17 for the western half.

Most of the tributaries from the main valley mouth to about 550 kilometers from the valley mouth appear to have U-shaped cross-sections in their median and headward reaches and V-shaped cross-sections where they meet the main valley. Also, most of the 26 tributaries on which depth measurements were made have longitudinal profiles which display a somewhat flattened slope around 200 meters below the Smooth Plains datum. Finally, all the tributaries measured from the valley mouth to 520 kilometers from the valley mouth were found to have steeply sloping longitudinal profiles where they meet the main valley.

That the headward reaches of Nirgal Vallis are at approximately the same depth below the Smooth Plains surface as the heads of the tributaries is perhaps strongly suggestive of groundwater sapping above a permeability boundary about 200 meters below the surface. This is similar (though the scale may be greater) to sapping channels observed by Laity and Malin (1985) in the Colorado Plateau. The steepening of the tributaries where they join the main valley might indicate they were abandoned as the main valley developed headward. The relatively smooth, uniform longitudinal slope of the valley floor and its much greater depth towards the mouth beyond this 200 meter depth is suggestive of liquid water flow and transport of material out of the valley.

REFERENCES

Baker, V.R. (1982) *The Channels of Mars*. Austin, University of Texas Press.

Laity, J.E. and Malin, M.C. (1985) Sapping processes and the development of theater-headed valley networks on the Colorado Plateau. *Geol. Soc. Am. Bull.* **96:** 203-217.

Parker, T.J., and Pieri, D.C. (1984) Geomorphology and geology of the southwestern Margaritifer Sinus and Argyre regions of Mars. 1. Geological and geomorphological overview. NASA TM-87563, p. 361-363.

Pieri, D.C. (1980) Geomorphology of martian valleys. NASA TM-81979, p. 1-160.

Sharp, R.P. and Malin, M.C. (1975) Channels on Mars. *Geol. Soc. Am. Bull.* **86:** 331-342.

Chapter 14

The Effect of Slope on Experimental Drainage Patterns: Possible Application to Mars

Loren Phillips

There has been no systematic investigation of the effect of increasing slope on drainage pattern development, and quantitative relations between pattern character and slope have not been developed. To provide this information, eight experiments with different initial ground slopes were conducted in the TERF (tilting erosion-runoff flume). The major features of this flume are accurate slope and base level control, a versatile sprinkler system, and ease of operation and data collection. A homogeneous mixture of sand, silt, and clay (D_{50} = 0.2 mm) was installed in the TERF, and miniature drainage networks were formed by mist-fall erosion and runoff. Incremental base level lowering accomplished maximum extension of the networks. Preliminary results of these experiments indicate that, for the experimental material used:

1. Glock's stages of network evolution developed during all experiments, but they were only obvious on moderate to steep slopes ($\geq$ 3%).
2. Channel generations (groups of morphologically similar channels that evolve at different times during the development of a drainage network) formed during all experiments.
3. There was a definite pattern change from dendritic at 1.06% slope (junction angle range: 32°-109°; mean = 64.4°, s = 21.2) to subdendritic at 2.13% slope (junction angle range: 28°-115°; mean = 61.3°, s = 17.0) to subparallel at 2.93% and 3.72% slope (junction angle range: 15°-90°; mean = 43.55°, s = 15.0) to parallel at 5% slope and higher (junction angle range: 25°-60°; mean = 40.0°, s = 10.0).

Drainage patterns exhibiting both parallelism and channel generations occur on both Earth and Mars. Some Wyoming drainage patterns show marked parallelism at 2.36% ground slope, and channel generations also appear to be present. Of the martian patterns studied, junction angle ranges and means indicate that they are subparallel to parallel patterns. Although there is a great disparity of age and scale between martian and experimental networks, junction angles and patterns are similar for both. Therefore, the formation of martian channels by surface runoff cannot be discounted.

Chapter 15

Groundwater Sapping As a Submarine Geomorphic Process

James M. Robb

Although the creation of submarine canyons by the discharge of groundwater was suggested by Douglas Johnson during the 1930s, there was little direct evidence of the process until recently, when sidescan-sonar images from part of the Continental Slope off New Jersey became available. Those images show valleys and canyons that comprise series of steep-walled basins resembling subaerial features attributed to groundwater sapping. The basins appear to be located along the slope where the same stratigraphic intervals crop out. Excess pore pressures and discharge of groundwater at such intervals, enhanced by jointing, could cause slow, particle-by-particle cliff face retreat as well as increased rates of slope failure. Seismic profiling and stratigraphic sampling show that the slope truncates seaward-dipping clastic and chalky strata of Tertiary age and that there is stratigraphic continuity below the Continental Shelf from subaerial outcrops, as Johnson had postulated in his early work. Digital hydrologic modeling, using permeability data from offshore wells, indicates that eustatic sea level lowerings could have induced discharge of groundwater at the Continental Slope. Fresh interstitial water thought to be relict from Pleistocene time has been found under the Continental Shelf as far as 100 km offshore. There are apparent kluftkarren and rillenkarren on calcareous outcrops as deep as 2000 m below sea level on the lower slope, which may be evidence of former fresh-water discharge and solution by corrosive freshwater-seawater mixtures.

Unlike the subaerial realm, where groundwater that discharges from the soil will run downslope and transform its potential energy into work, removing more soil and transporting it away, groundwater that discharges into open water does not have the same potential energy, as it is supported by a medium of similar density; particles dislodged by it from the cliff face or bottom surface remain where they fall. Direct gravity would thus appear to be a relatively more important agent in the submarine world, and additional mechanisms must be supplied if the concept of unimpeded removal of material at a slope base is to apply to erosional schemes. Consequently, although groundwater seepage face erosion can help to explain some submarine erosional features, groundwater discharge is probably not an adequate agent to create subsea valley networks. The conceptual differences in the submarine and subaerial environment which this example illustrates may be applicable to studies of extraterrestrial geologic processes under heavy atmospheres.